

EXTREME MEDICINE

SCIENTIFIC AND PRACTICAL REVIEWED JOURNAL OF FMBA OF RUSSIA

EDITOR-IN-CHIEF Veronika Skvortsova, DSc, professor, RAS corresponding member

DEPUTY EDITOR-IN-CHIEF Igor Berzin, DSc, professor; Daria Kryuchko, DSc

EDITORS Vsevolod Belousov, DSc, professor; Anton Keskinov, PhD

TRANSLATORS Nadezda Tikhomirova, Vyacheslav Vityuk

DESIGN AND LAYOUT Marina Doronina

EDITORIAL BOARD

Agapov VK, DSc, professor (Moscow, Russia)
Baranov VM, member of RAS, DSc, professor (Moscow, Russia)
Bogomolov AV, DSc, professor (Moscow, Russia)
Boyko AN, DSc, professor (Moscow, Russia)
Borisevich IV, DSc, professor (Moscow, Russia)
Bushmanov AY, DSc, professor (Moscow, Russia)
Valenta R, PhD, professor (Moscow, Russia)
Daikhes NA, member of RAS, DSc, professor (Moscow, Russia)
Dubina MV, member of RAS, DSc, professor (Saint-Petersburg, Russia)
Dudarenko SV, DSc (Saint-Petersburg, Russia)
Ilyin LA, member of RAS, DSc, professor (Moscow, Russia)
Lobzin YV, member of RAS, DSc, professor (Saint-Petersburg, Russia)
Nikiforov VV, DSc, professor (Moscow, Russia)

Olesova VN, DSc, professor (Moscow, Russia)
Petrov RV, member of RAS, DSc, professor (Moscow, Russia)
Sadilov AS, DSc, professor (Saint-Petersburg, Russia)
Rembovsky VR, DSc, professor (Saint-Petersburg, Russia)
Samoilov AS, member of RAS, DSc, professor (Moscow, Russia)
Sergienko VI, member of RAS, DSc, professor (Moscow, Russia)
Sidorcevic SV, DSc (Moscow, Russia)
Troitsky AV, DSc, professor (Moscow, Russia)
Ushakov IB, member of RAS, DSc, professor (Moscow, Russia)
Khaitov MR, member of RAS, DSc, professor (Moscow, Russia)
Khaitov RM, member of RAS, DSc, professor (Moscow, Russia)
Chechetkin AV, DSc, professor (Saint-Petersburg, Russia)
Yudin SM, DSc, professor (Moscow, Russia)

ADVISORY BOARD

Aklev AV, DSc, professor (Chelyabinsk, Russia)
Arakelov SA, DSc, professor (Saint-Petersburg, Russia)
Baklaushev VP, DSc, professor (Moscow, Russia)
Degteva MO, PhD (Chelyabinsk, Russia)
Efimenko NV, DSc, professor (Pyatigorsk, Russia)
Kazakevich EV, DSc, professor (Arkhangelsk, Russia)
Katuntsev VP, DSc, professor (Moscow, Russia)
Klimanov VA, DSc, professor (Moscow, Russia)
Klinov DV, PhD (Moscow, Russia)
Koshurnikova NA, DSc, professor (Ozersk, Russia)
Minnullin IP, DSc, professor (Saint-Petersburg, Russia)

Mosyagin IG, DSc, professor (Saint-Petersburg, Russia)
Panasenkov OM, DSc, professor (Moscow, Russia)
Rogozhnikov VA, DSc, (Moscow, Russia)
Romanov SA, PhD (Ozersk, Russia)
Sotnichenko SA, DSc (Vladivostok, Russia)
Suranova TG, PhD, docent (Moscow, Russia)
Takhauov RM, DSc, professor (Seversk, Russia)
Shandala NK, DSc, professor (Moscow, Russia)
Shinkarev SM, DSc (Moscow, Russia)
Shipulin GA, PhD (Moscow, Russia)
Yakovleva TV, DSc (Moscow, Russia)

SUBMISSION editor@fmbs.press

CORRESPONDENCE editor@fmbs.press

COLLABORATION manager@fmbs.press

ADDRESS Volokolamskoe shosse, 30, str. 1, Moscow, 123182, Russia

Indexed in Scopus in 2022

Indexed in RSCI. IF 2018: 0,570

Listed in HAC 31.01.2020 (№ 1292)

Open access to archive



ВЫСШАЯ
АТТЕСТАЦИОННАЯ
КОМИССИЯ (ВАК)



Issue DOI: 10.47183/mes.2022-01

The mass media registration certificate № 25124 issued on July 27, 2006

Founder and publisher: Federal medical-biological agency fmbs.gov.ru

The journal is distributed under the terms of Creative Commons Attribution 4.0 International License www.creativecommons.org



Approved for print 31.03.2022
Circulation: 500 copies. Printed by Print.Formula
www.print-formula.ru

МЕДИЦИНА ЭКСТРЕМАЛЬНЫХ СИТУАЦИЙ

НАУЧНО-ПРАКТИЧЕСКИЙ РЕЦЕНЗИРУЕМЫЙ ЖУРНАЛ ФМБА РОССИИ

ГЛАВНЫЙ РЕДАКТОР Вероника Скворцова, д. м. н., профессор, член-корреспондент РАН

ЗАМЕСТИТЕЛЬ ГЛАВНОГО РЕДАКТОРА Игорь Берзин, д. м. н., профессор; Дарья Крючко, д. м. н.

НАУЧНЫЕ РЕДАКТОРЫ Всеволод Белоусов, д. м. н., профессор; Антон Кескинов, к. м. н.

ПЕРЕВОДЧИКИ Надежда Тихомирова, Вячеслав Витюк

ДИЗАЙН И ВЕРСТКА Марины Дорониной

РЕДАКЦИОННАЯ КОЛЛЕГИЯ

В. К. Агапов, д. м. н., профессор (Москва, Россия)
В. М. Баранов, д. м. н., профессор, академик РАН (Москва, Россия)
А. В. Богомолов, д. т. н., профессор (Москва, Россия)
А. Н. Бойко, д. м. н., профессор (Москва, Россия)
И. В. Борисевич, д. м. н., профессор (Москва, Россия)
А. Ю. Бушманов, д. м. н., профессор (Москва, Россия)
Р. Валента, д. м. н., профессор (Москва, Россия)
Н. А. Дайхес, д. м. н., профессор, член-корр. РАН (Москва, Россия)
М. В. Дубина, д. м. н., профессор, академик РАН (Санкт-Петербург, Россия)
С. В. Дударенко, д. м. н., доцент (Санкт-Петербург, Россия)
Л. А. Ильин, д. м. н., профессор, академик РАН (Москва, Россия)
Ю. В. Лобзин, д. м. н., профессор, академик РАН (Санкт-Петербург, Россия)
В. В. Никифоров, д. м. н., профессор (Москва, Россия)

В. Н. Олесова, д. м. н., профессор (Москва, Россия)
Р. В. Петров, д. м. н., профессор, академик РАН (Москва, Россия)
А. С. Радилов, д. м. н., профессор (Санкт-Петербург, Россия)
В. Р. Рембовский, д. м. н., профессор (Санкт-Петербург, Россия)
А. С. Самойлов, д. м. н., профессор, член-корр. РАН (Москва, Россия)
В. А. Сергиенко, д. м. н., профессор, член-корр. РАН (Москва, Россия)
С. В. Сидоркевич, д. м. н. (Москва, Россия)
А. В. Троицкий, д. м. н., профессор (Москва, Россия)
И. Б. Ушаков, д. м. н., профессор, академик РАН (Москва, Россия)
М. Р. Хаитов, д. м. н., профессор, член-корр. РАН (Москва, Россия)
Р. М. Хаитов, д. м. н., профессор, академик РАН (Москва, Россия)
А. В. Четкин, д. м. н., профессор (Санкт-Петербург, Россия)
С. М. Юдин, д. м. н., профессор (Москва, Россия)

РЕДАКЦИОННЫЙ СОВЕТ

А. В. Аклеев, д. м. н., профессор (Челябинск, Россия)
С. А. Аракелов, д. б. н., профессор (Санкт-Петербург, Россия)
В. П. Баклаушев, д. м. н., профессор (Москва, Россия)
М. О. Дегтева, к. т. н. (Челябинск, Россия)
Н. В. Ефименко, д. м. н., профессор (Пятигорск, Россия)
Е. В. Казакевич, д. м. н., профессор (Архангельск, Россия)
В. П. Катунцев, д. м. н., профессор (Москва, Россия)
В. А. Климанов, д. ф.-м. н., профессор (Москва, Россия)
Д. В. Клинов, к. ф. м. н., (Москва, Россия)
Н. А. Кошурникова, д. м. н., профессор (Озерск, Россия)
И. П. Миннуллин, д. м. н., профессор (Санкт-Петербург, Россия)

И. Г. Мосягин, д. м. н., профессор (Санкт-Петербург, Россия)
О. М. Панасенко, д. б. н., профессор (Москва, Россия)
В. А. Рогожников, д. м. н. (Москва, Россия)
С. А. Романов, к. б. н. (Озерск, Россия)
С. А. Сотниченко, д. м. н. (Владивосток, Россия)
Т. Г. Суранова, к. м. н., доцент (Москва, Россия)
Р. М. Тахауов, д. м. н., профессор (Северск, Россия)
Н. К. Шандала, д. м. н., профессор (Москва, Россия)
С. М. Шинкарев, д. т. н. (Москва, Россия)
Г. А. Шипулин, к. м. н. (Москва, Россия)
Т. В. Яковлева, д. м. н. (Москва, Россия)

ПОДАЧА РУКОПИСЕЙ editor@fmba.press

ПЕРЕПИСКА С РЕДАКЦИЕЙ editor@fmba.press

СОТРУДНИЧЕСТВО manager@fmba.press

АДРЕС РЕДАКЦИИ Волоколамское шоссе, д. 30, стр. 1, г. Москва, 123182, Россия

Журнал включен в Scopus в 2022 г.

Журнал включен в РИНЦ. IF 2018: 0,570

Журнал включен в Перечень 31.01.2020 (№ 1292)

Здесь находится открытый архив журнала

Scopus®

НАУЧНАЯ ЭЛЕКТРОННАЯ
БИБЛИОТЕКА
LIBRARY.RU



ВЫСШАЯ
АТТЕСТАЦИОННАЯ
КОМИССИЯ (ВАК)

CYBERLENINKA

DOI выпуска: 10.47183/mes.2022-01

Свидетельство о регистрации средства массовой информации № ФС77-25124 от 27 июля 2006 года

Учредитель и издатель: Федеральное медико-биологическое агентство fmba.gov.ru

Журнал распространяется по лицензии Creative Commons Attribution 4.0 International www.creativecommons.org



Подписано в печать 31.03.2022
Тираж 500 экз. Отпечатано в типографии Print.Formula
www.print-formula.ru

METHOD	5
<hr/>	
Development of PCR test for detection of the SARS-CoV-2 genetic variants Alpha, Beta, Gamma, Delta Shipulin GA, Savochkina YuA, Shuryaeva AK, Shivyagina EE, Nosova AO, Davydova EE, Luparev AR, Malova TV, Yudin SM Разработка ПЦР-теста для выявления генетических вариантов альфа, бета, гамма, дельта вируса SARS-COV-2 Г. А. Шипулин, Ю. А. Савочкина, А. К. Шуряева, Е. Е. Шивлягина, А. О. Носова, Е. Е. Давыдова, А. Р. Лупарев, Т. В. Малова, С. М. Юдин	
REVIEW	12
<hr/>	
Liver damage in patients with COVID-19 Vologzhanin DA, Golota AS, Kamilova TA, Makarenko SV, Scherbak SG Поражение печени у больных COVID-19 Д. А. Вологжанин, А. С. Голота, Т. А. Камилова, С. В. Макаренко, С. Г. Щербак	
REVIEW	20
<hr/>	
PAMAM dendrimers and prospects of their application in medicine Popova EV, Krivorotov DV, Gamazkov RV, Radilov AS Дендримеры PAMAM и перспективы их применения в медицине Е. В. Попова, Д. В. Криворотов, Р. В. Гамазков, А. С. Радиллов	
ORIGINAL RESEARCH	27
<hr/>	
Specifics of the workload-dependent dynamics of psycho-emotional exhaustion among medical staff of a COVID hospital Nazaryan SE, Samoilov AS, Sedin VI Особенности динамики психоэмоционального истощения у медицинского персонала COVID-госпиталя с различной интенсивностью трудовой нагрузки С. Е. Назарян, А. С. Самойлов, В. И. Седин	
ORIGINAL RESEARCH	33
<hr/>	
The effect of a single procedure of combined micropolarization on autonomic regulation and sensorimotor reactions Sivachenko IB, Medvedev DS, Fedorova TA, Tsimbal MV, Steinberg NV, Moiseenko GA Влияние однократной процедуры комбинированной микрополяризации на вегетативную регуляцию и сенсорно-моторные реакции И. Б. Сиваченко, Д. С. Медведев, Т. А. Фёдорова, М. В. Цимбал, Н. В. Штейнберг, Г. А. Моисеенко	
ORIGINAL RESEARCH	40
<hr/>	
Antimicrobial and antiviral activity of three-component complex of chlorhexidine-EDTA-zinc Galinkin VA, Enikeev AKh, Podolskaya EP, Gladchuk AS, Vinogradova TI, Zabolotnykh NV, Dogonadze MZ, Krasnov KA Антимикробная и вирулицидная активность трехкомпонентного комплекса хлоргексидин-ЭДТА-цинк В. А. Галынкин, А. Х. Еникеев, Е. П. Подольская, А. С. Гладчук, Т. И. Виноградова, Н. В. Заболотных, М. З. Догондзе, К. А. Краснов	
ORIGINAL RESEARCH	47
<hr/>	
Modelling myeloablative cytostatic therapy with cyclophosphamide is accompanied by gastrointestinal stasis in rats Schäfer TV, Ivnitsky JuJu, Rejniuk VL Моделирование миелоабляционной цитостатической терапии циклофосфаном сопровождается желудочно-кишечным стазом у крыс Т. В. Шефер, Ю. Ю. Ивницкий, В. Л. Рейнюк	

Detection of ultra-low concentrations of bromodihydrochlorophenylbenzodiazepine (phenazepam) and its metabolites in biological objects

Volkova AA, Kalekin RA, Moskaleva NE, Astashkina OG, Orlova AM, Markin PA

Обнаружение бромдигидрохлорфенилбензодиазепамина (феназепама) и его метаболита в биологическом объекте при сверхнизких концентрациях

А. А. Волкова, Р. А. Калёкин, Н. Е. Москалева, О. Г. Асташкина, А. М. Орлова, П. А. Маркин

Hepatitis B, C and TTV virus infection in highly trained athletes

Melnikova LI, Kozhanova TV, Ilchenko LYU, Morozov IA, Soboleva NV, Nguyen Thi-Hanh, Kruglova IV, Gordeychuk IV

Инфицированность вирусами гепатитов В, С и ТТВ высококвалифицированных спортсменов

Л. И. Мельникова, Т. В. Кожанова, Л. Ю. Ильченко, И. А. Морозов, Н. В. Соболева, Nguyen Thi-Hanh, И. В. Круглова, И. В. Гордейчук

Focal laser photocoagulation of the optic disc peripapillary neovascularization in patient with proliferative diabetic retinopathy

Takhchidi KhP, Takhchidi NKH, Kasminina TA, Tebina EP

Фокальная лазерная коагуляция перипапиллярной неоваскуляризации диска зрительного нерва при пролиферативной диабетической ретинопатии

Х. П. Тахчиди, Н. Х. Тахчиди, Т. А. Касминина, Е. П. Тебина

DEVELOPMENT OF PCR TEST FOR DETECTION OF THE SARS-COV-2 GENETIC VARIANTS ALPHA, BETA, GAMMA, DELTA

Shipulin GA, Savochkina YuA, Shuryaeva AK , Shivyagina EE, Nosova AO, Davydova EE, Luparev AR, Malova TV, Yudin SM


Centre for Strategic Planning and Management of Biomedical Health Risks of Federal Medical Biological Agency, Moscow, Russia

The emergence of novel SARS-CoV-2 genetic variants with increased transmissivity and reduced antibody neutralization efficiency is a threat to global public health. Reverse transcription polymerase chain reaction (RT-PCR) with the use of fluorescent probes, which make it possible to detect the single nucleotide substitutions, is a technique suitable for screening the SARS-CoV-2 RNA-containing samples for the already known functionally significant mutations in the S-gene, identification of which allows to define and differentiate the most epidemiologically significant genetic variants. The study was aimed to develop an assay for the large-scale monitoring of the spread of the SARS-CoV-2 top-priority variants. Based on the whole-genome alignment of the SARS-CoV-2 sequences, deposited in the GISAID database, primers and LNA-modified probes were selected to detect mutations in the S gene, typical for the Alpha, Beta/Gamma and Delta variants of concern (VOC). The developed reagent kit for detection of the key mutations in the SARS-CoV-2 S gene by the real time RT-PCR has good analytical and diagnostic characteristics and was authorized as a medical device (reagent) for *in vitro* use. The results of detecting the VOC and the key mutations with the use of the developed reagent kit were consistent with the data of the whole genome sequencing of 1,500 SARS-CoV-2 RNA samples. The developed reagent kit and the subsequent SARS-CoV-2 RNA sequencing assay used to perform the epidemiological monitoring of SARS-CoV-2 variants made it possible to promptly report the emergence of the Delta genetic variant in Russia, and to trace the dynamic changes in the prevalence of Delta in Moscow Region in April–September 2021.

Keywords: coronavirus, COVID-19, SARS-CoV-2, N501Y, P681H, 69-70del, E484K, B.1.1.7, B.1.351, P.1, VOC

Author contribution: Shipulin GA, Savochkina YuA, Davydova EE, Yudin SM — planning the experiment; Shipulin GA, Savochkina YuA, Yudin SM — literature analysis; Shuryaeva AK, Shivyagina EE, Nosova AO, Luparev AR, Malova TV — experimental procedure, data interpretation; Savochkina YuA, Shivyagina EE, Nosova AO — reagent kit development; Luparev AR — statistical analysis; Shipulin GA, Shuryaeva AK — manuscript writing and editing; Davydova EE, Yudin SM — manuscript editing.

Compliance with ethical standards: the study was performed in accordance with the requirements of the Declaration of Helsinki and GOST R ISO 14155-2014.

 **Correspondence should be addressed:** Anna K. Shuryaeva
Pogodinskaya, 10, str. 1, 119121, Moscow; ashuryaeva@cspmz.ru

Received: 15.12.2021 **Accepted:** 13.01.2022 **Published online:** 09.02.2022

DOI: 10.47183/mes.2022.003

РАЗРАБОТКА ПЦР-ТЕСТА ДЛЯ ВЫЯВЛЕНИЯ ГЕНЕТИЧЕСКИХ ВАРИАНТОВ АЛЬФА, БЕТА, ГАММА, ДЕЛЬТА ВИРУСА SARS-COV-2

Г. А. Шипулин, Ю. А. Савочкина, А. К. Шуряева , Е. Е. Шивлягина, А. О. Носова, Е. Е. Давыдова, А. Р. Лупарев, Т. В. Малова, С. М. Юдин


Центр стратегического планирования и управления медико-биологическими рисками здоровья Федерального медико-биологического агентства, г. Москва, Россия

Возникновение новых вариантов коронавируса SARS-CoV-2, обладающих повышенной трансмиссивностью и снижающих эффективность его нейтрализации выработанными ранее антителами, представляет угрозу для здоровья населения во всем мире. Метод полимеразной цепной реакции с обратной транскрипцией (ОТ-ПЦР) с флуоресцентными зондами, позволяющими детектировать единичные нуклеотидные замены, подходит для скрининга содержащих РНК SARS-CoV-2 образцов на наличие уже известных мутаций в S-гене, которые имеют функциональное значение, и выявление которых позволяет определять и дифференцировать геноварианты, имеющие наибольшее эпидемиологическое значение. Целью настоящей работы было разработать набор реагентов и методику для оперативного мониторинга распространения приоритетно значимых вариантов SARS-CoV-2. На основе выравнивания полногеномных последовательностей SARS-CoV-2, опубликованных в базе данных GISAID, были выбраны праймеры и LNA-модифицированные зонды для выявления мутаций в S-гене, характерных для генетических линий альфа, бета/гамма и дельта особой эпидемиологической значимости (VOC). Разработан и зарегистрирован набор реагентов в формате ОТ-ПЦР в реальном времени для выявления наиболее значимых мутаций в S-гене SARS-CoV-2, продемонстрированы его высокие аналитические и диагностические характеристики. Показано соответствие результатов выявления линий VOC и их основных мутаций разработанным набором с данными полногеномного секвенирования для 1500 образцов РНК SARS-CoV-2. Применение набора реагентов в сочетании с последующим секвенированием РНК SARS-CoV-2 в рамках проведения эпидемиологического мониторинга позволило оперативно установить факт появления на территории России геноварианта дельта и в дальнейшем отследить динамику изменения его распространенности в Московском регионе в период с апреля по сентябрь 2021 г.

Ключевые слова: коронавирус, COVID-19, SARS-CoV-2, N501Y, P681H, 69-70del, E484K, B.1.1.7, B.1.351, P.1, изоляты особой эпидемиологической значимости

Вклад авторов: Г. А. Шипулин, Ю. А. Савочкина, Е. Е. Давыдова, С. М. Юдин — планирование эксперимента; Г. А. Шипулин, Ю. А. Савочкина, С. М. Юдин — анализ литературы; А. К. Шуряева, Е. Е. Шивлягина, А. О. Носова, А. Р. Лупарев, Т. В. Малова — постановка эксперимента и интерпретация результатов; Ю. А. Савочкина, Е. Е. Шивлягина, А. О. Носова — разработка набора реагентов; А. Р. Лупарев — статистический анализ; Г. А. Шипулин, А. К. Шуряева — написание и редактирование рукописи; Е. Е. Давыдова, С. М. Юдин — редактирование рукописи.

Соблюдение этических стандартов: исследование проведено в соответствии с требованиями Хельсинкской декларации и ГОСТ Р ИСО 14155-2014.

 **Для корреспонденции:** Анна Константиновна Шуряева
ул. Погодинская, д. 10, стр. 1, 119121, г. Москва; ashuryaeva@cspmz.ru

Статья получена: 15.12.2021 **Статья принята к печати:** 13.01.2022 **Опубликована онлайн:** 09.02.2022

DOI: 10.47183/mes.2022.003

A novel coronavirus, causing the dangerous respiratory disease in humans, COVID-19, was found at the end of the year 2019 in China. After the whole genome sequencing the virus was classified as a betacoronavirus and referred to as SARS-CoV-2 [1–3]. High mutagenic capability of coronaviruses is well known [4]. The majority of emerging mutations do not affect the properties of the virus, however, some mutations can result in functional alterations, including fast viral spread and/or more severe illness.

Since the start of SARS-CoV-2 pandemic, a large number of genome sequences were published in the GISAID database [5], which made it possible to trace both the viral spread and the emergence of mutations in the viral genome.

In December 2020, British authorities declared a rapid increase in the number of COVID-19 cases. The sharp spike in morbidity was caused by the novel SARS-CoV-2 coronavirus genetic variant, which differed from the reference genome. This variant carried mutations in the gene encoding the S protein [6, 7]. Based on the phylogenetic analysis, the new British lineage of SARS-CoV-2 was named B.1.1.7 and classified as a variant of concern (VOC). The B.1.1.7 variant has a number of typical mutations in the spike protein, such as N501Y, A570D, D614G, and P681H, as well as amino acid deletions 69-70 and 144Y [8, 9]. Simultaneously, one more epidemiologically significant lineage was detected, which caused the outbreak in various provinces of the Republic of South Africa. This lineage is known as B.1.351. The South African strain contains nine spike mutations in addition to D614G, including the mutation cluster (for example, 242–244del and R246I) in the spike protein N-terminal domain (NTD), three mutations (K417N, E484K and N501Y) in the receptor binding domain (RBD), and one mutation (A701V) located close to the furin cleavage site [10, 11]. In January 2021, experts of the National Institute of Infectious Diseases, Japan, discovered a novel SARS-CoV-2 variant, the P.1 lineage, the isolates of which were identified in tourists coming from Brazil. Some mutations present in the Brazilian strain were previously discovered in the British and South African variants. This isolate contains 12 mutations in the spike protein, including N501Y and E484K [12]. Later the discussed above coronavirus genetic lineages were named using the letters of the Greek alphabet in accordance with the nomenclature, introduced by the WHO: Alpha (B.1.1.7 and subvariants Q.1–Q.8), Beta (B.1.351), Gamma (P.1). All three SARS-CoV-2 genetic variants listed above are considered the variants of concern (VOC) by the WHO and ECDC, and circulate all over the world [6].

In the spring of 2021 in India the new SARS-CoV-2 lineage B.1.617.2 was discovered, which spread rapidly and gave rise to the new wave of the pandemic, with the sharp rise in the incidence rate and the number of deaths in India and then in other countries in different parts of the world. Along with some closely related genetic lineages identified most recently, AY.1 and AY.2-124, the B.1.617.2 lineage contains the following typical mutations in the S protein: T19R, E156G, del157/158, L452R, T478K, D614G, P681R, and D950N, including mutations in the RBD [13]. Lineages B.1.617.2 and AY.1-124 are classified as the variants of concern, and are referred to as Delta in accordance with the WHO classification.

According to a number of reports, mutation N501Y in the S gene, found in the genomes of tree discussed above VOC out of four, affects the S protein-ACE2 binding affinity, which may result in increased transmissibility [14–16]. The presence of mutation E484K can allow the virus escape from monoclonal antibodies produced in response to the previous infection with SARS-CoV-2 containing no such mutation, or in response to vaccination [17–19].

It was shown for individuals infected with the Alpha lineage, that the mean duration of the acute infection was longer compared to the values obtained for the strains of other lineages (13.3 days vs. 8.2 days, respectively) [20]. To date, there is no evidence that the SARS-CoV-2 Alpha genetic variant has the potential to escape from monoclonal antibodies, produced in response to vaccination [8, 21–23]. However, according to literature, the South African and Brazilian variants could reduce the efficacy of some vaccines against COVID-19 [7, 24]. Structural analysis of the RBD mutation L452R and the P681R mutation, located in the furin cleavage site, has shown that these mutations may help to increase the efficacy of SARS-CoV-2 binding to the ACE2 receptor and the S1-S2 cleavage rate, thus contributing to the increased transmissibility. The presence of this mutation in RBD indicates the reduced binding with the selected monoclonal antibodies, and may affect their neutralization potency [13, 25].

Based on the foregoing, detection of various coronavirus variants and tracing the spread of the SARS-CoV-2 isolates, being the variants of utmost epidemiological significance, is an important challenge.

Currently, viral genome sequencing is the most common technique, allowing one to discover the rapidly emerging SARS-CoV-2 variants. However, studies involving the use of genome sequencing are expensive and time-consuming. Moreover, the method is also limited by the more stringent requirements to viral load in the sample compared to PCR. Reverse transcription polymerase chain reaction (RT-PCR) is a method, which enables screening the samples containing the SARS-CoV-2 RNA for the already known functionally significant mutations in the S gene of coronavirus, identification of which allows one to define and differentiate the viral VOC of utmost epidemiological significance. The use of oligonucleotide probes with modified LNA nucleotides enables the successful differentiation of even single nucleotide substitutions in the assayed gene sequence [26]. RT-PCR is recommended to increase the output and performance of screening for the top-priority genetic variants by the guidelines on the detection and identification of SARS-CoV-2 variants, issued by the experts of the WHO and ECDC [27]. There are reagent kits of foreign production for detection of important mutations in the gene encoding the S protein by RT-PCR. For example, reagent kit, manufactured by the Korean company PowerChek, identifies mutations, typical for the lineages Delta, Alpha, Beta, and Gamma, and the kit, produced by the French company ID, detects mutations L452R, E484K, and E484Q. In Russia only the reagent kits for detection of mutations typical for the Alpha lineage have been registered (manufactured by the Central Research Institute of Epidemiology and DNA-Technology LLC), the other lineages are not covered.

Thus, the development of the domestic reagent kit for the timely monitoring of the top-priority SARS-CoV-2 variants spread is extremely relevant. For this purpose we have developed the RT-PCR-based method and the reagent kit for detection of the range of mutations in the S gene of coronavirus, typical for four genetic variants of utmost epidemiological significance, as well as for detection of RNA of the SARS-CoV-2 variants Delta, Alpha, and Beta/Gamma (without differentiation between the latter) by identification of the relevant combination of key mutations. The study was aimed to develop the reagent kit allowing one to identify mutations N501Y, P681H and the deletion 69-70del, the combination of which is typical for the SARS-CoV-2 Alpha genetic lineage, mutation E484K, which in combination with the mutation N501Y is typical for the Beta and Gamma lineages, mutations P681R and L452R, the

Table. The RNA targets with corresponding fluorescent probes to be detected for each RT-PCR mixture of the kit

Dye of fluorescent probe	RNA target to be detected		
	FAM	JOE	ROX
2-A	mutation N501Y in the S gene of SARS-CoV-2	fragment of codon 501 of the S gene of SARS-CoV-2 with no mutation N501Y	deletion 69-70del in the S gene of SARS-CoV-2
2-B	fragment of codon 484 of the S gene of SARS-CoV-2 with no mutation E484K	mutation E484K in the S gene of SARS-CoV-2	mutation E484Q in the S gene of SARS-CoV-2
2-C	mutations P681H/R in the S gene of SARS-CoV-2	mutation L452R in the S gene of SARS-CoV-2	mutation P681R in the S gene of SARS-CoV-2

combination of which is typical for the Delta lineage, as well as to detect the presence of each of the listed above mutations. The kit may be used as a monitoring tool enabling the prompt acquisition of data on the dynamic changes in the spread of the top-priority SARS-CoV-2 strains (or genetic variants), carrying the functionally significant mutations.

METHODS

Design of oligonucleotides for amplification of the S gene target regions

The whole genome alignment of the SARS-CoV-2 sequences, deposited in the GISAID database (accessed 05.10.2021), was used to select the diagnostic primers and probes for detection of mutations, typical for the most epidemiologically significant SARS-CoV-2 genetic lineages. Based on the alignment data, regions carrying the relevant mutations were defined in the viral S gene, primers and LNA-modified probes were selected to detect the following mutations in the genome of the SARS-CoV-2 coronavirus: N501Y, deletions 69-70del, P681H and P681R, L452R, E484K, E484Q. Oligonucleotides were selected in accordance with the standard requirements for selection of primers and TaqMan probes [28, 29] with the use of the Oligo Calc [30] and OligoAnalyzer Tool [31] online resources. Thermodynamic properties and secondary structure of fluorescent probes were assessed using the Mfold Web Server [32]. Oligonucleotides were synthesized by the Genterra (Russia).

Clinical samples

Nasopharyngeal and oropharyngeal swabs (n = 10,297) were obtained at the Head Center for Hygiene and Epidemiology of the Federal Medical Biological Agency from patients with symptoms of ARVI from December 2020 to September 2021. Swab samples were collected in the test tubes, containing transport medium (Central Research Institute of Epidemiology; Russia), and stored at a temperature of -70 °C before testing.

RNA extraction

RNA was extracted using the AmpliTest RIBO-prep kit (FSBI SPC FMBA; Russia) in accordance with the manufacturer's guidelines. RNA was eluted in 50 µl of RNA elution buffer. RNA samples were stored at a temperature not exceeding -70 °C before using.

RT-PCR

Multiplex RT-PCR was carried out in accordance with the instructions. In addition to RNA samples, each test included the positive control samples (PCS) A, B, C, PCS W for the wild type, and the negative control.

Each sample was tested for the presence of mutations, typical for the VOC Alpha, Delta, Beta/Gamma, in three test tubes, containing mixtures 2-A, 2-B, and 2-C. Fluorescence signal accumulation curves for three different channels were analyzed (Table). The volume of RNA solution to be tested was 10 µl.

Amplification program included the following thermal cycling steps: 50 °C — 15 min, 95 °C — 15 min. The following steps were repeated in 45 cycles: 95 °C — 15 s, 60 °C — 30 s, 72 °C — 15 s.

The AmpliTest SARS-CoV-2 VOC v.2 reagent kit was optimized using the Rotor-Gene Q (Qiagen; Germany), CFX96 (Bio-Rad Laboratories; USA), and DTprime (DNA-Technology; Russia) systems.

Positive control samples (PCS)

The mixture of recombinant plasmids containing the amplified target S-gene fragments, being the targets of the selected primers and probes, was used as a PCS.

The PCR products were purified using the MiniElute Gel Extraction Kit (Qiagen; Germany), ligated into the pGEM-T plasmid vector (Promega; USA), and transformed in *Escherichia coli*. Recombinant plasmids of individual clones were purified using the Plasmid Miniprep Kit (Axygen; USA). The PCS nucleotide sequences were confirmed by Sanger sequencing (cycle sequencing) using the ABI PRISM Big Dye v.3.1 kit (Thermo Fisher Scientific; USA) in accordance with the manufacturer's guidelines, and the Applied Biosystems Sanger Sequencing 3500 Series Genetic Analyzer (Thermo Fisher Scientific; USA). The forward and reverse PCR primers, flanking the fragment to be amplified, were used for sequencing.

The sequencing reaction was carried out in 5 µL of reaction mixture in the 0.2 mL thin wall microtubes. The reaction mixture contained 0.8 µL of specific primer (forward or reverse) with a concentration of 1 µM and 1 µL of the Ready Reaction BigDye Terminator v3.1 mixture (Thermo Fisher Scientific; USA). The components were mixed carefully, and thermal cycling was performed in the SimpliAmp VeriFlex 96 thermal cycler (Thermo Fisher Scientific; USA) in accordance with the following program: initial denaturation 2 min at 95 °C, then 45 cycles (denaturation 20 s at 95 °C, primer annealing 30 s at 60 °C, elongation 1 min at 68 °C). Capillary electrophoresis was performed in the Applied Biosystems Sanger Sequencing 3500 Genetic Analyzer (Thermo Fisher Scientific; USA) after the sample purification of excess dideoxynucleotides and salts.

Four PCSs were developed for the reagent kit: PCS A, containing the fragment of the SARS-CoV-2 S-gene codon 501 carrying the mutation N501Y, and the S-gene fragment carrying the deletion 69-70del; PCS B, containing the mixture of recombinant plasmids with the fragments of the SARS-CoV-2 S-gene codon 484 carrying mutations E484K and E484Q; PCS C, containing plasmids carrying mutations P681H, L452R

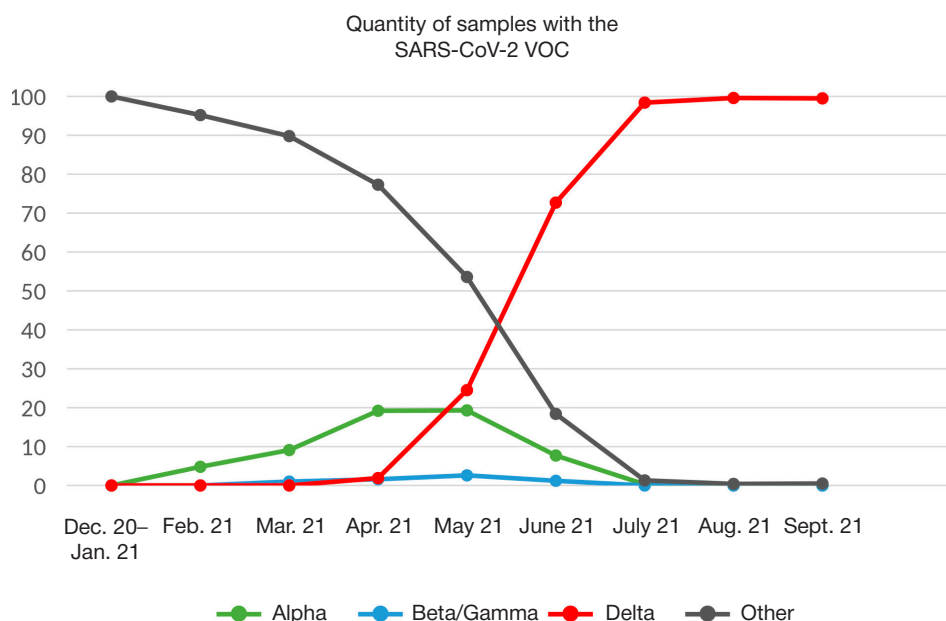


Fig. The results for the SARS-CoV-2 VOC spread monitoring performed from December 2020 to September 2021. The samples (total $n = 10,297$) were collected in Moscow and Moscow Region

and P681R in the SARS-CoV-2 S gene; PCS W, containing plasmids with the fragments of the SARS-CoV-2 S-gene codons 484 and 501 with no mutations N501Y and E484K.

The concentration of each PCS was measured by Droplet Digital PCR (ddPCR) with the use of the QX200 Droplet Digital PCR System (Bio-Rad Laboratories; USA). PCSs were introduced at the stage of RT-PCR as the separate samples.

Analytical sensitivity and specificity

To assess the analytical sensitivity, we used the SARS-CoV-2 RNA samples, obtained by extraction from biomaterial (smears from the mucous membrane of nasopharynx and oropharynx), which were studied using the diagnostic system developed in order to identify the minimum dilution, at which the samples were detected as positive. The concentration of each sample was previously measured by ddPCR using the QX200 Droplet Digital PCR System (Bio-Rad Laboratories; USA). The sensitivity threshold was defined based on the minimum dilution detected in three iterations.

To assess the analytical specificity of the reagent kit, we used RNA of the SARS-CoV-2 strain No. GK2020/1 from the collection of the N. F. Gamaleya National Research Center, as well as RNA of the strains of coronaviruses HCoV 229E, HCoV OC43, HCoV NI63, SARS-CoV HKU39849, MERS-CoV (European Virus Archive Global 011N-03868 — Coronavirus RNA specificity panel), strains of influenza A virus (H1N1) (ATCC VR-1469), influenza A virus (H3N2) (ATCC VR-776) and influenza B virus (Victoria Lineage) (ATCC VR-1930) from the American Type Culture Collection (ATCC; USA), strains of *Streptococcus pneumoniae* (№ 131116), *Streptococcus pyogenes* (№ 130001), *Haemophilus influenzae* (№ 151221), *Staphylococcus aureus* (№ 201108), *Klebsiella pneumoniae* from the collection of pathogenic microorganisms of the Scientific Centre for Expert Evaluation of Medicinal Products of the Ministry of Health of the Russian Federation, strains of human parainfluenza viruses types 1, 2, 3, human rhinoviruses types 13, 17, 26 from the State Collection of the Smorodintsev Research Institute of Influenza in a concentration not less than 1×10^6 GE/mL.

Whole genome sequencing (WGS)

Whole genome sequencing (WGS) was used as a reference method for identification of mutations in the RNA samples.

Samples with the cycle threshold (Ct) in RT-PCR not exceeding 25 were used for sequencing. Reverse transcription of the RNA samples was performed using the Reverta-L reagent kit (Centre for Strategic Planning of FMBA; Russia). The resulting cDNA was amplified using the AmpliSeq for Illumina SARS-CoV-2 Research Panel (Illumina; USA), containing 247 amplicons in two pools, which covered the entire SARS-CoV-2 genome. Libraries for the high-throughput sequencing were prepared using the AmpliSeq Library PLUS kit (Illumina; USA). The quality of libraries was evaluated by capillary electrophoresis with the Agilent Bioanalyzer 2100 (Agilent; USA). The library concentrations were measured with the Qubit 4 Fluorometer (Thermo Fisher Scientific; USA) using the HS Qubit dsDNA reagent kit (Thermo Fisher Scientific; USA). Sequencing was carried out with the use of the Illumina NextSeq 550 system (Illumina; USA) and the NextSeq 500/550 v2.5 kit (300 cycles) (Illumina; USA). All the procedures were carried out in accordance with the guidelines, issued by the manufacturers.

Statistical analysis

The diagnostic sensitivity (percentage of positive test results in the group of positive samples) was calculated as $A/(A+B) \times 100\%$, and the diagnostic specificity (percentage of negative test results in the group of negative samples) was calculated as $A/(A+B) \times 100\%$, where B was the number of assayed samples, which tested positive using the kit, of the total number of samples, and A was the number of assayed samples, which tested negative using the kit, of the total number of samples with the true positive results. The 95% confidence intervals for the diagnostic characteristics were calculated by the Clopper-Pearson method.

RESULTS

When developing the reagent kit, we have selected the SARS-CoV-2 S-gene regions, flanking mutations, typical for the

SARS-CoV-2 genetic lineages Alpha, Beta/Gamma, and Delta, to be the targets. We have selected primers and probes for identification of mutations N501Y, P681H and the deletion 69–70del, the combination of which is typical for the SARS-CoV-2 Alpha genetic lineage (B.1.1.7), mutations P681R and L452R, the combination of which is typical for the Delta genetic lineage (B.1.617.2 and all the AY variants), mutation E484K, which in combination with N501Y is typical for the Beta and Gamma genetic lineages (B.1.351/P.1, these variants have not been differentiated).

The reagent kit has been developed in the format of using three RT-PCR mixtures for analysis. Each mixture enables the detection of three markers, involving registration in three different fluorescence channels. In addition to the key mutations in the S gene, the range of genetic markers, identified using the kit, includes two codons, E484 and N501, matching with the reference SARS-CoV-2 RNA sequence. These serve as endogenous controls for the exclusion of false positive results.

The samples of all the listed above viruses and bacteria were tested in order to define the analytical specificity, no false positive results were obtained. When assaying RNA of the SARS-CoV-2 strain No. GK2020/1 from the collection of the N. F. Gamaleya National Research Center using the kit, no mutations were found in the codons 501, 484, 681, and 69–70 of the SARS-CoV-2 S gene, the results corresponded to the whole genome nucleotide sequence of this isolate, deposited in the GISAID database (EPI_ISL_421275). The following result was obtained for all samples containing no SARS-CoV-2 RNA: the samples have no SARS-CoV-2 RNA for analysis.

To assess the analytical sensitivity, we used the biomaterial samples with the known concentration of the SARS-CoV-2 viral RNA, defined by ddPCR. The genetic variants were reproducibly detected up to the SARS-CoV-2 RNA concentration of 1×10^3 copies/mL, which defined the analytical sensitivity of the reagent kit.

The diagnostic characteristics of the reagent kit developed were assessed in the clinical trial, involving studying the SARS-CoV-2 RNA samples with genotypes defined by WGS or Sanger sequencing of the S gene. To assess the diagnostic sensitivity, a total of 192 nasopharyngeal and oropharyngeal swab samples were analyzed, including 32 samples containing the SARS-CoV-2 RNA with a combination of mutations in the S gene, characteristic of the Alpha genetic lineage (B.1.1.7), 28 samples containing the SARS-CoV-2 RNA with a combination of mutations, characteristic of the Beta/Gamma genetic lineages (B.1.351/P1), 50 samples containing the SARS-CoV-2 RNA of the Delta genetic lineage (B.1.617.2 and all the AY variants). To assess the diagnostic specificity, a total of 82 RNA samples obtained from nasopharyngeal and oropharyngeal swabs were analyzed, which contained the SARS-CoV-2 RNA with no mutations under analysis. All the target mutations and their combinations, corresponding to the Delta, Alpha or Beta/Gamma genetic lineages, were identified in all samples. No discordant (nonspecific) results were registered. Thus, the diagnostic sensitivity (DS) of 100% was defined (DS with the 95% level of confidence was 94.2–100% for the Delta lineage, 91.1–100% for the Alpha lineage, 89.9–100% for the Beta/Gamma lineages). The diagnostic specificity was 100% (with 95% level of confidence it was 96.4–100%).

The further practical use of the reagent kit showed full compliance of VOC and their key mutations' identification results with the results of WGS performed in 1500 samples of viral RNA of the genetic lineages Alpha, Beta, Gamma, and others (collected from March to May 2021), as well as Delta (collected from June to August 2021). All the samples carried

the relevant combinations of mutations in the S gene, based on which the following SARS-CoV-2 genetic lineages were defined: Delta ($n = 750$), Alpha ($n = 302$), Beta/Gamma ($n = 32$), and others ($n = 416$). The RT-PCR results were completely matched with the data of WGS, so high diagnostic performance of the reagent kit was shown.

From December 1, 2020 to September 30, 2021 more than 10,000 clinical samples of the SARS-CoV-2 RNA were tested, collected in Moscow and Moscow Region within the framework of monitoring the spread of the SARS-CoV-2 VOC. The findings were split per month and presented as a percentage of the variants identified (Fig.). During the studied period (December 2020 to September 2021) we observed the emergence of VOC or single functionally significant mutations and their subsequent replacement by the novel SARS-CoV-2 virus variants. Thus, in the samples, obtained from December 2020 to January 2021, no isolates were found carrying mutations, typical for VOC. During the period the gradual increase in the proportion of distinct lineages was observed. In five months the proportion of the SARS-CoV-2 Beta/Gamma lineages samples changed from 0 to 1.6%, and the proportion of samples belonging to the Alpha lineage increased from 0 to 19.2%. The proportion of the Delta variant rose rapidly to 25% by the end of May, reached 87% by mid-June 2021, exceeded 95% in the first week of July, and was above 99% during the next months until the end of the studied period.

DISCUSSION

The emergence of the novel SARS-CoV-2 variants remains a grave worldwide concern, since the new variants can have the potential of higher transmissibility, affect the disease duration and severity, reduce the vaccine efficacy, and increase the mortality rate [6, 7, 14–20, 24].

Currently, WGS is the most widely used versatile method for identification of the new SARS-CoV-2 variants. Unfortunately, the method is very time-consuming and expensive. RT-PCR is an efficient alternative method, suitable for identification of the previously defined mutations, the markers of the key lineages, the detection of which is important for monitoring the spread of the genetic variants, and understanding the epidemiological situation.

The outcome of the study is the real time RT-PCR diagnostic test system for identification of the functionally significant mutations allowing one to define the SARS-CoV-2 VOC. The analysis includes the following steps: RNA extraction, RNA reverse transcription, cDNA amplification with the real time fluorescence hybridization detection, and data interpretation.

The kit provided allows one to distinguish RNA of the SARS-CoV-2 Alpha, Beta/Gamma and Delta variants from the other genetic lineages based on the combinations of typical mutations. According to a number of studies [15–23], the presence of distinct mutations (E484K, N501Y, P681H, P681R), associated with different genetic variants of coronavirus, results in the functionally significant alterations in the S-protein structure, including those contributing to the increased transmissibility, reduced neutralization efficiency of antibodies, produced in response to infection with the earlier circulating variants of the virus or in response to vaccination. That is why the detection of individual mutations, without taking into account the combinations of mutations, is also of some epidemiological significance.

The kit shows high analytical sensitivity (1×10^3 copies/mL of the SARS-CoV-2 RNA) for each of the genetic variants to be detected, and 100% analytical specificity in the tested panel of

microorganisms. The diagnostic specificity with the 95% level of confidence is 94.2–100% for the Delta lineage, 91.1–100% for the Alpha lineage, 89.9–100% for the Beta/Gamma lineages, and the diagnostic specificity is 96.4–100% with the 95% level of confidence.

The use of the reagent kit developed within the framework of epidemiological monitoring made it possible to detect the emergence of the SARS-CoV-2 Delta variant in Moscow in April 2021 in a timely manner, and to report promptly the dramatic increase in the proportion of Delta strains among the SARS-CoV-2 variants, detected in the surveyed patients in Moscow Region. It is important to note that the emergence and further spread of the Delta variant in Russia have resulted in the almost complete substitution of the other coronavirus lineages.

References

1. Bogoch II, Watts A, Thomas-Bachli A, Huber C, Kraemer MUG, Khan K, et al. Pneumonia of unknown aetiology in Wuhan, China: potential for international spread via commercial air travel. *J Travel Med.* 2020; 27 (2): 1–3.
2. Hui DS, I Azhar E, Madani TA, Ntoumi F, Kock R, Dar O, et al. The continuing 2019-nCoV epidemic threat of novel coronaviruses to global health — The latest 2019 novel coronavirus outbreak in Wuhan, China. *Int J Infect Dis.* 2020; 91: 264–6.
3. Rothan HA, Byrareddy SN. The epidemiology and pathogenesis of coronavirus disease (COVID-19) outbreak. *J Autoimmun.* 2020 May; 109:102433.
4. Sánchez CM, Gebauer F, Suñé C, Mendez A, Dopazo J, Enjuanes L. Genetic evolution and tropism of transmissible gastroenteritis coronaviruses. *Virology.* 1992 Sep; 190 (1): 92–105.
5. GISAID EpiFlu™ Database. Available from: <http://www.GISAID.org>.
6. World Health Organization. Available from: <https://www.who.int>.
7. Luring AS, Hodcroft EB. Genetic variants of SARS-CoV-2 — What do they mean? *JAMA.* 2021; 325: 529–31.
8. CDC 2021. Emerging SARS-CoV-2 variants. Available from: <https://www.cdc.gov/coronavirus/2019-ncov/more/science-and-research/scientific-brief-emerging-variants.html>.
9. Grubaugh ND, Hodcroft EB, Fauver JR, Phelan AL, Cevik M. Public health actions to control new SARS-CoV-2 variants. *Cell.* 2021;184 (5): 1127–32.
10. Tegally H, Wilkinson E, Giovanetti M, Iranzadeh A, Fonseca V, Giandhari J, et al. Emergence and rapid spread of a new severe acute respiratory syndrome-related coronavirus 2 (SARS-CoV-2) lineage with multiple spike mutations in South Africa. *MedRxiv.* 2020; 12.21.20248640.
11. Nelson G, Buzko O, Spilman PR, Niazi K, Rabizadeh S, Soon-Shiong PR. Molecular dynamic simulation reveals E484K mutation enhances spike RBD-ACE2 affinity and the combination of E484K, K417N and N501Y mutations (501Y.V2 variant) induces conformational change greater than N501Y mutant alone, potentially resulting in an escape mutant. *bioRxiv.* 2021.01.13.426558.
12. National Institute of Infectious Diseases of JAPAN Brief report 12.01.2021. Available from: <https://www.niid.go.jp/niid/images/epi/corona/covid19-33-en-210112.pdf>.
13. Cherian S, Potdar V, Jadhav S, Yadav P, Gupta N, Das M, et al. Convergent evolution of SARS-CoV-2 spike mutations, L452R, E484Q and P681R, in the second wave of COVID-19 in Maharashtra, India. *Microorganisms.* 2021; 9 (7): 1542.
14. Lacobucci G. Covid-19: New UK variant may be linked to increased death rate, early data indicate. *BMJ.* 2021; 372: n230.
15. Santos JC, Passos GA. The high infectivity of SARS-CoV-2 B.1.1.7 is associated with increased interaction force between Spike-ACE2 caused by the viral N501Y mutation. *bioRxiv.* 2020.12.29.424708.
16. Davies NG, Abbott S, Barnard RC, Jarvis CI, Kucharski AJ, Munday JD, et al. Estimated transmissibility and impact of SARS-CoV-2 lineage B.1.1.7 in England. *Science.* 2021; 372 (6538): eabg3055.
17. Cele S, Gazy I, Jackson L, Hwa SH, Tegally H, Lustig G, et al. Escape of SARS-CoV-2 501Y.V2 from neutralization by convalescent plasma. *Nature.* 2021; 593 (7857): 142–6.
18. Wibmer CK, Ayres F, Hermanus T, Madzivhandila M, Kgagudi P, Oosthuysen B, et al. SARS-CoV-2 501Y.V2 escapes neutralization by South African COVID-19 donor plasma. *Nat Med.* 2021; 27: 622–5.
19. Garcia-Beltran WF, Lam EC, St Denis K, Nitido AD, Garcia ZH, Hauser BM, et al. Multiple SARS-CoV-2 variants escape neutralization by vaccine-induced humoral immunity. *Cell.* 2021; 184 (9): 2372–2383.e9.
20. Kissler S, Fauver JR, Mack C, Tai C, Breban MI, et al. Densely sampled viral trajectories suggest longer duration of acute infection with B.1.1.7 variant relative to non-B.1.1.7 SARS-CoV-2. Harvard University's DASH repository 2021. *medRxiv.* 2021.
21. Callaway E, Mallapaty S. Novavax offers first evidence that COVID vaccines protect people against variants. *Nature.* 2021; 590: 17.
22. Greaney AJ, Loes AN, Crawford KHD, Starr TN, Malone KD, Chu HY, et al. Comprehensive mapping of mutations to the SARS-CoV-2 receptor-binding domain that affect recognition by polyclonal human serum antibodies. *Cell Host Microbe.* 2021; 29 (3): 463–476.e6.
23. Wu K, Werner AP, Moliva JL, Koch M, Choi A, et al. mRNA-1273 vaccine induces neutralizing antibodies against spike mutants from global SARS-CoV-2 variants. *BioRxiv.* 2021. 01.25.427948.
24. Elbe S, Buckland-Merrett G. Data, disease and diplomacy: GISAID's innovative contribution to global health. *Global challenges (Hoboken, NJ).* 2017; 1: 33–46.
25. Starr TN, Greaney AJ, Hilton SK, Ellis D, Crawford KHD, Dingens AS, et al. Deep mutational scanning of SARS-CoV-2 receptor binding domain reveals constraints on folding and ACE2 binding. *Cell.* 2020; 182 (5): 1295–1310.e20.
26. You Y, Moreira BG, Behlke MA, Owczarzy R. Design of LNA probes that improve mismatch discrimination. *Nucleic Acids Res.* 2006; 34 (8): e60.
27. European Centre for Disease Prevention and Control, WHO Regional Office for Europe. Methods for the detection and identification of SARS-CoV-2 variants. 3 March 2021. ECDC and WHO Regional Office for Europe: Stockholm and Copenhagen. 2021.
28. Van Pelt-Verkuil E, van Belkum A, Hays JP. Principles and Technical Aspects of PCR Amplification. Springer Science & Business Media. 2008; 330 p.
29. Yuryev A. Methods in Molecular Biology: PCR Primer Design. Humana Press. 2007; 432 p.
30. Kibbe WA. OligoCalc: an online oligonucleotide properties calculator. *Nucleic Acids Res.* 2007. Available from: <http://biotools.nubic.northwestern.edu/OligoCalc.html>.
31. Integrated DNA Technologies. OligoAnalyzer Tool. Available from:

CONCLUSIONS

The highly sensitive, specific, and easy to use AmpliTest SARS-CoV-2 VOC v.2 reagent kit for identification of mutations in the S gene of coronavirus, typical for the Alpha, Beta/Gamma and Delta genetic lineages, by RT-PCR has been developed in the Centre for Strategic Planning of the Federal Medical Biological Agency. The kit was validated using the samples containing the coronavirus RNA with genotypes, determined by the SARS-CoV-2 genome sequencing. The PCR results showed a perfect match with the sequencing data. The use of the PCR reagent kit enables fast and efficient assessment of the spread of the coronavirus genetic variants, and immediately taking the appropriate anti-epidemic measures based on the data obtained.

<https://www.idtdna.com/pages/tools/oligoanalyzer>.

32. The mfold Web Server (Hosted by The RNA Institute, College

of Arts and Sciences). Available from: <http://unafold.rna.albany.edu/?q=mfold/DNA-Folding-Form>.

Литература

1. Bogoch II, Watts A, Thomas-Bachli A, Huber C, Kraemer MUG, Khan K, et al. Pneumonia of unknown aetiology in Wuhan, China: potential for international spread via commercial air travel. *J Travel Med.* 2020; 27 (2): 1–3.
2. Hui DS, I Azhar E, Madani TA, Ntoumi F, Kock R, Dar O, et al. The continuing 2019-nCoV epidemic threat of novel coronaviruses to global health — The latest 2019 novel coronavirus outbreak in Wuhan, China. *Int J Infect Dis.* 2020; 91: 264–6.
3. Rothan HA, Byrareddy SN. The epidemiology and pathogenesis of coronavirus disease (COVID-19) outbreak. *J Autoimmun.* 2020 May; 109:102433.
4. Sánchez CM, Gebauer F, Suñé C, Mendez A, Dopazo J, Enjuanes L. Genetic evolution and tropism of transmissible gastroenteritis coronaviruses. *Virology.* 1992 Sep; 190 (1): 92–105.
5. GISAID EpiFlu™ Database. Available from: <http://www.GISAID.org>.
6. World Health Organization. Available from: <https://www.who.int>.
7. Luring AS, Hodcroft EB. Genetic variants of SARS-CoV-2 — What do they mean? *JAMA.* 2021; 325: 529–31.
8. CDC 2021. Emerging SARS-CoV-2 variants. Available from: <https://www.cdc.gov/coronavirus/2019-ncov/more/science-and-research/scientific-brief-emerging-variants.html>.
9. Grubaugh ND, Hodcroft EB, Fauver JR, Phelan AL, Cevik M. Public health actions to control new SARS-CoV-2 variants. *Cell.* 2021;184 (5): 1127–32.
10. Tegally H, Wilkinson E, Giovanetti M, Iranzadeh A, Fonseca V, Giandhari J, et al. Emergence and rapid spread of a new severe acute respiratory syndrome-related coronavirus 2 (SARS-CoV-2) lineage with multiple spike mutations in South Africa. *MedRxiv.* 2020; 12.21.20248640.
11. Nelson G, Buzko O, Spilman PR, Niazi K, Rabizadeh S, Soon-Shiong PR. Molecular dynamic simulation reveals E484K mutation enhances spike RBD-ACE2 affinity and the combination of E484K, K417N and N501Y mutations (501Y.V2 variant) induces conformational change greater than N501Y mutant alone, potentially resulting in an escape mutant. *bioRxiv.* 2021.01.13.426558.
12. National Institute of Infectious Diseases of JAPAN Brief report 12.01.2021. Available from: <https://www.niid.go.jp/niid/images/epi/corona/covid19-33-en-210112.pdf>.
13. Cherian S, Potdar V, Jadhav S, Yadav P, Gupta N, Das M, et al. Convergent evolution of SARS-CoV-2 spike mutations, L452R, E484Q and P681R, in the second wave of COVID-19 in Maharashtra, India. *Microorganisms.* 2021; 9 (7): 1542.
14. Lacobucci G. Covid-19: New UK variant may be linked to increased death rate, early data indicate. *BMJ.* 2021; 372: n230.
15. Santos JC, Passos GA. The high infectivity of SARS-CoV-2 B.1.1.7 is associated with increased interaction force between Spike-ACE2 caused by the viral N501Y mutation. *bioRxiv.* 2020.12.29.424708.
16. Davies NG, Abbott S, Barnard RC, Jarvis CI, Kucharski AJ, Munday JD, et al. Estimated transmissibility and impact of SARS-CoV-2 lineage B.1.1.7 in England. *Science.* 2021; 372 (6538): eabg3055.
17. Cele S, Gazy I, Jackson L, Hwa SH, Tegally H, Lustig G, et al. Escape of SARS-CoV-2 501Y.V2 from neutralization by convalescent plasma. *Nature.* 2021; 593 (7857): 142–6.
18. Wibmer CK, Ayres F, Hermanus T, Madzivhandila M, Kgagudi P, Oosthuysen B, et al. SARS-CoV-2 501Y.V2 escapes neutralization by South African COVID-19 donor plasma. *Nat Med.* 2021; 27: 622–5.
19. Garcia-Beltran WF, Lam EC, St Denis K, Nitido AD, Garcia ZH, Hauser BM, et al. Multiple SARS-CoV-2 variants escape neutralization by vaccine-induced humoral immunity. *Cell.* 2021; 184 (9): 2372–2383.e9.
20. Kissler S, Fauver JR, Mack C, Tai C, Breban MI, et al. Densely sampled viral trajectories suggest longer duration of acute infection with B.1.1.7 variant relative to non-B.1.1.7 SARS-CoV-2. *Harvard University's DASH repository.* 2021.
21. Callaway E, Mallapaty S. Novavax offers first evidence that COVID vaccines protect people against variants. *Nature.* 2021; 590: 17.
22. Greaney AJ, Loes AN, Crawford KHD, Starr TN, Malone KD, Chu HY, et al. Comprehensive mapping of mutations to the SARS-CoV-2 receptor-binding domain that affect recognition by polyclonal human serum antibodies. *Cell Host Microbe.* 2021; 29 (3): 463–476.e6.
23. Wu K, Werner AP, Moliva JI, Koch M, Choi A, et al. mRNA-1273 vaccine induces neutralizing antibodies against spike mutants from global SARS-CoV-2 variants. *BioRxiv.* 2021. 01.25.427948.
24. Elbe S, Buckland-Merrett G. Data, disease and diplomacy: GISAID's innovative contribution to global health. *Global challenges (Hoboken, NJ).* 2017; 1: 33–46.
25. Starr TN, Greaney AJ, Hilton SK, Ellis D, Crawford KHD, Diggins AS, et al. Deep mutational scanning of SARS-CoV-2 receptor binding domain reveals constraints on folding and ACE2 binding. *Cell.* 2020; 182 (5): 1295–1310.e20.
26. You Y, Moreira BG, Behlke MA, Owczarzy R. Design of LNA probes that improve mismatch discrimination. *Nucleic Acids Res.* 2006; 34 (8): e60.
27. European Centre for Disease Prevention and Control, WHO Regional Office for Europe. Methods for the detection and identification of SARS-CoV-2 variants. 3 March 2021. ECDC and WHO Regional Office for Europe: Stockholm and Copenhagen. 2021.
28. Van Pelt-Verkuil E, van Belkum A, Hays JP. Principles and Technical Aspects of PCR Amplification. Springer Science & Business Media. 2008; 330 p.
29. Yuryev A. Methods in Molecular Biology: PCR Primer Design. Humana Press. 2007; 432 p.
30. Kibbe WA. OligoCalc: an online oligonucleotide properties calculator. *Nucleic Acids Res.* 2007. Available from: <http://biotools.nubic.northwestern.edu/OligoCalc.html>.
31. Integrated DNA Technologies. OligoAnalyzer Tool. Available from: <https://www.idtdna.com/pages/tools/oligoanalyzer>.
32. The mfold Web Server (Hosted by The RNA Institute, College of Arts and Sciences). Available from: <http://unafold.rna.albany.edu/?q=mfold/DNA-Folding-Form>.

LIVER DAMAGE IN PATIENTS WITH COVID-19

Vologzhanin DA^{1,2}, Golota AS¹ ✉, Kamilova TA¹, Makarenko SV^{1,2}, Scherbak SG^{1,2}¹ City Clinical Hospital No. 40 of the Kurortny District, Saint Petersburg, Russia² St Petersburg University, Saint Petersburg, Russia

The clinical spectrum of SARS-CoV-2 infection continues to expand, raising important fundamental issues regarding the SARS-CoV-2 cellular tropism and pathogenic mechanisms. Liver damage is observed in patients with all forms of COVID-19, especially severe and critical forms, which could be due to the direct viral damage, immune dysregulation (systemic inflammatory response and cytokine storm), hypoxia-ischemia, drug-induced hepatotoxicity, and concomitant chronic disorders. Liver damage, defined primarily by elevated transaminase levels, is often observed in patients with COVID-19 and correlates with clinical outcomes, including mortality. Diagnostic criteria, pathogenesis, clinical characteristics, treatment, and prognosis of liver injury in COVID-19 should be clarified in further clinical trials. Currently, there is a critical shortage of proven treatment options for patients with COVID-19, resulting in an urgent need to study the multiple organ failure and liver damage pathogenesis in patients with this disease. The review provides information about the pathophysiological mechanisms of the SARS-CoV-2-induced liver damage and the development of liver failure in COVID-19. Information sources were searched in the PubMed database using the keywords "liver damage in COVID-19" and "immune liver damage in COVID-19".

Keywords: coronavirus SARS-CoV-2, COVID-19, liver damage, systemic hepatotoxicity, immune liver damage, drug-induced hepatotoxicity, concomitant chronic liver disease

Author contribution: Golota AS, Kamilova TA — data search and analysis, manuscript writing; Vologzhanin DA, Makarenko SV, Scherbak SG — manuscript discussion and editing.

✉ **Correspondence should be addressed:** Aleksandr S. Golota
Borisova, 9, lit. B, 197706, Saint Petersburg, Russia; golotaa@yahoo.com

Received: 14.03.2022 **Accepted:** 27.03.2022 **Published online:** 31.03.2022

DOI: 10.47183/mes.2022.009

ПОРАЖЕНИЕ ПЕЧЕНИ У БОЛЬНЫХ COVID-19

Д. А. Вологжанин^{1,2}, А. С. Голота¹ ✉, Т. А. Камилова¹, С. В. Макаренко^{1,2}, С. Г. Щербак^{1,2}¹ Городская больница № 40 Курортного административного района, Санкт-Петербург, Россия² Санкт-Петербургский государственный университет, Санкт-Петербург, Россия

Спектр клинических проявлений инфекции SARS-CoV-2 продолжает расширяться, возникают важные фундаментальные вопросы, касающиеся ее клеточного тропизма и патогенетических механизмов. Повреждение печени происходит при всех формах COVID-19, особенно при тяжелых и крайне тяжелых, что может быть связано с прямым вирусным поражением, иммунной дисрегуляцией (системным воспалительным ответом и цитокиновым штормом), гипоксическим/ишемическим повреждением, лекарственной гепатотоксичностью и сопутствующими хроническими заболеваниями. Повреждение печени, определяемое в основном по повышению уровней трансаминаз, часто обнаруживают у пациентов с COVID-19, и оно коррелирует с клиническими исходами, включая смертность. Диагностические критерии, патогенез, клинические характеристики, лечение и прогноз поражения печени при COVID-19 должны быть уточнены в дальнейших клинических исследованиях. В настоящее время критически не хватает проверенных вариантов лечения пациентов с COVID-19, что приводит к неотложной необходимости изучения патогенеза полиорганной недостаточности и повреждения печени при этом заболевании. В обзоре представлена информация о патофизиологических механизмах повреждения печени коронавирусом SARS-CoV-2 и развитии печеночной недостаточности при COVID-19. Поиск источников информации проведен в базе данных PubMed по ключевым словам «liver damage in COVID-19» и «immune liver damage in COVID-19».

Ключевые слова: коронавирус SARS-CoV-2, COVID-19, повреждение печени, системная гепатотоксичность, иммунное повреждение печени, лекарственная гепатотоксичность, сопутствующее хроническое заболевание печени.

Вклад авторов: А. С. Голота, Т. А. Камилова — поисково-аналитическая работа, написание текста статьи; Д. А. Вологжанин, С. В. Макаренко, С. Г. Щербак — обсуждение и редактирование текста статьи.

✉ **Для корреспонденции:** Александр Сергеевич Голота
ул. Борисова, д. 9, лит. Б, 197706, г. Санкт-Петербург, Россия; golotaa@yahoo.com

Статья получена: 14.03.2022 **Статья принята к печати:** 27.03.2022 **Опубликована онлайн:** 31.03.2022

DOI: 10.47183/mes.2022.009

SARS-CoV-2 coronavirus is a respiratory pathogen causing COVID-19. Complications of COVID-19 affect almost all organs, including liver. Direct virus cytotoxicity, dysregulated immune responses, microcirculatory disorders and thrombosis contribute to the systemic toxicity in COVID-19. The diversity of the COVID-19 manifestations is associated with the broad organotropism of SARS-CoV-2.

SARS-CoV-2 infects cells by means of the multifunctional cellular receptor, ACE2 (angiotensin-converting enzyme-2), which is found on the cell membranes in all organs, including liver, and makes the tissue vulnerable to the coronavirus invasion. Cellular serine protease TMPRSS2 (transmembrane protease serine 2) is involved in the SARS-CoV-2 invasion,

contributing to the virus internalization into target cells [1]. ACE2 and TMPRSS2 are expressed in the cells of many tissues, including gastric glandular cells, enterocytes, hepatocytes, cholangiocytes, and endothelial cells [2, 3]. Elevated ACE2 expression in hepatocytes has been revealed in patients with liver fibrosis/cirrhosis [2, 4]. This finding is very important: concomitant liver disease may increase the SARS-CoV-2 liver tropism.

Hepatic dysfunction may influence the multisystem manifestations of COVID-19, such as acute respiratory distress syndrome (ARDS), coagulopathy, and multiple organ failure. Liver is the main human organ involved in metabolism and detoxification, that is why even a moderate decline in liver

function can alter the safety profiles and therapeutic efficacy of antiviral drugs metabolized in the liver [4].

Epidemiological data on liver injury in patients with COVID-19

The prevalence of liver injury in patients with severe COVID-19 (74.4%) is higher than in patients with the mild course of the disease (43.0%). Patients with severe COVID-19 admitted to an intensive care unit (ICU) had a more severe hepatic dysfunction compared to patients with the milder disease. The prevalence of elevated hepatic transaminase plasma levels in patients with COVID-19, which are particularly high in severe cases, reached 53% in survivors [5, 6] and 78% in the deceased [5]. Elevated serum levels of aspartate transaminase (AST) were observed in almost 18% of patients with mild COVID-19 and 56% of patients with severe disease; elevated levels of alanine aminotransferase (ALT) were found in almost 20% of patients with mild COVID-19 and 28% of patients with the severe disease. Elevated levels of cholestatic enzymes, alkaline phosphatase (ALP) and gamma glutamyltransferase (GGT), were observed in 6.1 and 21.1% of patients with COVID-19, respectively [7].

Elevated levels of transaminases and bilirubin and the reduced albumin concentration in patients with COVID-19 correlate with the length of hospital stay, risk of admission to ICU and 30-day mortality. In the majority of patients, transaminase levels are back to normal after recovery. The patients with persistently elevated transaminase levels are severely ill or have a chronic liver disease (CLD). Elevated levels of GGT and ALP in patients with COVID-19 are indicative of damage to the bile duct cells in the liver. Liver injury could be secondary to the bile duct cell damage, since there are no viral inclusions in the biopsy specimens taken from some patients, and the pathological changes manifest themselves in the form of microvascular steatosis and moderate lobular and portal inflammation. Furthermore, the extent of liver injury positively correlates with the infection severity [8].

According to systematic review with meta-analysis of 11 studies (793 patients), abnormally low serum albumin levels were found in 79% (40–99%) of patients [9]. When performing meta-analysis, only the baseline laboratory data obtained at admission were taken into account.

In general, hepatic dysfunction is typical for 76.3% of patients, and liver injury is typical for 21.5% of patients [10].

Mechanisms underlying liver damage in COVID-19

Pathogenesis of liver injury caused by COVID-19 have not been properly clarified, since the available data are scarce and contradictory. The mechanisms of hepatocellular injury are multifactorial and include direct viral damage, immune-mediated injury, hypoxia-ischemia, thrombosis, and drug-induced hepatotoxicity [8, 10].

Direct viral damage to the liver

Infection of hepatocytes with SARS-CoV-2, mediated by the ACE2 cellular receptor, results in the acute cytopathic liver injury and is associated with the high mortality [3]. Foci of periportal and centrilobular necrosis without significant inflammation are reported [11].

In addition to hepatocellular pattern of the liver enzyme level elevation, COVID-19-associated liver injury can manifest itself in the form of cholestatic pattern. ACE2 expression on the biliary epithelial cells results in the direct viral infection. Swelling of endothelium of the hepatic artery branches in the portal tract

together with luminal narrowing are observed, endophlebitis of the portal vein, endotheliitis, and blood clots in the branches of the portal vein emerge [12].

ACE2 expression on the majority of cholangiocytes (59.7% of cells) and a relatively weak expression on hepatocytes (2.6%; the average expression levels are 20 times lower than in cholangiocytes) suggest that SARS-CoV-2 contributes to liver injury, causing cholangiocyte dysfunction. SARS-CoV-2 infection decreased cell-cell tight junction between cholangiocytes and reduces their barrier function. Assessment of liver biopsy specimens in fatal cases has revealed coronavirus in the cytoplasm of hepatocytes. Considerable hepatocyte apoptosis in combination with the presence of the CD4 and CD8 T cells in the lobular and portal tracts is indicative of the direct liver infection with SARS-CoV-2. These data demonstrate the SARS-CoV-2 ability to infect hepatocytes, despite low ACE2 expression [10].

Immune-mediated liver injury

In the course of the SARS-CoV-2 infection, 80% of immune cells entering liver are represented by CD8 T cells. CD4 T cell infiltration correlates with B cell activation, and the levels of neutralizing antibodies against SARS-CoV-2 and pro-inflammatory cytokines (IL1 β , IL6 and TNF α), as well as the SARS-CoV-2 hepatic clearance [8]. IL6 is a factor of acute liver injury in patients with COVID-19, which induces liver sinusoidal endotheliopathy with neutrophil infiltration and a hypercoagulable phenotype [13]. The hypercoagulable and inflammatory phenotypes of the liver sinusoidal endothelial cells are considered the marker of endothelial damage and mortality predictor in patients with liver cirrhosis and COVID-19 [14].

Sudden deterioration of liver function at the advanced stage of the disease is associated with systemic inflammatory response, which can damage multiple organs, including liver. Moreover, patients with lymphocytopenia more often suffer from liver dysfunction [15]. Inflammatory changes, such as hepatocyte swelling and steatosis, liver sinus cell proliferation, Kupffer cell hyperplasia, and immune cell infiltration are found in liver cells of patients with severe COVID-19 [16].

Post-mortem examination of some patients with COVID-19 revealed cholestatic features, such as bile duct proliferation, portal inflammatory infiltrates, and, in a number of cases, canalicular/ductular bile plugs [17]. Cytokine storm typical for the SARS-CoV-2-associated viral sepsis could be the main contributing factor, since inflammatory cytokines IL6, TNF α and IL1 β could cause hepatocellular cholestasis. Persistent systemic IL6 signaling induced by the SARS-CoV-2 infection inhibits albumin synthesis. Hypoalbuminemia associated with the cytokine storm and cholestasis resulting from inhibition of hepatobiliary excretion could be considered part of the COVID-19 acute phase. IL6 provides strong mitogenic stimulation of cholangiocytes, which induce proliferative and pro-inflammatory phenotypes [4].

In those infected with SARS-CoV-2, elevated C-reactive protein (CRP) levels and lymphopenia are considered independent risk factors for liver injury [18]. Taking into account the fact that histopathological examination has revealed no signs of severe inflammatory liver injury [19], alterations in the levels of hepatic enzymes in patients with SARS-CoV-2 could be due to hepatitis being the secondary response to the SARS-CoV-2-induced systemic inflammation [10].

Hypoxic hepatitis

Hepatic sinus endothelial cells contribute to perfusion disorders, responding to inflammatory signals. Ischemia-reperfusion injury

in the liver could result in inflammation due to activation of Kupffer cells, neutrophils, and platelets. In the conditions of ischemia and hypoxia, inhibition of the cell survival signaling pathway in hepatocytes results in hepatocyte necrosis. In patients with ARDS, hypoxia induces oxidative stress, persistent elevation of the levels of reactive oxygen species, and secretion of pro-inflammatory substances that cause hepatocyte damage and necrosis [8].

Hypoxia is a typical sign of severe COVID-19 and the main regulator of hepatocellular ACE2 expression. This may explain the fact that extrapulmonary dissemination of SARS-CoV-2 is observed mainly in patients with ARDS and other hypoxic conditions. Gene expression analysis has shown that primary hepatocytes infected with SARS-CoV-2 are characterized by overexpression of pro-inflammatory cytokines together with inhibition of key metabolic processes. These data illustrate the comprehensive nature of liver injury in patients with COVID-19 and the mutual influence of multiple SARS-CoV-2-activated molecular pathways involved. Biliary ducts of patients with COVID-19 are subject to hypoxia due to respiratory failure (exacerbated by the peribiliary arterial plexus obliteration resulting from vasculitis/thrombogenesis). Thus, poor blood circulation and hypoxia, as well as continuous inflammatory stimulation, are the main triggers of damage to the bile duct epithelium in patients with severe COVID-19 [4].

Coagulation and thrombosis

Elevated levels of hypercoagulability markers, D-dimer, fibrinogen and factor FVIII, were found in 100, 74 and 100% of patients with the extremely severe COVID-19. Microvascular thrombosis may result in the end-stage liver disease. Autopsy has revealed infiltration of lymphocytes and monocytes in the portal area with sinus thrombosis and congestion; hepatocyte degeneration and lobular necrosis have been found in the liver [16]. These data show that in patients with COVID-19 hypercoagulation is one of the causes of liver damage.

Coronavirus therapy-induced hepatotoxicity

Drug-induced liver injury results in varying degree liver damage, observed in patients with COVID-19. Antiviral drugs (oseltamivir, abidor, lopinavir, and ritonavir), antibiotics, steroids and hormones which have side effects, including liver damage, are widely used in treatment of COVID-19. In particular, the use of lopinavir/ritonavir increases the likelihood of liver injury by 4 times. Liver metabolizes the majority of drugs for SARS-CoV-2. Elevated levels of ALT, ALP, bilirubin, and GGT, were observed in individuals infected with SARS-CoV-2, who were treated with lopinavir, ritonavir, and remdesivir [20].

Liver damage was more likely in patients who received medications of several types, and high-dose hormones. Liver injury disrupts metabolism and drug excretion and increases the antiviral drug toxicity. That is why great importance should be attached to the liver function monitoring, although in the majority of COVID-19 cases mild liver injury is observed, which is of a temporary nature and returns to normal without any specific treatment. Patients with severe liver injury need targeted hepatoprotective therapy. Treatment of the COVID-19-associated liver damage is based on inhibition of inflammation and correction of hypoxemia aimed at preventing the multiple organ dysfunction syndrome, as well as on one or two hepatoprotective drugs depending on the patient's liver dysfunction [15].

Hepatotoxic therapeutic agents include antiviral drugs that target the virus itself (remdesivir), IL6 and its effector

signaling pathways (tocilizumab and baricitinib), and systemic inflammation (dexamethasone) together with antibiotics and steroids.

The randomized clinical trials have shown that the combination of remdesivir, the antiviral drug used in treatment of SARS-CoV-2 infection, with baricitinib, the JAK protein kinase inhibitor, improve the COVID-19 outcomes compared with the use of remdesivir only [21].

Coformulated drug lopinavir/ritonavir can cause liver necrosis and suppress hepatocyte proliferation. The drug induces inflammation and exacerbates liver injury due to increased oxidative stress. Lopinavir/ritonavir administration results in 7-fold increase in the hepatic enzyme levels [20].

Dexamethasone reduces the levels of biomarkers of endothelial damage (angiopoietin-2, intercellular adhesion molecules ICAM-1 and sRAGE) and inflammation (CRP) [22].

The use of endogenous cytokines, interferons, released by cells in response to viral infection (including SARS-CoV-2), in treatment of COVID-19 in order to inhibit replication of the pathogen resulted in leukopenia, lymphopenia, hepatocyte injury, autoimmune hepatitis, and other severe side effects [8].

Baricitinib, the JAK-STAT signaling pathway inhibitor, affects hyperinflammatory status arising from the SARS-CoV-2 infection, and is capable of preventing endocytosis and viral infection. However, the drug increases the risk of thrombosis and leads to liver injury. The increasing number of the reported cases of liver damage, cholestasis and hepatitis developing in the considerable number of patients who received JAK inhibitors to treat COVID-19, attracts attention [23].

Tocilizumab, anti-IL-6 receptor monoclonal antibody, is used as part of combination therapy in severe COVID-19 cases. Tocilizumab therapy must be discontinued if the levels of hepatic enzymes exceed the upper limit of normal more than three times [8].

These data indicate that it is necessary to regularly monitor the hepatic enzyme levels during treatment of patients with COVID-19 in order to minimize the risk of complications [24].

Taking into account the increased risk of death from COVID-19 in patients with CLD, European Association for the Study of the Liver (EASL), American Association for the Study of Liver Diseases (AASLD), and Belgian Liver and Intestine Advisory Committee (BeLIAC) have recommended to give priority to vaccination against COVID-19 to patients with CLD and liver transplant recipients [25].

COVID-19-associated liver damage in patients with no concomitant chronic liver disease

Liver injury (predominantly hepatocellular rather than cholestatic) observed at admission correlates with clinical outcomes (ICU admission, mechanical ventilation, death). Patients having normal AST levels at admission and patients with abnormal levels of AST, ALT and ALP at peak hospitalization are at higher risk of mechanical ventilation [26]. Analysis of biopsy specimens has shown that the coronavirus-induced liver damage is the main cause of liver dysfunction in COVID-19 patients with no CLD. SARS-CoV-2 causes hepatic cytopathy with massive apoptosis and the presence of binuclear (less mature) hepatocytes being the predominant histological features [18, 27].

Among 900 COVID-19 patients, 28% had elevated levels of at least one hepatic enzyme [24]. Liver examination in patients with COVID-19 revealed endotheilitis [28] and fibrin microthrombi in hepatic sinusoids [29]. Liver study performed during autopsy revealed the dilated portal vein

and the increased number of the portal vein branches, partial thrombosis or complete obstruction of the portal and sinusoidal vessels, portal tract fibrosis, and microthrombi in hepatic sinusoids. None of these patients had CLD before or at admission to hospital. All liver specimens showed minimum signs of inflammation. Histopathological findings indicate a secondary nature of intrahepatic vasculature abnormalities to systemic changes caused by the virus [30].

Microvesicular steatosis is considered the main COVID-19-associated hepatocellular alteration. However, signs of liver damage, such as ground glass hepatocytes, fibrin aggregates in the sinusoidal lumen, sinusoidal dilatation and hepatocyte atrophy, dilated Disse spaces, and intrasinusoidal deposition of fibrin and red blood cells are also found in patients with no steatosis. Sinusoidal dilatation and Kupffer cell activation are the signs of thrombotic sinusoiditis. Intrahepatic vasculature abnormalities, including sinusoidal microthrombi, were found in the liver of 15% of patients who died from COVID-19: this was a marker of liver disease caused by SARS-CoV-2. A body of observations allows us to consider severe thrombotic sinusoiditis as a negative prognostic factor in patients with COVID-19 [17]. Liver injury can be also associated with the interaction between the intrahepatic cytotoxic T cells and Kupffer cells. Hypoxia and shock can cause ARDS, hypoxia/reperfusion-induced dysfunction, and hepatic ischemia. Indirect damage to the liver sinusoidal endothelium could result from systemic inflammation or iatrogenic causes (mechanic ventilation) [4].

Autopsy of the deceased COVID-19 patients' liver also revealed portal fibrosis accompanied by considerable pericyte activation. Liver autopsy performed in patients with COVID-19 revealed SARS-CoV-2 RNA in blood vessel lumens and endothelial cells of portal veins [30]. Inflammation mediated by endothelium is a possible mechanism of sustained liver injury, since endotheliopathy persists in patients with long COVID-19 [31].

Micro- and macrovesicular steatosis was observed when performing liver autopsy in patients with COVID-19, for whom SARS-CoV-2 infection was the only factor of liver damage. Microvesicular steatosis usually results from the genetic or acquired disorders of mitochondrial β -oxidation. In patients with COVID-19, SARS-CoV-2 affects mitochondrial activity and causes mitochondrial cristae abnormalities, thus worsening the liver metabolic status [18].

COVID-19-associated ARDS could be accompanied by the right ventricular dysfunction resulting in congestive hepatopathy due to elevated central venous pressure. In cases of sustained hemodynamic and/or respiratory failure hypoxia leads to hepatocyte death, defined as the centrilobular necrosis when performing histopathological examination. Furthermore, acute right-sided heart failure and the resulting hepatic congestion in patients with COVID-19 could be caused by hypercoagulation [4]. However, in the majority of cases, SARS-CoV-2-associated liver injury was mild and failed to meet the diagnostic criteria for hypoxic hepatitis even in patients admitted to ICU [7].

Coagulopathy characterized by elevated levels of D-dimer and fibrinogen is one of the features of COVID-19. Elevated levels of D-dimer are associated with severe COVID-19 and high mortality. High levels of D-dimer were found in almost all patients (96%) who died from severe COVID-19; elevated ALT levels were found in the majority of patients (62%), which pointed to the link between liver injury, hepatic vein thrombosis and coagulopathy. None of the patients had a history of CLD or portal hypertension [30]. Autopsy revealed the platelet-fibrin microthrombi in hepatic sinusoids and platelet aggregation in the portal vein in at least 50% of patients [30, 32].

In 86% of cases, autopsy of patients who died from severe COVID-19-associated pneumonia revealed moderate centrilobular necrosis associated with minimum portal or lobular inflammation; steatosis and cholestasis were found in 57% of cases, and in 36% of cases discrete proliferation of bile ducts was observed. Although most of patients were treated with drugs having low hepatotoxicity, hypoxia resulting from severe lung injury could reduce the tolerance of hepatocytes to toxic damage. The combination of hypoxia caused by severe pneumonia and drug toxicity was the most likely cause of liver injury in the deceased patients with COVID-19 [19].

The correlation between liver injury and COVID-19 severity has been confirmed [33]. Abnormal liver function test results at admission to hospital increase the risk of severe COVID-19-associated pneumonia [20]. The COVID-19 severity correlates with the AST and ALT levels, particularly in patients admitted to ICU [24]. In patients admitted with liver diseases, the risk of death correlates with the grade of liver damage: the risk is 1.4 times higher in patients with grade I liver injury, and 2.8 times higher in patients with grade II liver damage [34]. Thus, liver damage is an independent prognostic factor of mortality in patients infected with SARS-CoV-2.

COVID-19 in patients with concomitant liver disease

According to meta-analysis of epidemiological studies, the overall prevalence of CLD in patients with COVID-19 is 3%. SARS-CoV2 infection in patients with CLD is associated with higher mortality compared to other etiologies [13]. In case of liver disease diagnosed before the COVID-19 infection, coronavirus affects the emergence, severity, prognosis of COVID-19, as well as the treatment success [8]. Individuals with CLD are more likely to be infected with SARS-CoV-2 due to weak immune response. Half of the patients with abnormal liver function test results have CLD, including non-alcoholic fatty liver disease (NAFLD), alcoholic liver disease, and chronic hepatitis B [20]. NAFLD is the most common dysmetabolic liver disease in the world being an independent risk factor of the COVID-19 progression (OR 6.4). The disorder is associated with the higher risk of liver dysfunction and the longer viral clearance period. Moreover, it increases the risk of severe COVID-19 progression related to metabolic dysfunction [35].

The study of patients within the Yale-New Haven Health System (USA) confirmed that the patients with abnormal liver tests were at high risk of severe disease. Liver injury was predominantly hepatocellular rather than cholestatic. In these patients, liver abnormalities increased at peak hospitalization. Multivariate analysis made it possible to reveal the relationship between the liver function indicators and clinical outcomes (admission to ICU, mechanical ventilation, and death) [26]. In COVID-19 with elevated serum transaminase levels, it is necessary to take into account the SARS-CoV-2-associated reactivation of the existing liver diseases, including autoimmune disorders.

Pro-inflammatory environment occurring in patients with hepatocellular and cholangiocellular COVID-19-associated injury contributes to activation of hepatic stellate cells, and, as a result, to fibrosis induction in patients with CLD [4]. Activation and proliferation of Kupffer cells resulting from systemic inflammation are often observed, particularly in the liver specimens obtained from the deceased patients with COVID-19 [8].

Chronic liver damage determines immunosuppression, which significantly increases patient mortality, as it has been shown in the observational study of 17,425,445 patients with COVID-19 [36].

Patients with liver cancer are also at high risk of coronavirus infection, especially those undergoing chemotherapy or immunotherapy in the hospital [37]. Cancer patients infected with SARS-CoV-2 have a poorer prognosis compared to COVID-19 patients having no cancer; in such patients, mortality reaches 20% [38].

Liver transplant

The risk of infection and severe course of COVID-19 during the perioperative and the early post-transplant period is higher because of the high levels of immunosuppression [39]. At the same time, hyperactive response of innate immunity can cause liver damage and multiple organ failure; immunosuppression reduces the risk of hyperinflammation and cytokine storm in the liver transplant recipients [15].

The registry of patients with COVID-19 and CLD contains the data of 1588 patients with CLD and no cirrhosis, 772 patients with cirrhosis, and 280 liver transplant recipients [40]. Acute hepatic decompensation occurred in 46% of patients with cirrhosis, while 21% of them had no respiratory symptoms. In patients with acutely decompensated liver disease, mortality is two times higher than in patients with compensated cirrhosis (44% vs. 22%; $p < 0.001$) [41].

Pathogenic gut–liver axis in COVID–19

Since the beginning of the pandemic, gastrointestinal (GI) symptoms were reported as the distinctive features of COVID-19 along with the respiratory and hepatic symptoms. According to meta-analysis of 60 studies involving 4,243 patients with COVID-19, the prevalence of GI symptoms is 17.6% [42]. GI symptoms can appear before or even in the absence of respiratory symptoms [43].

SARS-CoV-2 identification in fecal samples and the combination of GI and liver symptoms are indicative of the gut–liver axis dysregulation in these patients. High expression of ACE2 receptor in the gastrointestinal epithelium (100 times higher than on hepatocytes) allows SARS-CoV2 to enter the cells of biliary ducts and suppress liver function [8]. The COVID-19-induced bowel infection can disrupt the intestinal epithelial barrier and gut vascular barrier leading to the viral translocation into liver through the portal vein. Subsequently, SARS-CoV-2 virions released by the infected hepatocytes, enter the bile [44]. Biliary tract provides the direct link between the liver and the gut, that is why SARS-CoV-2 can reach the gut and infect the

gut through bile, causing reinfection. Thus, the prospective hepatobiliary mechanism can create a vicious cycle explaining the worst outcome in patients with the symptoms of liver disease and GI symptoms [4, 45].

When comparing the deceased patients with the critically ill survivors, immunomodulatory and tissue proteins associated with the COVID-19 survival were identified in blood plasma [46]. Comparison of the organ-specific “death signatures” revealed the significant correlation between the liver signature and the levels of ALT and AST. Proteins associated with the COVID-19 severity included THBS2 (thrombospondin 2), ACTA2 (actin alpha 2), HGF (hepatocyte growth factor), PDGFRA (platelet-derived growth factor receptor A) of Kupffer cells, TACSTD2 (tumor-associated calcium signal transducer 2) of cholangiocytes, CA2 (carbonic anhydrase 2), and BLVRB (biliverdin reductase B) of erythroid cells of the liver. Thus, blood plasma proteome could be used as the liquid biopsy for studying the potential therapeutic targets, and the diagnosis and stratification of patients at high risk being the candidates for personalized therapy [46].

CONCLUSION

SARS-CoV-2 coronavirus mainly affects respiratory tract. However, it shows tropism to the liver and bile ducts. That is why hepatologists are increasingly involved in combating the novel coronavirus infection. Medical practitioners predict the increasing prevalence of liver diseases in the months and years ahead, since SARS-CoV-2 is capable of directly infecting and causing damage to the liver tissue.

The course and outcome of COVID-19 depend largely on the patient's health and concomitant diseases. NAFLD, hepatitis B and C, liver cirrhosis, hepatic cancer, and taking immunosuppressants after the liver transplant result in immunodeficiency. Complications occur earlier and to a greater extent in patients with systemic immunodeficiency.

With the spread of the pandemic and publishing the new data on the effects of coronaviruses on the infected body it has become possible to define the risk factors for hepatic complications in patients infected with SARS-CoV-2. Studying the clinical data of patients with COVID-19 and liver diseases is important for identification of hepatic complications, prediction of the response to treatment, creation of the hepatic complication risk models, and development of the guidelines for patients with liver diseases and coronavirus infection.

References

1. Skok K, Stelzl E, Trauner M, et al. Post-mortem viral dynamics and tropism in COVID-19 patients in correlation with organ damage. *Virchows Arch.* 2021; 478 (2): 343–53. DOI: 10.1007/s00428-020-02903-8.
2. Ackermann M, Verleden SE, Kuehnel M, et al. Pulmonary vascular endothelialitis, thrombosis, and angiogenesis in Covid-19. *N Engl J Med.* 2020; 383 (2): 120–8. DOI:10.1056/NEJMoa2015432.
3. Cabibbo G, Rizzo GEM, Stornello C, Craxi A. SARS-CoV-2 infection in patients with a normal or abnormal liver. *J Viral Hepat.* 2021; 28 (1): 4–11. DOI: 10.1111/jvh.13440.
4. Nardo AD, Schneeweiss-Gleixner M, Bakail M, et al. Pathophysiological mechanisms of liver injury in COVID-19. *Liver Int.* 2021; 41 (1): 20–32. DOI: 10.1111/liv.14730.
5. Amin M. COVID-19 and the liver: overview. *Eur J Gastroenterol Hepatol.* 2021; 33 (3): 309–11. DOI: 10.1097/MEG.0000000000001808.
6. Yadav DK, Singh A, Zhang Q, et al. Involvement of liver in COVID-19: systematic review and meta-analysis. *Gut.* 2021; 70 (4): 807–9. DOI: 10.1136/gutjnl-2020-322072.
7. Kulkarni AV, Kumar P, Tevethia HV, et al. Systematic review with meta-analysis: liver manifestations and outcomes in COVID-19. *Aliment Pharmacol Ther.* 2020; 52 (4): 584–99. DOI: 10.1111/apt.15916.
8. Wang X, Lei J, Li Z, Yan L. Potential Effects of Coronaviruses on the Liver: An Update. *Front Med (Lausanne).* 2021; 8: 651658. DOI: 10.3389/fmed.2021.651658.
9. Merola E, Pravadelli C, de Pretis G. Prevalence of liver injury in patients with coronavirus disease 2019 (COVID-19): a systematic review and meta-analysis. *Acta Gastroenterol Belg.* 2020; 83 (3): 454–60. PMID: 33094594.
10. Mohandas S, Vairappan B. SARSCoV2 infection and the gut–liver axis. *J Dig Dis.* 2020; 21 (12): 687–95. DOI: 10.1111/1751-

- 2980.12951.
11. Li Y, Xiao SY. Hepatic involvement in COVID-19 patients: Pathology, pathogenesis, and clinical implications. *J Med Virol.* 2020; 92 (9): 1491–4. DOI: 10.1002/jmv.25973.
 12. Butikofer S, Lenggenhager D, Wendel Garcia PD, et al. Secondary sclerosing cholangitis as cause of persistent jaundice in patients with severe COVID-19. *Liver Int.* 2021; 41 (10): 2404–17. DOI: 10.1111/liv.14971.
 13. McConnell MJ, Kondo R, Kawaguchi N, Iwakiri Y. COVID-19 and liver injury: role of inflammatory endotheliopathy, platelet dysfunction and thrombosis. *Hepatol Commun.* 2022; 6 (2): 255–69. DOI: 10.1002/hep4.1843.
 14. Kaur S, Hussain S, Kolhe K, et al. Elevated plasma ICAM1 levels predict 28-day mortality in cirrhotic patients with COVID-19 or bacterial sepsis. *JHEP Rep.* 2021; 3 (4): 100303. DOI: 10.1016/j.jhepr.2021.100303.
 15. Zhao J-N, Fan Y, Wu S-D. Liver injury in COVID-19: A minireview. *World J Clin Cases.* 2020; 8 (19): 4303–10. DOI: 10.12998/wjcc.v8.i19.4303.
 16. Beigmohammadi MT, Jahanbin B, Safaei M, et al. Pathological findings of postmortem biopsies from lung, heart, and liver of 7 deceased COVID-19 patients. *Int J Surg Pathol.* 2021; 29 (2): 135–45. DOI: 10.1177/1066896920935195.
 17. Fanni D, Cerrone G, Saba L, et al. Thrombotic sinusoiditis and local diffuse intrasinusoidal coagulation in the liver of subjects affected by COVID-19: the evidence from histology and scanning electron microscopy. *Eur Rev Med Pharmacol Sci.* 2021; 25 (19): 5904–12. DOI: 10.26355/eurrev_202110_26866.
 18. Wang Y, Liu S, Liu H, et al. SARS-CoV-2 infection of the liver directly contributes to hepatic impairment in patients with COVID-19. *J Hepatol.* 2020; 73 (4): 807–16. DOI: 10.1016/j.jhep.2020.05.002.
 19. Schmit G, Lelotte J, Vanhaebost J, et al. The liver in COVID-19-related death: protagonist or innocent bystander? *Pathobiology.* 2021; 88 (1): 88–94. DOI: 10.1159/000512008.
 20. Cai Q, Huang D, Yu H, et al. COVID-19: abnormal liver function tests. *J Hepatol.* 2020; 73 (3): 566–74. DOI: 10.1016/j.jhep.2020.04.006.
 21. Stebbing J, Sanchez Nieves G, Falcone M, et al. JAK inhibition reduces SARS-CoV-2 liver infectivity and modulates inflammatory responses to reduce morbidity and mortality. *Sci Adv.* 2021; 7 (1): eabe4724. DOI: 10.1126/sciadv.abe4724.
 22. Kim WY, Kweon OJ, Cha MJ, et al. Dexamethasone may improve severe COVID-19 via ameliorating endothelial injury and inflammation: A preliminary pilot study. *PLoS One.* 2021; 16 (7): e0254167. DOI: 10.1371/journal.pone.0254167.
 23. Raschi E, Caraceni P, Poluzzi E, De Ponti F, Baricitinib, JAK inhibitors and liver injury: a cause for concern in COVID-19? *Expert Opin Drug Saf.* 2020; 19: 1367–69. DOI: 10.1080/14740338.2020.1812191.
 24. Naeem A, Khamuani MK, Kumar P, et al. Impact of coronavirus diseases on liver enzymes. *Cureus.* 2021; 13 (9): e17650. DOI: 10.7759/cureus.17650.
 25. Cornberg M, Buti M, Eberhardt CS, Grossi PA, Shouval D. EASL position paper on the use of COVID-19 vaccines in patients with chronic liver diseases, hepatobiliary cancer and liver transplant recipients. *J Hepatol.* 2021; 74 (4): 944–51. DOI: 10.1016/j.jhep.2021.01.032.
 26. Hundt MA, Deng Y, Ciarleglio MM, et al. Abnormal liver tests in COVID-19: a retrospective observational cohort study of 1827 patients in a major U.S. hospital network. *Hepatology.* 2020; 72 (4): 1169–76. DOI: 10.1002/HEP.31487.
 27. Pirisi M, Rigamonti C, D'Alfonso S, et al. Liver infection and COVID-19: the electron microscopy proof and revision of the literature. *Eur Rev Med Pharmacol Sci.* 2021; 25 (4): 2146–51. DOI: 10.26355/eurrev_202102_25120.
 28. Varga Z, Flammer AJ, Steiger P, et al. Endothelial cell infection and endotheliitis in COVID-19. *Lancet.* 2020; 395 (10234): 1417–18. DOI: 10.1016/S0140-6736(20)30937-5.
 29. Duarte-Neto AN, Monteiro RA, da Silva LF, et al. Pulmonary and systemic involvement in COVID-19 patients assessed with ultrasound-guided minimally invasive autopsy. *Histopathology.* 2020; 77: 186–97. DOI: 10.1111/his.14160.
 30. Sonzogni A, Previtali G, Seghezzi M, et al. Liver histopathology in severe COVID 19 respiratory failure is suggestive of vascular alterations. *Liver Int.* 2020; 40 (9): 2110–16. DOI: 10.1111/liv.14601.
 31. Fogarty H, Townsend L, Morrin H, et al. Persistent endotheliopathy in the pathogenesis of long COVID syndrome. *J Thromb Haemost.* 2021; 19 (10): 2546–53. DOI: 10.1111/jth.15490.
 32. Rapkiewicz A, Carsons S, Pittaluga S, et al. Megakaryocytes and platelet-fibrin thrombi characterize multi-organ thrombosis at autopsy in COVID-19: A case series. *EClinicalMedicine.* 2020; 24: 100434. DOI: 10.1016/j.eclim.2020.100434.
 33. Musa S. Hepatic and gastrointestinal involvement in coronavirus disease 2019 (COVID-19): What do we know till now? *Arab J Gastroenterol.* 2020; 21 (1): 3–8. DOI: 10.1016/j.ajg.2020.03.002.
 34. Chen LY, Chu HK, Bai T, et al. Liver damage at admission is an independent prognostic factor for COVID-19. *J Dig Dis.* 2020; 21 (9): 512–18. DOI: 10.1111/1751-2980.12925.
 35. Mushtaq K, Khan MU, Iqbal F, et al. NAFLD is a predictor of liver injury in COVID-19 hospitalized patients but not of mortality, disease severity on the presentation or progression — The debate continues. *J Hepatol.* 2021; 74 (2): 482–84. DOI: 10.1016/j.jhep.2020.09.006.
 36. Williamson EJ, Walker AJ, Bhaskaran K, et al. OpenSAFELY: factors associated with COVID-19-related hospital death in the linked electronic health records of 17 million adult NHS patients. *Nature.* 2020; 584 (7821): 430–36. DOI: 10.1038/s41586-020-2521-4.
 37. Barry A, Apisarnthanarax S, O'Kane GM, et al. Management of primary hepatic malignancies during the COVID-19 pandemic: recommendations for risk mitigation from a multidisciplinary perspective. *Lancet Gastroenterol Hepatol.* 2020; 5 (8): 765–75. DOI: 10.1016/S2468-1253(20)30182-5.
 38. Gosain R, Abdou Y, Singh A, et al. COVID-19 and cancer: a comprehensive review. *Curr Oncol Rep.* 2020. 8; 22 (5): 53. DOI: 10.1007/s11912-020-00934-7.
 39. D'Antiga L. Coronaviruses and immunosuppressed patients: the facts during the Third Epidemic. *Liver Transpl.* 2020; 26 (6): 832–4. DOI: 10.1002/lt.25756.
 40. SECURE CIRRHOSIS REGISTRY. <https://covidcirrhosis.web.unc.edu/updates-and-data/>. Accessed 14.12.2021.
 41. Marjot T, Moon AM, Cook JA, et al. Outcomes following SARS-CoV-2 infection in patients with chronic liver disease: An international registry study. *J Hepatol.* 2021; 74 (3): 567–77. DOI: 10.1016/j.jhep.2020.09.024.
 42. Cheung KS, Hung IFN, Chan PPY, et al. Gastrointestinal manifestations of SARS-CoV-2 infection and virus load in fecal samples from a Hong Kong cohort: systematic review and meta-analysis. *Gastroenterology.* 2020; 159 (1): 81–95. DOI: 10.1053/j.gastro.2020.03.065.
 43. Amirian ES. Potential fecal transmission of SARS-CoV-2: Current Evidence and Implications for Public Health. *Int J Infect Dis.* 2020; 95: 363–70. DOI: 10.1016/j.ijid.2020.04.057.
 44. Han D, Fang Q, Wang X. SARS-CoV-2 was found in the bile juice from a patient with severe COVID-19. *J Med Virol.* 2021; 93 (1): 102–4. DOI: 10.1002/jmv.26169.
 45. Vespa E, Pugliese N, Colapietro F, Aghemo A. STAY (GI) HEALTHY: COVID-19 and gastrointestinal manifestations. *Tech Innov Gastrointest Endosc.* 2021; 23 (2): 179–89. DOI: 10.1016/j.tige.2021.01.006.
 46. Filbin MR, Mehta A, Schneider AM, et al. Longitudinal proteomic analysis of severe COVID-19 reveals survival-associated signatures, tissue-specific cell death, and cell-cell interactions. *Cell Rep Med.* 2021; 2 (5): 100287. DOI: 10.1016/j.xcrm.2021.100287.

Литература

- Skok K, Stelzl E, Trauner M, et al. Post-mortem viral dynamics and tropism in COVID-19 patients in correlation with organ damage. *Virchows Arch.* 2021; 478 (2): 343–53. DOI: 10.1007/s00428-020-02903-8.
- Ackermann M, Verleden SE, Kuehnel M, et al. Pulmonary vascular endothelialitis, thrombosis, and angiogenesis in Covid-19. *N Engl J Med.* 2020; 383 (2): 120–8. DOI:10.1056/NEJMoa2015432.
- Cabibbo G, Rizzo GEM, Stornello C, Craxi A. SARS-CoV-2 infection in patients with a normal or abnormal liver. *J Viral Hepat.* 2021; 28 (1): 4–11. DOI: 10.1111/jvh.13440.
- Nardo AD, Schneeweiss-Gleixner M, Bakail M, et al. Pathophysiological mechanisms of liver injury in COVID-19. *Liver Int.* 2021; 41 (1): 20–32. DOI: 10.1111/liv.14730.
- Amin M. COVID-19 and the liver: overview. *Eur J Gastroenterol Hepatol.* 2021; 33 (3): 309–11. DOI: 10.1097/MEG.0000000000001808.
- Yadav DK, Singh A, Zhang Q, et al. Involvement of liver in COVID-19: systematic review and meta-analysis. *Gut.* 2021; 70 (4): 807–9. DOI: 10.1136/gutjnl-2020-322072.
- Kulkarni AV, Kumar P, Tevethia HV, et al. Systematic review with meta-analysis: liver manifestations and outcomes in COVID-19. *Aliment Pharmacol Ther.* 2020; 52 (4): 584–99. DOI: 10.1111/apt.15916.
- Wang X, Lei J, Li Z, Yan L. Potential Effects of Coronaviruses on the Liver: An Update. *Front Med (Lausanne).* 2021; 8: 651658. DOI: 10.3389/fmed.2021.651658.
- Merola E, Pravadelli C, de Pretis G. Prevalence of liver injury in patients with coronavirus disease 2019 (COVID-19): a systematic review and meta-analysis. *Acta Gastroenterol Belg.* 2020; 83 (3): 454–60. PMID: 33094594.
- Mohandas S, Vairappan B. SARS-CoV2 infection and the gut-liver axis. *J Dig Dis.* 2020; 21 (12): 687–95. DOI: 10.1111/1751-2980.12951.
- Li Y, Xiao SY. Hepatic involvement in COVID-19 patients: Pathology, pathogenesis, and clinical implications. *J Med Virol.* 2020; 92 (9): 1491–4. DOI: 10.1002/jmv.25973.
- Butikofer S, Lenggenhager D, Wendel Garcia PD, et al. Secondary sclerosing cholangitis as cause of persistent jaundice in patients with severe COVID-19. *Liver Int.* 2021; 41 (10): 2404–17. DOI: 10.1111/liv.14971.
- McConnell MJ, Kondo R, Kawaguchi N, Iwakiri Y. COVID-19 and liver injury: role of inflammatory endotheliopathy, platelet dysfunction and thrombosis. *Hepatol Commun.* 2022; 6 (2): 255–69. DOI: 10.1002/hep4.1843.
- Kaur S, Hussain S, Kolhe K, et al. Elevated plasma ICAM1 levels predict 28-day mortality in cirrhotic patients with COVID-19 or bacterial sepsis. *JHEP Rep.* 2021; 3 (4): 100303. DOI: 10.1016/j.jhepr.2021.100303.
- Zhao J-N, Fan Y, Wu S-D. Liver injury in COVID-19: A minireview. *World J Clin Cases.* 2020; 8 (19): 4303–10. DOI: 10.12998/wjcc.v8.i19.4303.
- Beigmohammadi MT, Jahanbin B, Safaei M, et al. Pathological findings of postmortem biopsies from lung, heart, and liver of 7 deceased COVID-19 patients. *Int J Surg Pathol.* 2021; 29 (2): 135–45. DOI: 10.1177/1066896920935195.
- Fanni D, Cerrone G, Saba L, et al. Thrombotic sinusoiditis and local diffuse intrasinusoidal coagulation in the liver of subjects affected by COVID-19: the evidence from histology and scanning electron microscopy. *Eur Rev Med Pharmacol Sci.* 2021; 25 (19): 5904–12. DOI: 10.26355/eurev_202110_26866.
- Wang Y, Liu S, Liu H, et al. SARS-CoV-2 infection of the liver directly contributes to hepatic impairment in patients with COVID-19. *J Hepatol.* 2020; 73 (4): 807–16. DOI: 10.1016/j.jhep.2020.05.002.
- Schmit G, Lelotte J, Vanhaebost J, et al. The liver in COVID-19-related death: protagonist or innocent bystander? *Pathobiology.* 2021; 88 (1): 88–94. DOI: 10.1159/000512008.
- Cai Q, Huang D, Yu H, et al. COVID-19: abnormal liver function tests. *J Hepatol.* 2020; 73 (3): 566–74. DOI: 10.1016/j.jhep.2020.04.006.
- Stebbing J, Sanchez Nievas G, Falcone M, et al. JAK inhibition reduces SARS-CoV-2 liver infectivity and modulates inflammatory responses to reduce morbidity and mortality. *Sci Adv.* 2021; 7 (1): eabe4724. DOI: 10.1126/sciadv.abe4724.
- Kim WY, Kweon OJ, Cha MJ, et al. Dexamethasone may improve severe COVID-19 via ameliorating endothelial injury and inflammation: A preliminary pilot study. *PLoS One.* 2021; 16 (7): e0254167. DOI: 10.1371/journal.pone.0254167.
- Raschi E, Caraceni P, Poluzzi E, De Ponti F. Baricitinib, JAK inhibitors and liver injury: a cause for concern in COVID-19? *Expert Opin Drug Saf.* 2020; 19: 1367–69. DOI: 10.1080/14740338.2020.1812191.
- Naeem A, Khamuani MK, Kumar P, et al. Impact of coronavirus diseases on liver enzymes. *Cureus.* 2021; 13 (9): e17650. DOI: 10.7759/cureus.17650.
- Cornberg M, Buti M, Eberhardt CS, Grossi PA, Shouval D. EASL position paper on the use of COVID-19 vaccines in patients with chronic liver diseases, hepatobiliary cancer and liver transplant recipients. *J Hepatol.* 2021; 74 (4): 944–51. DOI: 10.1016/j.jhep.2021.01.032.
- Hundt MA, Deng Y, Ciarleglio MM, et al. Abnormal liver tests in COVID-19: a retrospective observational cohort study of 1827 patients in a major U.S. hospital network. *Hepatology.* 2020; 72 (4): 1169–76. DOI: 10.1002/HEP.31487.
- Pirisi M, Rigamonti C, D'Alfonso S, et al. Liver infection and COVID-19: the electron microscopy proof and revision of the literature. *Eur Rev Med Pharmacol Sci.* 2021; 25 (4): 2146–51. DOI: 10.26355/eurev_202102_25120.
- Varga Z, Flammer AJ, Steiger P, et al. Endothelial cell infection and endotheliitis in COVID-19. *Lancet.* 2020; 395 (10234): 1417–18. DOI: 10.1016/S0140-6736(20)30937-5.
- Duarte-Neto AN, Monteiro RA, da Silva LF, et al. Pulmonary and systemic involvement in COVID-19 patients assessed with ultrasound-guided minimally invasive autopsy. *Histopathology.* 2020; 77: 186–97. DOI: 10.1111/his.14160.
- Sonzogni A, Previtali G, Seghezzi M, et al. Liver histopathology in severe COVID 19 respiratory failure is suggestive of vascular alterations. *Liver Int.* 2020; 40 (9): 2110–16. DOI: 10.1111/liv.14601.
- Fogarty H, Townsend L, Morrin H, et al. Persistent endotheliopathy in the pathogenesis of long COVID syndrome. *J Thromb Haemost.* 2021; 19 (10): 2546–53. DOI: 10.1111/jth.15490.
- Rapkiewicz A, Carsons S, Pittaluga S, et al. Megakaryocytes and platelet-fibrin thrombi characterize multi-organ thrombosis at autopsy in COVID-19: A case series. *EClinicalMedicine.* 2020; 24: 100434. DOI: 10.1016/j.eclinm.2020.100434.
- Musa S. Hepatic and gastrointestinal involvement in coronavirus disease 2019 (COVID-19): What do we know till now? *Arab J Gastroenterol.* 2020; 21 (1): 3–8. DOI: 10.1016/j.ajg.2020.03.002.
- Chen LY, Chu HK, Bai T, et al. Liver damage at admission is an independent prognostic factor for COVID-19. *J Dig Dis.* 2020; 21 (9): 512–18. DOI: 10.1111/1751-2980.12925.
- Mushtaq K, Khan MU, Iqbal F, et al. NAFLD is a predictor of liver injury in COVID-19 hospitalized patients but not of mortality, disease severity on the presentation or progression — The debate continues. *J Hepatol.* 2021; 74 (2): 482–84. DOI: 10.1016/j.jhep.2020.09.006.
- Williamson EJ, Walker AJ, Bhaskaran K, et al. OpenSAFELY: factors associated with COVID-19-related hospital death in the linked electronic health records of 17 million adult NHS patients. *Nature.* 2020; 584 (7821): 430–36. DOI: 10.1038/s41586-020-2521-4.
- Barry A, Apisarnthanarax S, O'Kane GM, et al. Management of primary hepatic malignancies during the COVID-19 pandemic: recommendations for risk mitigation from a multidisciplinary perspective. *Lancet Gastroenterol Hepatol.* 2020; 5 (8): 765–75. DOI: 10.1016/S2468-1253(20)30182-5.
- Gosain R, Abdou Y, Singh A, et al. COVID-19 and cancer: a comprehensive review. *Curr Oncol Rep.* 2020; 22 (5): 53. DOI: 10.1007/s11912-020-00934-7.
- D'Antiga L. Coronaviruses and immunosuppressed patients: the facts during the Third Epidemic. *Liver Transpl.* 2020; 26 (6): 832–4. DOI: 10.1002/lt.25756.

40. SECURE CIRRHOSIS REGISTRY. <https://covidcirrhosis.web.unc.edu/updates-and-data/>. Accessed 14.12.2021.
41. Marjot T, Moon AM, Cook JA, et al. Outcomes following SARS-CoV-2 infection in patients with chronic liver disease: An international registry study. *J Hepatol.* 2021; 74 (3): 567–77. DOI: 10.1016/j.jhep.2020.09.024.
42. Cheung KS, Hung IFN, Chan PPY, et al. Gastrointestinal manifestations of SARS-CoV-2 infection and virus load in fecal samples from a Hong Kong cohort: systematic review and meta-analysis. *Gastroenterology.* 2020; 159 (1): 81–95. DOI: 10.1053/j.gastro.2020.03.065.
43. Amirian ES. Potential fecal transmission of SARS-CoV-2: Current Evidence and Implications for Public Health. *Int J Infect Dis.* 2020; 95: 363–70. DOI: 10.1016/j.ijid.2020.04.057.
44. Han D, Fang Q, Wang X. SARS-CoV-2 was found in the bile juice from a patient with severe COVID-19. *J Med Virol.* 2021; 93 (1): 102–4. DOI: 10.1002/jmv.26169.
45. Vespa E, Pugliese N, Colapietro F, Aghemo A. STAY (GI) HEALTHY: COVID-19 and gastrointestinal manifestations. *Tech Innov Gastrointest Endosc.* 2021; 23 (2): 179–89. DOI: 10.1016/j.tige.2021.01.006.
46. Filbin MR, Mehta A, Schneider AM, et al. Longitudinal proteomic analysis of severe COVID-19 reveals survival-associated signatures, tissue-specific cell death, and cell-cell interactions. *Cell Rep Med.* 2021; 2 (5): 100287. DOI: 10.1016/j.xcrm.2021.100287.

PAMAM DENDRIMERS AND PROSPECTS OF THEIR APPLICATION IN MEDICINE

Popova EV ✉, Krivorotov DV, Gamazkov RV, Radilov AS

Research Institute of Hygiene, Occupational Pathology and Human Ecology of the Federal Medical Biological Agency, Leningrad region, Russia

Development of drug delivery systems based on branched biocompatible polymers is one of the most promising areas of modern nanopharmaceutics. Researchers have been exploring this area several decades now, and the results of their efforts quickly find their way into production. Dendrimers, a new class of universal synthetic polymers with a highly functional surface, have a number of unique properties: constant size, high degree of branching, multivalence, solubility in water, definite molecular weight, internal cavities. With the release of VivaSol gel, the first dendrimer-based commercialized product, the "model range" of dendrimer carriers has grown significantly. Poly(amide-amine) (PAMAM) dendrimers, which consist of an alkyldiamine core and tertiary amine branches, are believed to be among the most promising compounds that can be used in the development of the new generation drugs. However, they were kept out of the list of clinically acceptable compounds for a long time because of their toxicity, unclear behavior in living systems and pharmacokinetic profile, as well the difficulties associated with establishing a therapeutic dose. This review presents basic information about PAMAM dendrimers and attempts to assess the prospects of their application in treatment of various diseases, including COVID-19.

Keywords: dendrimers, drugs, COVID 19, drug delivery systems**Author contribution:** all authors of the article took equal parts in the literature search and analysis, data interpretation, manuscript authoring and preparation.✉ **Correspondence should be addressed:** Elena Viktorovna Popova
Bekhtereva, 1, korp. 3, litera R, St. Petersburg, 192019, Russia; arabka2008@mail.ru**Received:** 10.03.2022 **Accepted:** 24.03.2022 **Published online:** 30.03.2022**DOI:** 10.47183/mes.2022.008

ДЕНДРИМЕРЫ ПАМАМ И ПЕРСПЕКТИВЫ ИХ ПРИМЕНЕНИЯ В МЕДИЦИНЕ

Е. В. Попова ✉, Д. В. Криворотов, Р. В. Гамазков, А. С. Радилов

Научно-исследовательский институт гигиены, профпатологии и экологии человека Федерального медико-биологического агентства, Ленинградская область, Россия

Разработка систем доставки лекарственных веществ на основе разветвленных биосовместимых полимеров — одно из наиболее перспективных направлений современной нанофармацевтики. Исследования в данной области ведут уже не одно десятилетие, а их результаты активно внедряют в производство. Дендримеры — новый класс универсальных синтетических полимеров с поверхностью высокой степени функциональности, — обладают уникальными свойствами: постоянством размера, высокой степенью разветвления, многовалентностью, растворимостью в воде, четко определенной молекулярной массой, наличием внутренних полостей. С выпуском первого коммерческого продукта на основе дендримера — геля VivaSol, «модельный ряд» дендримерных носителей существенно разросся. Поли(амид)аминовые дендримеры, состоящие из алкилдиаминового ядра и третичных аминовых ветвей, считают одними из наиболее перспективных соединений для разработки препаратов нового поколения. Однако их клиническая адаптация долгое время была ограничена вследствие их токсичности, неопределенности поведения в живых системах и фармакокинетического профиля, а также сложности в подборе терапевтической дозы. В обзоре представлены основные сведения о дендримерах ПАМАМ и сделана попытка оценить перспективы их применения в терапии различных заболеваний, в том числе COVID-19.

Ключевые слова: дендримеры, лекарственные препараты, COVID-19, системы доставки**Вклад авторов:** все авторы статьи в равнозначной степени внесли вклад в поиск и анализ литературы, интерпретацию полученных данных, подготовку и оформление рукописи.✉ **Для корреспонденции:** Елена Викторовна Попова
ул. Бехтерева, д. 1, корп. 3, литера Р, г. Санкт-Петербург, 192019, Россия; arabka2008@mail.ru**Статья получена:** 10.03.2022 **Статья принята к печати:** 24.03.2022 **Опубликована онлайн:** 30.03.2022**DOI:** 10.47183/mes.2022.008

In the field of pharmaceutical chemistry, the top priority task is the development of drug and vaccine delivery systems. Today, pharmaceutical giants are working on the new systems that would deliver drugs, vaccines and siRNA. Oncology remains one of the leading areas of their practical application. However, since 2019, when the COVID-19 pandemic began, a task considered particularly urgent is the development of targeted drug delivery systems, i.e., those that deliver antiviral and standard therapy drugs to target organs (brain, lungs, intestines). There is a wide range of new delivery systems available nowadays, which necessitates regular systematization of information about their actual applicability in clinical practice. The primary reason behind the interest in three-dimensional branched monodisperse polymer dendrimers is their unique and stable structure [1], which can be designed during stepwise synthesis, something unachievable with other polymers. As a result, their unique geometry and valence properties are

completed with the low degree of polydispersity. Constant charge and size enable formation of well-defined complexes with various drugs.

The purpose of this review is to summarize information about the various drug compounds delivery systems based on PAMAM dendrimers that are described in the scientific literature and used by the pharmaceutical industry. A subject that received more attention is the trend of using this type of carriers in the fight against COVID-19.

Use of PAMAM dendrimers for drug delivery: prospects

PAMAM dendrimers can be successfully used to solve various biomedical problems. Dendrimers-based delivery systems can be carriers of both hydrophilic and hydrophobic compounds [2]. However, the adoption of unmodified PAMAM dendrimers into clinical practice is limited because of their

toxicity, unpredictable behavior in living organisms, unknown bioavailability, biocompatibility, or pharmacokinetic profile. Moreover, it is hard to establish the effective therapeutic dose of the complex and expensive to produce them.

PAMAM dendrimers are extremely small (1–200 nm), which significantly improves their chances of avoiding capture and destruction by the reticuloendothelial system [3]. One of the downsides of PAMAM dendrimer cations of higher generations is their ability to destroy cell membranes [4].

It is known that dendrimers are capable of passing through the blood-brain barrier, which means they can deliver the carried drugs into the brain. PAMAM dendrimers are most often used in the therapies of brain disorders [5]. For example, there are PAMAM dendrimer and carbamazepine (antiepileptic drug) complexes that are part of the Alzheimer's disease treatment protocols [6]. Caproyl-modified G2 (second generation) PAMAM dendrimers are effective carriers of insulin in a nasal delivery system [7].

A G5 PAMAM dendrimer known for its low solubility in water has the proven capability of delivering haloperidol, a neuroleptic drug, to the brain [8]. A smaller dose of haloperidol-dendrimer complex administered nasally produced a therapeutic effect comparable to that of intraperitoneal administration of this drug.

A group of researchers has analyzed the possibilities of using dendrimers as delivery systems carrying immunogenic peptides into a living organism. Since the bioavailability of peptides is insufficient to induce immunogenic reactions unprotected peptides tend to degrade when acted upon by proteases, there was designed an experimental complex for nasal administration with G4 PAMAM dendrimers as adjuvant and carrier of the pPGT122 peptide epitope [9].

Cationic G5 and G7 PAMAM dendrimers loaded with ¹⁴C accumulate in the pancreas, which can be used in the treatment of diabetes mellitus. In addition, these dendrimers have been shown to be rapidly (< 2 h) excreted by the kidneys in the urine [10].

Dendrimers can also be used as systems for delivering proteins into the body: ribonucleases, alcohol dehydrogenases, aldolases etc., including blood plasma proteins, human serum albumin and γ -globulin [11].

Drugs used in ophthalmology

Up to 105 million people around the world suffer from glaucoma, a common and severe chronic eye disease that can manifest itself in a variety of clinical forms in people of different ages (including newborns) and races [12]. There are many new glaucoma medications available on the market today, but their choice is still limited.

In a study, PAMAM dendrimers were shown to be capable of delivering antiglaucoma drugs, pilocarpine nitrate and tropicamide [13]. Loading pilocarpine nitrate onto PAMAM dendrimers also increased its bioavailability.

There was developed a hydrogel (mcDH) of G5 PAMAM dendrimer and polyethylene glycol diacrylate (PEG-DA) [14]. Based on the hydrogel, a new brimonidine antiglaucoma drug was designed. The authors of this study have also investigated cytotoxicity of the NIH3T3 delivery system to fibroblasts, brimonidine release kinetics *in vitro*, the ability of this agent to penetrate rabbit's cornea.

A report published in 2017 described a fast-dissolving nanofiber scaffold of PAMAM dendrimer and brimonidine tartrate that, according to the authors, is an alternative to eye drops [15]. The experiment, which lasted three weeks, was designed to compare the response to brimonidine tartrate eye

drops and the said scaffold in a brown Norwegian rat model; the response to the two drug forms compared was similar. The researchers have also noted high solubility of the scaffolds, complete biocompatibility and efficient delivery of brimonidine.

A number of *in vitro* and *ex vivo* studies have shown that PAMAM-based hydrogels can enhance penetration of anti-glaucoma drugs into eye tissues, which translates into smaller dosages and higher efficacy.

Drugs used in oncology

The growing incidence of cancer in the population and the advancements in the methods of treatment of this pathology have increased the rate of development of this area of medical science. Radiation therapy (RT) is one of the most commonly used types of cancer treatment. Its key tasks are to ensure complete resorption of the tumor tissue, inhibit its growth and alleviate symptoms of the disease. This treatment option is not without limitations: in particular, to make RT efficient, it is necessary to very accurately target the radiation and keep it targeted on the tumor throughout the procedure. In this connection, much development effort is now invested into dendrimer-based radiopharmaceuticals. Conceptually, this type of medications are designed to deliver the radioactive nuclide straight into the tumor tissue and in the concentration required, thus protecting healthy tissues from radiation exposure. Radiolabeled dendrimers allow using less radiolabels, which consequently reduces their toxicity and tumor resistance [16]. For example, PAMAM dendrimers can specifically target A549 human lung carcinoma cells overexpressing the $\alpha v \beta 3$ integrin. The dendrimer, in turn, can be effectively labeled with the ¹³¹I radiolabel and subsequently used in radiation treatment of a lung carcinoma that overexpresses the $\alpha v \beta 3$ integrin [17].

The modern anticancer chemotherapy arsenal includes about a hundred drugs and several groups of substances with similar chemical structure, anticancer action and source of origin. All anticancer drugs aim to inhibit cell proliferation and kill tumor cells. What is promising about dendrimers is they ability to form complexes with chemotherapeutic agents, deliver them to the affected organs and subsequently release in high concentrations. Thus, the main goals of chemotherapy are realized: relapse-free survival of the patient after surgery (adjuvant chemotherapy), reduction of the degree of surgery invasiveness (neoadjuvant chemotherapy), improvement of the quality of life (maintenance chemotherapy).

Anticancer agents with carboxyl groups, such as methotrexate (MTX) or doxorubicin (DOX), interact well with PAMAM dendrimers' core and surface. The rate of incorporation of these agents increases with the generation of dendrimers: for example, 4G PAMAM dendrimer can accommodate up to 26 MTX molecules (with additional polyethylene glycol (PEG) chains).

Doxorubicin is one of the anticancer drugs commonly conjugated to dendrimers [18], the resulting complex applicable in treatments of breast, bladder, stomach cancers and gliomas. PAMAM dendrimers are known to penetrate intestinal epithelial barriers, which makes them usable as carriers in oral delivery systems. In one study, PAMAM dendrimers functionalized with folic acid (widely used as a vector for anticancer drugs) and labeled with isothiocyanate were carrying doxorubicin; the complex proved to be highly efficient [19].

There is a large number of research papers that report on development of drug vectors based on PAMAM dendrimers and designed to deliver antitumor drugs, such as fluorouracil [20], gemcitabine [21], berberine [22], thalidomide [23], paclitaxel [24], cisplatin [25], and malloapelta B [26].

A standard chemotherapy drug used against advanced pancreatic cancer is gemcitabine. One of its drawbacks is the short half-life. Most researchers that invest time and effort into development of dendrimer-based gemcitabine delivery systems seek to design an efficient, least toxic complex for cancer treatment [27].

The isoquinoline alkaloid berberine (BBR), a protoberberine, is used in traditional medicine to treat conditions such as type 2 diabetes and hypercholesterolemia. Since BBR inhibits growth of cancer cells and induces apoptosis, it is also used in cancer therapy. A complex of PAMAM dendrimer and BBR was designed and its anticancer activity studied on human breast cancer cells MCF-7 and MDA-MB-468 [22, 28]. The PAMAM-BBR system showed a more potent anticancer effect than BBR alone. Covalent cross-linking of BBR with dendrimer's amino groups allowed increasing the load of the agent carried and even enhance its anticancer activity. The hemolytic toxicity and hypoglycemic effects of BBR were reduced.

Another study demonstrated a complex of trastuzumab and PAMAM dendrimer linked with paclitaxel or docetaxel, which can specifically target SKBR3 HER-2-positive cells. The designed conjugates proved to be even more toxic towards HER-2-positive human breast cancer cells than the agent alone or as part of a simple PAMAM-trastuzumab conjugate [29].

Cis-dichlorodiaminoplatin(II) (cisplatin), an anticancer drug, binds DNA via intracavitary cross-links to d(GpG) (dG = deoxyguanosine) and d(ApG) (dA = deoxyadenosine), which impairs DNA replication and transcription and causes cell death. Cisplatin is very effective against many solid tumors, including ovarian cancer. However, tumors become resistant to cisplatin with time and, in addition, it has systemic side effects, nephrotoxicity and neurotoxicity [25]. Compared to uncombined cisplatin, PAMAM-cisplatin complexes showed greater efficacy against all ovarian cancer cell lines, even those resistant to cisplatin. In a variety of cell lines resistant to cisplatin, the G4 PAMAM dendrimer and cisplatin conjugates caused formation of DNA adducts, increased expression of apoptotic genes and high caspase activity while exhibiting better cytotoxicity properties [30].

Genistein (4,5,7-Trihydroxyisoflavone), found in soybean and chickpea, has a wide range of physiological and pharmacological functions. It is known to inhibit the growth of human melanoma cells at the G2/M transition and has been shown to inhibit DNA strand breaks mediated by $H_2O_2/Cu(II)$ by acting as a direct scavenger of reactive oxygen species with an OH group at the C-4 position, which enables its antioxidant activity [31].

Loading of the G4 and G5 PEGylated PAMAM dendrimer with 5-fluorouracil (5FU, anticancer drug) allowed reducing the amount of agent lost in delivery and decreased its hemolytic toxicity [20]. It took 90 molecules of the drug to fully load the G4 PAMAM-NH₂ dendrimer. A group of researchers suggested [32] a way to increase the synergistic anticancer efficacy by developing a system for co-delivery of the miR-205 gene vector and the 5FU target drug on an acetylated PAMAM conjugated to an LHRH peptide (LHRH-G5.0NHAC). The optimized co-delivery system was then evaluated for synergistic anticancer effect *in vitro* and *in vivo*.

It is known that folate receptors (FR) are highly expressed in many types of tumor cells (e.g., breast carcinoma) [33]. Polyethylene glycol-modified G4 PAMAM dendrimers were functionalized with folic acid (FA), then the complex was extended with 5FU and 99mTc (technetium-99m) and became the new PEG-PAMAM G4-FA-5FU-99mTc complex. Compared to other nanocarriers and normal cells, the FA-specific complex showed high breast cancer cells penetration capacity.

In one study, PAMAM dendrimer was used to co-deliver miR-21 antisense oligonucleotide (as-miR-21) and 5FU to a human glioblastoma while increasing cytotoxicity of the 5FU antisense therapy [34]. Antisense therapy seeks to stop synthesis of the protein involved in the development of the disease by inhibiting translation of its mRNA with complementary antisense oligonucleotides.

Another study describes a PEG core PAMAM dendrimer-based gemcitabine delivery system that contains anionic carboxylic acid groups modified with PEG chains that were simultaneously conjugated with Flt1 antibodies [35]. Flt1 is the vascular endothelial growth factor (VEGF) receptor 1, which promotes angiogenesis in histomorphological varieties of cancer. Extended with gemcitabine, this system became more efficient in reducing tumor burden in a pancreatic cancer xenograft model. Moreover, this gemcitabine delivery system has also changed the growth dynamics of myeloid cells and decreased their amount in bone marrow.

Dendrimers are also vital components of the anticancer drugs targeted delivery vector systems. The vectors are monoclonal antibodies and tumor-specific proteins that can recognize and bind tumor-specific antigens. Folic acid can be called a promising vector candidate enabling targeted delivery of anticancer drugs. Cell membranes of most tumors (carcinomas, gliomas) have a folic acid receptor. After binding to the receptor, the drug-dendrimer complex enters the cell by means of the receptor-mediated endocytosis and releases the drug.

Antiviral drugs

In the last two centuries, viral diseases have been among the most pressing medical and social problems. Some acute viral infections claim the lives of up to 14 million people worldwide each year, according to WHO. Viruses are non-cellular life forms that can infect living organisms by penetration through epithelium of the gastrointestinal tract (enterovirus, adenovirus), epithelium of the respiratory tract (rhinovirus), skin (papilloma virus, chickenpox), mucous membranes, placenta, during blood transfusions, organ transplantation operations, breastfeeding.

One of the key requirements for the newly designed antiviral drugs is the ability to selectively suppress a certain stage of virus reproduction without affecting the vital processes of other body cells; another key requirement is high bioavailability that allows keeping concentration of the drug in target cells at the level needed to cure and counteract development of drug resistance.

Loading of antiviral drugs on dendrimers enables delivery to target organs and prolongation of action of the drugs, which in turn ensures efficacy of drug therapy. The most common antiviral drugs are interferon derivatives, inhibitors of viral RNA, enzymes (neuraminidase) that release new virions. Scientists have been designing interferon-dendrimer complexes for several years now. In one of the studies, researchers have successfully formed a complex of arginine-modified PAMAM dendrimer and interferon beta used in glioblastoma therapies, which was then studied in mice [36]. Authors of another work managed to create a PAMAM dendrimer-based transdermal delivery system with interferon regulatory factor 3 (IFN 3).

In the literature, there are solitary mentions of designed complexes of a dendrimer and an antiviral drug, for example, acyclovir [37].

PAMAM dendrimers and COVID-19

There are five classes of drugs that are used in the standard COVID-19 treatment protocol: anti-inflammatory (non-specific

anti-inflammatory drugs), systemic corticosteroids (glucocorticosteroids), vitamins, antivirals and anticoagulants. Targeted delivery can soften the systemic effects drugs have on the body, increase their bioavailability, reduce the dose and toxic load on the organs that eliminate them from the body.

Combination drug therapy relying on delivery systems is one of the promising ways of treatment of complicated COVID-19 cases. It allows not only to reduce the dosage of the administered drugs, but also to achieve several therapeutic goals. For example, COVID-19-induced inflammation in the lungs calls for non-specific anti-inflammatory, antiviral drugs, corticosteroids and anticoagulants. These medications are administered parenterally and act systemically, which significantly increases the number of side effects and iatrogenic complications associated with their use.

Antivirals in COVID-19 therapies

PAMAM dendrimer cations themselves are known to possess antiviral properties and act against herpes virus (HSV) and influenza [38]. Cationic dendrimers with NH₂ and OH groups interacted with negatively charged envelope of the MERS-CoV virus and thus blocked it [39]. Another study investigated antiviral activity of G1 polyamidoamine dendrimers conjugated with 3'-siallactose or 6'-sialyllactose; the targets were various strains of the influenza virus [40]. The authors noted that the complexes prevented penetration of the virus into cells. The analysis of hemagglutination inhibition data revealed that human and swine influenza viruses were inhibited by (6SL)-PAMAM dendrimer complexes and, to a lesser extent, (3SL)-PAMAM dendrimer complexes.

Brain is one of the organs affected by the new coronavirus infection. The main problem in establishing the therapeutic dose of a drug designed to work in the brain lies with the need to pass the blood-brain barrier. This fact underpins the importance of development of systems capable of reaching the focus of the disease through the physiological barriers of the body and releasing a therapeutic dose of the drug carried in the tissue affected by the virus.

Anti-inflammatory drugs in COVID-19 therapies

Severe post-COVID-19 complications develop because of the systemic inflammatory response of the body with excessive production of cytokines. Tumor necrosis factor alpha (TNF α) plays a central role in most inflammatory lung diseases, such as chronic obstructive pulmonary disease, asthma, acute respiratory distress syndrome and acute lung injury. Theoretically, TNF α is a promising target for siRNA-based therapy against acute and chronic lung inflammation. Authors of one of the studies used G3 PAMAM dendrimers to deliver TNF α -targeted siRNA to the lungs [41]. They investigated the efficacy and safety of the resulting complex (dendriplex) in a mice model of acute pneumonia. Dendriplexes were shown to efficiently deliver the agent, ensure high transfection efficacy and high uptake of RAW264.7 by macrophages.

There was described a G2 PAMAM dendrimer and dexamethasone-based heme oxygenase 1 (HO-1) delivery system designed to treat ischemic stroke [42]. HO-1 is an antioxidant enzyme that has anti-inflammatory and immunomodulatory effects. Dexamethasone, an anti-inflammatory corticosteroid drug, is a common component of treatment protocols for a variety of acute inflammatory diseases. In particular, it is used to alleviate cerebral edema in ischemic stroke. Therefore, the combined delivery of the

HO-1 gene and dexamethasone may have an additive effect on ischemic brain structures.

N-acetylcysteine is a mucolytic expectorant anti-inflammatory drug prescribed in cases of infectious and respiratory diseases of the upper and lower respiratory tract. A group of researchers has found that PAMAM-COOH anionic dendrimer and N-acetylcysteine (NAC) conjugates can efficiently address neuroinflammations [43]. The antioxidant and anti-inflammatory potency of the PAMAM-(COOH)-(NAC) complex was assessed in microglial cells in vitro. Compared to NAC alone, the complex proved to produce a more intense antioxidant effect [44]. In addition, microglial cells (resident macrophages of the central nervous system) were used to investigate cytotoxicity, cellular uptake and the efficacy of the delivery system. The cellular uptake of dendrimers was rapid, with a well-defined drug release rate.

Delivery of the PAMAM dendrimer and methylprednisolone complex to the lungs is a promising pattern in drug therapy of COVID-19. With G5 PAMAM dendrimer as a carrier for methylprednisolone and the complex administered nasally, the dendrimer was demonstrated to persist in the lung for five days [45]. Repeated daily administrations over the next five days showed that the complex did not cause any observable non-specific inflammatory reactions in the lungs.

It is known that COVID-19 may be accompanied by an aggressive inflammatory response of the body with active release of inflammatory cytokines. Such response is called a cytokine storm. It is an uncontrolled overactive reaction of the immune system to the infecting SARS-CoV-2 virus; the result is extensive lung damage combined with multiple organ failure. Cytokine storm is one of the main causes of death of COVID-19 patients. The countermeasures adopted in the clinical practice involve administration of immunosuppressants, recombinant humanized monoclonal antibodies to interleukin IL6 and IL1 receptors: tocilizumab, sarilumab, levilumab, olokizumab, canakinumab. Development of the target delivery systems for these drugs is an important task in the context of treatment of complicated new coronavirus infection cases.

Anticoagulants in COVID-19 therapies

Intravascular thrombosis is one of the formidable complications associated with COVID-19. To arrest its development, standard treatment protocols always include administration of drugs that inhibit coagulation hemostasis and prevent formation of blood clots. PAMAM dendrimers can be used as antithrombotic agents in anticoagulant therapy [19]. Arginine- and FA-modified G4 and G5 dendrimers carrying coumarin-3-carboxylic acid showed a good antithrombotic effect, high hemocompatibility, hemocompatibility and stability. Another dendrimer-based complex suggested for treatment of venous thrombosis is the complex of PAMAM dendrimer and enoxaparin, the efficacy of which was demonstrated in mice model experiments [46].

The PAMAM dendrimer-heparin complexes can be formed both by incorporating the drug into the dendrimer and by electrostatic interaction with functional groups. It was discovered that such a complex created through electrostatic interactions improves biocompatibility of the dendrimer itself while reducing the cytotoxicity [47]. A G3 PAMAM dendrimer was used to carry enoxaparin to the lungs, which ultimately resulted in prevention of thrombosis in blood vessels [48].

Immunobiological drugs

Since interfering RNA therapy has been shown effective in treatment of the new coronavirus infection, development of

siRNA and mRNA vaccines became an increasingly popular activity. Inhaled PAMAM dendrimer-siRNA complex may be a much more specific and safe therapeutic agent against COVID 19.

CONCLUSION

It is obvious that the interest in development of dendrimer-based delivery systems (employing their various classes of dendrimers) will continue to grow. In this connection, it seems promising rely on such systems to improve the methods of delivery of the already registered drugs used in the treatment standards. The advantages that underpin the importance of the respective efforts include targeted effect on the organs,

accumulation of high therapeutic concentrations of drugs in the lesions, reduced side effects and complications from the treatment. Today, many of the drugs based on dendrimers are already commercially available and approved for clinical use.

The scientific community pays special attention to the development of delivery systems not just for cancers but also for COVID-19. In the fall of 2020, Starpharma announced the completion of testing of a nasal spray against SARS-CoV-2 based on the SPL7013 dendrimer. The G4 SPL7013 consists of a divalent benzylhydramine core, outgoing from the core of L-lysine branches with 32 surface groups of naphthalenesulfonic acid (DNAA), which impart hydrophobicity and a high anionic charge to the dendrimer surface [49].

References

1. Kharwade R, More S, Warokar A, Agrawal P, Mahajan N. Starburst PAMAM dendrimers: Synthetic approaches, surface modifications, and biomedical applications. *Arabian Journal of Chemistry*. 2020; 13 (7): 6009–39.
2. Abedi-Gaballu F, Dehghan G, Ghaffari M, Yekta R, Abbaspour-Ravasjani S, et al. PAMAM dendrimers as efficient drug and gene delivery nanosystems for cancer therapy. *Applied materials today*. 2018; 12: 177–90.
3. Hannon G, Lysaght J, Liptrott NJ, Prina-Mello A. Immunotoxicity considerations for next generation cancer nanomedicines. *Advanced Science*. 2019; 6 (19): 1900133.
4. Fox LJ, Richardson RM, Briscoe WH. PAMAM dendrimer — cell membrane interactions. *Advances in Colloid and Interface Science*. 2018; 257: 1–18.
5. Florendo M, Figacz A, Srinageshwar B, Sharma A, Swanson D, et al. Use of Polyamidoamine Dendrimers in Brain Diseases. *Molecules*. 2018; 23: 2238.
6. Igartúa DE, Martínez CS, Temprana CF, Alonso S del V, Jimena Prieto M. PAMAM dendrimers as a carbamazepine delivery system for neurodegenerative diseases: A biophysical and nanotoxicological characterization. *International Journal of Pharmaceutics*. 2018; 544 (1): 191–202.
7. Yan C, Gu J, Lv Y, Shi W, Wang Y, et al. Caproyl-Modified G2 PAMAM Dendrimer (G2-AC) Nanocomplexes Increases the Pulmonary Absorption of Insulin. *AAPS PharmSciTech*. 2019; 20: 298.
8. Xie H, Li L, Sun Y, Wang Y, Gao S, et al. An Available Strategy for Nasal Brain Transport of Nanocomposite Based on PAMAM Dendrimers via In Situ Gel. *Nanomaterials*. 2019; 9 (2): 147.
9. Alberto RFR, Martiniano B, Saúl RH, Jazmín GM, Mara GS, et al. In silico and in vivo studies of gp120-HIV-derived peptides in complex with G4-PAMAM dendrimers. *RSC Advances*. 2020; 10 (35): 20414–26.
10. Kheraldine H, Rachid O, Habib AM, Moustafa A-E, Benter IF, et al. Emerging innate biological properties of nano-drug delivery systems: A focus on PAMAM dendrimers and their clinical potential. *Advanced Drug Delivery Reviews*. 2021; 178: 113908.
11. Thiagarajan G, Sadekar S, Greish K, Ray A, Ghandehari H. Evidence of oral translocation of anionic G6.5 dendrimers in mice. *Molecular pharmaceutics*. 2013; 10 (3): 988–98.
12. Baxrushina EO, Anurova MN, Demina NB, Lapik IV, Turaeva AR, i dr. Sistemy dostavki oftal'mologicheskix preparatov (obzor). *Razrabotka i registraciya lekarstvennyx sredstv*. 2020; 10 (1): 57–66. Russian.
13. Prajapati SK, Jain A. Dendrimers for Advanced Drug Delivery. In *Advanced Biopolymeric Systems for Drug Delivery*. Eds: Springer, Cham. 2020; 339–60.
14. Wang J, Williamson GS, Lancina III MG, Yang H. Mildly cross-linked dendrimer hydrogel prepared via aza-Michael addition reaction for topical brimonidine delivery. *Journal of biomedical nanotechnology*. 2017; 13 (9): 1089–96.
15. Belamkar A, Harris A, Zukerman R, Siesky B, Oddone F, et al. Sustained release glaucoma therapies: Novel modalities for overcoming key treatment barriers associated with topical medications. *Annals of Medicine*. 2022; 54 (1): 343–58.
16. Liko F, Hindre F, Fernandez-Megia E. Dendrimers as innovative radiopharmaceuticals in cancer radionanotherapy. *Biomacromolecules*. 2016; 17 (10): 3103–14.
17. Jinhe Z, Ruimin W, Jianqiu Z, Yongming C, Wang X, et al. RGDyC peptide-Modified PAMAM Dendrimer Conjugates Labeled with Radionuclide¹³¹I for SPECT Imaging and Radiotherapy of Lung Carcinoma. *Journal of Nuclear Medicine*. 2019; 60 (1): 1056.
18. Marcinkowska M, Sobierajska E, Stanczyk M, Janaszewska A, Chworos A, et al. Conjugate of PAMAM Dendrimer, Doxorubicin and Monoclonal Antibody—Trastuzumab: The New Approach of a Well-Known Strategy. *Polymers*. 2018; 10: 187.
19. Araújo R, Santos S, Igne Ferreira E, Giarolla J. New Advances in General Biomedical Applications of PAMAM Dendrimers. *Molecules*. 2018; 23 (11): 2849–76.
20. Bhadra D, Bhadra S, Jain S, Jain NK. A PEGylated dendritic nanoparticulate carrier of fluorouracil. *Int J Pharm*. 2003; 257 (1–2): 111–24.
21. Surekha B, Kommana NS, Dubey SK, Kumar AP, Shukla R, et al. PAMAM dendrimer as a talented multifunctional biomimetic nanocarrier for cancer diagnosis and therapy. *Colloids and Surfaces B: Biointerfaces*. 2021; 204: 111837.
22. Gupta L, Sharma AK, Gothwal A, Khan MS, Khinchi MP, et al. Dendrimer encapsulated and conjugated delivery of berberine: A novel approach mitigating toxicity and improving in vivo pharmacokinetics. *International journal of pharmaceutics*. 2017; 528 (1–2): 88–99.
23. Chen G, Jaskula-Sztul R, Harrison A, Dammalapati A, Xu W, et al. KE108-conjugated unimolecular micelles loaded with a novel HDAC inhibitor thailandepsin-A for targeted neuroendocrine cancer therapy. *Biomaterials*. 2016; 97: 22–33.
24. Srivastava A, Tripathi PK. PAMAM dendrimer-vitamin conjugate for delivery of paclitaxel as anticancer agent. *International Journal of Green Pharmacy*. 2020; 14 (4): 360–6.
25. Xu X, Li Y, Lu X, Sun Y, Luo J, et al. Glutaryl polyamidoamine dendrimer for overcoming cisplatin-resistance of breast cancer cells. *Journal of Nanoscience and Nanotechnology*. 2018; 18 (10): 6732–9.
26. Le PN, Pham DC, Nguyen DH, Tran NQ, Dimitrov V, et al. Poly (N-isopropylacrylamide)-functionalized dendrimer as a thermosensitive nanopatform for delivering malloapelta B against HepG2 cancer cell proliferation. *Advances in Natural Sciences: Nanoscience and Nanotechnology*. 2017; 8 (2): 025014.
27. Parsian M, Mutlu P, Yalcin S, Tezcaner A, Gunduz U. Half generations magnetic PAMAM dendrimers as an effective system for targeted gemcitabine delivery. *International Journal of Pharmaceutics*. 2016; 515 (1–2): 104–13.
28. Majidzadeh H, Araj-Khodaei M, Ghaffari M, Torbati M, Dolatabadi JEN, et al. Nano-based delivery systems for berberine: A modern anti-cancer herbal medicine. *Colloids and Surfaces B: Biointerfaces*.

- 2020; 194: 111188.
29. Marcinkowska M, Stanczyk M, Janaszewska A, Gajek A, Ksiezak M, et al. Molecular Mechanisms of Antitumor Activity of PAMAM Dendrimer Conjugates with Anticancer Drugs and a Monoclonal Antibody. *Polymers*. 2019; 11 (9): 1422.
 30. Yellepeddi VK, Kumar A, Maher DM, Chauhan SC, Vangara KK, et al. Biotinylated PAMAM dendrimers for intracellular delivery of cisplatin to ovarian cancer: role of SMVT. *Anticancer research*. 2011; 31 (3): 897–906.
 31. Chanphai P, Tajmir-Riahi HA. Encapsulation of micronutrients resveratrol, genistein, and curcumin by folic acid-PAMAM nanoparticles. *Molecular and Cellular Biochemistry*. 2018; 449 (1): 157–66.
 32. Tang Q, Liu D, Chen H, He D, Pan W, et al. Functionalized PAMAM-Based system for targeted delivery of miR-205 and 5-fluorouracil in breast cancer. *Journal of Drug Delivery Science and Technology*. 2022; 67: 102959.
 33. Narmani A, Arani MAA, Mohammadnejad J, Vaziri AZ, Solymani S, et al. Breast tumor targeting with PAMAM-PEG-5FU-99mTc as a new therapeutic nanocomplex: in in-vitro and in-vivo studies. *Biomedical Microdevices*. 2020; 22 (2): 1–13.
 34. Ren Y, Kang CS, Yuan XB, Zhou X, Xu P, et al. Co-delivery of as-miR-21 and 5-FU by poly (amidoamine) dendrimer attenuates human glioma cell growth in vitro. *Journal of Biomaterials Science, Polymer Edition*. 2010; 21 (3): 303–14.
 35. Yoyen-Ermis D, Ozturk-Atar K, Kursunel MA, Aydin C, Ozkazanc D, et al. Tumor-induced myeloid cells are reduced by gemcitabine-loaded PAMAM dendrimers decorated with anti-Flt1 antibody. *Molecular pharmaceutics*. 2018; 15 (4): 1526–33.
 36. Bai CZ, Choi S, Nam K, An S, Park JS. Arginine modified PAMAM dendrimer for interferon beta gene delivery to malignant glioma. *International journal of pharmaceutics*. 2013; 445 (1–2): 79–87.
 37. Chauhan AS. Dendrimers for drug delivery. *Molecules*. 2018; 23 (4): 938.
 38. Bourne N, Stanberry LR, Kern ER, Holan G, Matthews B, et al. Dendrimers, a new class of candidate topical microbicides with activity against herpes simplex virus infection. *Antimicrobial agents and chemotherapy*. 2000; 44 (9): 2471–4.
 39. Vahedifard F, Chakravarthy K. Nanomedicine for COVID-19: The role of nanotechnology in the treatment and diagnosis of COVID-19. *Emergent materials*. 2021; 4 (1): 75–99.
 40. Günther SC, Maier JD, Vetter J, Podvalnyy N, Khanzhin N, et al. Antiviral potential of 3'-sialyllactose-and 6'-sialyllactose-conjugated dendritic polymers against human and avian influenza viruses. *Scientific reports*. 2020; 10 (1): 1–9.
 41. Bohr A, Tsapis N, Foged C, Andreana I, Yang M, et al. Treatment of acute lung inflammation by pulmonary delivery of anti-TNF- α siRNA with PAMAM dendrimers in a murine model. *European Journal of Pharmaceutics and Biopharmaceutics*. 2020; 156: 114–120.
 42. Jeon P, Choi M, Oh J, Lee M. Dexamethasone-Conjugated Polyamidoamine Dendrimer for Delivery of the Heme Oxygenase-1 Gene into the Ischemic Brain. *Macromolecular Bioscience*. 2015; 15 (7): 1021–8.
 43. Wang B, Navath RS, Romero R, Kannan S, Kannan R. Anti-inflammatory and anti-oxidant activity of anionic dendrimer-N-acetyl cysteine conjugates in activated microglial cells. *International journal of pharmaceutics*. 2009; 377 (1–2): 159–68.
 44. Kurtoglu YE, Navath RS, Wang B, Kannan S, Romero R, et al. Poly (amidoamine) dendrimer-drug conjugates with disulfide linkages for intracellular drug delivery. *Biomaterials*. 2009; 30 (11): 2112–21.
 45. Inapagolla R, Guru BR, Kurtoglu YE, Gao X, Lieh-Lai M, et al. In vivo efficacy of dendrimer-methylprednisolone conjugate formulation for the treatment of lung inflammation. *International journal of pharmaceutics*. 2010; 399 (1–2): 140–7.
 46. Vaidya A, Jain S, Pathak K, Pathak D. Dendrimers: Nanosized multifunctional platform for drug delivery. *Drug Delivery Letters*. 2018; 8 (1): 3–19.
 47. Thanh VM, Nguyen TH, Tran TV, Ngoc UTP, Ho MN, et al. Low systemic toxicity nanocarriers fabricated from heparin-mPEG and PAMAM dendrimers for controlled drug release. *Materials Science and Engineering: C*. 2018; 82: 291–8.
 48. Pandey P, Mehta M, Shukla S, Wadhwa R, Singhvi G, et al. Emerging nanotechnology in chronic respiratory diseases. *Nanofabrications in Human Health*. 2020: 449–68.
 49. Paull JRA, Luscombe CA, Castellarnau A, Heery GP, Bobardt MD, Galloway PA. Protective Effects of Astodimer Sodium 1% Nasal Spray Formulation against SARS-CoV-2 Nasal Challenge in K18-hACE2 Mice. *Viruses*. 2021; 13: 1656.

Литература

1. Kharwade R, More S, Warokar A, Agrawal P, Mahajan N. Starburst PAMAM dendrimers: Synthetic approaches, surface modifications, and biomedical applications. *Arabian Journal of Chemistry*. 2020; 13 (7): 6009–39.
2. Abedi-Gaballu F, Dehghan G, Ghaffari M, Yekta R, Abbaspour-Ravasjani S, et al. PAMAM dendrimers as efficient drug and gene delivery nanosystems for cancer therapy. *Applied materials today*. 2018; 12: 177–90.
3. Hannon G, Lysaght J, Liptrott NJ, Prina-Mello A. Immunotoxicity considerations for next generation cancer nanomedicines. *Advanced Science*. 2019; 6 (19): 1900133.
4. Fox LJ, Richardson RM, Briscoe WH. PAMAM dendrimer — cell membrane interactions. *Advances in Colloid and Interface Science*. 2018; 257: 1–18.
5. Florendo M, Figacz A, Srinageshwar B, Sharma A, Swanson D, et al. Use of Polyamidoamine Dendrimers in Brain Diseases. *Molecules*. 2018; 23: 2238.
6. Igarúa DE, Martínez CS, Temprana CF, Alonso S del V, Jimena Prieto M. PAMAM dendrimers as a carbamazepine delivery system for neurodegenerative diseases: A biophysical and nanotoxicological characterization. *International Journal of Pharmaceutics*. 2018; 544 (1): 191–202.
7. Yan C, Gu J, Lv Y, Shi W, Wang Y, et al. Caproyl-Modified G2 PAMAM Dendrimer (G2-AC) Nanocomplexes Increases the Pulmonary Absorption of Insulin. *AAPS PharmSciTech*. 2019; 20: 298.
8. Xie H, Li L, Sun Y, Wang Y, Gao S, et al. An Available Strategy for Nasal Brain Transport of Nanocomposite Based on PAMAM Dendrimers via In Situ Gel. *Nanomaterials*. 2019; 9 (2): 147.
9. Alberto RFR, Martiniano B, Saúl RH, Jazmín GM, Mara GS, et al. In silico and in vivo studies of gp120-HIV-derived peptides in complex with G4-PAMAM dendrimers. *RSC Advances*. 2020; 10 (35): 20414–26.
10. Kheraldine H, Rachid O, Habib AM, Moustafa A-E, Benter IF, et al. Emerging innate biological properties of nano-drug delivery systems: A focus on PAMAM dendrimers and their clinical potential. *Advanced Drug Delivery Reviews*. 2021; 178: 113908.
11. Thiagarajan G, Sadekar S, Greish K, Ray A, Ghandehari H. Evidence of oral translocation of anionic G6.5 dendrimers in mice. *Molecular pharmaceutics*. 2013; 10 (3): 988–98.
12. Бахрушина Е. О., Анурова М. Н., Демина Н. Б., Лапик И. В., Тураева А. Р., и др. Системы доставки офтальмологических препаратов (обзор). Разработка и регистрация лекарственных средств. 2020; 10 (1): 57–66.
13. Prajapati SK, Jain A. Dendrimers for Advanced Drug Delivery. In *Advanced Biopolymeric Systems for Drug Delivery*. Eds: Springer, Cham. 2020; 339–60.
14. Wang J, Williamson GS, Lancina III MG, Yang H. Mildly cross-linked dendrimer hydrogel prepared via aza-Michael addition reaction for topical brimonidine delivery. *Journal of biomedical nanotechnology*. 2017; 13 (9): 1089–96.
15. Belamkar A, Harris A, Zukerman R, Siesky B, Oddone F, et al. Sustained release glaucoma therapies: Novel modalities for overcoming key treatment barriers associated with topical medications. *Annals of Medicine*. 2022; 54 (1): 343–58.
16. Liko F, Hindre F, Fernandez-Megia E. Dendrimers as

- innovative radiopharmaceuticals in cancer radionanotherapy. *Biomacromolecules*. 2016; 17 (10): 3103–14.
17. Jinhe Z, Ruimin W, Jianqiu Z, Yongming C, Wang X, et al. RGDyC peptide-Modified PAMAM Dendrimer Conjugates Labeled with Radionuclide¹³¹I for SPECT Imaging and Radiotherapy of Lung Carcinoma. *Journal of Nuclear Medicine*. 2019; 60 (1): 1056.
 18. Marcinkowska M, Sobierajska E, Stanczyk M, Janaszewska A, Chworos A, et al. Conjugate of PAMAM Dendrimer, Doxorubicin and Monoclonal Antibody—Trastuzumab: The New Approach of a Well-Known Strategy. *Polymers*. 2018; 10: 187.
 19. Araújo R, Santos S, Igne Ferreira E, Giarolla J. New Advances in General Biomedical Applications of PAMAM Dendrimers. *Molecules*. 2018; 23 (11): 2849–76.
 20. Bhadra D, Bhadra S, Jain S, Jain NK. A PEGylated dendritic nanoparticulate carrier of fluorouracil. *Int J Pharm*. 2003; 257 (1–2): 111–24.
 21. Surekha B, Kommana NS, Dubey SK, Kumar AP, Shukla R, et al. PAMAM dendrimer as a talented multifunctional biomimetic nanocarrier for cancer diagnosis and therapy. *Colloids and Surfaces B: Biointerfaces*. 2021; 204: 111837.
 22. Gupta L, Sharma AK, Gothwal A, Khan MS, Khinchi MP, et al. Dendrimer encapsulated and conjugated delivery of berberine: A novel approach mitigating toxicity and improving in vivo pharmacokinetics. *International journal of pharmaceutics*. 2017; 528 (1–2): 88–99.
 23. Chen G, Jaskula-Sztul R, Harrison A, Dammalapati A, Xu W, et al. KE108-conjugated unimolecular micelles loaded with a novel HDAC inhibitor thailandepsin-A for targeted neuroendocrine cancer therapy. *Biomaterials*. 2016; 97: 22–33.
 24. Srivastava A, Tripathi PK. PAMAM dendrimer-vitamin conjugate for delivery of paclitaxel as anticancer agent. *International Journal of Green Pharmacy*, 2020; 14 (4): 360–6.
 25. Xu X, Li Y, Lu X, Sun Y, Luo J, et al. Glutaryl polyamidoamine dendrimer for overcoming cisplatin-resistance of breast cancer cells. *Journal of Nanoscience and Nanotechnology*. 2018; 18 (10): 6732–9.
 26. Le PN, Pham DC, Nguyen DH, Tran NQ, Dimitrov V, et al. Poly (N-isopropylacrylamide)-functionalized dendrimer as a thermosensitive nanoplatform for delivering malloapelta B against HepG2 cancer cell proliferation. *Advances in Natural Sciences: Nanoscience and Nanotechnology*. 2017; 8 (2): 025014.
 27. Parsian M, Mutlu P, Yalcin S, Tezcaner A, Gunduz U. Half generations magnetic PAMAM dendrimers as an effective system for targeted gemcitabine delivery. *International Journal of Pharmaceutics*. 2016; 515 (1–2): 104–13.
 28. Majidzadeh H, Araj-Khodaei M, Ghaffari M, Torbati M, Dolatabadi JEN, et al. Nano-based delivery systems for berberine: A modern anticancer herbal medicine. *Colloids and Surfaces B: Biointerfaces*. 2020; 194: 111188.
 29. Marcinkowska M, Stanczyk M, Janaszewska A, Gajek A, Ksiezak M, et al. Molecular Mechanisms of Antitumor Activity of PAMAM Dendrimer Conjugates with Anticancer Drugs and a Monoclonal Antibody. *Polymers*. 2019; 11 (9): 1422.
 30. Yellepeddi VK, Kumar A, Maher DM, Chauhan SC, Vangara KK, et al. Biotinylated PAMAM dendrimers for intracellular delivery of cisplatin to ovarian cancer: role of SMVT. *Anticancer research*. 2011; 31 (3): 897–906.
 31. Chanphai P, Tajmir-Riahi HA. Encapsulation of micronutrients resveratrol, genistein, and curcumin by folic acid-PAMAM nanoparticles. *Molecular and Cellular Biochemistry*. 2018; 449 (1): 157–66.
 32. Tang Q, Liu D, Chen H, He D, Pan W, et al. Functionalized PAMAM-Based system for targeted delivery of miR-205 and 5-fluorouracil in breast cancer. *Journal of Drug Delivery Science and Technology*. 2022; 67: 102959.
 33. Narmani A, Arani MAA, Mohammadnejad J, Vaziri AZ, Solymani S, et al. Breast tumor targeting with PAMAM-PEG-5FU-99mTc as a new therapeutic nanocomplex: in in-vitro and in-vivo studies. *Biomedical Microdevices*. 2020; 22 (2): 1–13.
 34. Ren Y, Kang CS, Yuan XB, Zhou X, Xu P, et al. Co-delivery of as-miR-21 and 5-FU by poly (amidoamine) dendrimer attenuates human glioma cell growth in vitro. *Journal of Biomaterials Science, Polymer Edition*. 2010; 21 (3): 303–14.
 35. Yoyen-Ermis D, Ozturk-Atar K, Kursunel MA, Aydin C, Ozkazanc D, et al. Tumor-induced myeloid cells are reduced by gemcitabine-loaded PAMAM dendrimers decorated with anti-Flt1 antibody. *Molecular pharmaceutics*. 2018; 15 (4): 1526–33.
 36. Bai CZ, Choi S, Nam K, An S, Park JS. Arginine modified PAMAM dendrimer for interferon beta gene delivery to malignant glioma. *International journal of pharmaceutics*. 2013; 445 (1–2): 79–87.
 37. Chauhan AS. Dendrimers for drug delivery. *Molecules*. 2018; 23 (4): 938.
 38. Bourne N, Stanberry LR, Kern ER, Holan G, Matthews B, et al. Dendrimers, a new class of candidate topical microbicides with activity against herpes simplex virus infection. *Antimicrobial agents and chemotherapy*. 2000; 44 (9): 2471–4.
 39. Vahedifard F, Chakravarthy K. Nanomedicine for COVID-19: The role of nanotechnology in the treatment and diagnosis of COVID-19. *Emergent materials*. 2021; 4 (1): 75–99.
 40. Günther SC, Maier JD, Vetter J, Podvalnyy N, Khanzhin N, et al. Antiviral potential of 3'-sialyllactose-and 6'-sialyllactose-conjugated dendritic polymers against human and avian influenza viruses. *Scientific reports*. 2020; 10 (1): 1–9.
 41. Bohr A, Tsapis N, Foged C, Andreana I, Yang M, et al. Treatment of acute lung inflammation by pulmonary delivery of anti-TNF- α siRNA with PAMAM dendrimers in a murine model. *European Journal of Pharmaceutics and Biopharmaceutics*. 2020; 156: 114–120.
 42. Jeon P, Choi M, Oh J, Lee M. Dexamethasone-Conjugated Polyamidoamine Dendrimer for Delivery of the Heme Oxygenase-1 Gene into the Ischemic Brain. *Macromolecular Bioscience*. 2015; 15 (7): 1021–8.
 43. Wang B, Navath RS, Romero R, Kannan S, Kannan R. Anti-inflammatory and anti-oxidant activity of anionic dendrimer-N-acetyl cysteine conjugates in activated microglial cells. *International journal of pharmaceutics*. 2009; 377 (1–2): 159–68.
 44. Kurtoglu YE, Navath RS, Wang B, Kannan S, Romero R, et al. Poly (amidoamine) dendrimer-drug conjugates with disulfide linkages for intracellular drug delivery. *Biomaterials*. 2009; 30 (11): 2112–21.
 45. Inapagolla R, Guru BR, Kurtoglu YE, Gao X, Lieh-Lai M, et al. In vivo efficacy of dendrimer-methylprednisolone conjugate formulation for the treatment of lung inflammation. *International journal of pharmaceutics*. 2010; 399 (1–2): 140–7.
 46. Vaidya A, Jain S, Pathak K, Pathak D. Dendrimers: Nanosized multifunctional platform for drug delivery. *Drug Delivery Letters*. 2018; 8 (1): 3–19.
 47. Thanh VM, Nguyen TH, Tran TV, Ngoc UTP, Ho MN, et al. Low systemic toxicity nanocarriers fabricated from heparin-mPEG and PAMAM dendrimers for controlled drug release. *Materials Science and Engineering: C*. 2018; 82: 291–8.
 48. Pandey P, Mehta M, Shukla S, Wadhwa R, Singhvi G, et al. Emerging nanotechnology in chronic respiratory diseases. *Nanoformulations in Human Health*. 2020: 449–68.
 49. Paull JRA, Luscombe CA, Castellamau A, Heery GP, Bobardt MD, Gallay PA. Protective Effects of Astodimer Sodium 1% Nasal Spray Formulation against SARS-CoV-2 Nasal Challenge in K18-hACE2 Mice. *Viruses*. 2021; 13: 1656.

SPECIFICS OF THE WORKLOAD-DEPENDENT DYNAMICS OF PSYCHO-EMOTIONAL EXHAUSTION AMONG MEDICAL STAFF OF A COVID HOSPITAL

Nazaryan SE ✉, Samoilov AS, Sedin VI

Burnasyan Federal Medical Biophysical Center, Moscow, Russia

In the beginning of 2020 there appeared an urgent need for substantial advancement of the medical and psychological support for medical personnel involved in medical care provided to patients with the new coronavirus infection (COVID-19) in hospital settings. This need originated from the necessity to diagnose the risks of doctors developing mental states that adversely affect their professional performance and, subsequently, lead to disorders. In addition, there are under-researched matters of dependence of the prevalence of destructive mental states on the intensity of workload experienced by doctors in the "red zones", where the risk of patient fatalities is high. This study aimed to investigate the workload-dependent dynamics of psycho-emotional exhaustion among the medical staff of a COVID hospital. We analyzed the psychological tests (MBI, Maslach Burnout Inventory) that 121 people completed during a four-week assignment in the "infectious" zone and two weeks in the observation department. Seventy-nine doctors comprised the heavy workload group and 42 were in the moderate workload group. The study showed that healthcare workers experiencing heavier workloads exhibit high values of the psycho-emotional exhaustion indicators more often. We registered significant differences ($p \leq 0.05$) by the Emotional Exhaustion scale at the third and fifth weeks of the study. By the fifth week, i.e., when the assignment in the "infectious zone" was over, heavy workload group had the median of 25 (23.5; 27), while in the moderate workload group it was 14 (14; 15), which is 56% lower.

Keywords: healthcare workers, COVID-19, psycho-emotional state, professional burnout, psychological testing, psycho-emotional exhaustion, emotional exhaustion, depersonalization, professional degradation

Author contributions: VI Sedin — study planning, data analysis and interpretation; SE Nazaryan — literature analysis, data collection, processing of the results; AS Samoilov — study planning.

Compliance with the ethical standards: the study was approved by the Ethical Committee of A.I. Burnasyan Federal Medical Biophysical Center (minutes #34 of April 7, 2020). All participants signed the informed consent form agreeing to psychological examination and rehabilitation program activities.

✉ **Correspondence should be addressed:** Svetlana E. Nazaryan
Marshala Novikova, 23, Moscow, 123098, Russia; sveta-nazaryan@yandex.ru

Received: 01.03.2022 **Accepted:** 15.03.2022 **Published online:** 28.03.2022

DOI: 10.47183/mes.2022.010

ОСОБЕННОСТИ ДИНАМИКИ ПСИХОЭМОЦИОНАЛЬНОГО ИСТОЩЕНИЯ У МЕДИЦИНСКОГО ПЕРСОНАЛА COVID-ГОСПИТАЛЯ С РАЗЛИЧНОЙ ИНТЕНСИВНОСТЬЮ ТРУДОВОЙ НАГРУЗКИ

С. Е. Назарян ✉, А. С. Самойлов, В. И. Седин

Федеральный медицинский биофизический центр имени А. И. Бурназяна, Москва, Россия

С начала 2020 г. появилась острая потребность в развитии медико-психологического обеспечения медицинского персонала, задействованного в оказании медицинской помощи пациентам с новой коронавирусной инфекцией (COVID-19) в стационарных условиях. Она продиктована необходимостью диагностики рисков развития у врачей психических состояний, приводящих к снижению эффективности профессиональной деятельности и, в итоге, к заболеваниям. Кроме того, недостаточно изучены вопросы влияния на распространенность деструктивных психических состояний у медиков интенсивности нагрузки при работе непосредственно в «красной зоне» в отделениях с повышенным риском смертности у пациентов. Целью работы было изучить динамику психоэмоционального истощения у медперсонала COVID-госпиталя с различной интенсивностью трудовой нагрузки. Проанализированы результаты психологического обследования 121 человека с использованием «Опросника профессионального выгорания Маслаха» (MBI) в течение четырехнедельной работы в «заразной» зоне и двухнедельного пребывания в обсервации. В группу с высокой интенсивностью нагрузки вошло 79 медиков, в группу со средней интенсивностью — 42. Показано, что у медперсонала, чей труд был связан с большей интенсивностью, чаще встречается высокий уровень показателей психоэмоционального истощения. Так, по шкале «Эмоциональное истощение» достоверные различия ($p \leq 0,05$) получены на третьей и пятой неделях исследования. На пятой неделе исследования, т. е. после окончания работы в «заразной зоне», в группе с высокой интенсивностью нагрузки медиана составила 25 (23,5; 27), в то время как в группе со средней интенсивностью она была на 56% ниже и составила 14 (14; 15).

Ключевые слова: медицинский персонал, COVID-19, психоэмоциональное состояние, профессиональное выгорание, психологическое обследование, психоэмоциональное истощение, эмоциональное истощение, деперсонализация, редукция профессиональных достижений

Вклад авторов: В. И. Седин — планирование исследования, анализ и интерпретация данных; С. Е. Назарян — анализ литературы, сбор данных, обработка результатов; А. С. Самойлов — планирование исследования.

Соблюдение этических стандартов: исследование одобрено этическим комитетом Федерального медицинского биофизического центра имени А. И. Бурназяна (протокол № 34 от 7 апреля 2020 г.). Все участники подписали информированное согласие на психологическое обследование и использование реабилитационной программы.

✉ **Для корреспонденции:** Светлана Евгеньевна Назарян
ул. Маршала Новикова, д. 23, г. Москва, 123098, Россия; sveta-nazaryan@yandex.ru

Статья получена: 01.03.2022 **Статья принята к печати:** 15.03.2022 **Опубликована онлайн:** 28.03.2022

DOI: 10.47183/mes.2022.010

Healthcare professionals, especially those working in COVID hospitals where the conditions are excessively stressful, run the risk of development of psycho-emotional exhaustion and other negative mental conditions, like persistently bad mood, deteriorating health, sleep disorders, asthenia, emotional exhaustion, professional burnout [1–4]. These problems call for

solutions, which, in turn, necessitate development of a program and implementation of preventive psycho-corrective measures designed to counter progression of negative mental states and, ultimately, deterioration of professional effectiveness [5]. Many researchers note that extreme conditions of work peculiar to activities of many medical professionals translate into high risks

of development of negative mental conditions, e.g., persistently bad mood, deteriorating health, sleep disorders, asthenia, emotional exhaustion, professional burnout etc [1, 6, 7].

Previously, researchers have confirmed the leading role of psycho-emotional stress in the development of negative states when working conditions are extreme [8, 9]. For healthcare professionals, work inside quarantine, so-called "infectious" zones, in direct contact with COVID-19 patients, is the leading factor driving development of the aforementioned mental health disorders [10, 11]. A good example is the study that involved over 2000 Italian healthcare workers at the peak of the COVID-19 pandemic. The researchers found that medical professionals manning intensive care units and helping infected patients first-hand exhibited symptoms of post-traumatic stress disorder (66%), high level of anxiety (64%) and severe depression (42%). The findings included the conclusion that healthcare personnel of the departments where patients run high risk of death are more susceptible to mental health disorders [12]. Similar studies were conducted in the Russian Federation [2, 4, 13, 14]. One of them involved 248 people, its objective was to investigate professional burnout and emotional maladjustment among medical workers. According to the results of this study, over 60% of medical professionals experience emotional burnout, 23% suffer manifestations of symptoms of depression and 25% have high level of anxiety [13]. Authors of the study state that the frequency of identification of these symptoms in healthcare personnel working directly with COVID-19 patients is higher than in those who do not work with them. When the same sample of medical professionals was re-examined 4 months later, the occurrence of burnout symptoms decreased to 35%, depression symptoms — to 8.3%, but the frequency of high anxiety cases has grown to 29.3%.

It is well-known that distribution of workload among healthcare workers in COVID hospitals is not uniform. This fact is confirmed by the regulatory documents [15, 16] describing specifics of work of medical and nursing staff. Management of COVID hospitals, which sets the pay rates for various departments thereof, is also well aware of the non-uniform distribution of workload.

This study aimed to investigate the specifics of workload-dependent dynamics of psycho-emotional exhaustion among medical staff of a COVID hospital.

METHODS

Criteria for inclusion of medical workers in the study: permanent stay in a COVID-hospital; work in "infectious" zone and observation department; provision of medical care (as part of professional duties) in direct contact with infected patients of the COVID hospital. The exclusion criteria were refusal to participate in the study, violation of the study plan.

The study sample included 121 people, 87 female and 34 male. Forty-two of them were medical doctors, 79 — nursing staff. Twenty-six doctors and 53 nurses made up the heavy workload group: they discharged their professional duties in the "infectious" zone of the COVID hospital, in departments where the risks of patient mortality and medical personnel infection were high (intensive care units, emergency room and departments for patients with severe disease). The moderate workload group included 20 doctors and 22 nurses working in the COVID hospital departments where the risk of mortality among patients was low (two aftercare departments).

The level of workload was assessed by experts; the assessment factored in the intensity of work in the departments of the COVID hospital, the likelihood of patient deaths infection

of the staff with coronavirus. The experts ($n = 12$) were medical doctors with at least 10 years of experience in intensive care units and managers of the clinical departments of the Center the study was conducted at. The participating healthcare professionals were distributed into heavy and moderate workload groups. Experts found no doctors nor nurses whose workload could be qualified as "light."

To identify signs of emotional burnout, the state of the medical personnel of the COVID hospital was monitored remotely with the help of a the questionnaire (Google Form) the link to which was sent to the participants via WhatsApp messenger. In this work, we used the Maslach Burnout Inventory (MBI) adapted by N. E. Vodopyanova [17]. The results of the testing were analyzed by the three scales of the methodology: Emotional Exhaustion, Depersonalization and Professional Degradation. The study lasted six weeks: four weeks of work in the "infectious" zone and two weeks in the observation department. The participants were tested before starting their work in the "infectious" zone, thus giving the baseline data. After that, the testing was done every week, online.

We checked distribution of the data with the Kolmogorov-Smirnov test. Since it was not normal for most of the data, the subsequent statistical analysis was performed with nonparametric data analysis method: Mann-Whitney U test (pairwise comparison of the two groups at each time point). The differences were considered significant when the level of significance was $p \leq 0.05$.

RESULTS

In order to obtain the baseline values of Emotional Exhaustion, Depersonalization and Professional Degradation indicators under the Professional Burnout Questionnaire methodology, we tested the participants (psychological examination) before they started working in the "infectious" zone (Table 1).

The baseline values learned through the initial examination were compared with the reference values [17]; there were no negative deviations identified, which indicates the participants did not have signs of professional burnout before starting work in the "infectious" zone.

Table 2 presents the analysis of results of psychological examination of healthcare workers that had different levels of workload while working in the "infectious" zone and the observation department.

Figure 1 shows dynamics of the Emotional Exhaustion indicator depending on the level of workload throughout the study.

In the first week, neither the participants working in the departments where the risk of patient mortality was high nor those discharging duties in the rehabilitation treatment departments exhibited noticeable signs of emotional exhaustion. In the first group, the values of this indicator were in the range of 15.65 ± 4.89 , the range for the second group was 16.21 ± 4.29 .

In the heavy workload group, the highest values of the Emotional Exhaustion indicator (outside the normal range) were registered on the fifth week of the study: 25.08 ± 2.36 . By the end of the study, the values went down to the upper limit of the range of low level of emotional exhaustion and equaled 15.08 ± 2.63 .

In the moderate workload group, the highest values of the Emotional Exhaustion indicator, which lay within the average level range, were recorded on the fourth week of the study: 22.93 ± 2.83 . Further, by the fifth week, the values decreased and equaled 14.21 ± 1.05 , and by the end of the study, they returned to the normal range (15.43 ± 2.58).

Table 1. Mean professional burnout values, initial examination, by gender

Indicators (scales) of the methods	Men (<i>n</i> = 34)	Women (<i>n</i> = 87)	Reference values
Emotional exhaustion	16,65 ± 4,25	15,53 ± 4,81	16,0–24,0
Depersonalization	3,21 ± 1,47	2,78 ± 1,37	6,0–10,0
Deterioration of personal achievements	37,85 ± 1,88	36,79 ± 2,34	31,0–36,0

The differences registered on the third and fifth weeks were significant.

Figure 2 shows the dynamics of the Depersonalization indicator. The initial examination revealed no signs of depersonalization in either of the groups. The values of this indicator recorded in the heavy workload group were 2.85 ± 1.41 , in the moderate workload group — 3.00 ± 1.43 .

In the first group, by the end of the second week of the study the values of this indicator started climbing (5.28 ± 2.01) and peaked in the third week, reaching 7.30 ± 1.16 . After that, the trend is downward: 6.24 ± 1.28 from the fourth week and 4.76 ± 1.33 by the end of the study.

The second group shows similar dynamics. The values of this indicator grow up from the second week (5.76 ± 2.24) and reach their maximum levels (7.57 ± 1.21) in the third week of the study. By the end of the fourth week the values equaled 6.67 ± 1.59 , they were going down and reached the level of 3.81 ± 1.21 by the end of the sixth week.

The differences registered on the fifth and sixth weeks were significant.

The analysis of median values revealed the greatest intergroup differences at the fifth week of the study. Then, this value for the heavy workload group was at the level of 6 (5; 7), and in the moderate workload group it was 4 (3; 4). In both groups, the values of the Depersonalization indicator were going up from the first to the third week, remained consistently high through the fourth week and started going down from the fifth week. The revealed dynamics was more pronounced in the heavy workload group, which is the result of the larger number of patients treated and significant emotional and physical stress.

Figure 3 visualizes the Professional Deterioration indicator dynamics throughout the study.

Initial examination revealed no signs of manifestation of the condition behind this indicator in either of the groups, with its values being 37.00 ± 2.32 and 37.26 ± 2.19 , respectively.

In the heavy workload group, the values of this indication decrease through the second week of the study (34.87 ± 1.71)

and reach the minimum level on the third week (30.49 ± 1.91). From the end of the fourth week (34.11 ± 1.33), the trend becomes upward: on the fifth week, the values are in the range of 36.58 ± 2.20 , and on the sixth — 39.73 ± 1.37 . This fact signals of the signs of professional deterioration associated with peak loads (the second and third weeks).

A similar trend was noted in the moderate workload group. The values of the indicator decrease from the second to the third week of the study (35.24 ± 1.82 and 30.29 ± 1.99 , respectively). After that, they start to go up, with the final examination revealing no signs of professional deterioration (39.88 ± 1.19).

The values of this indicator remained within the reference range throughout the study; no significant intergroup differences were found. The lack of such differences was further confirmed by the median values and the interquartile range of the data. In terms of this indicator, the comparison groups exhibited maximum heterogeneity at the fifth week of the study, but the values showing the level of Professional Deterioration were not significantly different: 37 (35; 38) and 36 (34; 38), respectively.

DISCUSSION

Numerous studies conducted by scientists from different countries confirm that every second healthcare worker involved in the treatment of patients with the new coronavirus infection has psychological maladjustment disorders and shows symptoms of increasing fatigue, irritability, and aggression. According to the authors of these studies, it is the awareness of the high risk of contracting the potentially lethal disease, understanding the imperfection of drug therapy and the process of care provision to patients with severe complications that are most stressful for the healthcare professionals working in the quarantine zones [18–23].

The results obtained are consistent with the data reported by other researchers. The authors confirm that healthcare personnel of the departments where patients run high risk of death are more susceptible to mental health disorders [24, 25].

Table 2. Summary data on the dynamics of the workload-dependent professional burnout indicators (groups of participating healthcare workers)

Method	Group, workload level	Week of the study					
		1	2	3	4	5	6
		M ± SD	M ± SD	M ± SD	M ± SD	M ± SD	M ± SD
Emotional exhaustion	Group 1, heavy <i>n</i> = 79	15,65 ± 4,89	19,57 ± 2,93	19,76 ± 2,92	22,06 ± 2,91	25,08 ± 2,36	15,08 ± 2,63
	Group 2, moderate <i>n</i> = 42	16,21 ± 4,29	19,19 ± 2,87	12,67 ± 9,92*	22,93 ± 2,83	14,21 ± 1,05*	15,43 ± 2,58
Depersonalization	Group 1, heavy <i>n</i> = 79	2,85 ± 1,41	5,28 ± 2,01	7,30 ± 1,16	6,24 ± 1,28	5,82 ± 1,59	4,76 ± 1,33
	Group 2, moderate <i>n</i> = 42	3,00 ± 1,43	5,76 ± 2,24	7,57 ± 1,21	6,67 ± 1,59	3,36 ± 1,03*	3,81 ± 1,21*
Deterioration of personal achievements	Group 1, heavy <i>n</i> = 79	37,00 ± 2,32	34,87 ± 1,71	30,49 ± 1,91	34,11 ± 1,33	36,58 ± 2,20	39,73 ± 1,37
	Group 2, moderate <i>n</i> = 42	37,26 ± 2,19	35,24 ± 1,82	30,29 ± 1,99	34,12 ± 1,35	36,12 ± 2,48	39,88 ± 1,19

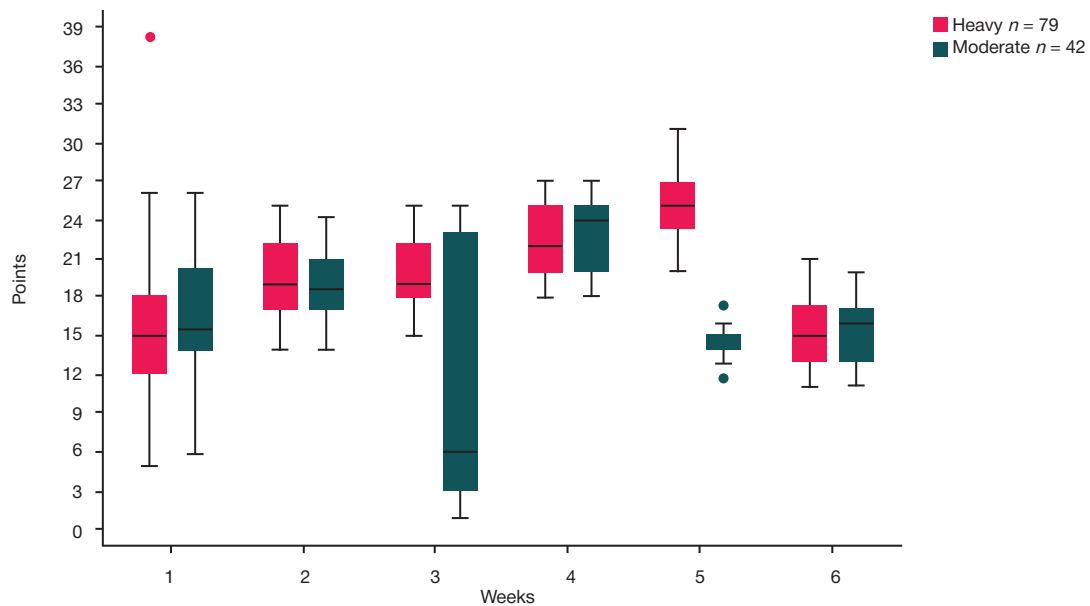


Fig. 1. Emotional Exhaustion indicator dynamics, groups with different level of workload (Me [Q₁; Q₃])

Summarizing the results of our study, we can trace the general dynamics of psycho-emotional states of healthcare professionals working under extreme conditions. The level of workload and the very character of work done by medical staff are associated with specific mental burden, which makes the person use various kinds of resources to cope.

The three scales of the Professional Burnout Questionnaire showed that in the second, third and fourth weeks of the study, the mental state of the participating healthcare professionals (both groups) was characterized by moderate manifestations of psychasthenia, apathy and emotional emptiness. Overall, the first week of the study was uneventful in terms of pronounced emotional shocks, which may indicate that the preliminary training of the medical personnel was high quality. At the second week, we registered manifestations of emotional exhaustion and depersonalization, which is the result of high saturation of the participants' work with emotions. The Emotional Exhaustion indicator values continue to grow through the third and fourth weeks of the study and finally go beyond the reference range. During the fifth and sixth weeks, the downward trend persists for the Emotional Exhaustion and Depersonalization indicator values, while the Professional Deterioration indicator shows growth, which can manifest in underestimation of one's competence, increased dissatisfaction with oneself,

underestimation of the value of work done (professional activities), negative self-perception in the professional sphere, appearance of the sense of failure, indifference to work.

CONCLUSIONS

In terms of psycho-emotional disorders, the most difficult were the second, third and fourth weeks of work in the "infectious" zone. The Workload Level and the associated specifics of professional activity should be accounted for when evaluating the dynamics of the indicators studied. The component to be paid special attention to in the analysis of the data is the interquartile range, which was larger at the beginning and decreased by the end of work in the "infectious" zone, which means the values registered then reflect the state of the majority of study participants. Medical personnel working in heavy workload departments had to deal with severe cases and patient mortality more often; in this connection, the dynamics of their psychological state is peculiar in its low variability and high values of indicators of the psycho-emotional burnout. The peculiarities of the dynamics of development of negative psychological conditions in healthcare professionals working in difficult epidemiological conditions are important factors in the process of designing preventive and corrective psychological

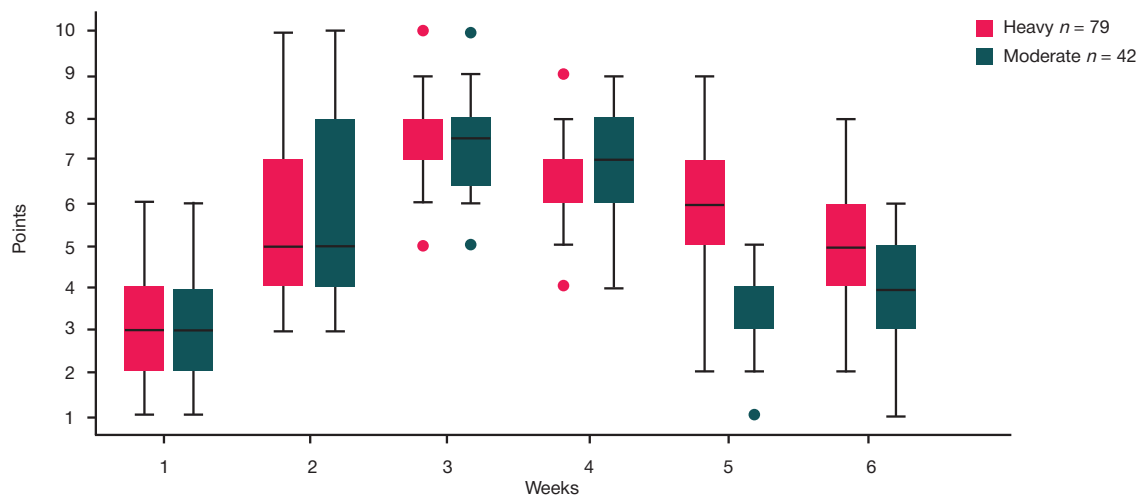


Fig. 2. Depersonalization indicator dynamics, groups with different level of workload (Me [Q₁; Q₃])

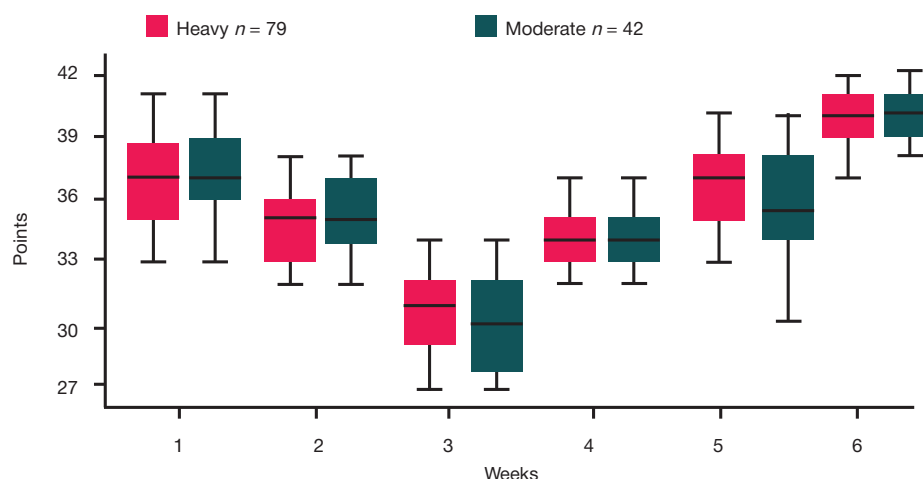


Fig. 3. Professional Deterioration indicator dynamics, groups with different level of workload (Me [Q₁; Q₃])

support and recovery programs for those who discharge their professional duties in extreme conditions with limited opportunities for direct contact in the context of psychological support rendered to them. In this case, the relevant methods are those of cognitive-behavioral therapy (reading or online

viewing of lectures containing sections about possible negative mental states and methods for their self-correction, methods for switching internal behavioral attitudes — psychophysical gymnastics) and art therapy, which can be applied without external assistance.

References

- Bushmanov AYu, Galstyan IA, Solovov VYu, Konchalovskij MV. Uroki dlya zdravooxraneniya: avariya na ChAEHS i pandemiya COVID-19. Medicinskaya radiologiya i radiacionnaya bezopasnost'. 2020; 65 (3): 79–84. Russian.
- Nazaryan SE, Samojlov AS, Pustovojt VI, Petrova MS. Psixoehmocional'noe sostoyanie medicinskix sotrudnikov, uchastvuyushix v rabote infekcionnyx stacionarov COVID-19. V sbornike: Materialy XX yubilejnogo Vserossijskogo foruma «Zdravnica-2021»; 15–17 iyunya 2021 g.; Moskva, 2021; s. 86–89. Russian.
- Sedin VI, Kolyuchkin SN. Teoriya i praktika beskontaktnoj psixodiagnostiki. Apparatnye sredstva v psixologicheskoy podgotovke. V sbornike: Materialy mezhhregional'noj nauchno-prakticheskoy konferencii psixologov silovyx struktur «Nauchno-metodicheskie aspekty ispol'zovaniya programmno-apparatnyx sredstv i trenazherov v psixologicheskoy podgotovke voennosluzhashchix»; 25 oktyabrya, 2017 g.; Moskva, 2018; s. 59–63. Russian.
- Xolmogorova AB, Petrikov SS, Suroegina AYU, Mikita OYu, Raxmanina AA, Roj AP. Problema professional'nogo vygoraniya i psixicheskogo zdorov'ya medicinskix rabotnikov vo vremya pandemii COVID-19. Zhurnal im. N. V. Sklifosovskogo. Neotlozhnaya medicinskaya pomoshh'. 2020; 9 (3): 321–37. Russian.
- Samojlov AS, Nazaryan SE. Programma vosstanovleniya dlya medicinskix rabotnikov v usloviyax medicinskoj mobilizacii. Sovremennye voprosy biomeditsiny. 2020; 3: 35–37. Russian.
- Bulygina VG. Vliyaniye ehkstremaal'nyx faktorov sluzhebnoj deyatel'nosti na psixicheskoe zdorov'e specialistov opasnyx professij (obzor zarubezhnyx issledovaniy). V sb.: V. G. Bulygina, S. V. Shport, A. A. Dubinskij, M. M. Pronicheva. Mediko-biologicheskie i social'no-psixologicheskie problemy bezopasnosti v chrezvychajnyx situatsiyax. 2017; 3: 93–100. Russian.
- Sobolnikov VV. Psixologiya professional'noj deyatel'nosti v osobyax i ehkstremaal'nyx usloviyax. M.: Yurajt, 2019; 190 s. Russian.
- Bhattacharyya M, Pal MS, Sharma YK, Majumdar D. Changes in sleep patterns during prolonged stays in Antarctica. Int J Biometeorol. 2008; 52 (8): 869–79.
- Ushakov IB, Ujba VV, Sapeckij AO. Mediko-biologicheskie riski, svyazannye s vypolneniem dal'nix kosmicheskix poletov. Medicina ehkstremaal'nyx situatsij. 2017; 1: 43–64. Russian.
- Lee SA. How much “Thinking” about COVID-19 is clinically dysfunctional? Brain, Behavior, and Immunity. 2020; 87: 97–98.
- Labrague LJ, de Los Santos JAA. COVID-19 anxiety among front-line nurses: Predictive role of organisational support, personal resilience and social support. J Nurs Manag. 2020; 28 (7): 1653–61.
- Luceño-Moreno L, Talavera-Velasco B, García-Albuérne Y, Martín-García J. Symptoms of posttraumatic stress, anxiety, depression, levels of resilience and burnout in Spanish health personnel during the COVID-19 Pandemic. Int J Environ Res Public Health. 2020; 17 (15): 5514.
- Petrikov SS, Xolmogorova AB, Suroegina AYU, Mikita OYu, Roj AP, Raxmanina AA. Professional'noe vygoranie, simptomy ehmoacional'nogo neblagopoluchiya i distressa u medicinskix rabotnikov vo vremya ehpidemii COVID-19. Konsul'tativnaya psixologiya i psixoterapiya. 2020; 65 (3): 8–45. Russian.
- Sorokin MYU, Kasyanov ED, Rukavishnikov GV, Makarevich OV, Neznakov NG, Lutova NB, i dr. Psixologicheskie reakcii naseleniya kak faktor adaptatsii k pandemii COVID-19. Obozrenie psixiatrii i medicinskoj psixologii imeni V. M. Bextereva. 2020; (2): 87–94. Russian.
- Prikaz Ministerstva truda i social'noj zashhity Rossijskoj Federacii ot 31 iyulya 2020 g № 475n Ob utverzhenii professional'nogo standarta «Medicinskaya sestra/medicinskij brat». Dostupno po ssylke: <https://normativ.kontur.ru/document?moduleId=1&documentId=370329>. Russian.
- Metodicheskie rekomendacii MP 3.1.0229-21 «Rekomendacii po organizacii protivoehpideemicheskix meropriyatij v medicinskix organizatsiyax, osushhestvlyayushhix okazanie medicinskoj pomoshhi pacientam s novoj koronavirusnoj infekciej (COVID-19) (podozreniem na zaboolevanie) v stacionarnyx usloviyax» (utv. Federal'noj sluzhboj po nadzoru v sfere zashhity prav potrebitel' i blagopoluchiya cheloveka 18 yanvarya 2021 g.). Dostupno po ssylke: <https://base.garant.ru/400232151/>. Russian.
- Vodopyanova NE, Starchenkova EN. Sindrom vygoraniya: Diagnostika i profilaktika. 2-e izd. SPb.: Piter, 2008; 254 s. Russian.
- Arafa A, Mohammed Z, Mahmoud O. Elshazley M, Ewis A. Depressed, anxious, and stressed: What have healthcare workers on the frontlines in Egypt and Saudi Arabia experienced during the COVID-19 pandemic? Journal of Affective Disorders. 2021; 278: 365–71.
- Gorini A, Fiabane E, Sommaruga M, Barbieri S, Sottotetti F, Rovere MT et al. Mental health and risk perception among Italian healthcare workers during the second month of the Covid-19

- pandemic. *Archives of Psychiatric Nursing*. 2020. 34 (6): 537–44.
20. Huang JZ, Han MF, Luo TD, Ren AK, Zhou XP. Mental health survey of medical staff in a tertiary infectious disease hospital for COVID-19. *Zhonghua Lao Dong Wei Sheng Zhi Ye Bing Za Zhi*. 2020; 38 (3): 192–5.
 21. Lasalvia A, Bonetto C, Porru S, Carta A, Tardivo S, Bovo C, et al. Psychological impact of COVID-19 pandemic on healthcare workers in a highly burdened area of north-east Italy. *Epidemiol Psychiatr Sci*. 2020; DOI: 10.1017/S2045796020001158.
 22. Song X, Fu W, Liu X, Luo Z, Wang R, Zhou N. Mental health status of medical staff in emergency departments during the Coronavirus disease 2019 epidemic in China. *Brain, behavior, and immunity*. 2020; 88: 60–65.
 23. Zhu J, Sun L, Zhang L, Wang H, Fan A, Yang B. Prevalence and influencing factors of anxiety and depression symptoms in the first-line medical staff fighting against COVID-19 in Gansu. *Front Psychiatry*. 2020; 11: 386.
 24. Antonijevic J, Binic I, Zikic O, Manojlovic S, Tosic-Golubovic S, Popovic N. Mental health of medical personnel during the COVID-19 pandemic. *Brain and Behavior*. 2020; 10 (12): 01881.
 25. Rossi R, Socci V, Pacitti F, Siracusano A, Rossi A, Di Lorenzo G. Mental health outcomes among frontline and second-line health care workers during the Coronavirus disease 2019 (COVID-19) Pandemic in Italy. *JAMA Network Open*. 2020; 3 (5): 2010185.

Литература

1. Бушманов А. Ю., Галстян И. А., Соловьев В. Ю., Кончаловский М. В. Уроки для здравоохранения: авария на ЧАЭС и пандемия COVID-19. *Медицинская радиология и радиационная безопасность*. 2020. 65 (3): 79–84.
2. Назарян С. Е., Самойлов А. С., Пустовойт В. И., Петрова М. С. Психосоциальное состояние медицинских сотрудников, участвующих в работе инфекционных стационаров COVID-19. В сборнике: Материалы XX юбилейного Всероссийского форума «Здравница-2021»; 15–17 июня 2021 г.; Москва, 2021; с. 86–89.
3. Седин В. И., Колочкин С. Н. Теория и практика бесконтактной психодиагностики. Аппаратные средства в психологической подготовке. В сборнике: Материалы межрегиональной научно-практической конференции психологов силовых структур «Научно-методические аспекты использования программно-аппаратных средств и тренажеров в психологической подготовке военнослужащих»; 25 октября, 2017 г.; Москва, 2018; с. 59–63.
4. Холмогорова А. Б., Петриков С. С., Суроегина А. Ю., Микита О. Ю., Рахманина А. А., Рой А. П. Проблема профессионального выгорания и психического здоровья медицинских работников во время пандемии COVID-19. *Журнал им. Н. В. Склифосовского. Неотложная медицинская помощь*. 2020; 9 (3): 321–37.
5. Самойлов А. С., Назарян С. Е. Программа восстановления для медицинских работников в условиях медицинской мобилизации. *Современные вопросы биомедицины*. 2020; 3: 35–37.
6. Булыгина В. Г. Влияние экстремальных факторов служебной деятельности на психическое здоровье специалистов опасных профессий (обзор зарубежных исследований). В сб.: В. Г. Булыгина, С. В. Шпорт, А. А. Дубинский, М. М. Проничева. Медико-биологические и социально-психологические проблемы безопасности в чрезвычайных ситуациях. 2017; 3: 93–100.
7. Собольников В. В. Психология профессиональной деятельности в особых и экстремальных условиях. М.: Юрайт, 2019; 190 с.
8. Bhattacharyya M, Pal MS, Sharma YK, Majumdar D. Changes in sleep patterns during prolonged stays in Antarctica. *Int J Biometeorol*. 2008; 52 (8): 869–79.
9. Ушаков И. Б., Уйба В. В., Сапечкий А. О. Медико-биологические риски, связанные с выполнением дальних космических полетов. *Медицина экстремальных ситуаций*. 2017; 1: 43–64.
10. Lee SA. How much “Thinking” about COVID-19 is clinically dysfunctional? *Brain, Behavior, and Immunity*. 2020; 87: 97–98.
11. Labrague LJ, de Los Santos JAA. COVID-19 anxiety among front-line nurses: Predictive role of organisational support, personal resilience and social support. *J Nurs Manag*. 2020; 28 (7): 1653–61.
12. Luceño-Moreno L, Talavera-Velasco B, García-Albuera Y, Martín-García J. Symptoms of posttraumatic stress, anxiety, depression, levels of resilience and burnout in Spanish health personnel during the COVID-19 Pandemic. *Int J Environ Res Public Health*. 2020. 17 (15): 5514.
13. Петриков С. С., Холмогорова А. Б., Суроегина А. Ю., Микита О. Ю., Рой А. П., Рахманина А. А. Профессиональное выгорание, симптомы эмоционального неблагополучия и дистресса у медицинских работников во время эпидемии COVID-19. *Консультативная психология и психотерапия*. 2020; 65 (3): 8–45.
14. Сорокин М. Ю., Касьянов Е. Д., Рукавишников Г. В., Макаревич О. В., Незнанов Н. Г., Лутова Н. Б. и др. Психологические реакции населения как фактор адаптации к пандемии COVID-19. *Обзор психиатрии и медицинской психологии имени В. М. Бехтерева*. 2020; (2): 87–94.
15. Приказ Министерства труда и социальной защиты Российской Федерации от 31 июля 2020 г. 475н Об утверждении профессионального стандарта «Медицинская сестра/медицинский брат». Доступно по ссылке: <https://normativ.kontur.ru/document?moduleId=1&documentId=370329>.
16. Методические рекомендации МР 3.1.0229-21 «Рекомендации по организации противоэпидемических мероприятий в медицинских организациях, осуществляющих оказание медицинской помощи пациентам с новой коронавирусной инфекцией (COVID-19) (подозрением на заболевание) в стационарных условиях» (утв. Федеральной службой по надзору в сфере защиты прав потребителей и благополучия человека 18 января 2021 г.). Доступно по ссылке: <https://base.garant.ru/400232151/>.
17. Водопьянова Н. Е., Старченкова Е. Н. Синдром выгорания: Диагностика и профилактика. 2-е изд. СПб.: Питер, 2008; 254 с.
18. Arafa A, Mohammed Z, Mahmoud O, Elshazley M, Ewis A. Depressed, anxious, and stressed: What have healthcare workers on the frontlines in Egypt and Saudi Arabia experienced during the COVID-19 pandemic? *Journal of Affective Disorders*. 2021; 278: 365–71.
19. Gorini A, Fiabane E, Sommaruga M, Barbieri S, Sottotetti F, Rovere MT et al. Mental health and risk perception among Italian healthcare workers during the second month of the Covid-19 pandemic. *Archives of Psychiatric Nursing*. 2020. 34 (6): 537–44.
20. Huang JZ, Han MF, Luo TD, Ren AK, Zhou XP. Mental health survey of medical staff in a tertiary infectious disease hospital for COVID-19. *Zhonghua Lao Dong Wei Sheng Zhi Ye Bing Za Zhi*. 2020; 38 (3): 192–5.
21. Lasalvia A, Bonetto C, Porru S, Carta A, Tardivo S, Bovo C, et al. Psychological impact of COVID-19 pandemic on healthcare workers in a highly burdened area of north-east Italy. *Epidemiol Psychiatr Sci*. 2020; DOI: 10.1017/S2045796020001158.
22. Song X, Fu W, Liu X, Luo Z, Wang R, Zhou N. Mental health status of medical staff in emergency departments during the Coronavirus disease 2019 epidemic in China. *Brain, behavior, and immunity*. 2020; 88: 60–65.
23. Zhu J, Sun L, Zhang L, Wang H, Fan A, Yang B. Prevalence and influencing factors of anxiety and depression symptoms in the first-line medical staff fighting against COVID-19 in Gansu. *Front Psychiatry*. 2020; 11: 386.
24. Antonijevic J, Binic I, Zikic O, Manojlovic S, Tosic-Golubovic S, Popovic N. Mental health of medical personnel during the COVID-19 pandemic. *Brain and Behavior*. 2020; 10 (12): 01881.
25. Rossi R, Socci V, Pacitti F, Siracusano A, Rossi A, Di Lorenzo G. Mental health outcomes among frontline and second-line health care workers during the Coronavirus disease 2019 (COVID-19) Pandemic in Italy. *JAMA Network Open*. 2020; 3 (5): 2010185.

THE EFFECT OF A SINGLE PROCEDURE OF COMBINED MICROPOLARIZATION ON AUTONOMIC REGULATION AND SENSORIMOTOR REACTIONS

Sivachenko IB^{1,3}✉, Medvedev DS^{1,2}, Fedorova TA¹, Tsimbal MV¹, Steinberg NV¹, Moiseenko GA³

¹ Research Institute of Hygiene, Occupational Pathology and Human Ecology of the Federal Medical Biological Agency, St. Petersburg, Russia

² North-Western State Medical University named after I.I. Mechnikov, St. Petersburg, Russia

³ Pavlov Institute of Physiology, St. Petersburg, Russia

Micropolarization was already proved an effective method for restoring impaired brain functions and improving intracerebral processes in the absence of impairments. Combining stimulation methods is a promising approach: a combination of electrode positioning methods can increase the efficacy of the procedures and find application in various fields, from sports through machinery operation to support of operatives of the Ministry of Emergency Situations, etc. This study aimed to assess the effect of a single combined micropolarization procedure on the functional state of the autonomic nervous system and sensorimotor reactions of conventionally healthy individuals. It involved 31 people and relied on the methods enabling evaluation of sensorimotor reactions, cardiorythmography with spectral analysis of heart rate variability and pupillary reflexes assessment. Volunteers underwent the combined micropolarization procedure once, the duration of the procedure was 40 minutes. The most effective combinations were transspinal plus transcranial micropolarization with positioning in the region of premotor cortex (short-term shift of the autonomic balance towards parasympathetic influence by 48.7%; optimization of the pupil recovery function by 26.4%; increase in interference immunity by 32.2%) and "solar" plus transcranial micropolarization in the area of the temporal zone of cerebral cortex (15.8% increase of the orthostatic test transition period ratio; 6.2% deceleration of the visual-motor reaction).

Keywords: transcranial micropolarization, functional state, autonomic regulation, sensorimotor reactions, transcranial stimulation, direct current

Author contribution: Sivachenko IB — planning, coordination and organization of the study, analysis of the results, conclusions and discussion; Medvedev DS — organization of the study, research supervision, conclusions and discussion; Fedorova TA, Tsimbal MV, Steinberg NV — execution of the practical part of the study with volunteers, processing of the data obtained; Moiseenko GA — consulting, analysis of the results, conclusions and discussion.

Compliance with ethical standards: the study was approved by the Ethics Committee of the Research Institute of Hygiene, Occupational Pathology and Human Ecology of FMBA of Russia (minutes #2 of February 28, 2019). All volunteers signed the informed written consent to participation in the study.

✉ **Correspondence should be addressed:** Ivan B. Sivachenko
Bekhtereva st., 1, korp. 3, St. Petersburg, 192019, Russia; avans_d@mail.ru

Received: 02.03.2022 **Accepted:** 15.03.2022 **Published online:** 24.03.2022

DOI: 10.47183/mes.2022.006

ВЛИЯНИЕ ОДНОКРАТНОЙ ПРОЦЕДУРЫ КОМБИНИРОВАННОЙ МИКРОПОЛЯРИЗАЦИИ НА ВЕГЕТАТИВНУЮ РЕГУЛЯЦИЮ И СЕНСОРНО-МОТОРНЫЕ РЕАКЦИИ

И. Б. Сиваченко^{1,3}✉, Д. С. Медведев^{1,2}, Т. А. Фёдорова¹, М. В. Цимбал¹, Н. В. Штейнберг¹, Г. А. Моисеенко³

¹ Научно-исследовательский институт гигиены, профпатологии и экологии человека Федерального медико-биологического агентства, Санкт-Петербург, Россия

² Северо-Западный государственный медицинский университет имени И. И. Мечникова, Санкт-Петербург, Россия

³ Институт физиологии имени И. П. Павлова, Санкт-Петербург, Россия

Метод микрополяризации уже показал свою эффективность для восстановления нарушенных мозговых функций, а также для улучшения внутримозговых процессов в норме. Перспективным направлением представляется комбинирование методов стимуляции, поскольку сочетание методов позиционирования электродов может повысить результативность процедур и найти применение в различных сферах деятельности: сопровождении операторов, спортсменов, сотрудников МЧС и др. Целью исследования было оценить влияние однократной комбинированной микрополяризации на функциональное состояние вегетативной нервной системы и сенсорно-моторные реакции условно здоровых лиц. В исследовании с участием 31 человека использовали методики для оценки сенсорно-моторных реакций, кардиоритмографии со спектральным анализом вариабельности сердечного ритма, проводили оценку зрачковых рефлексов. Процедуру комбинированной микрополяризации добровольцы проходили однократно, в течение 40 мин. Наиболее эффективными оказались схемы комбинации трансспинальной и транскраниальной микрополяризации с позиционированием в области премоторной зоны коры головного мозга (краткосрочное смещение вегетативного баланса в сторону парасимпатического влияния — на 48,7%; оптимизация функции восстановления зрачка — на 26,4%; увеличение помехоустойчивости — на 32,2%), и комбинации «солнечной» и транскраниальной микрополяризации в области проекции височной зоны коры головного мозга (увеличение коэффициента переходного периода в ортостатической пробе — на 15,8%; замедления зрительно-моторной реакции — на 6,2%).

Ключевые слова: транскраниальная микрополяризация, функциональное состояние, вегетативная регуляция, сенсорно-моторные реакции, транскраниальная стимуляция, постоянный ток

Вклад авторов: И. Б. Сиваченко — планирование, координация и организация исследования, анализ результатов, выводы и обсуждение; Д. С. Медведев — организация исследования, научное руководство, выводы и обсуждение; Т. А. Фёдорова, М. В. Цимбал, Н. В. Штейнберг — проведение практической части исследования с добровольцами, обработка полученных данных; Г. А. Моисеенко — консультирование, анализ результатов, выводы и обсуждение.

Соблюдение этических стандартов: исследование одобрено этическим комитетом НИИ ГПЭЧ ФМБА России (протокол № 2 от 28 февраля 2019 г.). Все добровольцы подписали информированное согласие на участие в исследовании.

✉ **Для корреспонденции:** Иван Борисович Сиваченко
ул. Бехтерева, д. 1, к. 3, г. Санкт-Петербург, 192019, Россия; avans_d@mail.ru

Статья получена: 02.03.2022 **Статья принята к печати:** 15.03.2022 **Опубликована онлайн:** 24.03.2022

DOI: 10.47183/mes.2022.006

Recent studies have shown that micropolarization is effective in both functional restoration following pathological processes [1, 2] and functional improvement when intracerebral processes are normal [3–5]. Micropolarization was demonstrated [5–7] to reduce the severity of manifestations of the chronic fatigue syndrome; normalize autonomic regulation processes (vascular tone, blood pressure, stimulation of humoral and cellular immunity); normalize psychophysiological state, produce anti-stress and antidepressant effects, alleviate fatigue, improve performance etc.

Methods that combine cerebral cortex transcranial micropolarization and additional spinal nerves transspinal stimulation (both direct current and magnetic impulses) seem to show promise [6, 7].

Transspinal micropolarization is a method for treatment of cerebral functional disorders associated with vascular tone regulation [7]. Transspinal micropolarization optimizes the parasympathetic effect on the heart rate by engaging the neural pathway for autonomic nervous system (ANS) activation [6].

Earlier studies [8, 9] suggested the option of "solar" micropolarization, which implies acting on the solar plexus area where there is a large cluster of autonomic neurons that receive up to 90% of signals from the metasympathetic nervous system of the abdominal region and are closely connected with the vagus and sympathetic nerves. The neural ganglia in the solar plexus region play an important regulatory role on the part of the ANS.

Thus, in order to improve the methodology supporting practical use of micropolarization, it seems important to evaluate and compare the effects of various approaches to combined micropolarization.

The purpose of this study was to assess the effect of a single combined micropolarization procedure on the functional state of the ANS and sensorimotor reactions of conventionally healthy individuals.

METHODS

The study involved 31 volunteers, students of the St. Petersburg Medical and Social Institute (20 people) and other educational establishment (11 people), aged 20–25 years, 17 male and 14 female. The inclusion criteria were: signed voluntary informed consent; permission to participate given by a neurologist and a physician following relevant examinations. The exclusion criteria were: acute mental disorders, convulsive conditions, epilepsy; trauma and brain tumors; infectious lesions of the central nervous system (CNS); hypertension or hypotension, hydrocephalus; thyrotoxicosis; atrial fibrillation, skin damage at the electrode sites; implanted pacemakers; a history of clinically significant allergic reactions, alcoholism, drug addiction.

The assessment of the state of the nervous system relied on the following methods: 1) cardiorythmography (GHR) with spectral analysis of heart rate variability (VNS Micro hardware and software system, Neurosoft; Russia); 2) Pupillometry test for assessment of pupillary reflexes (KSRZRs-01 digital pupillometric complex; Research Institute of Hygiene, Occupational Pathology and Human Ecology of the FMBA; Russia); 3) test for evaluation of spatio-temporal reactions — RDO (reaction to a moving object), PZMR (simple visual-motor response test), interference immunity.

The key criteria for assessment of autonomic reactions to a single micropolarization procedure were the classic heart rate variability indications: frequency range in high, medium and low regions, their interrelation, orthostatic test index and pupillary reaction indicators.

The time of pupil constriction and dilatation reflects the functions of cholinergic (parasympathetic) and adrenergic (sympathetic) constituents of the pupil's dual innervation. The speed of pupil constriction and dilation reflects the activity of parasympathetic and sympathetic components when the pupil constricts or dilates, and the amplitude of constriction indicates vegetative activity in the pupillomotor system. If the difference between initial and final diameters of the pupil is greater than 0.45 mm, the pupil's restoration is abnormal, which is associated with the predominance of parasympathetic activity, a sign of fatigue. To quantify the pupillary reaction, we processed the pupillogram (automated mathematical processing) factoring in the generally accepted pupillometric indicators: the pupil diameter before the light stimulus; final diameter of the pupil; time of the latent period of pupillary reaction; time of pupil constriction (parasympathetic phase); time of pupil dilation (sympathetic phase); average rate of pupil constriction; average rate of pupil dilation; amplitude of the pupil constriction. Pupil reaction is a reliable indicator of the level of attention [10].

The RDO (Reaction to a moving object), PZMR (simple visual-motor response) and Attention and Interference Immunity tests allowed evaluating the speed and quality characteristics of sensory and motor processes and indirectly estimate the balance of mental processes in the context of the specifics of higher nervous activity (since the response time depends on the properties of excitation and inhibition processes and the person's functional state, the level of fatigue in particular).

After testing, the participants underwent 40 minutes of the combined micropolarization procedure, followed by another testing session.

The combination included transspinal, transcranial and "solar" micropolarization in varying patterns.

For transspinal micropolarization, we used 200 μ A direct current delivered through the cutaneous electrodes

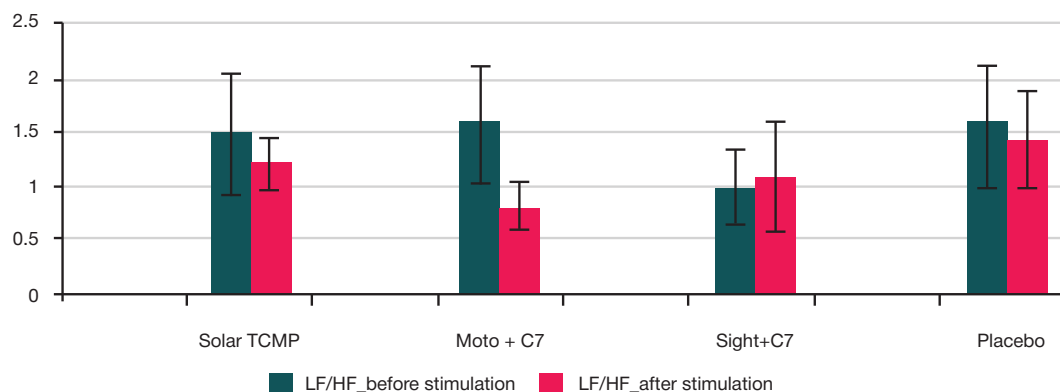


Fig. 1. Change in the LF/HF ratio after the micropolarization procedure. * — statistically significant changes ($p < 0.05$; Wilcoxon test)

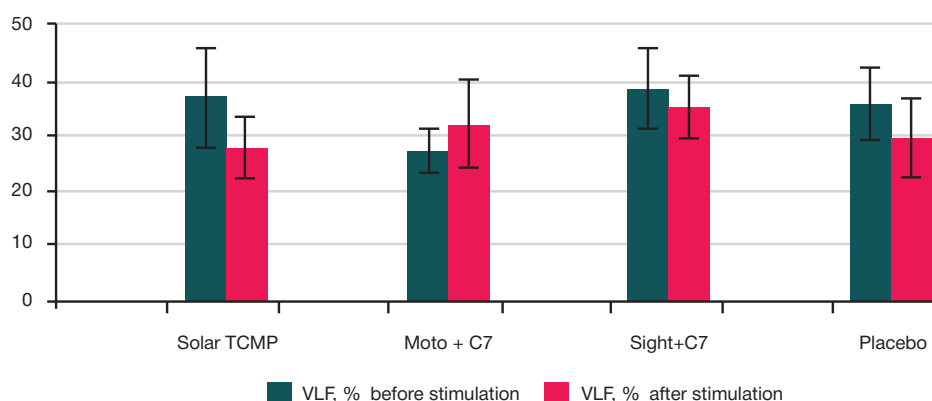


Fig. 2. Changes in the VLF component of the heart rate range after the micropolarization procedure

applied above the spinal canal where spinal nerves exit it; anode was placed laterally from the spinous process of the seventh cervical vertebra (C7), cathode — contralateral to the lumbosacral zone at the level of spinous processes (L5–S1).

For transcranial micropolarization, we used 200 μ A direct current delivered to the primary visual cortex plane (anode — O1 of the left hemisphere, cathode — contralateral lumbosacral zone at the level of spinous processes L5–S1), primary motor cortex plane (anode — M1, cathode — right shoulder area), temporal cortex plane (anode — T3, cathode — the area of the right shoulder).

"Solar" micropolarization procedure employed 200 μ A direct current delivered to the solar plexus area through an anode just below the umbilical region and a cathode on the right shoulder.

The sample was divided into four groups.

– Group 1 (8 people), single procedure, combination of transspinal and transcranial micropolarization, the latter applied in the primary motor cortex area. The pattern of application and the group were called "Moto + C7."

– Group 2 (8 people), single procedure, combination of transspinal and transcranial micropolarization, the latter applied in the primary visual cortex area. This pattern of application (and the group) was named "Sight + C7."

– Group 3 (8 people), single procedure, transcranial and "solar" micropolarization, the former applied in the temporal zone, the latter — above autonomic ganglia of the solar plexus. This pattern, together with the group, was dubbed "Solar TCMP."

– Group 4 (7 people), placebo: the participants had the electrodes applied as in the "Moto + C7" pattern, but there was no current running through them throughout the procedure. This group was called "Placebo."

RESULTS

Figures 1–4 show the average values of the spectral analysis of heart rate variability for all four groups before and after the single micropolarization procedure.

We have registered significant ($p < 0.05$; Wilcoxon test) changes in the LF/HF indicator (Fig. 1). This indicator was detected decreasing by 48.7% from the baseline level in the Group 1, where the current was directed at the premotor cortex area ("Moto + C7"). Relative to the placebo group, the decrease in LF/HF was 43.5%. Against the comparison group, no significant changes in the dynamics of the indicator were detected. The values of this indicator tended to decrease in groups 2 and 3, too, where the micropolarization procedure was of the combined type with different electrode application spots.

We identified no significant differences ($p > 0.05$; Wilcoxon test) between all groups, "Placebo" included, in the values of the VLF indicator (the lowest frequency range of the heart rate variability) (Fig. 2). This indicator shows the level of neurohumoral activity.

The total spectral power of the heart rate TP reflects the total contribution of all assessed components to the regulation of the ANS. Same as for the previous indicator, we identified no significant differences between the groups for this one, either (Fig. 3, $p > 0.05$).

The K30:15 ratio increased by 15.8% in Group 3, "Solar TCMP"; the change is significant ($p < 0.05$; Wilcoxon test) (Fig. 4). It should be noted that this is the only group where we detected a significant change in this indicator. Relative to the placebo group, the increase was 12.8%.

Figures 5–7 show the values of the integral characteristics of the central nervous system before and after the single micropolarization procedure through all the four groups.

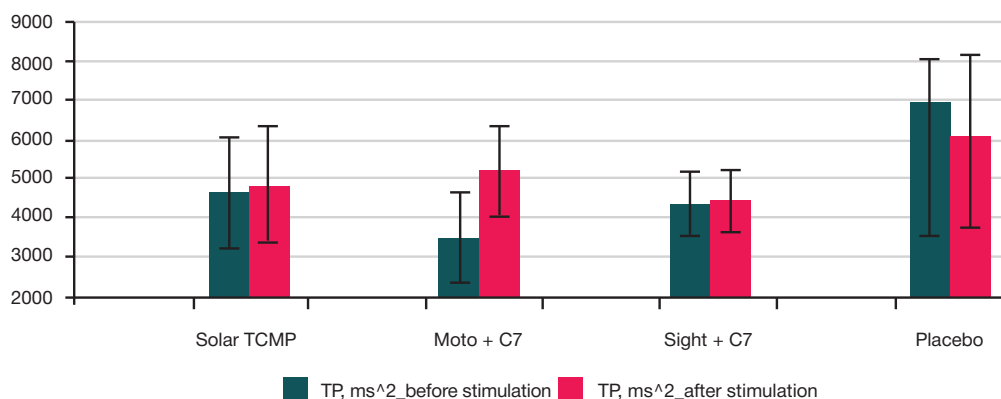


Fig. 3. Change in the total spectral power (TP) after the micropolarization procedure

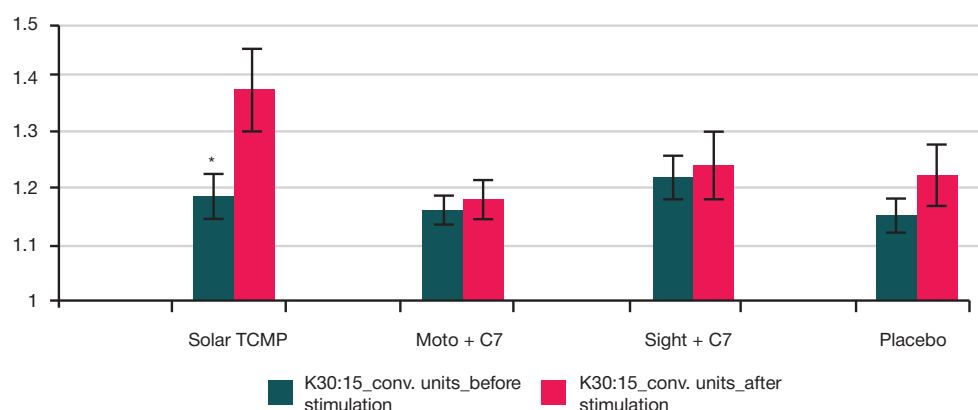


Fig. 4. Change in the K30:15 ratio after the micropolarization procedure. * — statistically significant changes ($p < 0.05$; Wilcoxon test)

We identified significant ($p < 0.05$) changes in the mean reaction time with the simple visual-motor response test (Fig. 5). In the "Solar TCMP" group, this indicator has grown by 6.2% relative to the baseline initial level.

There were identified no significant differences in the "balance of mental processes" indicator registered with the RDO (reaction to a moving object) test ($p > 0.05$).

The interference resistance value significantly increased by 32.2% ($p < 0.05$; Wilcoxon test) in group 1 ("Moto + C7") after the procedure. The participants in this group had an increased level of attention and interference immunity (Fig. 7). Relative to the placebo group, the increase was 12.8%.

Pupillometry done after the micropolarization procedure allowed identifying a small number of statistically significant differences in the changing values of indicators (see Table). In the group where electrodes were applied to the solar ganglia and temporal zones, the pupil diameter decreased by 26.4% from the initial to the final states, which is significant. In absolute figures, the diameter value in this group was more than 0.45 mm, which confirms the insufficient recovery of the pupil.

The analysis of pupillometry indicator values before and after the "Sight + C7" pattern procedure reveals specific peculiarities of the pupil dilation time alteration, one of which is the slight yet significant (2.2%) shortening of the dilation time that characterizes activation of parasympathetic regulation mechanisms.

DISCUSSION

The combination of anodic transcranial stimulation with the electrode on the primary motor cortex plane (anode — M1,

cathode — right shoulder) and transspinal stimulation (anode — C7, cathode — contralateral to the lumbosacral zone at the level of the spinous processes L5-S1) had a positive effect on autonomic regulation: the parasympathetic and sympathetic influence were optimized (LF/HF ratio was reduced), which, presumably, improved attention focusing (increased interference immunity).

The low-frequency and high-frequency parts of the heart rate variability range reflect the activity of the sympathetic and parasympathetic divisions of the ANS. The LF/HF ratio characterizes the vegetative balance and gives an idea of the involvement of the central link of regulation. The mentioned reduction of this ratio can be interpreted as signaling of the growing activity of the parasympathetic part of the ANS.

Pupil diameter monitoring and K30:15 value obtained from the orthostatic test allowed discovering activation of the recovery processes in response to the combination of transcranial stimulation at the temporal zone (anode — T3, cathode — right shoulder area) and stimulation above the solar plexus.

The K30:15 ratio characterizes the speed of optimization of the person's condition when he/she stands up from the supine position (orthostatic test). The registered dynamics allow assuming that a single micropolarization procedure improves general condition of the body.

The pupil function has links to various parts of the central and autonomic nervous systems, which allows considering it a sensitive probe capable of reporting the functional state of a person [11]. Autonomic nervous system, which enables adaptation of the body both to various environmental influences and to high physical loads, is one of the first bodily systems to respond to such influences/loads. In healthy people,

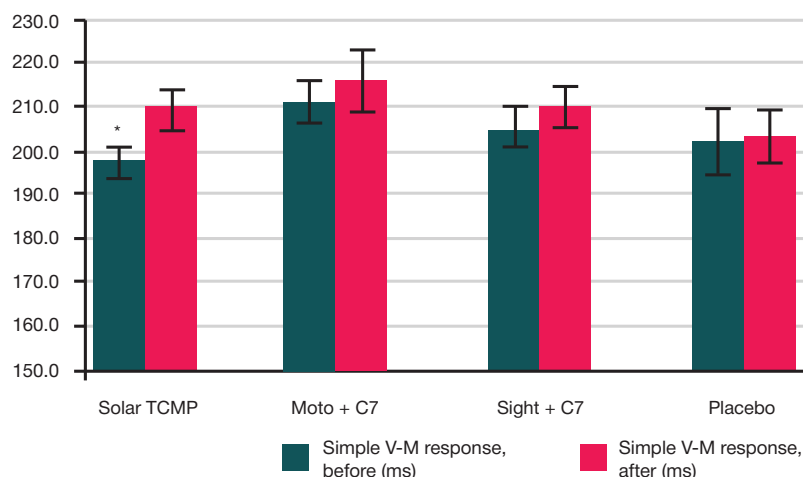


Fig. 5. Change in the mean reaction time (simple visual-motor response test) after the micropolarization procedure. * — statistically significant changes ($p < 0.05$; Wilcoxon test)

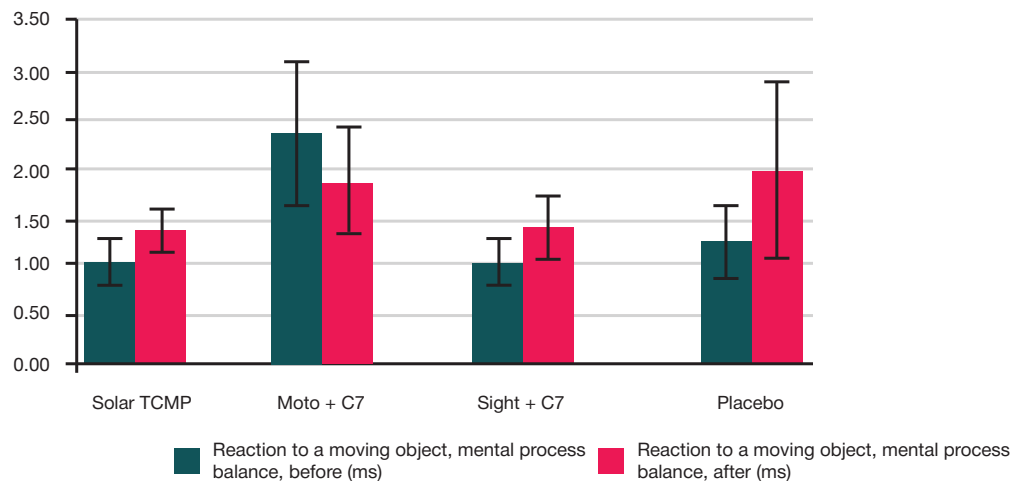


Fig. 6. Change in the balance of inhibition and excitation (RDO test) after the micropolarization procedure

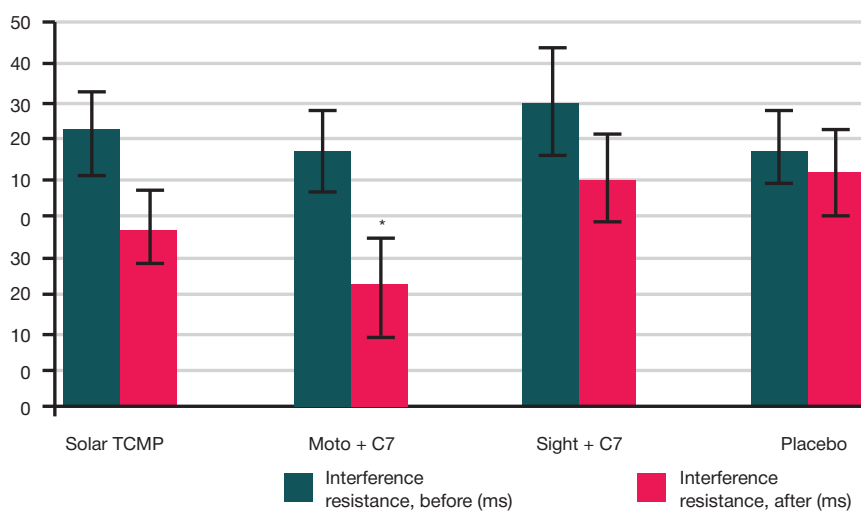


Fig. 7. Change of interference immunity values after the micropolarization procedure. * — statistically significant changes ($p < 0.05$; Wilcoxon test)

pupil function largely depends on the state of the ANS, which adds to the importance of its testing because the fatigue-related impairment of this function may manifest before other symptoms signaling of the CNS and ANS fatigue and deterioration of the adaptive capabilities. A smaller difference between the initial and final diameters of the pupil indicates optimization of action of the sympathetic and parasympathetic divisions of the ANS. The results of this study are consistent with the data reported by

other authors who researched the pupillomotor system reaction in people undergoing adjustment procedures [12, 13].

As for the modulation of sensorimotor reactions, we registered activation of the inhibition processes, which is confirmed by the increased visual-motor response time. The changes of the mean reaction time detected with the simple visual-motor response test can be interpreted as signaling of the growing inhibitory influences. The effect may come from the

Table. Dynamics of pupillometry indicator values after the micropolarization procedure

Group	Solar TCMP		Moto + C7		Sight + C7		Placebo	
	Before stimulation	After stimulation	Before stimulation	After stimulation	Before stimulation	After stimulation	Before stimulation	After stimulation
Di	6,26 ± 0,30	6,03 ± 0,28	5,97 ± 0,32	6,18 ± 0,17	5,52 ± 0,41	5,75 ± 0,40	5,82 ± 0,30	5,94 ± 0,27
Tl	0,28 ± 0,01	0,28 ± 0,01	0,28 ± 0,01	0,29 ± 0,01	0,28 ± 0,01	0,28 ± 0,01	0,28 ± 0,01	0,27 ± 0,01
Ac	1,67 ± 0,12	1,64 ± 0,08	1,57 ± 0,10	1,61 ± 0,07	1,60 ± 0,14	1,66 ± 0,11	1,61 ± 0,09	1,61 ± 0,12
Tc	0,51 ± 0,03	0,53 ± 0,02	0,46 ± 0,03	0,48 ± 0,02	0,46 ± 0,02	0,51 ± 0,02	0,48 ± 0,03	0,51 ± 0,03
Td	2,21 ± 0,03	2,20 ± 0,02	2,26 ± 0,03	2,23 ± 0,02	2,26 ± 0,02	2,21 ± 0,02*	2,24 ± 0,03	2,22 ± 0,03
Vc	3,28 ± 0,17	3,14 ± 0,16	3,46 ± 0,14	3,38 ± 0,18	3,46 ± 0,23	3,24 ± 0,14	3,40 ± 0,17	3,20 ± 0,16
Vd	0,76 ± 0,06	0,75 ± 0,04	0,67 ± 0,07	0,72 ± 0,03	0,72 ± 0,06	0,83 ± 0,10	0,72 ± 0,05	0,73 ± 0,06
Df	5,73 ± 0,29	5,63 ± 0,26	5,71 ± 0,31	5,75 ± 0,14	5,19 ± 0,35	5,39 ± 0,33	5,31 ± 0,32	5,42 ± 0,29
Di-Df	0,53 ± 0,06	0,39 ± 0,06*	0,26 ± 0,05	0,44 ± 0,07	0,33 ± 0,08	0,36 ± 0,13	0,51 ± 0,12	0,52 ± 0,11

Note: Di (mm) — initial pupil diameter before the light stimulus; Df (mm) — final pupil diameter; Tl (s) — time of the latent period of pupillary reaction; Tc (s) — pupil constriction time (parasympathetic phase); Td (s) — pupil dilation time (sympathetic phase); Vc (mm/s) — average pupil constriction speed; Vd (mm/s) — average pupil dilation speed; Ac (mm) — amplitude of pupil constriction. Pupil reaction is a reliable indicator of the level of attention; * — value is significant with respect to background ($p < 0.05$; Wilcoxon test).

increased contribution of parasympathetic part of the ANS to the regulation of the functional state.

There were no significant effects detected for the combination of transcranial stimulation in the primary visual cortex plane (anode — O1, cathode — L5-S1) and transspinal stimulation (anode — C7, cathode — L5-S1).

The revealed effects of micropolarization pattern combinations enable further improvement of the methods of micropolarization procedures. The tested patterns may find practical application in professional sports. For example, optimization of the autonomic regulation processes is of paramount importance for athletes in biathlon, where it is extremely important to switch between dynamic and static physical loads in an optimal way.

CONCLUSIONS

This study assessed the effect of a single combined micropolarization procedure on the functional state of the ANS

and sensorimotor reactions of conventionally healthy individuals. We tested three electrode positioning patterns. The results of the study show that the considered combinations of patterns produce different effects. The most effective combinations were: 1) transspinal plus transcranial micropolarization with electrode positioning in the region of premotor cortex, which triggered a short-term shift of the autonomic balance towards parasympathetic influence (by the LF/HF ratio) by 48.7%; optimization of the pupil recovery function by 26.4%; increase in interference immunity by 32.2%; 2) "solar" plus transcranial micropolarization in the area of the temporal zone of cerebral cortex, which increased the K30:15 ratio by 15.8% (discovered with an orthostatic test) and the visual-motor reaction deceleration by 6.2%. Further investigation of the characteristics of exposure time and current strength in the context of combined micropolarization procedures seems promising; such studies may be aimed at selecting the more effective stimulation modes.

References

1. Lipatova AS, Kade AX, Trofimenko AI, Polyakov PP. Korrekciya stress-inducirovannykh nejroimmunoendokrinnykh narushenij u samcov krysa s nizkoj ustojchivost'yu k stressu primeneniem transkraniyal'noj ehlektrostimulyacii. Chelovek i ego zdorov'e. 2018; 3: 58–68. Russian.
2. Knyazeva OV, Belousova MV, Prusakov VF, Zaikova FM. Primenenie transkraniyal'noj mikropolyarizacii v kompleksnoj rehabilitacii detej s rasstrojstvom ehkspressivnoj rechi. Vestnik sovremennoj klinicheskoy mediciny. 2019; 1: 64–69. Russian.
3. Karkishhenko NN, Vartanov AA, Chudina YuA, Chajvanov DB. Algoritm rascheta variabel'nosti i velichiny vozdejstviya ehlektricheskogo toka na osnove matematicheskoy modeli rastekaniya toka pri transkraniyal'noj mikropolyarizacii po dannym stereotakticheskix koordinat. Biomedicina. 2017; 1: 4–9. Russian.
4. Bragina OA, Semyachkina-Glushkovskaya OV, Trofimov AO, Bragin DE. O mexanizmax modulyacii mozgovogo krovotoka pri transkraniyal'noj ehlektricheskoy stimulyacii. Medicinskij al'manax. 2018; 5(56): 68–71. Russian.
5. Chajvanov DB, Chudina YuA. Primenenie nejromodulyacii dlya korrekcii psixofunkcional'nyx sostoyanij v processe transaktnogo analiza. Vestnik RUDN. Seriya: Psixologiya i pedagogika. 2011; 4: 38–43. Russian.
6. Muravyev SV, Kravcova EYu, Cherkasova VG, Antropov ES, Vliyanie transvertebral'noj mikropolyarizacii spinного mozga na sistemu vegetativnoj regulyacii po dannym variacionnoj kardiointervalografii u detej i podrostkov s zabolevaniyami pozvonochnika. Medicinskij al'manax. 2017; 2 (47): 66–69. Russian.
7. Sirbiladze GK, Suslova GA, Pinchuk DYU, Sirbiladze TK. Vozmozhnost' primeneniya transspinal'noj mikropolyarizacii dlya korrekcii cerebral'nogo krovoobrashcheniya. Peditriya. 2017; 6: 50–55. Russian.
8. Skoromec TA, Naryshkin AG, Gorelik AL. Solyarnaya mikropolyarizaciya v kompleksnom lechenii bol'nyx s zabolevaniyami vegetativnoj nevrnoj sistemy. Metodicheskie rekomendacii. SPb.: Izd. Centr SPb NIPNI im. V.M. Bextereva, 2011; 13 s. Russian.
9. Naryshkin AG, Galanin IV, Gorelik AL, Skoromec TA, Vtorov AV, Lisichik MV, i dr. Nespecificheskij metod lecheniya somatofornnyx, vegetativnyx i gipotalamicheskix rasstrojstv. Obozrenie psixiatrii i medicinskoj psixologii. 2015; 3: 56–63. Russian.
10. Suvorov NF, Tairov OP. Psixofiziologicheskie mexanizmy izbiratel'nogo vnimaniya. L.: Nauka, 1985; 286 s. Russian.
11. Bakutkin VV. Issledovanie zrachkovyx reakcij v medicinskoj praktike. Saratov: Amirit, 2017; 120 s. Russian.
12. Filipe JA. Assessment of autonomic function in high level athletes by pupillometry. Auton Neurosci. 2003; 104 (1): 66–72.
13. Stang J. Assessment of Parasympathetic Activity in Athletes: Comparing Two Different Methods. Medicine and Science in Sports and Exercise. 2016; 48 (2): 316–22.

Литература

1. Липатова А. С., Каде А. Х., Трофименко А. И., Поляков П. П. Коррекция стресс-индуцированных нейроиммуноэндокринных нарушений у самцов крыс с низкой устойчивостью к стрессу применением транскраниальной электростимуляции. Человек и его здоровье. 2018; 3: 58–68.
2. Князева О. В., Белоусова М. В., Прусаков В. Ф., Зайкова Ф. М. Применение транскраниальной микрополяризации в комплексной реабилитации детей с расстройством экспрессивной речи. Вестник современной клинической медицины. 2019; 1: 64–69.
3. Каркищенко Н. Н., Вартанов А. А., Чудина Ю. А., Чайванов Д. Б. Алгоритм расчета вариабельности и величины воздействия электрического тока на основе математической модели растекания тока при транскраниальной микрополяризации по данным стереотактических координат. Биомедицина. 2017; 1: 4–9.
4. Брагина О. А., Семьякина-Глушковская О. В., Трофимов А. О., Брагин Д. Е. О механизмах модуляции мозгового кровотока при транскраниальной электрической стимуляции. Медицинский альманах. 2018; 5 (56): 68–71.
5. Чайванов Д. Б., Чудина Ю. А. Применение нейромодуляции для коррекции психофункциональных состояний в процессе транскраниального анализа. Вестник РУДН. Серия: Психология и педагогика. 2011; 4: 38–43.
6. Муравьев С. В., Кравцова Е. Ю., Черкасова В. Г., Антропов Е. С., Влияние трансвертебральной микрополяризации спинного мозга на систему вегетативной регуляции по данным вариационной кардиоинтервалографии у детей и подростков с заболеваниями позвоночника. Медицинский альманах. 2017; 2 (47): 66–69.
7. Сирбиладзе Г. К., Сусллова Г. А., Пинчук Д. Ю., Сирбиладзе Т. К. Возможность применения трансспинальной микрополяризации для коррекции церебрального кровообращения. Педиатрия. 2017; 6: 50–55.
8. Скоромец Т. А., Нарышкин А. Г., Горелик А. Л. Солярная микрополяризация в комплексном лечении больных с заболеваниями вегетативной нервной системы.

- Методические рекомендации. СПб.: Изд. Центр СПб НИПНИ им. В.М. Бехтерева, 2011; 13 с.
9. Нарышкин А. Г., Галанин И. В., Горелик А. Л., Скоромец Т. А., Второв А. В., Лисичик М. В., и др. Неспецифический метод лечения соматоформных, вегетативных и гипоталамических расстройств. Обозрение психиатрии и медицинской психологии. 2015; 3: 56–63.
 10. Суворов Н. Ф., Таиров О. П. Психофизиологические механизмы избирательного внимания. Л.: Наука, 1985; 286 с.
 11. Бакуткин В. В. Исследование зрачковых реакций в медицинской практике. Саратов: Амирит, 2017; 120 с.
 12. Filipe JA. Assessment of autonomic function in high level athletes by pupillometry. Auton Neurosci. 2003; 104 (1): 66–72.
 13. Stang J. Assessment of Parasympathetic Activity in Athletes: Comparing Two Different Methods. Medicine and Science in Sports and Exercise. 2016; 48 (2): 316–22.

ANTIMICROBIAL AND ANTIVIRAL ACTIVITY OF THREE-COMPONENT COMPLEX OF CHLORHEXIDINE-EDTA-ZINC

Galinkin VA¹, Enikeev AKh¹, Podolskaya EP^{2,3}, Gladchuk AS^{2,4}, Vinogradova TI⁵, Zabolotnykh NV⁵, Dogonadze MZ⁵, Krasnov KA² ✉

¹ ООО "РОСБИО", St. Petersburg, Russia

² Federal State-Financed Institution Golikov Research Clinical Center of Toxicology under the Federal Medical Biological Agency, St. Petersburg, Russia

³ Institute of Analytical Instrumentation, St. Petersburg, Russia

⁴ Saint Petersburg State University, St Petersburg, Russia

⁵ Saint-Petersburg State Research Institute of Phthisiopulmonology, St. Petersburg, Russia

Chlorhexidine bigluconate (CHX) is widely used as a disinfectant, but it is not effective against spore-forming microorganisms, as well as viruses. In this work, a method has been found to increase the biocidal activity of chlorhexidine by using it as part of a complex including ethylenediaminetetraacetic acid (EDTA) and zinc chloride. The structure of the three-component complex CHX-EDTA-zinc is proved by the MALDI-MS method. The biocidal activity of the chlorhexidine complex has been studied *in vitro* and *in vivo* experiments. It is shown that the complex is significantly superior to chlorhexidine alone, both in terms of activity level and in the breadth of biocidal action. In relation to the studied bacterial and fungal strains, the CHX-EDTA-Zn complex was 4–5 times more active than chlorhexidine bigluconate. In concentrations from 1.0 mg/ml to 0.008 mg/ml (depending on the type of micro-organism), *in vitro* the complex showed both bacteriostatic and bactericidal effects against the main pathogens of bacterial diseases of birds. In clinical conditions, the complex has shown high efficiency in the treatment of dermatitis in small domestic and farm animals. Also, *in vitro* and *in vivo*, the complex showed unexpectedly high antitubercular activity comparable to that of monofloxacin, including on drug-resistant strains of mycobacteria. *in vitro* experiments involving polio virus and adenovirus have shown that the CHX-EDTA-Zn complex possesses virulent action.

Keywords: chlorhexidine, EDTA, zinc, complex, MALDI, antiseptic, anti-tuberculosis, antiviral activity

Funding: ООО "РОСБИО"

Author contribution: Galinkin VA — organization of microbiological and virological research; Enikeev AKh — general management; Podolskaya EP — mass spectrometric analysis; Gladchuk AS — chemical-analytical studies; Vinogradova TI — management of studies of anti-tuberculosis activity; Zabolotnykh NV — study of antitubercular activity *in vitro*; Dogonadze MZ — study of antitubercular activity in animals; Krasnov KA — data processing and interpretation, preparation of the materials for publication.

Compliance with ethical standards: all procedures with animal models were carried out in accordance with the Directive 2010/63/EU of the European Parliament and of the Council of the European Union (2010) on protection of animals used for scientific purposes.

✉ **Correspondence should be addressed:** Konstantin A. Krasnov
Bekhtereva, 1/2, k. 54, St. Petersburg, 199106, Russia; krasnov_tox@mail.ru

Received: 27.12.2021 **Accepted:** 12.01.2022 **Published online:** 07.02.2022

DOI: 10.47183/mes.2022.002

АНТИМИКРОБНАЯ И ВИРУЛИЦИДНАЯ АКТИВНОСТЬ ТРЕХКОМПОНЕНТНОГО КОМПЛЕКСА ХЛОРГЕКСИДИН-ЭДТА-ЦИНК

В. А. Галынкин¹, А. Х. Ениеев¹, Е. П. Подольская^{2,3}, А. С. Гладчук^{2,4}, Т. И. Виноградова⁵, Н. В. Заболотных⁵, М. З. Догонадзе⁵, К. А. Краснов² ✉

¹ ООО «РОСБИО», Санкт-Петербург, Россия

² Научно-клинический центр токсикологии имени С. Н. Голикова Федерального медико-биологического агентства, Санкт-Петербург, Россия

³ Институт аналитического приборостроения, Санкт-Петербург, Россия

⁴ Санкт-Петербургский государственный университет, Санкт-Петербург, Россия

⁵ Санкт-Петербургский научно-исследовательский институт фтизиопульмонологии, Санкт-Петербург, Россия

Хлоргексидина биглюконат (ХГ) широко используют в качестве дезинфицирующего средства, однако он мало эффективен в отношении спорообразующих микроорганизмов, а также вирусов. Целью работы было повысить биоцидную активность хлоргексидина путем его использования в составе комплекса, включающего этилендиаминететрауксусную кислоту (ЭДТА) и хлорид цинка. Структура трехкомпонентного комплекса ХГ-ЭДТА-цинк доказана методом МАЛДИ-МС, биоцидная активность изучена в экспериментах *in vitro* и *in vivo*. Показано, что комплекс значительно превосходит индивидуальный хлоргексидин, как по уровню активности, так и по широте биоцидного действия. В отношении изученных бактериальных и грибных штаммов комплекс ХГ-ЭДТА-Zn был в 4–5 раз активнее, чем биглюконат хлоргексидина. В концентрации 1,0–0,008 мг/мл (в зависимости от вида микроорганизма) *in vitro* комплекс проявлял как бактериостатическое, так и бактерицидное действие в отношении основных возбудителей бактериальных болезней птиц. В клинических условиях показана его высокая эффективность при лечении дерматитов у мелких домашних и сельскохозяйственных животных; *in vitro* и *in vivo* выявлена высокая противотуберкулезная активность, сопоставимая с препаратом монофлуксаценом, в том числе на лекарственно устойчивых штаммах микобактерий. В экспериментах *in vitro* на примере вируса полиомиелита и аденовируса доказано наличие у комплекса ХГ-ЭДТА-Zn вирулицидного действия.

Ключевые слова: хлоргексидин, ЭДТА, цинк, комплекс, МАЛДИ, антисептическая, противотуберкулезная, противовирусная активность

Финансирование: ООО «РОСБИО»

Вклад авторов: В. А. Галынкин — организация микробиологических и вирусологических исследований; А. Х. Ениеев — общее руководство; Е. П. Подольская — масс-спектрометрический анализ; А. С. Гладчук — химико-аналитические исследования; Т. И. Виноградова — руководство исследованиями противотуберкулезной активности; Н. В. Заболотных — изучение противотуберкулезной активности *in vitro*; М. З. Догонадзе — изучение противотуберкулезной активности на животных; К. А. Краснов — обработка и интерпретация данных, подготовка материалов к печати.

Соблюдение этических стандартов: все процедуры с модельными животными были проведены в соответствии с Правилами лабораторной практики и директивой Европейского парламента и Совета Европейского союза 2010/63/ЕС (2010 г.) о защите животных, используемых для научных целей.

✉ **Для корреспонденции:** Константин Андреевич Краснов
ул. Бехтерева, д. 1/2, к. 54, г. Санкт-Петербург, 199106, Россия; krasnov_tox@mail.ru

Статья получена: 27.12.2021 **Статья принята к печати:** 24.01.2022 **Опубликована онлайн:** 07.02.2022

DOI: 10.47183/mes.2022.002

Disinfectants are widely used in medical practice, everyday life and in many other areas of human activity. Disinfection measures are especially important in the context of epidemics or the risk of spread of dangerous infections, which makes provision of medical institutions and general population with effective antiseptic agents a task of national importance. Generally, such agents are expected to effectively suppress all types of pathogenic microflora, including causative pathogens of microbial, fungal and viral infections, as well as to be safe for humans and the environment. The currently existing agents meet these requirements only partially, so the matter of development of new ones remains urgent.

Chlorhexidine (1.6-di-[bis-(4-chlorophenyl)biguanide]hexane bigluconate) is one of the most famous antiseptics. It has been used medical, veterinary and household environments for over 60 years now; to this day, it remains one of the most popular antiseptic agents [1]. It is popular because of its strong bactericidal effect against a wide range of gram-positive and gram-negative microorganisms, including fungi, as well as because of the ability to remain highly active in contact with various biological substrates (blood, saliva, pus, etc.) [2].

A chlorhexidine molecule consists of two symmetrical chlorophenyl-substituted biguanide groups connected by a hydrophobic hexamethylene chain. At physiological pH, it exists as a bication [3]. Like most cationic antiseptics, chlorhexidine has its antimicrobial action realized at the level of the cell membrane [4].

Chlorhexidine is the primary active ingredient in various topical disinfectants; it is used to treat wounds, burns, to sterilize the surgical field, skin. Chlorhexidine is a component of anti-cold solutions and rinses [5]. It is indispensable in dentistry, where it became acknowledged as a "golden standard" and once served as a reference agent for the new antiseptics development efforts [6].

However, chlorhexidine has a number of significant drawbacks. In particular, at room temperature, it has practically no effect on bacterial spores, which makes it of little use against spore-forming pathogens [5]. Acid-resistant microorganisms [7], including pathogens of tuberculosis and leprosy, also exhibit high resistance to chlorhexidine. Another serious drawback of chlorhexidine is lack of pronounced virucidal activity. Although chlorhexidine has some effect on HIV, herpes 1 and 2, influenza A [2, 5], it is all but ineffective against most viruses, including, according to the recent clinical studies, such as SARS-CoV-2 [8].

Last but not least, the efficacy of all such commonly used agents diminishes with emergence of resistant microbial strains. For a long time it was believed that microorganisms cannot become resistant to chlorhexidine [2], but recent data refute this opinion. For example, it was established that *K. pneumoniae* can adapt to chlorhexidine, which leads to the appearance of pathogenic strains that are practically insensitive to the recommended antiseptic concentrations [9].

As our studies show, antiseptic potency of chlorhexidine can be increased by combining it with other chemicals. In this connection, it seems interesting to study the specific activity of chlorhexidine in the presence of excipients it creates a complex with, such as Trilon B (ethylenediaminetetraacetic acid disodium salt, EDTA) and zinc chloride. Zinc salts and complexes are moderately active against microbes, fungi and viruses [10], while EDTA, although it is not antiseptic individually, can form stable complexes with most metal cations [11] and improve permeability of cell membranes for other substances, including zinc and, possibly, chlorhexidine. The purpose of this work was to study the molecular structure of the new chlorhexidine complex and to thoroughly investigate its biocidal properties.

METHODS

The complex compound 0.2% chlorhexidine bigluconate water solution, 1% ethylenediaminetetraacetic acid disodium salt (EDTA) and 0.5% zinc chloride was provided by OOO Rosbio (St. Petersburg).

Mass spectrometry

The technique selected for the analysis was MALDI-MS, matrix-assisted laser desorption/ionization mass spectrometry. The original complex solution was diluted with water 100 times. 0.5 µl of the resulting solution were applied to the MALDI target cell, followed by 0.5 µl of the matrix solution (5 mg/ml). The mixture was then dried. The matrix was 2,5-dihydroxybenzoic acid dissolved in 70% acetonitrile with the addition of 0.1% trifluoroacetic acid (TFA). The samples were left to dry at room temperature and then examined with an ultrafleXtreme MALDI-TOF/TOF mass spectrometer (Bruker Daltonics; Germany) at the Science Park of St. Petersburg State University.

The mass spectra were recorded in the range m/z 600–1500 in the "reflectron" mode with detection of positive ions. For one spectrum, 15,000 instances of sample irradiation with a Nd:YAG 355 nm laser were summed up. The mass spectrometer was calibrated with a Peptide Calibration Standard II calibration mixture (Bruker Daltonics; Germany).

The elemental composition of the chlorhexidine-EDTA-Zn complex was determined by the standard method (CHN analysis), and the quantitative content of zinc was established with the help of inductively coupled plasma atomic emission spectroscopy enabled by the Optima 2100DV spectrometer (Perkin Elmer; USA). To isolate the individual complex, the initial solution was concentrated by evaporation in a vacuum to 1/10 of the primary volume, then the precipitated crystalline product was separated, washed with water and dried in air at 40 °C to constant weight. The resulting complex was a colorless fine crystalline powder, partially soluble in water. The initial solution contained 0.34% of this complex, which is 0.2% in terms of pure chlorhexidine. Elemental analysis data: found C — 44.50%, H — 5.21%, N — 19.44%, Zn — 7.57%. $C_{32}H_{44}Cl_2N_{12}O_8Zn$ — MW 858.21; calculated C — 44.64%, H — 5.15%, N — 19.52%, Zn — 7.60%. MALDI-MS mass spectrum data: m/z 859.27.

In vitro and in vivo microbiological studies

The *in vitro* experiments and clinical trials of antiseptic properties of the chlorhexidine-EDTA-Zn complex on animals were carried out at the Vitebsk State Academy of Veterinary Medicine (Belarus) and Agrokombinat Yubileyny (Belarus). The preparation was serially diluted in Petri dishes; each microorganism was tested in two series of experiments that made use of cultures grown on two different nutrient media [12].

The *in vivo* experiments included treatment of dermatitis in domestic and farm animals (dogs, cats, rabbits and sheep). The antiseptic was applied once a day for 5–14 days.

Investigation of antitubercular activity

This part of the study was carried out at Saint-Petersburg State Research Institute of Phthisiopulmonology of the Ministry of Healthcare of the Russian Federation. *In vitro*, the antitubercular activity of the complex was tested on *Mycobacterium tuberculosis* H37Rv, a sensitive reference strain (Institute of Hygiene and Epidemiology, Prague, 1976), and a clinical isolate

Table 1. Antimicrobial activity of the CHX-EDTA-Zn complex in comparison with chlorhexidine bigluconate (CHX)

Antiseptic	Culture					
	<i>Bac. subtilis</i>	<i>E. coli</i>	<i>Bac. mycoides</i>	<i>Sac. cerevisiae</i>	<i>P. breri-compactum</i>	<i>Asp. niger</i>
	Area of the no-growth zone, cm ²					
CHX-EDTA-Zn complex	16.8	13.7	15.2	16.8	19.4	18.5
CHX	3.6	4.1	4.1	4.0	4.4	3.6
CHX/Complex activity index	4.7	3.3	3.7	4.2	4.4	5.1

of *M. tuberculosis* 5582 with multidrug resistance (collection of MBT strains of Saint-Petersburg State Research Institute of Phthiopulmonology). The minimum inhibitory concentration (MIC) was determined with the help of the REMA method [13] on cultures of *M. tuberculosis* H37Rv and clinical isolate 5582 with resistance to isoniazid, rifampicin, streptomycin, and pyrazinamide. The MIC value was taken as the minimum drug concentration at which the average fluorescence level did not significantly exceed 1% of the level registered for the control MBT culture that grew without inhibition. Bacterial growth was registered both visually, by the change in the color of resazurin from blue to pink, and using a FLUOstar Optima plate fluorimeter (Germany) at an excitation wavelength of 520 nm and emission wavelength of 590 nm.

In vivo, the antitubercular activity of the complex was studied in male C57black/6 mice weighing 16–18 g (Andreevka nursery, Scientific Center for Biomedical Technologies of the Federal Medical Biological Agency; Russia) [14, 15], with two models of tuberculosis, first involving infection with the standard test strain *M. tuberculosis* H37Rv, second — with the drug-resistant strain 5582. In both series of experiments animals received medications from the fourth day on after the infection. All preparations were administered intragastrically, daily, with the exception of Saturdays and Sundays, until the end of the experiment. The CHX-EDTA-Zn complex was administered in two doses, 7 mg/kg and 14 mg/kg. Moxifloxacin was the drug the efficacy of the complex was compared to. It was administered at an average therapeutic dose of 7 mg/kg. The total duration of the experiment was 40 days.

Table 2. CHX-EDTA-Zn complex activity against avian pathogens

Type of culture	Nutrient medium	Sample number and active substance concentration, mg/ml									
		1	2	3	4	5	6	7	8	9	10
		1.0	0.5	0.25	0.125	0.06	0.03	0.015	0.008	0.004	0.002
<i>E. coli-1</i>	Plain broth	–	–	–	–	–	–	–	–	+	+
	Endo medium	–	–	–	–	–	–	–	±	+	+
<i>E. coli-2</i>	Plain broth	–	–	–	–	–	–	–	–	+	+
	Endo medium	–	–	–	–	–	–	–	–	+	+
<i>S. enteritidis</i>	Plain broth	–	–	–	–	+	+	+	+	+	+
	Endo medium	±	±	±	±	+	+	+	+	+	+
<i>S. gallinarum</i>	Plain broth	–	–	–	–	–	–	+	+	+	+
	Endo medium	–	–	–	±	+	+	+	+	+	+
<i>S. typhimurium</i>	Plain broth	–	–	–	–	–	+	+	+	+	+
	Endo medium	–	–	±	±	±	+	+	+	+	+
<i>P. vulgaris</i>	Plain broth	–	–	–	+	+	+	+	+	+	+
	Plain agar	–	+	+	+	+	+	+	+	+	+
<i>St. aureus</i>	Plain broth	–	–	–	–	–	–	–	–	+	+
	Plain agar	–	–	–	+	+	+	+	+	+	+
<i>St. epidermidis</i>	Plain broth	–	–	–	–	–	–	–	–	–	+
	Plain agar	–	–	–	–	–	–	+	+	+	+

Note: “–” — complete absence of growth; “+” — growth of single colonies; “±” — normal growth.

Investigation of virucidal activity

The virucidal activity of the complex was studied at the Ivanovsky Institute of Virology in accordance with the Guidelines [16]. Vaccine strain of poliomyelitis virus (type 1, virus titer 6.5 lgTCID₅₀; M.P. Chumakov Research Institute of Poliomyelitis and Viral Encephalitis, Russia) and human adenovirus (type 5, virus titer 5.5 lg TCID₅₀; State Collection of Viruses of the Ivanovsky Institute of Virology, Russia) were employed. For the poliomyelitis virus, we used a transplantable Vero green monkey kidney cell culture, for the adenovirus — transplantable HEp2 cell line.

Statistical data processing

Statistica 7.0 software package (StatSoft; USA) enabled statistical processing. The metric indicators were presented as mean and error of mean ($M \pm m$). Student's *t*-test allowed establishing the significance of differences in metric indicators.

RESULTS

Biocidal activity assessment

The activity of 0.05% CHX-EDTA-Zn was compared in vitro with that of chlorhexidine bigluconate at the same concentration. For this comparison, we used a series of cultures of standard microorganisms. Table 1 shows the results of identification of the cultureless (no-growth) zones on Petri dishes.

Table 3. CHX-EDTA-Zn complex efficacy indicators in treatment of dermatitis in animals

Indicators	Animals	Serous catarrhal dermatitis	Purulent catarrhal dermatitis	Dermatitis of parasitic etiology (in complex therapy)
Number of experimental animals	Dogs	14	10	6
	Cats	7	2	–
	Rabbits	–	–	12
	Sheep	–	–	7
Duration of treatment, days	Dogs	5	7–10	6–14
	Cats	5	10–12	–
	Rabbits	–	–	6–9
	Sheep	–	–	6–12
Animals recovered	Dogs	11	9	5
	Cats	7	2	–
	Rabbits	–	–	10
	Sheep	–	–	7

Table 2 presents the results of *in vitro* assessment of antimicrobial activity against the main pathogens of bacterial diseases in birds.

At a concentration of 1.0–0.008 mg/ml (depending on the type of pathogen), the CHX-EDTA-Zn complex has both bacteriostatic and bactericidal effects against all studied pathogenic cultures.

Table 3 shows the results of *in vivo* studies in clinical conditions that involved treatment of dermatitis in domestic and farm animals.

Application of the antiseptic for 5–14 days let the animals recover completely. There were no allergic reactions or other negative side effects registered that could be attributed to the treatment.

The results of *in vitro* investigation of the antitubercular activity of the complex (against the *M. tuberculosis* 5582 strain) are shown in Fig. 1.

According to the results of *in vitro* testing on the *M. tuberculosis* H37Rv model, the CHX-EDTA-Zn complex has a pronounced antitubercular activity with the MIC value at 6.2 µg/ml.

Results of the *in vivo* investigation of antitubercular activity of the complex. Table 4 shows the results of investigation of therapeutic efficacy of the CHX-EDTA-Zn complex in comparison with moxifloxacin; Table 5 presents the data on inoculation of MBT from the lungs.

By the end of the experiment, on the 40th day from infection mortality in the control group (no treatment) was 70% among *M. tuberculosis* H37Rv cases and 40% among the strain 5582 cases. Moreover, both infection models have shown a sharp increase in the mass ratios of lungs and spleen, overall affection of the lung tissue with areas of necrosis. In the cultures of lung homogenates the MBT were recorded to grow continuously.

Therapeutic effect of the CHX-EDTA-Zn complex was confirmed in comparison with 7 mg/kg of moxifloxacin (average dose), a well-known antituberculous drug, in both models of tuberculosis, i.e. in mice infected with the standard test strain *M. tuberculosis* H37Rv and the drug-resistant strain 5582. The complex showed protective action and effectively prevented death of mice regardless of the model of tuberculosis (see

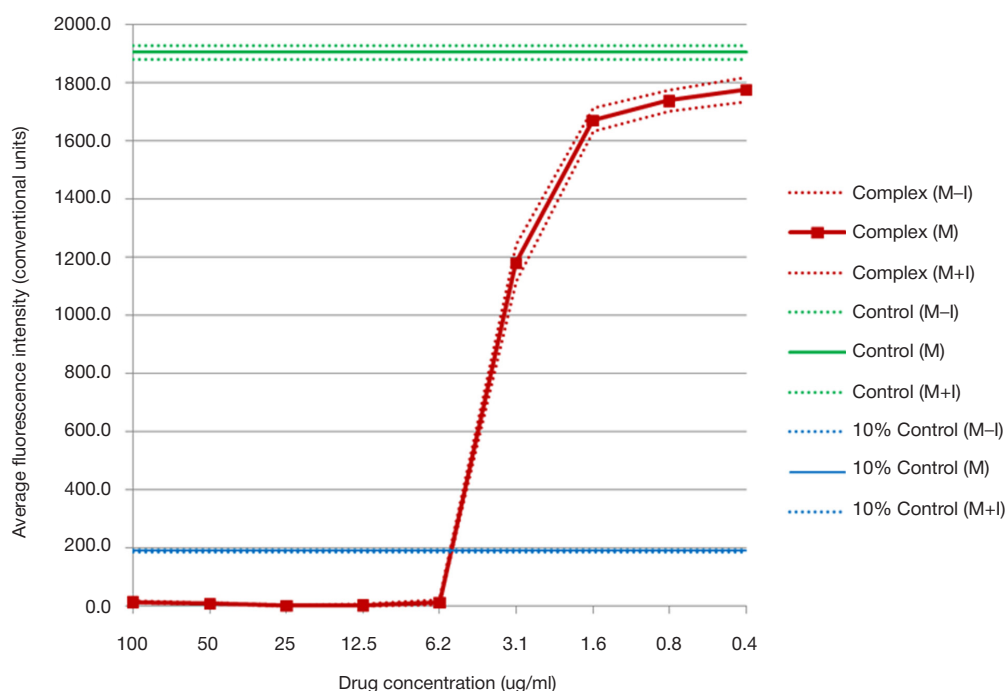


Fig. 1. Changes in the intensity of growth of the *M. tuberculosis* H37Rv test strain under the influence of the CHX-EDTA-Zn complex. M is the mean value, (M-I) and (M+I) are the lower and upper limits of the confidence interval (at $\alpha = 0.05$)

Table 4. Tuberculosis infection severity in mice infected with *M. tuberculosis* H37Rv and infected with drug-resistant strain 5582 (after 5 weeks from the start of the treatment)

Group №	Drug, dose <i>per os</i>	Lethality, %	Mass coefficients, c.u.		Lung injury index, c.u.
			lungs	spleen	
<i>M. tuberculosis</i> H37Rv infection model					
1	Infection control (untreated)	70	2.13 ± 0.18	1.89 ± 0.19	3.25 ± 0.11
2	Moxifloxacin 7.0 mg/kg	0	1.12 ± 0.06 $p_{1-2} < 0.001$	0.83 ± 0.03 $p_{1-2} < 0.002$	2.45 ± 0.03 $p_{1-2} < 0.001$
3	CHX-EDTA-Zn 7.0 mg/kg	0	1.28 ± 0.08 $p_{1-3} < 0.002$	1.05 ± 0.07 $p_{1-3} < 0.002$	2.55 ± 0.08 $p_{1-3} < 0.001$
4	CHX-EDTA-Zn 14 mg/kg	0	1.24 ± 0.09 $p_{1-4} < 0.002$	1.01 ± 0.09 $p_{1-4} < 0.002$	2.52 ± 0.05 $p_{1-4} < 0.001$
Multidrug-resistant 5582 strain infection model					
5	Infection control (untreated)	40	1.13 ± 0.03	1.05 ± 0.04	2.92 ± 0.04
6	Moxifloxacin 7.0 mg/kg	0	0.98 ± 0.04 $p_{1-2} < 0.01$	0.69 ± 0.05 $p_{1-2} < 0.001$	2.30 ± 0.08 $p_{1-2} < 0.001$
7	CHX-EDTA-Zn 14.0 mg/kg	0	1.01 ± 0.03 $p_{1-3} < 0.05$	0.91 ± 0.05 $p_{1-3} < 0.05$. $p_{2-3} < 0.01$	2.48 ± 0.05 $p_{1-3} < 0.001$ $p_{2-3} < 0.05$

Table 4). In the cases with drug-susceptible *M. tuberculosis* H37Rv, the CHX-EDTA-Zn complex significantly reduced the values of all registered parameters compared to the control group. The effect from administration of the 14 mg/kg dose was significantly more pronounced than that produced by the dose of 7.0 mg/kg, i.e. it was dose-dependent. In terms of reducing lung damage, 14 mg/kg of the CHX-EDTA-Zn complex in both models of tuberculosis were almost as effective as 7 mg/kg of moxifloxacin, although the former was slightly inferior to the latter in terms of spleen parameters.

Results of investigation of virulence activity Table 6 presents the results of assessing the potency of inhibition of viral reproduction expressed in TCID₅₀ units (50% tissue cytopathic infectious dose).

In both the suspension (mixing) and surface treatment tests, the solution of complex that contain of chlorhexidine 0.2%, inactivated the contaminating polio and human adenovirus in the course of 1–5 min.

DISCUSSION

It is known that EDTA forms a stable complex with the zinc cation (the $[ZnEDTA]^{2-}$ K_n instability constant is 3.2×10^{-17}) [11]. Preparation of a complex compound of chlorhexidine with EDTA has also been described [17]. However, more involved,

three-component complexes including EDTA, zinc and chlorhexidine, have not been studied. As we assumed, in an aqueous medium, chlorhexidine bigluconate, EDTA disodium salt and zinc chloride can form a complex compound with the structure shown in Fig. 2. Indeed, MALDI-MS study revealed a signal with m/z 859.27 that corresponds to the protonated form (MH⁺) of the predicted structure. Fragmentation of this ion leads to the appearance of corresponding signals: m/z 567.2 (ion of protonated adduct of chlorhexidine and zinc), m/z 505.3 (ion of protonated chlorhexidine) and m/z 353.3 (ion of protonated EDTA-Zn complex), which unambiguously proved its structure. Apparently, the structure of this complex includes a central four-coordinated doubly charged zinc cation, a doubly charged chlorhexidinium cation and a four-charged anion of a completely deprotonated EDTA molecule. The rather high stability of this ternary complex should also be noted: it persists under the harsh conditions of laser-induced evaporation.

The stability of the ternary complex of chlorhexidine, EDTA and zinc can be explained by intramolecular salt formation, which makes cationic and anionic fragments in this system stoichiometrically balance each other, ultimately forming an electrically neutral molecule.

The inclusion of chlorhexidine in the strong ternary complex with EDTA and zinc translates into improvement of biocidal activity (see Table 1). The CHX-EDTA-Zn complex is 4–5 times

Table 5. Inoculation of MBT from the lungs of mice infected with *M. tuberculosis* H37R and strain 5582 after 5 weeks of treatment with the CHX-EDTA-Zn complex

Group №	Drug, dose <i>per os</i>	Number of MBT colonies in the lungs, CFU × 10 ³	Number of viable mycobacteria in the lungs, lg
<i>M. tuberculosis</i> H37Rv infection			
1	Infection control (untreated)	129.6 ± 4.3	5.11 ± 0.01
2	Moxifloxacin 7.0 mg/kg	24.6 ± 4.6 $p_{1-2} < 0.001$	4.36 ± 0.09 $p_{1-2} < 0.001$
3	CHX-EDTA-Zn 7.0 mg/kg	41.99 ± 5.54 $p_{1-3} < 0.001$. $p_{2-3} < 0.05$	4.61 ± 0.05 $p_{1-3} < 0.001$. $p_{2-3} < 0.05$
4	CHX-EDTA-Zn 14 mg/kg	35.40 ± 3.19 $p_{1-4} < 0.001$	4.54 ± 0.05 $p_{1-4} < 0.001$
Multidrug-resistant 5582 strain infection			
6	Infection control (untreated)	18.39 ± 1.60	4.26 ± 0.04
7	Moxifloxacin 7.0 mg/kg	9.04 ± 1.57 $p_{1-2} < 0.01$	3.93 ± 0.07 $p_{1-2} < 0.01$
8	CHX-EDTA-Zn 14.0 mg/kg	11.48 ± 1.58 $p_{1-3} < 0.02$	4.04 ± 0.06 $p_{1-3} < 0.02$

Table 6. Virucidal activity of the CHX-EDTA-Zn complex

Object	Treatment method	Treatment time, min	Virus reproduction rate drop, lg TCID ₅₀	
			Polio	Adenovirus
Viral suspension	1 : 9 blend	5	3.5	4.0
Faux leather	Swab	1	4.0	4.0
		2 × 1.5	5.0	4.5
Latex	Swab	3	4.0	4.0
Metal	Swab	5	4.7	4.5
Glass	Swab	5	5.0	4.3
Plastic	Swab	5	4.3	4.3

more active against the studied bacterial and fungal strains than chlorhexidine bigluconate.

In vitro, the chlorhexidine complex also demonstrates high efficiency against the main avian pathogens (see Table 2), and *in vivo* it proved effective against dermatitis in domestic and farm animals — dogs, cats, rabbits and sheep (see Table 3). It can be concluded that the CHX-EDTA-Zn complex can be an effective medicine for treatment of bacterial and fungal skin diseases of various etiologies, healing of scratches, cracks, burns, infected wounds and pyoderma.

As our experiments show, the CHX-EDTA-Zn complex exhibits a significant anti-tuberculosis activity, which is quite unexpected, since chlorhexidine alone is very weak against *Mycobacterium tuberculosis* (MBT). In *in vitro* experiments, the activity (MIC) of the complex compared applied to the standard *M. tuberculosis* H37Rv strain (see Figure 1) is 6.2 µg/ml, and against the drug-resistant strain 5582 the activity is 2 times higher (MIC 3.1 µg/ml). In other words, the complex is twice as effective against the drug-resistant strain than the standard tuberculosis strain.

Even more surprising is the antituberculous activity of the CHX-EDTA-Zn complex established *in vivo*, when it was administered orally to mice, although it is known that chlorhexidine alone is practically not absorbed from the gastrointestinal tract. The reliability of the therapeutic effect of the drug is confirmed in two models of tuberculosis, based on animal survival data, on the results of assessment of the physiological parameters (see Table 4) and data on the MBT

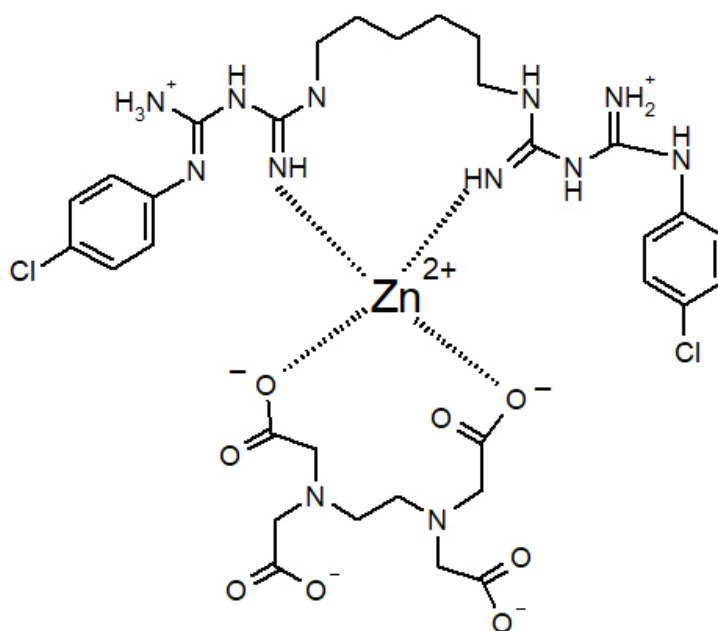
inoculation from the lungs (see Table 5). The complex is inferior to the moxifloxacin when used against the drug-sensitive strain *M. tuberculosis* H37Rv and almost as potent against the drug-resistant strain.

The results obtained allow considering the CHX-EDTA-Zn complex not only as a disinfectant, but also as a potential anti-tuberculosis drug that can be used as an adjuvant in the treatment of drug-resistant forms of tuberculosis.

The biocidal properties of the CHX-EDTA-Zn complex cover not only bacteria but also viruses (see Table 6). The results obtained indicate that the complex can be used to disinfect objects contaminated with these viruses.

CONCLUSIONS

The three-component complex of chlorhexidine, EDTA and zinc has a pronounced biocidal effect against pathogenic bacteria, fungi, *Mycobacterium tuberculosis* and viruses. It significantly exceeds chlorhexidine in terms of level of biocidal activity and the breadth of range of action. Overall, the chlorhexidine-EDTA-Zn complex appears to be a promising disinfectant that can be used to combat the spread of dangerous bacterial and viral infections. On models of experimental tuberculosis, when administered systemically, the CHX-EDTA-Zn complex exhibits a therapeutic effect comparable to that of moxifloxacin. This allows recommending this complex for further study as a possible treatment for drug-resistant forms of tuberculosis.

**Fig. 2.** Structural formula of the chlorhexidine-EDTA-zinc complex

References

1. Kvashnina DV, Kovalishena OV. Ocenka primeneniya hlorgeksidina kak antisepticheskogo sredstva. *Medicinskij al'manah*. 2016; 43 (3): 62–66. Russian.
2. Zverkov AV, Zuzova AP. Hlorgeksidin: proshloe, nastojashhee i budushhee odnogo iz osnovnyh antiseptikov. *Antimikrobnye preparaty*. 2013; 15 (4): 279–85. Russian.
3. Gilbert P, Moore LE. Cationic antiseptics: diversity of action under a common epithet. *J Appl Microbiol*. 2005; 99: 703–15.
4. Hugo WB. Disinfection mechanisms. In: Russell AD, Hugo WB, Ayliffe GAJ, eds. *Principles and practice of disinfection, preservation and sterilization*. Oxford: Blackwell, 1992; p. 187–210.
5. Mashkovskij MD. *Lekarstvennye sredstva*. M.: Novaja Volna, 2006. Russian.
6. Jones CG. Chlorhexidine: is it still the gold standard? *Periodontol*. 1997; 15: 55–62.
7. Junco-Lafuente MP, Baca-García P, Mesa-Aguado FL. Utilización de la clorhexidina en la prevención oral de pacientes de la tercera edad. *Revista del Ilustre Consejo General de Colegios de Odontólogos y Estomatólogos de España*. 2001; 6: 81–89.
8. Carouel F, Conte MP, Fisher J, Gonçalves LS, Dussart C, Llodra JC, Bourgeois D. COVID-19: A Recommendation to Examine the Effect of Mouthrinses With β -Cyclodextrin Combined With Citrox in Preventing Infection and Progression. *J Clin Med*. 2020; 9 (4): 1126.
9. Wand ME, Bock LJ, Bonney LC, Sutton JM. Mechanisms of Increased Resistance to Chlorhexidine and Cross-Resistance to Colistin following Exposure of *Klebsiella pneumoniae* Clinical Isolates to Chlorhexidine. *Antimicrob. Agents Chemother*. 2017; 61 (1): 1162–16.
10. Gupta M, Mahajan V, Mehta K, Chauhan P. Zinc Therapy in dermatology: a review. *Dermatology Research and Practice*. 2014; 9. Available from: <https://www.hindawi.com/journals/dr/2014/709152/>.
11. Djatlova NM, Temkina VYa, Popov KI. *Kompleksy i kompleksony metallov*. M.: Himija, 1988; 544 s. Russian.
12. *Metody laboratornyh issledovanij i ispytanij mediko-profilakticheskikh dezinfekcionnyh sredstv dlja ocenki ih jeffektivnosti i bezopasnosti: Rukovodstvo*. M.: Federal'nyj centr gigieny i jepidemiologii Rospotrebnadzora, 2010; 615 s. Russian.
13. Palomino J-C, Martin A, Camacho M, Guerra H, Swings J, Portaels F. Resazurin Microtitre Assay Plate — Simple and Inexpensive method for Detection of Dgug Resistance in *Mycobacterium tuberculosis*. *Antimicrob Agents Chemother*. 2002; 46 8: 2720–2.
14. Aleksandrova AE, Arijel BM. Ocenka tjazhesti tuberkuleznogo processa v legkih myshej. *Problemy tuberkuleza*. 1993; 3: 52–53. Russian.
15. Franzblau SG, DeGroot MA, Cho SH, Andries K, Nuermberger E, Ormel M, et al. Comprehensive analysis of methods used for the evaluation of compounds against *Mycobacterium tuberculosis*. *Tuberculosis*. 2012; 92: 453–88.
16. *Metodicheskie ukazaniya po izucheniju i ocenke virulicidnoj aktivnosti dezinficirujushih sredstv*. Rukovodstvo. MU 3.5.2431-08. M., 2010. Russian.
17. Rasimick BJ, Nekich M, Hladek MM, Barry L. Musikant BI, Deutsch AS. Interaction between Chlorhexidine Digluconate and EDTA. *JOE*. 2008; 34 (12): 1521–3.

Литература

1. Квашнина Д. В., Ковалишена О. В. Оценка применения хлоргексидина как антисептического средства. *Медицинский альманах*. 2016; 43 (3): 62–66.
2. Зверьков А. В., Зузова А. П. Хлоргексидин: прошлое, настоящее и будущее одного из основных антисептиков. *Антимикробные препараты*. 2013; 15 (4): 279–85.
3. Gilbert P, Moore LE. Cationic antiseptics: diversity of action under a common epithet. *J Appl Microbiol*. 2005; 99: 703–15.
4. Hugo WB. Disinfection mechanisms. In: Russell AD, Hugo WB, Ayliffe GAJ, eds. *Principles and practice of disinfection, preservation and sterilization*. Oxford: Blackwell, 1992; p. 187–210.
5. Машковский М. Д. *Лекарственные средства*. М.: Новая Волна, 2006.
6. Jones CG. Chlorhexidine: is it still the gold standard? *Periodontol*. 1997; 15: 55–62.
7. Junco-Lafuente MP, Baca-García P, Mesa-Aguado FL. Utilización de la clorhexidina en la prevención oral de pacientes de la tercera edad. *Revista del Ilustre Consejo General de Colegios de Odontólogos y Estomatólogos de España*. 2001; 6: 81–89.
8. Carouel F, Conte MP, Fisher J, Gonçalves LS, Dussart C, Llodra JC, Bourgeois D. COVID-19: A Recommendation to Examine the Effect of Mouthrinses With β -Cyclodextrin Combined With Citrox in Preventing Infection and Progression. *J Clin Med*. 2020; 9 (4): 1126.
9. Wand ME, Bock LJ, Bonney LC, Sutton JM. Mechanisms of Increased Resistance to Chlorhexidine and Cross-Resistance to Colistin following Exposure of *Klebsiella pneumoniae* Clinical Isolates to Chlorhexidine. *Antimicrob. Agents Chemother*. 2017; 61 (1): 1162–16.
10. Gupta M, Mahajan V, Mehta K, Chauhan P. Zinc Therapy in dermatology: a review. *Dermatology Research and Practice*. 2014; 9. Available from: <https://www.hindawi.com/journals/dr/2014/709152/>.
11. Дятлова Н. М., Темкина В. Я., Попов К. И. *Комплексы и комплексоны металлов*. М.: Химия, 1988; 544 с.
12. *Методы лабораторных исследований и испытаний медико-профилактических дезинфекционных средств для оценки их эффективности и безопасности: Руководство*. М.: Федеральный центр гигиены и эпидемиологии Роспотребнадзора, 2010; 615 с.
13. Palomino J-C, Martin A, Camacho M, Guerra H, Swings J, Portaels F. Resazurin Microtitre Assay Plate — Simple and Inexpensive method for Detection of Dgug Resistance in *Mycobacterium tuberculosis*. *Antimicrob Agents Chemother*. 2002; 46 8: 2720–2.
14. Александрова А. Е., Ариэль Б. М., Оценка тяжести туберкулезного процесса в легких мышей. *Проблемы туберкулеза*. 1993; 3: 52–53.
15. Franzblau SG, DeGroot MA, Cho SH, Andries K, Nuermberger E, Ormel M, et al. Comprehensive analysis of methods used for the evaluation of compounds against *Mycobacterium tuberculosis*. *Tuberculosis*. 2012; 92: 453–88.
16. *Методические указания по изучению и оценке вирулицидной активности дезинфицирующих средств*. Руководство. МУ 3.5.2431-08. М., 2010.
17. Rasimick BJ, Nekich M, Hladek MM, Barry L. Musikant BI, Deutsch AS. Interaction between Chlorhexidine Digluconate and EDTA. *JOE*. 2008; 34 (12): 1521–3.

MODELLING MYELOABLATIVE CYTOSTATIC THERAPY WITH CYCLOPHOSPHAMIDE IS ACCOMPANIED BY GASTROINTESTINAL STASIS IN RATS

Schäfer TV¹✉, Ivnitsky JuJu², Rejniuk VL²

¹ State Scientific Research Test Institute of the Military Medicine of Defense Ministry of the Russian Federation, Saint-Petersburg, Russia

² Golikov Research Clinical Center of Toxicology of the Federal Medical Biological Agency, Saint-Petersburg, Russia

Cyclophosphamide is used for the treatment of lymphoma, leukaemia, some solid tumours, and autoimmune disorders. When carrying out myeloablative cytostatic therapy, the doses of cyclophosphamide are prescribed, which cause irreversible pancytopenia. Early toxic effects of such doses are manifested by asthenic and emetic syndromes, limiting the treatment tolerance. Administration of cyclophosphamide in a dose of ≥ 600 mg/kg is accompanied by hyperammonaemia and symptoms, specific to the acute ammonium salt intoxication. Endotoxemia, resulting from the increase in the intestinal barrier permeability due to the impaired gastrointestinal motility, is considered the possible mechanism underlying these phenomena. The study was aimed to test this hypothesis. Radiographic assessment of the rat gastrointestinal peristalsis was performed within 25 h after administration of cyclophosphamide in a dose of 1000 mg/kg, which was equivalent to myeloablative dose for humans. Intraperitoneal, subcutaneous or intragastric administration of cyclophosphamide slowed down the gastrointestinal transit of bariumsulfate. In the case of subcutaneous cyclophosphamide injection, a moderate effect was observed. In the case of cyclophosphamide administered by gavage, the effect was manifested by a complete halt of transit. Thus, modelling myeloablative cytostatic therapy with cyclophosphamide in rats is associated with gastrointestinal stasis. The changes reported may promote the entry of the gut microbial products into the bloodstream and ensuing endotoxemia.

Keywords: cyclophosphamide, myeloablative cytostatic therapy, rat model, radiography, gastrointestinal stasis

Author contribution: Schäfer TV — developing the experimental model, study planning, experimental procedure, data processing and visualization; Ivnitsky JuJu — rationale, developing the experimental model, data interpretation; Rejniuk VL — setting up the experiment. All authors contributed to discussion, manuscript writing and editing.

Compliance with ethical standards: the study was carried out in accordance with the principles of bioethics, approved by the European Convention for the Protection of Vertebrate Animals used for Experimental and Other Scientific Purposes (ETS N 123).

✉ **Correspondence should be addressed:** Timur V. Schäfer
Lesoparkovaya, 4, Saint-Petersburg, 195043; schafer@yandex.ru

Received: 14.12.2021 **Accepted:** 15.01.2022 **Published online:** 31.01.2022

DOI: 10.47183/mes.2022.001

МОДЕЛИРОВАНИЕ МИЕЛОАБЛЯЦИОННОЙ ЦИТОСТАТИЧЕСКОЙ ТЕРАПИИ ЦИКЛОФОСФАНОМ СОПРОВОЖДАЕТСЯ ЖЕЛУДОЧНО-КИШЕЧНЫМ СТАЗОМ У КРЫС

Т. В. Шефер¹✉, Ю. Ю. Ивницкий², В. Л. Рейнюк²

¹ Государственный научно-исследовательский испытательный институт военной медицины Министерства обороны Российской Федерации, Санкт-Петербург, Россия

² Научно-клинический центр токсикологии имени академика С. Н. Голикова Федерального медико-биологического агентства, Санкт-Петербург, Россия

Циклофосфан применяют для лечения лимфом, лейкозов, некоторых солидных опухолей и аутоиммунных заболеваний. При миелоабляционной цитостатической терапии его назначают в дозах, вызывающих необратимую панцитопению. Ранние токсические эффекты при таких дозах проявляются астеническим и эметическим синдромами, ограничивающими переносимость лечения. Введение циклофосфана крысам в дозах ≥ 600 мг/кг сопровождается гипераммониемией и симптоматикой, характерной для острой интоксикации солями аммония. Возможным механизмом этих феноменов является эндотоксемия, обусловленная повышением проницаемости энтерогематического барьера вследствие нарушений моторики желудочно-кишечного тракта. Целью настоящей работы была проверка этой гипотезы. Рентгенологически изучали перистальтику желудочно-кишечного тракта крыс в течение 25 ч после введения циклофосфана в дозе 1000 мг/кг, биоэквивалентной его миелоабляционной дозе для человека. Внутривенное, подкожное или внутривентральное введение циклофосфана замедляло желудочно-кишечный транзит сульфата бария. При подкожном введении циклофосфана этот эффект был умеренным, а при внутривентральном — проявлялся полной остановкой транзита. Таким образом, моделирование на крысах миелоабляционной цитостатической терапии циклофосфаном сопряжено с развитием желудочно-кишечного стаза. Выявленные изменения могут способствовать поступлению в кровь продуктов жизнедеятельности кишечной микрофлоры и формированию эндотоксемии.

Ключевые слова: циклофосфан, миелоабляционная цитостатическая терапия, крысиная модель, рентгенография, желудочно-кишечный стаз

Вклад авторов: Т. В. Шефер — разработка экспериментальной модели, планирование исследования, экспериментальная часть, обработка и визуализация данных; Ю. Ю. Ивницкий — научный замысел, разработка экспериментальной модели, интерпретация результатов; В. Л. Рейнюк — организация экспериментальной части работы. Все авторы участвовали в обсуждении результатов, подготовке и редактировании рукописи статьи.

Соблюдение этических стандартов: исследование выполняли с соблюдением правил биоэтики, утвержденных Европейской конвенцией о защите позвоночных животных, используемых в экспериментальных и иных научных целях (ETS N 123).

✉ **Для корреспонденции:** Тимур Васильевич Шефер
ул. Лесопарковая, д. 4, г. Санкт-Петербург, 195043; schafer@yandex.ru

Статья получена: 14.12.2021 **Статья принята к печати:** 15.01.2022 **Опубликована онлайн:** 31.01.2022

DOI: 10.47183/mes.2022.001

Cyclophosphamide is used for the treatment of lymphoma, leukaemia, some solid tumours [1] and autoimmune disorders [2]. When carrying out myeloablative cytostatic therapy, the doses of cyclophosphamide are prescribed, which destroy the tumour, but cause fatal pancytopenia [3, 4].

Owing to subsequent allogeneic hematopoietic stem cell transplantation, these doses are an order of magnitude larger than the doses, used for conservative therapy [5], and exceed 120 mg/kg [6]. Early toxic effects of such doses of cyclophosphamide are manifested by asthenic and

emetic syndromes [7], limiting the drug tolerance. In rats, bioequivalent doses of cyclophosphamide (≥ 600 mg/kg) caused hyperammonaemia and symptoms, specific to the acute ammonium salt intoxication: ataxia, tremor, loss of reflexes, and seizure [8]. Increased permeability of the intestinal barrier could be the possible mechanism, underlying hyperammonaemia associated with acute cyclophosphamide intoxication [8–11]. Inhibition of intestinal peristalsis increases the permeability of the intestinal wall [12]. Thus, the study was aimed to assess the effects of the myeloablative dose of cyclophosphamide on gastrointestinal peristalsis.

METHODS

The study involved 24 male outbred albino rats with the body weight of 161–190 g, obtained from the Rappolovo laboratory animal nursery. The animals were treated in accordance with the Principles of Good Laboratory Practice, stated in the Order № 199n of the Ministry of Health of the Russian Federation, dated April 1, 2016 [13], and the requirements of the Guidelines for the Housing and Care of Laboratory Animals [14, 15]. Standard rat diet and ad libitum water access were provided. The day before the experiment the rats were deprived of food; however, access to water was not limited.

The rats were randomized into six groups, four animals per group. Water was administered in three control groups (intraperitoneal, subcutaneous, and intragastric routes). The freshly prepared aqueous cyclophosphamide solution in the amount of 10 mL/kg in a dose of 1000 mg/kg was administered in the corresponding three experimental groups. This was an absolutely lethal dose under either route of administration: all animals died within two weeks; in the case of intraperitoneal injection, the dose corresponded to 3.5 LD₅₀.

The 35% aqueous suspension of barium sulfate (10 mL/kg) was administered into the stomach of all rats using the gavage tube immediately after the cyclophosphamide administration. After 1, 3, 5, and 25 h the animals were placed in plastic pencil boxes, and the radiographic testing with the use of the Iconos R200 digital x-ray system (Siemens; Germany) was performed in a pairwise manner (experimental and control animals). X-ray images were assessed using the planimetric ruler by calculating the absolute and relative (percentage) values of the radiopaque shadow area in the stomach, duodenum, jejunum, cecum, descending colon, and rectum. The relative values other than zero or 100%, which were averaged for each group of animals, were ranked and assigned to one of the intervals (1–25, 26–50, 51–75, 76–99%), marked with various shades of grey; no shadow was marked with white, and the shadow of 100% of the injected barium mixture was marked with black. The data obtained were represented as a scheme.

RESULTS

An hour after the barium suspension administration to intact rats, a portion of the suspension passed from the stomach to the duodenum. After 3 h, the suspension was observed in the jejunum, and after 5 h it was also found in the cecum. Twenty-five hours after the start of the experiment the major portion of barium sulfate, found on the x-ray images, was in the descending colon and the rectum.

In the case of intraperitoneal administration of cyclophosphamide, barium suspension never reached the jejunum, and in the case of cyclophosphamide administered

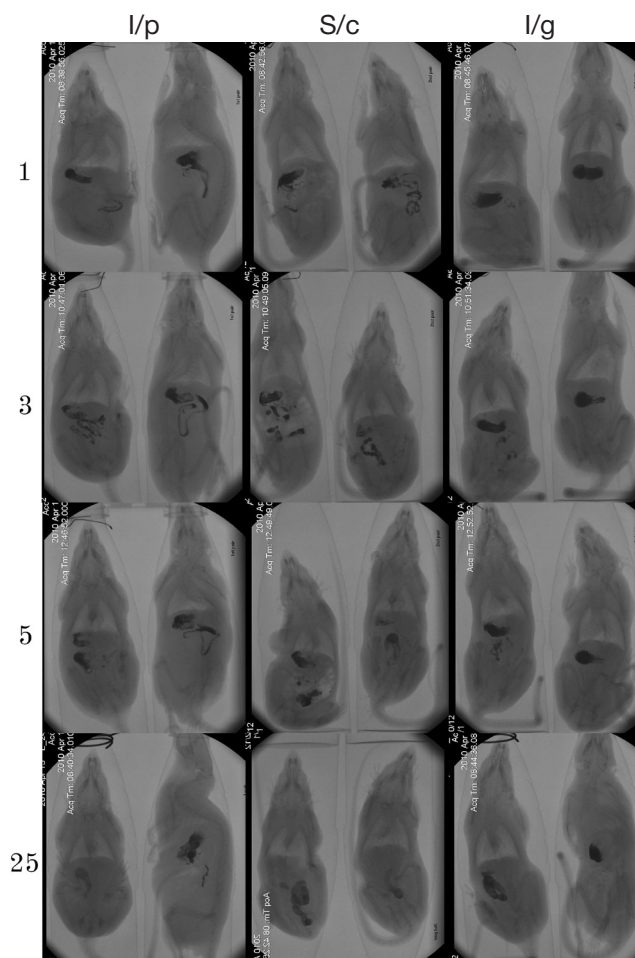


Fig. 1. X-ray radiography of rats performed at different times (specified on the left, hours) after administration of cyclophosphamide in a dose of 1000 mg (routes are specified on the top: i/p — intraperitoneal; s/c — subcutaneous; i/g — intragastric) and barium sulfate (i/g, immediately after cyclophosphamide administration). Control rats are shown on the left in each window

intragastrically, the suspension never left the stomach. Subcutaneous cyclophosphamide administration resulted in the less prominent slow-down of transit: after 3 h the radiopaque contrast medium left the stomach, however, after 25 h the medium did not reach the descending colon (Fig. 1, 2).

DISCUSSION

The development of gastrointestinal stasis in rats after cyclophosphamide administration is consistent with the earlier reported [16] slowing of gastric motility after the subcutaneous injection of cyclophosphamide in a dose of 50–200 mg/kg to rats. In the case of intragastric administration, the effect size could be due to the aldophosphamide (transport form of cyclophosphamide) hydrolysis in the acidic gastric contents with the formation of more active alkylating metabolites [17, 18].

In our study, the dose of cyclophosphamide corresponded to myeloablative dose for humans of 155 mg/kg [19]. Therefore, the data obtained clearly point to the possibility of developing gastrointestinal stasis in case of using cyclophosphamide to prepare the patients for the allogeneic hematopoietic stem cell transplantation.

Gastrointestinal stasis is a potentially fatal complication found in the intensive care unit patients [20, 21]. The condition increases the permeability of the intestinal barrier [22, 23], and results in the gram-negative bacterial lipopolysaccharides entering the bloodstream, developing systemic inflammation

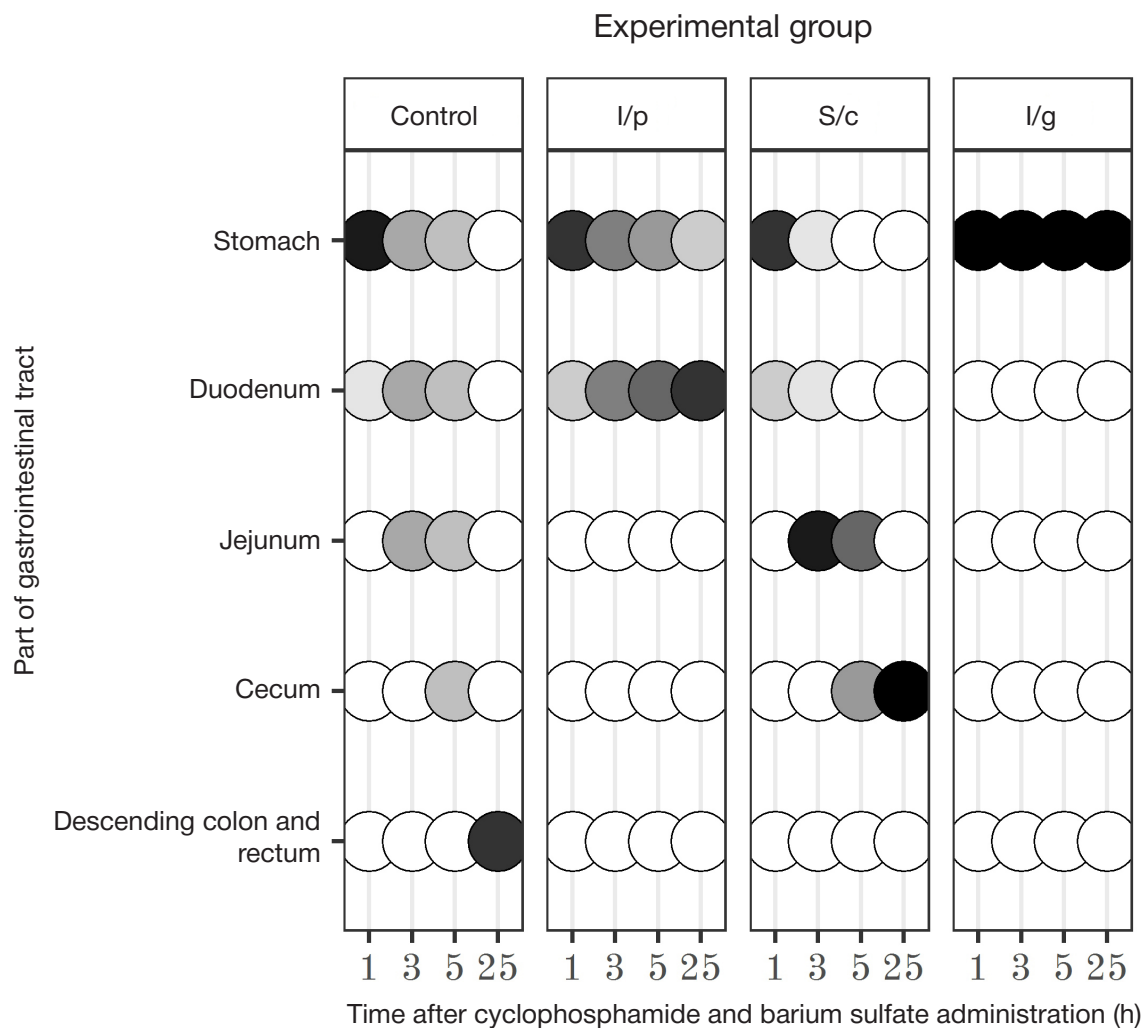


Fig. 2. Effects of cyclophosphamide administered in a dose of 1000 mg/kg on the barium suspension passage through the rat gastrointestinal tract. Shades of the circles are proportional to the percentage of the radiopaque shadow area in the corresponding section of the gastrointestinal tract: black circles — 100% of the administered barium sulfate; white circles — no barium sulfate

[24, 25] and sepsis [26]. Increased permeability of the intestinal barrier also results in the enhanced flux of toxic nitrogenous metabolites, such as ammonia, from chyme into the bloodstream. In rats, exacerbation of hyperammonaemia after the gavage with ammonium acetate against the background of acute cyclophosphamide intoxication leads to the rapid development of neurological disorders and significantly reduces the animals' life expectancy [27].

CONCLUSIONS

Modelling myeloablative cytostatic therapy in rats using cyclophosphamide results in gastrointestinal stasis. The changes in gastrointestinal peristalsis reported may contribute to the flux of the gut microbial products into the bloodstream and endotoxemia, and may be involved in the development of the cyclophosphamide early toxic effects.

References

- Emadi A, Jones RJ, Brodsky RA. Cyclophosphamide and cancer: golden anniversary. *Nature reviews. Clinical Oncology*. 2009; 6 (11): 638–47.
- Brodsky RA. High dose cyclophosphamide treatment for autoimmune disorders. *Scientific World Journal*. 2002; 28 (2): 1808–15.
- Kharfan-Dabaja MA, Reljic T, El-Asmar J, Nishihori T, Ayala E, Hamadani M, et al. Reduced-intensity or myeloablative allogeneic hematopoietic cell transplantation for mantle cell lymphoma: a systematic review. *Future Oncology*. 2016; 22 (12): 2631–42.
- Yee GC, McGuire TR. Allogeneic bone marrow transplantation in the treatment of hematologic diseases. *Clinical Pharmacology*. 1985; 4 (2): 149–60.
- Haïoun C, Lepage E, Gisselbrecht C, Salles G, Coiffier B, Brice P, et al. Survival benefit of high-dose therapy in poor-risk aggressive non-Hodgkin's lymphoma: final analysis of Etude des lymphomes de l'Adulte study. *Journal of Clinical Oncology*. 2000; 18: 3025–30.
- Atilla E, Atilla PA, Demirel T. A review of myeloablative vs reduced intensity/non-myeloablative regimens in allogeneic hematopoietic stem cell transplantations. *Balkan Medical Journal*. 2017; 34 (1): 1–9.
- Legeza VI, Geleev IS, Seleznyov AB. *Emetic syndrome*. Saint Petersburg: Foliant, 2005; 144 p. Russian.
- Ivnitsky JJ, Schäfer TV, Tyapin AA, Rejniuk VL. Changes in the chemical composition of the blood and brain of rats under the conditions of modeling the myeloablation regimen of cyclophosphamide administration. *Toxicologicheskii vestnik*. 2019; 156 (3): 13–8. Russian.
- Schäfer TV, Rejniuk VL, Ivnitsky JJ. Ammonia redistribution from the gastrointestinal tract to general circulation after intraperitoneal

- injection of cyclophosphamide to rats. *Bulletin of Experimental Biology and Medicine*. 2010; 150 (8): 170–6. Russian.
10. Dore MP, Pes GM, Murino A, Quarta Colosso B, Pennazio M. Short article: small intestinal mucosal injury in patients taking chemotherapeutic agents for solid cancers. *European Journal of Gastroenterology & Hepatology*. 2017; 29 (5): 568–71.
 11. Schäfer TV, Ivnitsky JJ, Rejniuk VL. Cyclophosphamide-induced leakage of gastrointestinal ammonia into the common bloodstream in rats. *Drug and Chemical Toxicology*. 2011; 34 (1): 25–31.
 12. Ghareghani M, Reiter RJ, Zibara K, Fathadi N. Latitude, vitamin D, melatonin, and gut microbiota act in concert to initiate multiple sclerosis: a new mechanistic pathway. *Frontiers in Immunology*. 2018; 9: 2484.
 13. On Approval of the Rules of Good Laboratory Practice: Order of the Ministry of Health of the Russian Federation from April 1, 2016, No 199n. Moscow, 2016.
 14. Guidelines for the maintenance and care of laboratory animals. Rules of equipment of premises and organization of procedures: GOST 33215–2014. Moscow: Standartinform, 2016; 12 p. Russian.
 15. Guidelines for the maintenance and care of laboratory animals. Rules for the maintenance and care of laboratory rodents and rabbits: GOST 33216–2014. Moscow: Standartinform, 2016; 15 p. Russian.
 16. Visnovský P. The effect of cyclophosphamide and methotrexate on gastric emptying and secretion in rats. *Bratislavské lekárske listy*. 1992; 93 (2): 90–2. Slovak.
 17. Anderson LW, Chen TL, Colvin OM, Grochow LB, Collins JM, Kennedy MJ, et al. Cyclophosphamide and 4-hydroxycyclophosphamide/aldophosphamide kinetics in patients receiving high-dose cyclophosphamide chemotherapy. *Clinical Cancer Research*. 1996; 2 (9): 1481–7.
 18. De Jonge ME, Huitema AD, Rodenhuis S, Beijnen JH. Clinical pharmacokinetics of cyclophosphamide. *Clinical Pharmacokinetics*. 2005; 44 (11): 1135–64.
 19. Habriev RU, editor. Guidelines for the experimental (preclinical) study of new pharmacological substances. Moscow: Medicina, 2005; 832 p. Russian.
 20. Deane AM, Chapman MJ, Reintam Blaser A, McClave SA, Emmanuel A. Pathophysiology and treatment of gastrointestinal motility disorders in the acutely ill. *Nutrition in Clinical Practice*. 2019; 34 (1): 23–36.
 21. Frazer C, Hussey L, Bemker M. Gastrointestinal motility problems in critically ill patients. *Critical care nursing clinics of North America*. 2018; 30 (1): 109–21.
 22. Herbert MK, Holzer P. Standardized concept for the treatment of gastrointestinal dysmotility in critically ill patients—current status and future options. *Clinical Nutrition*. 2008; 27 (1): 25–41.
 23. Ukleja A. Altered GI motility in critically ill patients: current understanding of pathophysiology, clinical impact, and diagnostic approach. *Nutrition in Clinical Practice*. 2010; 25 (1): 16–25.
 24. Buchholz BM, Bauer AJ. Membrane Tlr signaling mechanisms in the gastrointestinal tract during sepsis. *Neurogastroenterology and Motility*. 2010; 22: 232–45.
 25. Shimizu K, Ogura H, Asahara T, Nomoto K, Morotomi M, Nakahori Y, et al. Gastrointestinal dysmotility is associated with altered gut flora and septic mortality in patients with severe systemic inflammatory response syndrome: a preliminary study. *Neurogastroenterology and Motility*. 2011; 23 (4): 330–5.
 26. Chapman MJ, Nguyen NQ, Deane AM. Gastrointestinal dysmotility: clinical consequences and management of the critically ill patient. *Gastroenterology clinics of North America*. 2011; 40 (4): 725–39.
 27. Ivnitsky JJ, Schäfer TV, Rejniuk VL. Promotion of the toxic action of cyclophosphamide by digestive tract luminal ammonia in rats. *ISRN Toxicology [Internet]*. 2011. Article ID 450875. Available from: <https://www.hindawi.com/journals/isrn/2011/450875/>.

Литература

1. Emadi A, Jones RJ, Brodsky RA. Cyclophosphamide and cancer: golden anniversary. *Nature reviews. Clinical Oncology*. 2009; 6 (11): 638–47.
2. Brodsky RA. High dose cyclophosphamide treatment for autoimmune disorders. *Scientific World Journal*. 2002; 28 (2): 1808–15.
3. Kharfan-Dabaja MA, Reljie T, El-Asmar J, Nishihori T, Ayala E, Hamadani M, et al. Reduced-intensity or myeloablative allogeneic hematopoietic cell transplantation for mantle cell lymphoma: a systematic review. *Future Oncology*. 2016; 22 (12): 2631–42.
4. Yee GC, McGuire TR. Allogeneic bone marrow transplantation in the treatment of hematologic diseases. *Clinical Pharmacy*. 1985; 4 (2): 149–60.
5. Haioun C, Lepage E, Gisselbrecht C, Salles G, Coiffier B, Brice P, et al. Survival benefit of high-dose therapy in poor-risk aggressive non-Hodgkin's lymphoma: final analysis d'Etude des lymphomes de l'Adulte study. *Journal of Clinical Oncology*. 2000; 18: 3025–30.
6. Atilla E, Atilla PA, Demirer T. A review of myeloablative vs reduced intensity/non-myeloablative regimens in allogeneic hematopoietic stem cell transplantations. *Balkan Medical Journal*. 2017; 34 (1): 1–9.
7. Легеза В. И., Галеев И. Ш., Селезнев А. Б. Эметический синдром. СПб.: Фолиант, 2005; 144 с.
8. Ивницкий Ю. Ю., Шефер Т. В., Тяптин А. А., Рейнюк В. Л. Изменения химического состава крови и головного мозга крыс при моделировании миелоабляционного режима применения циклофосфана. *Токсикологический вестник*. 2019; 156 (3): 13–8.
9. Шефер Т. В., Рейнюк В. Л., Ивницкий Ю. Ю. Перераспределение аммиака из желудочно-кишечного тракта в общий кровоток при внутрибрюшинном введении циклофосфана крысам. *Бюллетень экспериментальной биологии и медицины*. 2010; 150 (8): 170–6.
10. Dore MP, Pes GM, Murino A, Quarta Colosso B, Pennazio M. Short article: small intestinal mucosal injury in patients taking chemotherapeutic agents for solid cancers. *European Journal of Gastroenterology & Hepatology*. 2017; 29 (5): 568–71.
11. Schäfer TV, Ivnitsky JJ, Rejniuk VL. Cyclophosphamide-induced leakage of gastrointestinal ammonia into the common bloodstream in rats. *Drug and Chemical Toxicology*. 2011; 34 (1): 25–31.
12. Ghareghani M, Reiter RJ, Zibara K, Fathadi N. Latitude, vitamin D, melatonin, and gut microbiota act in concert to initiate multiple sclerosis: a new mechanistic pathway. *Frontiers in Immunology*. 2018; 9: 2484.
13. Об утверждении Правил надлежащей лабораторной практики: Приказ Министерства здравоохранения Российской Федерации от 1 апреля 2016 г. № 199н. М., 2016.
14. Руководство по содержанию и уходу за лабораторными животными. Правила оборудования помещений и организации процедур: ГОСТ 33215–2014. М.: Стандартиформ, 2016; 12 с.
15. Руководство по содержанию и уходу за лабораторными животными. Правила содержания и ухода за лабораторными грызунами и кроликами: ГОСТ 33216–2014. М.: Стандартиформ, 2016; 15 с.
16. Visnovský P. The effect of cyclophosphamide and methotrexate on gastric emptying and secretion in rats. *Bratislavské lekárske listy*. 1992; 93 (2): 90–2 (на словацком языке).
17. Anderson LW, Chen TL, Colvin OM, Grochow LB, Collins JM, Kennedy MJ, et al. Cyclophosphamide and 4-hydroxycyclophosphamide/aldophosphamide kinetics in patients receiving high-dose cyclophosphamide chemotherapy. *Clinical Cancer Research*. 1996; 2 (9): 1481–7.
18. De Jonge ME, Huitema AD, Rodenhuis S, Beijnen JH. Clinical pharmacokinetics of cyclophosphamide. *Clinical Pharmacokinetics*. 2005; 44 (11): 1135–64.
19. Хабриев Р. У., редактор. Руководство по экспериментальному (доклиническому) изучению новых фармакологических веществ. М.: Медицина, 2005; 832 с.
20. Deane AM, Chapman MJ, Reintam Blaser A, McClave SA,

- Emmanuel A. Pathophysiology and treatment of gastrointestinal motility disorders in the acutely ill. *Nutrition in Clinical Practice*. 2019; 34 (1): 23–36.
21. Frazer C, Hussey L, Bemker M. Gastrointestinal motility problems in critically ill patients. *Critical care nursing clinics of North America*. 2018; 30 (1): 109–21.
 22. Herbert MK, Holzer P. Standardized concept for the treatment of gastrointestinal dysmotility in critically ill patients—current status and future options. *Clinical Nutrition*. 2008; 27 (1): 25–41.
 23. Ukleja A. Altered GI motility in critically ill patients: current understanding of pathophysiology, clinical impact, and diagnostic approach. *Nutrition in Clinical Practice*. 2010; 25 (1): 16–25.
 24. Buchholz BM, Bauer AJ. Membrane Tlr signaling mechanisms in the gastrointestinal tract during sepsis. *Neurogastroenterology and Motility*. 2010; 22: 232–45.
 25. Shimizu K, Ogura H, Asahara T, Nomoto K, Morotomi M, Nakahori Y, et al. Gastrointestinal dysmotility is associated with altered gut flora and septic mortality in patients with severe systemic inflammatory response syndrome: a preliminary study. *Neurogastroenterology and Motility*. 2011; 23 (4): 330–5.
 26. Chapman MJ, Nguyen NQ, Deane AM. Gastrointestinal dysmotility: clinical consequences and management of the critically ill patient. *Gastroenterology clinics of North America*. 2011; 40 (4): 725–39.
 27. Ivnitsky JJ, Schäfer TV, Rejniuk VL. Promotion of the toxic action of cyclophosphamide by digestive tract luminal ammonia in rats. *ISRN Toxicology [Internet]*. 2011. Article ID 450875. Available from: <https://www.hindawi.com/journals/isrn/2011/450875/>.

DETECTION OF ULTRA-LOW CONCENTRATIONS OF BROMODIHYDROCHLOROPHENYLBENZODIAZEPINE (PHENAZEPAM) AND ITS METABOLITES IN BIOLOGICAL OBJECTS

Volkova AA^{1,2}, Kalekin RA^{1,2}✉, Moskaleva NE^{1,3}, Astashkina OG^{1,4}, Orlova AM¹, Markin PA^{1,3}

¹ Russian Center of Forensic Medical Expertise, Moscow, Russia

² Peoples' Friendship University of Russia, Moscow, Russia

³ Sechenov First Moscow State Medical University, Moscow, Russia

⁴ Bureau of Forensic Medical Examination, Moscow, Russia

In extreme situations, reliable detection of the minimum therapeutic concentrations of psychotropic substances is important, since this allows one to provide adequate resuscitation. The group of benzodiazepine derivatives, which includes bromodihydrochlorophenylbenzodiazepine (phenazepam), is widely used in clinical practice. Along with the positive clinical effect, phenazepam has numerous side effects, capable of causing poisoning, even death. The study was aimed to develop the method for detection of the phenazepam metabolites by high-resolution HPLC–TMS suitable for achieving the aims and objectives of forensic medical expertise in case of the ultra-low urine substance concentrations. Urine of six patients (males and females aged 28–40), who were prescribed phenazepam and took the drug at minimum therapeutic concentrations on an ad hoc basis, was used during the study. Optimum conditions for the analyte chromatography after the urine sample preparation were defined with the phenazepam retention time of 7.05 ± 0.06 min; specific ions (m/z) 179, 183, 206, 242, 271, 285, 320, 348 (main) were defined for identification of phenazepam.

Keywords: phenazepam, bromodihydrochlorophenylbenzodiazepine, 3-hydroxyphenazepam, high-performance liquid chromatography, forensic chemistry research, chemical toxicological analysis, urine

Author contribution: Volkova AA, Kalekin RA, Orlova AM, Astashkina OG — data acquisition, manuscript writing; Volkova AA, Kalekin RA, Moskaleva NE, Markin PA — experimental procedure.

Compliance with ethical standards: the study was planned and conducted in accordance with the requirements of the Declaration of Helsinki of the World Medical Association (2000) and subsequent revisions thereto; the informed consent was submitted by all study participants.

✉ **Correspondence should be addressed to:** Roman A. Kalekin
Polikarpova, 12/13, Moscow, 125284, Russia; himija@rc-sme.ru

Received: 23.02.2022 **Accepted:** 11.03.2022 **Published online:** 25.03.2022

DOI: 10.47183/mes.2022.007

ОБНАРУЖЕНИЕ БРОМДИГИДРОХЛОРФЕНИЛБЕНЗОДИАЗЕПИНА (ФЕНАЗЕПАМА) И ЕГО МЕТАБОЛИТА В БИОЛОГИЧЕСКОМ ОБЪЕКТЕ ПРИ СВЕРХНИЗКИХ КОНЦЕНТРАЦИЯХ

А. А. Волкова^{1,2}, Р. А. Калёкин^{1,2}✉, Н. Е. Москалева^{1,3}, О. Г. Асташкина^{1,4}, А. М. Орлова¹, П. А. Маркин^{1,3}

¹ Российский центр судебно-медицинской экспертизы, Москва, Россия

² Российский университет дружбы народов, Москва, Россия

³ Первый Московский государственный медицинский университет имени И. М. Сеченова, Москва, Россия

⁴ Бюро судебно-медицинской экспертизы, Москва, Россия

В экстремальных ситуациях важна роль достоверного обнаружения психотропных веществ при минимальных терапевтических концентрациях, что позволит проводить адекватную реанимационную терапию. В медицинской практике широко используют группу производных бензодиазепинов, среди которых бромдигидрохлорфенилбензодиазепин (феназепам). Помимо положительного клинического эффекта феназепам обладает большим числом побочных эффектов, способных привести к отравлениям вплоть до летального исхода. Целью исследования было разработать методику обнаружения метаболитов феназепама методом ВЭЖХ–ТМС высокого разрешения для целей и задач судебно-медицинской экспертизы при наличии сверхнизких концентраций в моче. В исследовании использовали мочу шести пациентов (мужчин и женщин в возрасте 28–40 лет), принимавших феназепам в минимальных терапевтических концентрациях в разовых случаях, по назначению врача. По результатам исследования разработаны оптимальные условия хроматографирования аналитов после пробоподготовки мочи, с временем удерживания феназепама $7,05 \pm 0,06$ мин, выявлены характерные ионы (m/z) 179, 183, 206, 242, 271, 285, 320, 348 (основной) для идентификации феназепама.

Ключевые слова: феназепам, бромдигидрохлорфенилбензодиазепин, 3-гидроксифеназепам, высокоэффективная жидкостная хроматография, судебно-химическое исследование, химико-токсикологический анализ, моча

Вклад авторов: А. А. Волкова, Р. А. Калёкин, А. М. Орлова, О. Г. Асташкина — сбор данных, написание статьи; А. А. Волкова, Р. А. Калёкин, Н. Е. Москалева, П. А. Маркин — проведение экспериментальной части исследования.

Соблюдение этических стандартов: исследование спланировано и проведено с соблюдением требований Хельсинкской декларации Всемирной медицинской ассоциации (2000 г.) и последующих ее пересмотров; все участники подписали добровольное информированное согласие на участие в исследовании.

✉ **Для корреспонденции:** Роман Анатольевич Калёкин
ул. Поликарпова, д. 12/13, г. Москва, 125284, Россия; himija@rc-sme.ru

Статья получена: 23.02.2022 **Статья принята к печати:** 11.03.2022 **Опубликована онлайн:** 25.03.2022

DOI: 10.47183/mes.2022.007

In extreme situations, reliable detection of the minimum therapeutic concentrations of psychotropic substances is important, since this allows one to provide adequate resuscitation. Currently, benzodiazepine derivatives are among the most common psychotropic medications used in patients with anxiety disorders and other psychosomatic disorders. Bromodihydrochlorophenylbenzodiazepine (phenazepam) is the most potent benzodiazepine commonly used in medical practice [1–5]. Along with the positive clinical effect it has numerous side effects [6], which, in case of inappropriate medication use or non-medical use, may result in poisoning and even be fatal [7–9].

Bromodihydrochlorophenylbenzodiazepine is a benzodiazepine anxiolytic agent (tranquilizer) possessing anxiolytic, sedative-hypnotic, anticonvulsant and central muscle relaxant effects. The chemical name is 7-bromo-5-(ortho-chlorophenyl)-2,3-dihydro-1H-1,4-benzodiazepin-2-one; the molecular formula is $C_{15}H_{10}BrClN_2O$; in the Russian Federation, the compound is known mostly under the brand name of “Phenazepam”. The dosage forms are 0.5, 1.0 and 2.5 mg tablets [10], and the 1 mg/mL solution, 0.5 and 1.0 mL [11]. Bromodihydrochlorophenylbenzodiazepine is a prescription drug (prescription form № 148–1/u-88). As a potent substance, in 2021 it became a controlled drug. To phenazepam, the risk of substance abuse and withdrawal syndrome remains rather high, which is the cause of the poisoning cases. Side effects, such as hallucinations, euphoria, etc., define the abuse potential of the drug [1, 9].

Phenazepam is used in small quantities because of its huge therapeutic effect. The possibility of the effect manifold potentiation by other substances entails low concentrations of the substance in the body's biological objects. Non-medical use, combinations with other psychotropic medications or alcohol, and side effects may result in acute or fatal phenazepam intoxication, that is why development of the method for detection and identification of the ultra-low substance concentrations in biological objects using the advanced techniques still remains an urgent challenge posed by forensic chemistry and chemical toxicology studies. Simultaneous detection of the phenazepam metabolites and native substance (bromodihydrochlorophenylbenzodiazepine) makes it possible to actually verify the substance use by patient/victim and confirm the lack of false positive result in case of falsification in the form of adding the substance to the biological object. The most common non-invasive biological object used in medical laboratories (including the chemical toxicology laboratories) is the biological fluid, urine [12, 13].

Today, high performance liquid chromatography–tandem mass spectrometry (HPLC–TMS) is successfully used as a reliable, selective and sensitive method for screening, identification and quantification of small molecules [14–16]. The study was aimed to develop the method for detection of phenazepam and its major metabolite by high-resolution (HR) HPLC–TMS based on the Orbitrap technology suitable

for achieving the aims and objectives of forensic medical expertise in case of the ultra-low substance concentration in the biological object (urine).

METHODS

Urine samples were collected from patients ($n = 6$) in the morning on an empty stomach 8 ± 1 h after administration of the therapeutic concentrations of phenazepam (in tablets of 1 mg), prescribed due to psychosomatic disorder. Inclusion criteria: initial medication administration allowing to avoid deposition and concentration increase in the human body. Exclusion criteria: patients with comorbidities currently taking psychotropic medications; kidney disease; age over 45 or under 25. The average age of both male and female patients was 34 ± 6 years. The samples of biological fluid were collected anonymously using the non-invasive procedure on a voluntary basis, with the consent of the patient.

Bromodihydrochlorophenylbenzodiazepine, the active ingredient of phenazepam (LP-005121-191018), was assessed after purification of excipients. The working standards (WS) were prepared: alcohol solution containing 1 mg/mL of the test substance.

The following was used for assessment: high-resolution HPLC–TMS and Orbitrap technology [15, 16]; Orbitrap Exploris 120 mass spectrometer (ThermoFisher Scientific; USA), being the Orbitrap™ standalone unit with the atmospheric pressure chemical ionization (APCI) source for high-performance liquid chromatography–mass spectrometry.

Because of the phenazepam side effects being rather intense for benzodiazepine derivatives when referred to the forensic medical examination in order to perform chemical toxicological analysis, sample preparation was performed in accordance with the generally accepted procedure, developed for benzodiazepines derivatives. Phenazepam was isolated in two ways: 1) with no hydrolysis: 5 mL of native urine were alkalized to pH 10 by adding sodium hydroxide (3–6 mL); 2) by hydrochloric acid hydrolysis and subsequent liquid–liquid extraction: 5 mL of concentrated hydrochloric acid were added to 5 mL of the first-void urine and heated in the closed tube in a boiling water bath for an hour (acid hydrolysis). Then the solution was neutralized by alkalization with 60% sodium hydroxide to pH 10. Both options involved the subsequent chloroform extraction repeated two times: 10 mL in the separatory funnel, manually shaken moderately for 3 min. After settling chloroform was poured into the evaporating dish and evaporated to dryness on a water bath; solid residue was dissolved in 0.5 mL of acetonitrile and subjected to assessment.

Chromatographic conditions, HR HPLC–TMS

Thermo Scientific Xcalibur 4.4 software (Thermo Scientific; USA), TF Accucore PhenylHexyl column (100×2.1 mm, 2.6 mm) with the column temperature of 30 °C were used.

Table 1. Mobile phase gradient

Time, min	Liquid phase flow rate, mL/min	Mobile phase A, %	Mobile phase B, %
0	0.5	99.0	1.0
1.0	0.5	99.0	1.0
10.0	0.5	1.0	99.0
11.5	0.5	1.0	99.0
12.0	0.5	99.0	1.0
13.5	0.5	99.0	1.0

Table 2. Results of urine analysis by HR HPLC-TMS

Substance	Elemental composition	Theoretical mass of protonated ion, m/z	Experimental mass of protonated ion, m/z	Retention time, min ($n = 6$)	Statistical parameters of retention time*
Phenazepam	$C_{15}H_{10}BrClN_2O$	349.61	348.97	$a = 7.05$ (6.98; 7.05; 6.95; 7.15; 7.06; 7.11)	$\sigma^2 = 0.00572$; $\sigma = 0.07563$; $V = 1.07 \%$; $A/m_a = -0.07035$; $E/m_e = -2.14563$; $\bar{a} = 0.05667$
3-hydroxyphenazepam	$C_{15}H_{10}BrClN_2O_2$	365.61	364.97	$a = 6.77$ (6.65; 6.88; 6.77; 6.85; 6.70; 6.77)	$\sigma^2 = 0.00756$; $\sigma = 0.08695$; $V = 1.28 \%$; $A/m_a = -0.08377$; $E/m_e = -2.12896$; $\bar{a} = 0.06333$

Note: σ^2 — variance, σ — standard deviation; V — coefficient of variation; A/m_a — ratio of skewness to its error; E/m_e — ratio of kurtosis to its error; \bar{a} — mean deviation.

The combined mobile phase was previously prepared. To increase the speed of analysis and reduce the width of chromatographic peaks we used different gradients altering the composition of mobile phase and changed the flow rate of the delivered mobile phase. Mobile phase in the gradient mode: mobile phase A — 2 mM ammonium formate with 0.1% formic acid in water (pH 3.0), mobile phase B — 2 mM ammonium formate with 0.1% formic acid in the acetonitrile methanol mixture (1 : 1). The flow rate was 0.5 mL/min. The gradient mode details are provided in Table 1.

Detection was performed in the data-dependent acquisition mode. The full scan-ddMS2 mode was as follows: scan range 100–1000 m/z; RF Lens 50%, high resolution data acquisition (Orbitrap, 120,000 FWHM). Automatic scan range mode. Automatic detection of the ion injection time. Intensity threshold for fragmentation 2000. Peak detection 30%, isolation window 1 m/z, stepped collisional energy mode, absolute collision energy. Higher-energy collisional dissociation (HCD) of 15, 30, 45%. Fragment resolution of 30,000. Detection windows were adjusted by routine laboratory method in order to optimize the conditions of the qualitative and quantitative analysis. Ion exclusion mode was used after acquisition of one spectrum in 3 s.

The system was fitted with the ion source, the following settings were used: H-ESI ion source; positive-ion electrospray voltage of 3500 V; negative-ion electrospray voltage of 2500 V. Nebulizer gas — nitrogen 50 AU, auxiliary gas — nitrogen 13 AU. Capillary temperature — 280 °C; evaporation source temperature — 350 °C. Built-in mass calibration EASY-IC™ (fluoranthrene).

After chromatography, native compound, phenazepam, and its metabolite were identified using the mass spectral libraries:

TRACEFINDER 5.1 SP1; TOXFINDER 1.0; EFS_HRAM_Compound_Database; Toxicology_HRAM_Compound_Database; Thermo Scientific™ mzVault HRAM MS/MS spectral library; COMPOUND DISCOVERER 3.1; MzCloud.

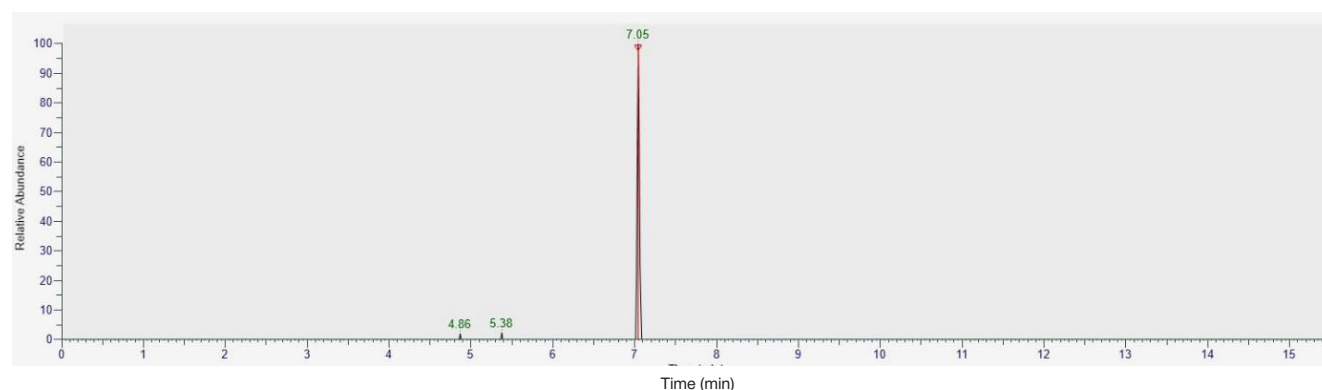
Student's t -test was used for statistical data processing. The differences were considered significant at $p < 0.05$.

RESULTS

The use of the selected scan mode made it possible to reach maximum sensitivity (due to the lack of collisional losses), which was essential for evaluation of the temporal detection windows, since the method, optimized for fast separation, could yield false-negative results due to low scan speed, whereas the significantly increased scan speed could result in the significantly reduced signal intensity, which was very important for detection of the low (therapeutic) concentrations of metabolites in biological fluids (urine). Chromatographic conditions, i.e. the mobile phase gradient combined with the temperature made it possible to reduce the quantity of compounds co-eluted from urine, and ensured reliable results (Fig. 1 and 3).

When performing isolation after hydrolysis, only the peak of phenazepam was observed (no 2-amino-5-bromo-2'-chlorobenzophenone was detected); peaks of phenazepam and 3-hydroxyphenazepam were observed when using no hydrolysis.

Phenazepam and its metabolite 3-hydroxyphenazepam were identified on the chromatograms using the selected ion approach. Detection was performed based on the retention time values with subsequent identification following the analysis of specific ions on the mass spectra of these compounds. Statistical analysis of the retention time values is provided in Table 2.

**Fig. 1.** Selected ion chromatogram (m/z 348) of the chloroform extract of urine containing phenazepam

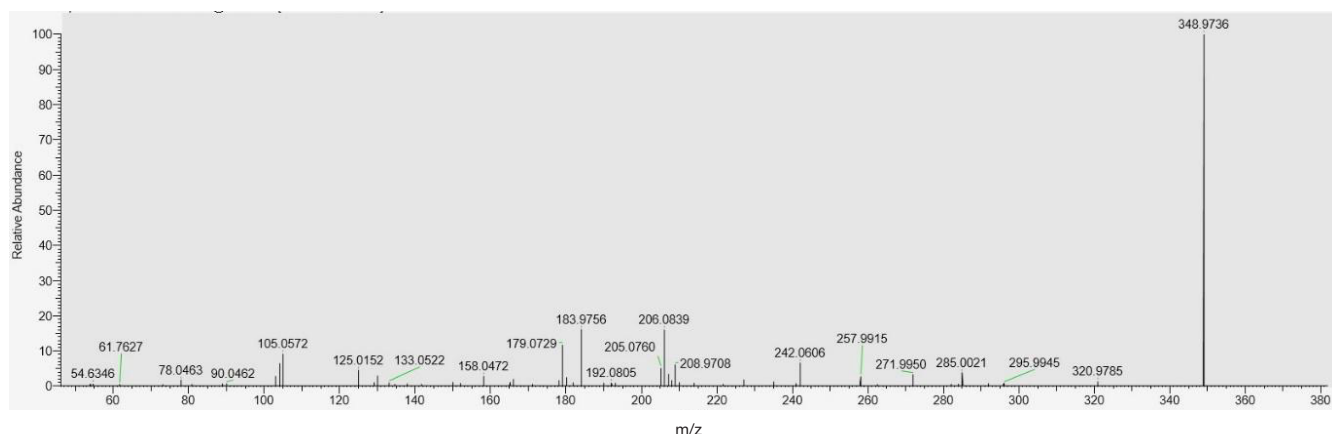


Fig. 2. Mass spectrum of phenazepam

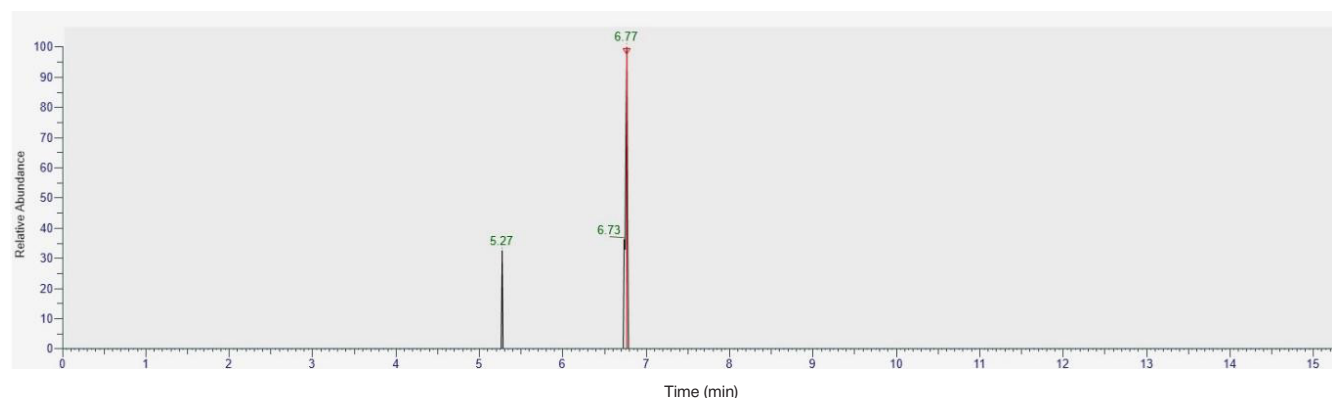


Fig. 3. Selected ion chromatogram (m/z 348) of the chloroform extract of urine containing 3-hydroxyphenazepam

In the body, phenazepam is metabolized to 3-hydroxyphenazepam. The percentage of native phenazepam excreted from the body is 47–89%, that is why identification is possible, and it is recommended to perform identification based on phenazepam.

Along with retention time, spectral characteristics of the test substances are considered a significant factor when performing identification (Fig. 2).

Statistical data processing and validation study (Table 3) were performed using the following parameters: analyte carryover assessment, determination of interference effects, ionization suppression/enhancement [17]. Parameters of validation characteristics met the acceptance criteria.

DISCUSSION

The acquired full range spectra of the test substances with the dissociated mass spectra of ions specific to the molecular fragments in various functional groups make it possible to distinguish ions specific to phenazepam: 179, 183, 206, 242, 271, 285, 320, 348 (main) m/z.

According to the data presented in Table 3, a specific ion could be distinguished for each test compound, however, identification requires the use of at least five. During the study

it is possible to perform analysis in the selected ion monitoring (SIM) mode using the selected ions. Ion at m/z 348 is the most intense ion in the mass spectra of phenazepam. It should be noted that ions of the “non-informative” range (i.e. below 150 AMU) are present in both test compounds, that is why identification results are heavily influenced by the components of the studied sample matrix and the “background” of the chromatography column. Therefore, it is recommended to use optimum data exceeding 150 AMU.

CONCLUSIONS

The method for identification of phenazepam in urine extracts by HR HPLC-TMS using the Orbitrap technology, allowing one to detect the ultra-low concentrations of phenazepam in the human biological objects (such as urine), has been developed, to be used in forensic chemistry and chemical toxicology studies. The retention time of the metabolite 3-hydroxyphenazepam after oral administration have been discovered and determined, specific ions to be used for identification have been defined. The method has been validated using the following parameters: analyte carryover assessment, determination of interference effects, ionization suppression/enhancement; according to these parameters, the method meets the acceptance criteria.

Table 3. Assessment of the parameters of validation characteristics used for identification of phenazepam and its metabolite by HR HPLC-TMS

Parameter	Result
Analyte carryover assessment	No analyte carryover revealed for 10 ng/mL
Determination of interference effects	No interference effects in the group of medications — metabolites of other benzodiazepine receptor agonists (clobazam, zaleplon, phenazepam)
Ionization suppression/enhancement	from –4,1 to 1,1% RSD < 11%

References

1. Dorofeeva OA. Kliniko-farmakologicheskie zakonomernosti terapevticheskogo dejstviya raznykh lekarstvennykh form fenazepamov u bol'nykh s trevozhnymi rasstrojstvami. Avtoreferat dissertacii na soiskanie uchenoj stepeni kandidata medicinskih nauk. Moskva, 2009. 24 s. Russian.
2. Kalekin RA. Sudebno-medicinskaya (ximicheskaya) ocenka nejroleptikov. Sudebno-ximicheskoe issledovanie i toksikologicheskaya xarakteristika nejroleptikov proizvodnykh benzamida. LAP LAMBERT. Academic Publishing GmbH & Co., 2012. 110 s. Russian.
3. Kalekin RA, Salomatin EM, Kalekina VA, Volkova AA. Laboratornaya diagnostika otravlenij nejroleptikami proizvodnymi benzamidami v narkologii: vozmozhnosti i problemy. Narkologiya. 2008; 7 (4–76): 33–37. Russian.
4. Kalekin RA, Salomatin EM, Kalekina VA, Volkova AA. Problemy i oshibki v sudebno-ximicheskix issledovaniyax na narkoticheskie i psixotropnye veshhestva. V sbornike: V. V. Kolkutin, redaktor. O problemnykh voprosax v organizacii proizvodstva sudebno-medicinskih ehkspertiz. Materialy Vserossijskoj nauchno-prakticheskoy konferencii. 2009, s. 313–317. Russian.
5. Kalekin RA, Salomatin EM, Kalekina VA. Perspektivy razrabotki sudebno-ximicheskogo i ximiko-toksikologicheskogo analiza nejroleptikov zameshennykh benzamidov. V sbornike: V. A. Klevno, redaktor. Sovremennye problemy mediko-kriminalisticheskix, sudebno-ximicheskix i ximiko-toksikologicheskix ehkspertnykh issledovaniy. Sbornik materialov Vsesoyuznoj nauchno-prakticheskoy konferencii, posvyashhennoj pamyati professora Yu. M. Kubickogo. 2007, s. 212–218. Russian.
6. Instrukciya po medicinskomu primeneniyu lekarstvennogo preparata Fenazepam LP-005121-191018. Russian.
7. Orlova AM, Kalekin RA, Volkova AA, Nevmyatova SR, Polushkina NV. Obnaruzhenie klobazama v moche metodom tonkoslojnoj xromatografii. Vestnik VGU, Ximiya. Biologiya. Farmaciya. 2021; 4: 18–24. Russian.
8. Orlova AM, Kalekin RA, Savchuk SA. Osobennosti issledovaniya pregabalina dlya celej i zadach sudebno-ximicheskix i ximiko-toksikologicheskix issledovaniy. Sudebnaya medicina. 2018; 4 (S1): 109. Russian.
9. Porseva NYu, Dvorskaya ON. Pravovye aspekty oborota snotvornyx preparatov, sposobnykh vyzyvat' lekarstvennuyu zavisimost'. Sovremennye problemy nauki i obrazovaniya. 2015; 3: 242. Russian.
10. Instrukciya po medicinskomu primeneniyu lekarstvennogo preparata Fenazepam R #003672/01-160609. Russian.
11. Instrukciya po medicinskomu primeneniyu lekarstvennogo preparata Fenazepam LSR-001772/09-100309. Russian.
12. Orlova AM, Kalekin RA, Pavlova AZ. Sudebno-medicinskaya ehkspertiza veshhestvennykh dokazatel'stv i vozmozhnosti issledovaniya pregabalina pri sudebno-ximicheskom i sudebno-toksikologicheskom issledovanii v kombinacii s drugimi sil'nodejstvuyushimi veshhestvami. Sudebno-medicinskaya nauka i praktika. Materialy nauchno-prakticheskoy konferencii molodyx uchenykh i specialistov. (28 noyabrya, 2018). M.: ANO IC, YurInfoZdrav, 2019; 13: 97–100. Russian.
13. Kalekin RA, Pavlova AZ, Orlova AM, Bulygina IE. K voprosu ustanovleniya fakta otravleniya psixotropnymi i sil'nodejstvuyushimi veshhestvami v biologicheskix ob'ektax ne invazivnogo otbora. Aktual'nye voprosy sudebnoj mediciny i obshhej patologii. Mater. nauch. prak. konf. Dekabr'skie chteniya v RUDN (21 dekabrya, 2018). M., 2019; s. 80–84. Russian.
14. Kalekin RA, Salomatin EM, Kalekina VA, Volkova AA. Differenciatsiya nejroleptikov gruppy proizvodnykh benzamidov metodom vysokoeffektivnoj zhidkostnoj xromatografii (VHhZhX). V sbornike: Materialy Vserossijskogo soveshaniya sudebno-medicinskih ehkspertov po primeneniyu pravil i medicinskih kriteriev opredeleniya stepeni tyazhesti vreda, prichinnogo zdorov'yu cheloveka. 2008, s. 226–8. Russian.
15. Helfer AG, Michely JA, Weber AA, Meyer MR, Maurer HH. Liquid chromatography-high resolution-tandem mass spectrometry using Orbitrap technology for comprehensive screening to detect drugs and their metabolites in blood plasma. Analytica Chimica Acta. 2017; 965: 83–95. Available from: <https://doi.org/10.1016/j.aca.2017.03.002>.
16. Helfer AG, Michely JA, Weber AA, Meyer MR, Maurer HH. Orbitrap technology for comprehensive metabolite-based liquid chromatographic-high resolution-tandem mass spectrometric urine drug screening — exemplified for cardiovascular drugs. Analytica Chimica Acta. 2015; 891: 221–33.
17. Barsegyan SS, Salomatin EM, Pleteneva TV, Maksimova TV, Dolinkin AO. V sbornike: R. A. Kalyokin, redaktor. Metodicheskie rekomendacii po validacii analiticheskix metodik, ispol'zuemykh v sudebno-ximicheskom i ximiko-toksikologicheskom analize biologicheskogo materiala. Metodicheskie rekomendacii. M.: RCSMEh, 2014. Russian.

Литература

1. Дорофеева О. А. Клинико-фармакологические закономерности терапевтического действия разных лекарственных форм феназепама у больных с тревожными расстройствами. Автореферат диссертации на соискание ученой степени кандидата медицинских наук. Москва, 2009. 24 с.
2. Калёкин Р. А. Судебно-медицинская (химическая) оценка нейролептиков. Судебно-химическое исследование и токсикологическая характеристика нейролептиков производных бензамида. LAP LAMBERT. Academic Publishing GmbH & Co., 2012. – 110 с.
3. Калёкин Р. А., Саломатин Е. М., Калёкина В. А., Волкова А. А. Лабораторная диагностика отравлений нейролептиками производными бензамида в наркологии: возможности и проблемы. Наркология. 2008; 7 (4–76): 33–37.
4. Калёкин Р. А., Саломатин Е. М., Калёкина В. А., Волкова А. А. Проблемы и ошибки в судебно-химических исследованиях на наркотические и психотропные вещества. В сборнике: В. В. Колкутин, редактор. О проблемных вопросах в организации производства судебно-медицинских экспертиз. Материалы Всероссийской научно-практической конференции. 2009, с. 313–317.
5. Калёкин Р. А., Саломатин Е. М., Калёкина В. А. Перспективы разработки судебно-химического и химико-токсикологического анализа нейролептиков замещенных бензамидов. В сборнике: В. А. Клевно, редактор. Современные проблемы медико-криминалистических, судебно-химических и химико-токсикологических экспертных исследований. Сборник материалов Всесоюзной научно-практической конференции, посвященной памяти профессора Ю. М. Кубицкого. 2007, с. 212–218.
6. Инструкция по медицинскому применению лекарственного препарата Феназепам ЛП-005121-191018.
7. Орлова А. М., Калёкин Р. А., Волкова А. А., Невмятова С. Р., Полушкина Н. В. Обнаружение кlobазам в моче методом тонкослойной хроматографии. Вестник ВГУ, Химия. Биология. Фармация. 2021; 4: 18–24.
8. Орлова А. М., Калёкин Р. А., Савчук С. А. Особенности исследования прегабалина для целей и задач судебно-химических и химико-токсикологических исследований. Судебная медицина. 2018; 4 (S1): 109.
9. Порсева Н. Ю., Дворская О. Н. Правовые аспекты оборота снотворных препаратов, способных вызывать лекарственную зависимость. Современные проблемы науки и образования. 2015; 3: 242.
10. Инструкция по медицинскому применению лекарственного препарата Феназепам Р №003672/01-160609.
11. Инструкция по медицинскому применению лекарственного

- препарата Феназепам ЛСР-001772/09-100309.
12. Орлова А. М., Калёкин Р. А., Павлова А. З. Судебно-медицинская экспертиза вещественных доказательств и возможности исследования прегабалина при судебно-химическом и судебно-токсикологическом исследовании в комбинации с другими сильнодействующими веществами. Судебно-медицинская наука и практика. Материалы научно-практической конференции молодых ученых и специалистов. (28 ноября, 2018). М.: АНО ИЦ, ЮрИнфоЗдрав, 2019; 13: 97–100.
 13. Калёкин Р. А., Павлова А. З., Орлова А. М., Булыгина И. Е. К вопросу установления факта отравления психотропными и сильнодействующими веществами в биологических объектах не инвазивного отбора. Актуальные вопросы судебной медицины и общей патологии. Матер. науч. прак. конф. Декабрьские чтения в РУДН (21 декабря, 2018), М., 2019; с. 80–84.
 14. Калёкин Р. А., Саломатин Е. М., Калёкина В. А., Волкова А. А. Дифференциация нейролептиков группы производных бензамидов методом высокоэффективной жидкостной хроматографии (ВЭЖХ). В сборнике: Материалы Всероссийского совещания судебно-медицинских экспертов по применению правил и медицинских критериев определения степени тяжести вреда, причиненного здоровью человека. 2008, с. 226–8.
 15. Helfer AG, Michely JA, Weber AA, Meyer MR, Maurer HH. Liquid chromatography-high resolution-tandem mass spectrometry using Orbitrap technology for comprehensive screening to detect drugs and their metabolites in blood plasma. *Analytica Chimica Acta*. 2017; 965: 83–95. Available from: <https://doi.org/10.1016/j.aca.2017.03.002>.
 16. Helfer AG, Michely JA, Weber AA, Meyer MR, Maurer HH. Orbitrap technology for comprehensive metabolite-based liquid chromatographic-high resolution-tandem mass spectrometric urine drug screening — exemplified for cardiovascular drugs. *Analytica Chimica Acta*. 2015; 891: 221–33.
 17. Барсегян С. С., Саломатин Е. М., Плетенева Т. В., Максимова Т. В., Долинкин А. О. В сборнике: Р. А. Калёкин, редактор. Методические рекомендации по валидации аналитических методик, используемых в судебно-химическом и химико-токсикологическом анализе биологического материала. Методические рекомендации. М.: РЦСМЭ, 2014.

HEPATITIS B, C AND TTV VIRUS INFECTION IN HIGHLY TRAINED ATHLETES

Melnikova LI¹✉, Kozhanova TV², Ilchenko LY^{2,3}, Morozov IA², Soboleva NV², Nguyen Thi-Hanh³, Kruglova IV⁴, Gordeychuk IV²¹ Clinical Hospital № 85 of Federal Medical-Biological Agency, Moscow, Russia² Chumakov Federal Scientific Center for Research and Development of Immune-and-Biological Products, Moscow, Russia³ Pirogov Russian National Research Medical University, Moscow, Russia⁴ Federal Scientific and Clinical Center for Sports Medicine and Rehabilitation of Federal Medical-Biological Agency, Moscow, Russia

Biomedical support is aimed at provision of the athletes' training at various stages of the training and competition process. Withholding of access to this process due to health problems resulting from hepatitis virus infection is a demanding task. The study was aimed to assess the detection rate of the hepatitis B virus, hepatitis C virus and TT virus infection markers in highly trained athletes. A total of 384 blood serum samples were collected from 240 males and 144 females aged 14–49 (athletes engaged in playing sports, precision sports, technical sports, etc.) within the framework of the multicenter open-label cross-sectional clinical trial. All athletes answered a questionnaire, which included demographic information, characteristics of sports, information about the infection risk factors, information about the fact of past acute viral hepatitis and vaccination. Markers of infection with hepatitis B virus, hepatitis C virus and TTV were identified in blood serum by enzyme immunoassay. HbsAg was detected in two surveyed athletes. Anti-HBcore (surrogate marker of latent HBV infection) was detected in 7% of samples (27/384); 1% of athletes (4/384) had a positive hepatitis C virus total antibody test (anti-HCV). Anti-HCV in combination with anti-HBcore was detected in one female athlete (14 years of age, tennis player). DNA of TTV, TTMDV and TTMV was detected in blood serum samples of 89.1%, 83.1% and 85.4% of athletes, respectively. High detection rate of the hepatitis virus markers was observed.

Keywords: highly trained athletes, hepatitis B, hepatitis C, hepatitis TTV, virus markers

Author contribution: Melnikova LI, Kruglova IV — collection of material, data analysis; Kozhanova TV — identification of markers of hepatitis virus infection, manuscript writing; Ilchenko LY — research design development, data analysis; Morozov IA — research design, manuscript editing; Soboleva NV — identification of the hepatitis virus infection markers, statistical data processing; Nguyen Thi-Hanh — literature analysis; Gordeychuk IV — manuscript editing, approval of the final version of the article.

Compliance with ethical standards: the study was approved by the Ethics Committee of the Clinical Hospital No. 85 of FMBA of Russia (protocol № 157 dated September 19, 2018). All subjects submitted the informed consent to blood sampling, identification of the hepatitis virus infection markers, and publication of results.

✉ **Correspondence should be addressed:** Lubov I. Melnikova
Kashirskoe shosse, 13G, Moscow, 115230, Russia; mel165@mail.ru

Received: 16.02.2022 **Accepted:** 05.03.2022 **Published online:** 22.03.2022

DOI: 10.47183/mes.2022.005

ИНФИЦИРОВАННОСТЬ ВИРУСАМИ ГЕПАТИТОВ В, С И ТТВ
ВЫСОКОКВАЛИФИЦИРОВАННЫХ СПОРТСМЕНОВЛ. И. Мельникова¹✉, Т. В. Кожанова², Л. Ю. Ильченко^{2,3}, И. А. Морозов², Н. В. Соболева², Nguyen Thi-Hanh³, И. В. Круглова⁴, И. В. Гордейчук²¹ Клиническая больница № 85 Федерального медико-биологического агентства, Москва, Россия² Федеральный научный центр исследований и разработки иммунобиологических препаратов имени М. П. Чумакова, Москва, Россия³ Российский национальный исследовательский медицинский университет имени Н. И. Пирогова, Москва, Россия⁴ Федеральный научно-клинический центр спортивной медицины и реабилитации Федерального медико-биологического агентства, Москва, Россия

Медико-биологическое сопровождение направлено на обеспечение подготовки спортсменов в различные периоды тренировочно-соревновательного процесса, отказ от допуска к нему из-за отклонений в состоянии здоровья вследствие инфицирования вирусами гепатитов является достаточно трудной задачей. Целью исследования было оценить частоту выявления маркеров инфицирования вирусами гепатитов В, С и ТТВ у высококвалифицированных спортсменов. В многоцентровом открытом одномоментном клиническом исследовании у 240 мужчин и 144 женщин в возрасте 14–49 лет (спортсменов игровых, сложнокоординационных, технических и других видов спорта). Получено 384 образца сыворотки крови. Все спортсмены заполняли анкету, включавшую демографические данные, характеристику вида спорта, сведения о факторах риска инфицирования, информацию о наличии перенесенного острого вирусного гепатита и вакцинопрофилактике. В сыворотке крови методом иммуноферментного анализа определяли маркеры инфицирования вирусами гепатитов В, С и ТТВ. У двух из обследуемых спортсменов выявлен HbsAg. В 7% (27/384) образцов обнаружены anti-HBcore (суррогатный маркер латентной HBV-инфекции), у 1% (4/384) спортсменов — суммарные антитела к вирусу гепатита С (anti-HCV). Anti-HCV был выявлен в сочетании с anti-HBcore у одной спортсменки (возраст — 14 лет, занимается теннисом). В образцах сывороток крови 89,1%, 83,1%, 85,4% спортсменов обнаружены DNA TTV, TTMDV и TTMV соответственно. Установлена высокая частота обнаружения маркеров вирусов гепатитов.

Ключевые слова: высококвалифицированные спортсмены, маркеры вирусов, гепатит В, гепатит С, гепатит ТТВ

Вклад авторов: Л. И. Мельникова, И. В. Круглова — сбор материала, анализ полученных данных; Т. В. Кожанова — определение маркеров инфицирования вирусов гепатитов, написание текста; Л. Ю. Ильченко — разработка дизайна исследования, анализ полученных данных; И. А. Морозов — дизайн исследования, редактирование текста; Н. В. Соболева — определение маркеров инфицирования вирусов гепатитов, статистическая обработка; Nguyen Thi-Hanh — обзор литературы; И. В. Гордейчук — редактирование и утверждение финального варианта статьи.

Соблюдение этических стандартов: этическим комитетом КБ № 85 ФМБА России (протокол № 157 от 19 сентября 2018 г.). Все участники подписали информированное согласие на взятие образца крови, определение маркеров вирусов гепатитов и публикацию полученных результатов.

✉ **Для корреспонденции:** Любовь Ивановна Мельникова
Каширское шоссе, 13, г. Москва, 115230, Россия; mel165@mail.ru

Статья получена: 16.02.2022 **Статья принята к печати:** 05.03.2022 **Опубликована онлайн:** 22.03.2022

DOI: 10.47183/mes.2022.005

Sport is one of the components of physical fitness, while high performance (elite) sport is an activity aimed at reaching peak athletic performance, which requires mobilization of emotional resources and body's functional capacity.

Peak athletic performance is reached due to the scientific and methodical support of the athlete training system at various stages of the training and competition process. Biomedical support involves investigation of the athletes' competitive activity together with the serial comprehensive, routine and detailed medical examinations (DME) performed in accordance with the specially designed programs in medical institutions [1, 2].

Viral hepatitis is a diffuse inflammatory liver disease caused by hepatotropic viruses. The infection has a variety of transmission routes and epidemiologic features [3].

Over the past 30 years, at least five different hepatitis viruses have been discovered: A (HAV), B (HBV), delta or D (HDV), C (HCV) and E (HEV) [3]. There is emerging evidence of the existence of other hepatotropic viruses capable of playing a role in the pathogenesis of both acute and chronic liver disease (CLD). Thus, hepatitis G virus (*Pegivirus*), TT virus and SEN virus were isolated from the samples collected from patients with acute or chronic hepatitis (CH) [4]. However, virological and epidemiological studies made it impossible to define the role of these viruses in the pathogenesis of the disease [3, 4].

Hepatitis B and C viruses remain the most important etiological factors of liver disease. Thus, in 2020 the acute hepatitis B infection incidence per 100,000 population was 0.35; the value for chronic hepatitis B infection was 4.4; the incidence of acute hepatitis C infection was 0.66; the value for chronic hepatitis C infection was 16.7 [5]. There are no official records of infection caused by hepatitis delta virus and *Torque teno virus* (TTV) in our country.

Taking into account the global prevalence of viral hepatitis it can be affirmed that athletes are also at risk of infection. They could be infected during the training session or the rest period. Athletes may get infected with viral hepatitis owing to activities not related to sports. However, there is some risk of virus transmission when practicing some sport. Furthermore, the team sport athletes maintain close contact with the team members for a long time; sharing food and drinks could increase the likelihood of the hepatitis virus fecal-oral transmission [6]. The actual prevalence of viral hepatitis among athletes is unknown [6, 7].

In this regard, questions arise about safety of sport and participation of athletes in the competitions after the diagnosis of acute or chronic viral hepatitis. Sports physicians should decide on the terms of the athlete's admission to training and competitions, understand the risk of viral transmission during sport, and be able to advise the athletes accordingly. Finally, specialists, who take care of the athletes' health, should be familiar with the strategies of the viral hepatitis prevention [8].

Athletes much more often get infected with HBV and HCV during activities not related to sport. These are unprotected sexual intercourse; the use of injection drugs, such as psychoactive substances and anabolic steroids; sharing personal items (for example, razors, toothbrushes, nail nippers). The cases of infection during tattooing, piercing and body painting have been reported [9].

Furthermore, healthcare professionals should consider the risk of the HBV and HCV horizontal transmission in athletes [10]. When playing sports, the infected blood could contaminate skin or mucous membranes of the other team members or individuals who come into contact with them [10].

The study was aimed to assess the detection rate for the HBV, HCV and TT infection markers in highly trained athletes.

METHODS

The multicenter open-label cross-sectional clinical trial was performed in the Center for Diagnosis and Management of Viral Hepatitis of the Clinical hospital No. 85 of FMBA of Russia and Federal Scientific and Clinical Center for Sports Medicine and Rehabilitation of FMBA of Russia.

Blood samples were collected from 384 athletes during the detailed medical examination. Inclusion criteria: highly trained athletes; age 14–49 years; informed consent to blood sampling, identification of the viral hepatitis markers, and publication of results.

All athletes completed the questionnaire, which had been developed by the researchers (Table 1).

Markers of viral hepatitis were identified in blood samples. Serological markers of HBV and HCV infection (hepatitis B surface antigen (HBsAg), antibody to hepatitis B core antigen (anti-HBcore), hepatitis C virus antibody (anti-HCV)) were identified by enzyme immunoassay using the number of test systems in accordance with the manufacturers' instructions. The following test systems were used: DS-EIA-HBsAg-0.01; DS-EIA-HBsAg-0.01 for confirmation; DS-EIA-anti-HBc; DS-EIA- SPECTRUM-G, DS-EIA-ANTI-HCV-SPECTRUM-GM (Diagnostic Systems; Russia).

Deoxyribonucleic acid (DNA) of viruses of the family *Anelloviridae* was detected in blood serum samples by polymerase chain reaction (PCR). Isolation of nucleic acids from the blood serum samples was performed using the kit for isolation of deoxyribonucleic acid/ribonucleic acid (DNA/RNA) from blood serum or plasma on the MP@SiO₂ magnetic particles (Sileks; Russia) in accordance with the manufacturer's protocol.

DNA of viruses of the family *Anelloviridae* in blood serum was identified by nested PCR [4], allowing one to distinguish between TTV, *Torque teno midi virus* (TTMDV), and *Torque teno mini virus* (TTMV) based on the amplified fragment size. The amplification product size was 112–117 nucleotides for TTV, 88 nucleotides for TTMDV and 70–72 nucleotides for TTMV. The product with the length of 207 base pairs (bp) was defined by 2% agarose gel electrophoresis conducted with TBE (Tris-borate-EDTA) buffer.

Statistical analysis of raw data involved calculation of the main selected indicators for quantitative variables. The detection rate of the serological markers (HBsAg, anti-HBcore, anti-HCV) and *Anelloviridae* virus DNA was calculated as a percentage of their total quantity in the sample.

RESULTS

The sample of athletes, whose blood samples were included in the study (384 out of 384), was randomized and represented by athletes engaged in different sports (playing sports, precision sports, technical sports, etc.) (Table 2).

Markers of HBV infection

Assessment of 384 blood samples revealed HBsAg in two individuals (male, fencing; female, volleyball). The detection rate of anti-HBcore in the general group was 7% (27/384). Female athletes were at higher risk of HBV infection compared to male athletes (18/144 and 9/240, respectively).

Analysis of personal data revealed the group of individuals with positive history. The following risk factors for infection predominated among athletes with anti-HBcore: dental care in 16 individuals (59.3%), injuries in 8 (29.6%), surgery in

Table 1. Questionnaire for highly trained athletes

Full name	Fill in or underline
Age (completed years)	
Gender	male / female
Place of birth	
Athletic discipline	
Athlete's qualification	
History of acute viral hepatitis	A, B, C, E (when?)
Vaccination against HAV	Yes, no (when?)
Vaccination against HBV	Yes, no (when?)
Surgical interventions	Yes, no (when?)
Transfusion of blood or blood substitutes	Yes, no (when?)
Dental care	Yes, no (when?)
Tattoos, piercings	Yes, no (when?)
Acupuncture	Yes, no (when?)
Traveling to foreign countries (which exactly?)	
Exposure to individuals with viral hepatitis	
Date of blood sampling	

Note: HAV — hepatitis A virus, HBV — hepatitis B virus.

9 (33.3%), acupuncture in 2 (7.4%), and tattooing in one individual (3.7%). There were no differences between males and females based on the risk factors. The average age of athletes with anti-HBcore was 16.1 ± 2.5 years.

Anti-HBcore was detected in blood serum of four artistic gymnasts, eight field hockey players, two pentathlon athletes, two hockey players, two golf players, two swimmers; single positive samples were obtained from freestyle skier, golf player, fencer, tennis player, artistic gymnast, universal martial arts fighter, and gun shooting athlete.

According to their personal data, only 11.7% of athletes (45/384) were vaccinated (three doses) against HBV. However, HBV infection markers (anti-HBcore) were found in one of them (female, artistic gymnastics). At this stage of the study, evaluation of the protective levels of the total hepatitis B surface antibody (anti-HBs) in athletes has not been completed.

The following was observed in HbsAg-positive patients: HBV DNA, viremia level exceeding 2000 IU/mL, elevation of alanine aminotransferase levels up to 1.5 of the reference limit (upper limit of normal), stage 1 fibrosis based on the transient elastography data. After 12 weeks of therapy with entecavir given at a dose of 0.5 mg/day, undetectable levels of HBV DNA were achieved. Therapy and follow-up were resumed.

Markers of HCV infection

According to the study, anti-HCV were found only in 1% of athletes (4/384). Combination therapy with sofosbuvir 400 mg/day and daclatasvir 60 mg/day was started after additional testing, which included assessing HCV RNA, viremia level, activity of chronic hepatitis C, and fibrosis stage. At the time of writing the article, the athletes had been followed up for 1.5–2 years after the antiviral therapy completion and achieving sustained virologic response.

Anti-HCV in combination with anti-HBcore were found in one female tennis player (aged 14). Biochemical indicators characterizing liver function (particularly, aminotransferases, bilirubin) did not exceed the upper limit of normal range. Abdominal ultrasound showed no abnormalities. Markers of viral replication, HBV DNA and HCV DNA, were assayed in

order to exclude latent viral infection, the negative test result was obtained. The athlete was further followed-up.

Markers of TTV, TTMDV, TTMV infection

According to the study, TTV was detected in 89.1% of athletes (342/384), TTMDV in 83.1% (319/384), and TTMV in 85.4% of athletes (328/384) (Table 3). The combination TTV + TTMDV + TTMV was detected in 69% of athletes (265/384). Biochemical indicators were within normal range.

DISCUSSION

The article presents the results of a study of 384 blood serum samples obtained from 384 highly trained athletes engaged in different sports. The detection rate of the hepatitis virus markers was high: 89.1% for TTV, 83.1% for TTMDV, 85.4% for TTMV, 7% for HBV, 1% for HCV.

It must be pointed out that the diagnosis of the hepatitis etiology limited to testing for HbsAg is ineffective, which allows patients with anti-HBcore to join the group of individuals with hepatitis of unknown etiology [4, 11]. Furthermore, such patients are most likely to infect other people.

Previously, only the presence of the stably detectable anti-HBcore was considered the sign of the past infection followed by the virus elimination and the disease remission [2]. However, anti-HBcore-positive patients generally have minimum serum levels of HBV DNA or HBV DNA that could be detected only in liver tissue. Today, the presence of anti-HBcore and the absence of HBsAg are considered the surrogate marker of latent HBV infection, and the lack of detectable HBV DNA in blood serum is not considered the fact precluding the infection.

Thus, the final judgement on the status of athletes with HbsAg is established through identification of the broader range of the HBV serological markers (anti-HBs, anti-HBe), confirmatory test for HbsAg and HBV DNA, and transient elastography aimed at detecting liver fibrosis and/or assessing the stage of fibrosis.

Along with HBV infection, hepatitis C virus (HCV) remains highly relevant. It is the major health and social issue in many of the world's countries, including the Russian Federation, owing

Table 2. Characteristics of athletes by gender and athletic discipline

Athletic discipline	Males	Females
Tennis	15	5
Universal martial arts	8	4
Biathlon	4	4
Bobsleigh	9	–
Volleyball	–	3
Canoe slalom	15	1
Golf	1	6
Judo	1	2
Luge	1	–
Track and field	12	10
Swimming	4	4
Jumping	3	1
Pentathlon	–	3
Artistic swimming	–	12
Ski cross	1	1
Slopestyle	1	–
Snowboard	1	–
Artistic gymnastics	15	6
Gun shooting sports	17	13
Sumo	5	10
Short-track speed skating	10	6
Football	–	12
Triathlon	–	1
Fencing	24	11
Freestyle skiing	19	8
Hockey	27	2
Field hockey	47	18
Chess	–	1
Total	240	144

to significant social and economic harm, global incidence, disease severity, and active involvement of people of working and childbearing age in the epidemic process [12].

According to the World Health Organization, the estimated number of people infected with HCV all over the world is 71 million [3]. However, the reported incidence rates for acute and chronic HCV do not fully reflect the population infection rate. HCV could remain asymptomatic for decades.

In our study, the detection rate of the most commonly identified HCV marker, anti-HCV, in athletes (1%) does not exceed the conditional average detection rate (3.5%)

obtained for this antibody in Eastern Europe [3] and, therefore, suggests low prevalence of HCV in the country. However, HCV co-infection with different hepatotropic and non-hepatotropic viruses could become the major underlying cause of the chronic hepatitis latency [4].

A decade after 1997, Japanese virologists H. Okamoto, T. Nishizawa, M. Ninomiya, et al, discovered viruses with genomes composed of one circular single-stranded DNA molecule [13, 14]. In 2009, the viruses were classified as a new family *Anelloviridae*. Already then we knew about the extremely high prevalence of viruses, which reached 100%

Table 3. Markers of hepatitis virus infection in athletes

Infection markers	Males, n (%)	Females, n (%)
anti-HBcore IgG	9/240 (3,8%)	18/144 (12,5%)
Of those: anti -HBcore IgG + TTV	9/9 (100%)	14/18 (77%)
anti -HBcore IgG + anti-HCV	0/9 (0%)	1/18 (5,5%)
mono anti-HCV	3/240 (0,8%)	1/144 (1,44%)
mono TTV	214/240 (89,2%)	128/144 (88,9%)
mono TTMDV	199/240 (82,9%)	120/144 (83,3%)
mono TTMV	206/240 (85,8%)	122/144 (84,7%)
TTV + TTMDV	184/240 (76,7%)	109/144 (75,7%)
TTMDV + TTMV	178/240 (74,2%)	106/144 (73,6%)
TTV + TTMDV + TTMV	168/240 (70%)	97/144 (67,4%)

not only in humans, but also in chimpanzee and African green monkeys. Such prevalence of viruses of the family *Anelloviridae* results from the properties of the parenterally transmitted and enteric viruses. It is believed that infection with these viruses is asymptomatic. The viruses are represented by numerous genera and genotypes (particularly, there are 29 genotypes of TTV (*genus Alphatorquevirus*), 12 genotypes of TTMV (*genus Betatorquevirus*), 15 genotypes of TTMDV (*genus Gammatorquevirus*)) [15]. Several viruses can coexist in the human body. Viruses are capable of affecting various organs and systems, but not all of them are related to liver disorders.

Over the past decade, the researchers observed not only the extremely high prevalence of these viruses in the populations of many countries, but also confirmed hepatotropism of some genotypes and their pathogenicity in the liver [15, 16].

The nature of chronic liver disease caused by viruses of this group has been described, the electron micrographs of TTV, TTMDV, TTMV have been obtained [17]. However, some researchers still believe in the non-pathogenic persistence of *Anelloviridae* family in humans assuming that their presence in human body results from centuries of the virus–host coevolution.

Unfortunately, English medical literature provides no data on the athletes' infection, which makes it impossible to perform analysis and compare the results with the data of similar foreign studies.

Analysis of personal data of the surveyed elite athletes, in who's serum samples anti-HBcore, anti-HCV and TTV/TTMDV/TTMV had been detected, showed that the athletes were unaware of their positive status.

All the above points to the need for assessment of the wider range of viral infection markers in athletes without being limited to testing for HBsAg and anti-HCV. Co-infection with different

hepatotropic and non-hepatotropic viruses, mutual influence of viruses, and their role in the development and progression of chronic liver diseases are the essential aspects of research.

CONCLUSIONS

Athletes are susceptible to the same viral infections as other representatives of human population, including infection with hepatitis viruses [18]. The risk of HBV and HCV infection spread does exist. However, the prevalence of these infections is not as high. Acute viral hepatitis in athlete does not require the long-term limitation of physical activity. Athletes diagnosed with acute hepatitis are under appropriate medical supervision aimed to prevent liver disease progression and chronification. In case of chronic hepatitis, efficient advanced therapeutic approaches make it possible to achieve the complete HCV elimination or clinical recovery in patients with chronic HBV infection. The prevalence of viral hepatitis in the population is high, that is why it is necessary to perform testing for the HBsAg, anti-HBcore and anti-HCV markers and acquire the data on vaccination against HAV and HBV when selecting children who would go to the sports sections and schools. Withholding of access to training and competition processes due to health problems resulting from hepatitis virus infection is a demanding task that elicits a negative reaction of the participating federation, relatives and people, who had used great moral and material resources to train the elite athlete. Currently, preventive vaccination against viral hepatitis is considered a modern strategy for prevention of infection and acute viral hepatitis progression. Vaccination should become a part of targeted training of athletes in order to reach peak athletic performance.

References

1. Samojlov AS, Razinkin SM, Petrova VV. Provedenie jetapnogo medicinskogo obsledovanija sportsmenov ciklicheskih vidov sporta na baze specializirovannogo centra sportivnoj mediciny. M.: FMBA Rossii, 2018; 65 s. Russian.
2. Meeusen R, Duclos M, Foster C, et al. Prevention, Diagnosis, and Treatment of the Overtraining Syndrome: Joint Consensus Statement of the European College of Sport Science and the American College of Sports Medicine. *Medicine and Science in Sports and Exercised*. 2013; 45 (1): 186–205. DOI: 10.1249/MSS.0b013e318279a10a.
3. Lanini S, Ustianowski A, Pisapia R, et al. Viral Hepatitis: Etiology, Epidemiology, Transmission, Diagnostics, Treatment, and Prevention. *Infect Dis Clin North Am*. 2019; 33 (4): 1045–62. DOI: 10.1016/j.idc.2019.08.004.
4. Ninomiya M, Nishizawa T, Takahashi M, et al. Identification and genomic characterization of a novel human torque teno virus of 3.2 kb. *J Gen Virol*. 2007; 88 (7): 1939–44. DOI: 10.1099/vir.0.82895-0.
5. O sostojanii sanitarno-jepidemiologicheskogo blagopoluchija naselenija v Rossijskoj Federacii v 2020 godu: Federal'naja sluzhba po nadzoru v sfere zashhity prav potrebitelej i blagopoluchija cheloveka, 2021; 256 s. Russian.
6. Harrington DW. Viral hepatitis and exercise. *Med Sci Sports Exerc*. 2000; 32: 422–30.
7. Melnikova LI, Ilchenko LYu, Zubkov YuP, Kruglova IV, Samojlov AS., Gordejchuk I. V. i dr. Sovremennaja laboratornaja diagnostika, protivovirusnaja terapija i profilaktika hronicheskikh gepatitov V, S, D u sportsmenov. Moskva, 2013; 70 s. Russian.
8. Bruckner P, Khan K: Common sports-related infections. In *Clinical Sports Medicine*, edn 2. Edited by Bruckner P, Khan K. Sydney: The McGraw-Hill Companies. 2000: 779–86.
9. Haley RW, Fischer RP: Commercial tattooing as a potentially important source of hepatitis C infection: clinical epidemiology of 626 consecutive patients unaware of their hepatitis C serological status. *Medicine*. 2001; 80: 134–51.
10. Tobe K, Matsuura K, Ogura T, et al.: Horizontal transmission of hepatitis B among players of an American football team. *Arch Intern Med*. 2000; 160: 2541–5.
11. Morozov IA, Ilchenko LJ, Fedorov IG. i dr. Skrytyj gepatit V: klinicheskoe znachenie i problemy diagnostiki. *Arhiv" vnutrennej mediciny*. 2012; 4 (6): 39–45. Russian.
12. HEPAHEALTH. Project Report. Risk Factors and the Burden of Liver Disease in Europe and Selected Central Asian Countries. [Electronic resource]. Available from: www.easl.eu (date of the application: 25.11.2021).
13. Nishizawa T, Okamoto H, Konishi K, Yoshizawa H, Miyakawa Y, Mayumi M. A Novel DNA Virus (TTV) Associated With Elevated Transaminase Levels in Posttransfusion Hepatitis of Unknown Etiology. *Biochem Biophys Res Commun*. 1997; 241 (1): 92–7. DOI: 10.1006/bbrc.1997.7765.
14. Virus Taxonomy: 2018b Release. Available from: <https://talk.ictvonline.org/taxonomy> (date of the application: 25.11.2021).
15. Al-Qahtani AA, Alabsi ES, Abu Odeh R, et al. Prevalence of anelloviruses (TTV, TTMDV, and TTMV) in healthy blood donors and in patients infected with HBV or HCV in Qatar. *J Virology*. 2016; 13 (1): 208–13. DOI: 10.1186/s12985-016-0664-6.
16. Itoh Y, Takahashi M, Fukuda M, et al. Visualization of TT virus particles recovered from the sera and feces of infected humans. *Biochem Biophys Res Commun*. 2000; 279 (2): 718–24. DOI: 10.1006/bbrc.2000.4013.
17. Morozov IA, Zverkova EA, Kyuregyan KK, i dr. Virusy roda *Anelloviridae* pri hronicheskij patologij pecheni. *Jeksperimental'naja klinicheskaja gastrojenterologija*. 2015; 7 (119): 4–11. Russian.
18. Ilchenko LYu, Morozov IA, Kozhanova TV, i dr. Vyjavljaemost' markerov inficirovanija virusami gepatitov u vysokokvalificirovannyh sportsmenov. *Arhiv" vnutrennej mediciny*. 2020; 4: 305–13. DOI: 10.20514/2226-6704-2020-10-4-305-313. Russian.

Литература

1. Самойлов А. С., Разинкин С. М., Петрова В. В. Проведение этапного медицинского обследования спортсменов циклических видов спорта на базе специализированного центра спортивной медицины. М.: ФМБА России, 2018; 65 с.
2. Meeusen R, Duclos M, Foster C, et al. Prevention, Diagnosis, and Treatment of the Overtraining Syndrome: Joint Consensus Statement of the European College of Sport Science and the American College of Sports Medicine. *Medicine and Science in Sports and Exercise*. 2013; 45 (1): 186–205. DOI: 10.1249/MSS.0b013e318279a10a.
3. Lanini S, Ustianowski A, Pisapia R, et al. Viral Hepatitis: Etiology, Epidemiology, Transmission, Diagnostics, Treatment, and Prevention. *Infect Dis Clin North Am*. 2019; 33 (4): 1045–62. DOI: 10.1016/j.idc.2019.08.004.
4. Ninomiya M, Nishizawa T, Takahashi M, et al. Identification and genomic characterization of a novel human torque teno virus of 3.2 kb. *J Gen Virol*. 2007; 88 (7): 1939–44. DOI: 10.1099/vir.0.82895-0.
5. О состоянии санитарно-эпидемиологического благополучия населения в Российской Федерации в 2020 году: Федеральная служба по надзору в сфере защиты прав потребителей и благополучия человека, 2021; 256 с.
6. Harrington DW. Viral hepatitis and exercise. *Med Sci Sports Exerc*. 2000; 32: 422–30.
7. Мельникова Л. И., Ильченко Л. Ю., Зубков Ю. П., Круглова И. В., Самойлов А. С., Гордейчук И. В. и др. Современная лабораторная диагностика, противовирусная терапия и профилактика хронических гепатитов В, С, D у спортсменов. Москва, 2013; 70 с.
8. Bruckner P, Khan K: Common sports-related infections. In *Clinical Sports Medicine*, edn 2. Edited by Bruckner P, Khan K. Sydney: The McGraw-Hill Companies. 2000: 779–86.
9. Haley RW, Fischer RP: Commercial tattooing as a potentially important source of hepatitis C infection: clinical epidemiology of 626 consecutive patients unaware of their hepatitis C serological status. *Medicine*. 2001; 80: 134–51.
10. Tobe K, Matsuura K, Ogura T, et al.: Horizontal transmission of hepatitis B among players of an American football team. *Arch Intern Med*. 2000; 160: 2541–5.
11. Морозов И. А., Ильченко Л. Ю., Федоров И. Г. и др. Скрытый гепатит В: клиническое значение и проблемы диагностики. *Архив внутренней медицины*. 2012; 4 (6): 39–45.
12. NEPAHEALTH. Project Report. Risk Factors and the Burden of Liver Disease in Europe and Selected Central Asian Countries. [Electronic resource]. Available from: www.easl.eu (date of the application: 25.11.2021).
13. Nishizawa T, Okamoto H, Konishi K, Yoshizawa H, Miyakawa Y, Mayumi M. A Novel DNA Virus (TTV) Associated With Elevated Transaminase Levels in Posttransfusion Hepatitis of Unknown Etiology. *Biochem Biophys Res Commun*. 1997; 241 (1): 92–7. DOI: 10.1006/bbrc.1997.7765.
14. Virus Taxonomy: 2018b Release. Available from: <https://talk.ictvonline.org/taxonomy> (date of the application: 25.11.2021).
15. Al-Qahtani AA, Alabsi ES, Abu Odeh R, et al. Prevalence of anelloviruses (TTV, TTMDV, and TTMV) in healthy blood donors and in patients infected with HBV or HCV in Qatar. *J Virology*. 2016; 13 (1): 208–13. DOI: 10.1186/s12985-016-0664-6.
16. Itoh Y, Takahashi M, Fukuda M, et al. Visualization of TT virus particles recovered from the sera and feces of infected humans. *Biochem Biophys Res Commun*. 2000; 279 (2): 718–24. DOI: 10.1006/bbrc.2000.4013.
17. Морозов И. А., Зверкова Е. А., Кюрегян К. К. и др. Вирусы рода *Anelloviridae* при хронической патологии печени. *Экспериментальная клиническая гастроэнтерология*. 2015; 7 (119): 4–11.
18. Ильченко Л. Ю., Морозов И. А., Кожанова Т. В. и др. Выявляемость маркеров инфицирования вирусами гепатитов у высококвалифицированных спортсменов. *Архив внутренней медицины*. 2020; 4: 305–13. DOI: 10.20514/2226-6704-2020-10-4-305-313.

FOCAL LASER PHOTOCOAGULATION OF THE OPTIC DISC PERIPAPILLARY NEOVASCULARIZATION IN PATIENT WITH PROLIFERATIVE DIABETIC RETINOPATHY

Takhchidi KhP, Takhchidi NKH, Kasminina TA, Tebina EP ✉

Pirogov Russian National Research Medical University, Moscow, Russia

Diabetic retinopathy (DR) is one of the most common complications of diabetes mellitus and one of the major causes of blindness in the developed world. Retinal laser photocoagulation is a gold standard for the treatment of DR. Despite its high efficiency, laser therapy has a number of limitations. The emergence of drugs, designed to inhibit the growth of the newly formed blood vessels, in ophthalmic practice made it possible to change treatment strategy in patients with retinal neovascularization. However, this method also has some adverse effects. Given the limitations on the repeated sessions of laser photocoagulation and the risks of ophthalmic complications after the intravitreal injection of the angiogenesis inhibitors, extraordinary situations, when there are negative results of treatment with the use of the described above techniques in one eye and disease progression in the single eye with preserved vision, become a serious problem when performing treatment. The clinical case reported has shown the feasibility of staged laser treatment in patient with the optic disc peripapillary neovascularization. Therapy has resulted in the regression of the newly formed blood vessels and visual function preservation.

Keywords: diabetic retinopathy, focal laser photocoagulation, multispectral imaging, angiogenesis inhibitors, peripapillary neovascularization

Author contribution: Takhchidi KhP — study concept and design, manuscript editing; Takhchidi NKH — literature analysis; Tebina EP — data acquisition and processing, manuscript writing; Kasminina TA — laser therapy.

Compliance with ethical standards: the patient submitted the informed consent to laser therapy and personal data processing.

✉ **Correspondence should be addressed:** Ekaterina P. Tebina
Volokolamskoe shosse, 30, korp. 2, Moscow, 123182, Russia; ekaterinatebina@mail.ru

Received: 15.01.2022 **Accepted:** 01.03.2022 **Published online:** 13.03.2022

DOI: 10.47183/mes.2022.004

ФОКАЛЬНАЯ ЛАЗЕРНАЯ КООГУЛЯЦИЯ ПЕРИПАПИЛЛЯРНОЙ НЕОВАСКУЛЯРИЗАЦИИ ДИСКА ЗРИТЕЛЬНОГО НЕРВА ПРИ ПРОЛИФЕРАТИВНОЙ ДИАБЕТИЧЕСКОЙ РЕТИНОПАТИИ

Х. П. Тахчиди, Н. Х. Тахчиди, Т. А. Касмынина, Е. П. Тебина ✉

Российский национальный исследовательский медицинский университет имени Н. И. Пирогова, Москва, Россия

Диабетическая ретинопатия (ДР) является одним из наиболее частых осложнений сахарного диабета и одной из ведущих причин развития слепоты в развитых странах. Золотой стандарт лечения ДР — лазерная коагуляция сетчатки. Несмотря на высокую эффективность лазерного лечения, данный метод имеет ограничения в использовании. Появление в клинической практике офтальмолога препаратов, направленных на ингибирование роста новообразованных сосудов, позволило изменить тактику лечения пациентов с неоваскуляризацией сетчатки. Однако и этот метод обладает рядом нежелательных побочных явлений. Учитывая ограничения в проведении повторных этапов лазерной коагуляции, а также рисков офтальмологических осложнений после интравитреального введения ингибиторов ангиогенеза, серьезной проблемой в лечении являются нестандартные ситуации, когда имеется отрицательный результат лечения вышеописанными технологиями на одном глазу и прогрессирование процесса на единственно зрячем другом глазу. Представленный клинический случай продемонстрировал возможность поэтапного лазерного лечения пациента с перипапиллярной неоваскуляризацией ДЗН. Результатом лечения явился регресс новообразованных сосудов с сохранением зрительных функций.

Ключевые слова: диабетическая ретинопатия, фокальная лазерная коагуляция, мультиспектральное исследование, ингибиторы ангиогенеза, перипапиллярная неоваскуляризация

Вклад авторов: Х. П. Тахчиди — концепция и дизайн исследования, редактирование текста; Н. Х. Тахчиди — анализ литературных данных; Е. П. Тебина — сбор и обработка материала, написание текста; Т. А. Касмынина — лазерное лечение пациента.

Соблюдение этических стандартов: от пациента получено добровольное информированное согласие на лазерное лечение и обработку персональных данных.

✉ **Для корреспонденции:** Екатерина Павловна Тебина
Волоколамское шоссе, д. 30, корп. 2, г. Москва, 123182, Россия; ekaterinatebina@mail.ru

Статья получена: 15.01.2022 **Статья принята к печати:** 01.03.2022 **Опубликована онлайн:** 13.03.2022

DOI: 10.47183/mes.2022.004

Currently, diabetes mellitus (DM) is a global issue. Microvascular complications of DM, such as diabetic retinopathy, nephropathy, neuropathy, are becoming the increasingly important disease manifestations and mortality causes [1].

Diabetic retinopathy (DR) is one of the most common complications of DM and one of the major causes of blindness in the developed world [2]. The prevalence of DR in the developed countries is about 3–4%; the percentage of affected individuals is higher in the older age groups. According to IDF (International Diabetes Federation), in 2017 there were 425 million people with DM all over the world. This indicator is expected to increase to 629 million people by 2040. A total of 3,029,397 patients with DM were registered in Russia in 2019,

among them about 294,000 people had type 1 DM (T1D), and 2,736,000 had type 2 DM (T2D) [3, 4].

Regardless of the type of DM, it is an undeniable fact that the longer is the age of DM, the higher is the risk of developing DR. DR is diagnosed in almost all patients with T1D and in more that 60% of patients with T2D within two decades after the disease onset. In the Wisconsin Epidemiologic Study of Diabetic Retinopathy (WESDR), blindness was diagnosed in 3.6% of patients with early-onset T1D and 1.6% of patients with adult-onset T2D. In 86% of cases, blindness in people with early-onset DM resulted from DR [5].

The DR triggers are as follows: chronic hyperglycemia, protein glycation, glucose oxidation through activation of

the polyol pathway, protein kinase activation, elevated levels of free radicals, impaired retinal microcirculation, endothelial dysfunction, hypoxia, increased production of the retinal pro-inflammatory cytokines and production of the vascular endothelial growth factor (VEGF), which result in edema and proliferation [6]. According to foreign and domestic literature, the efficiency of panretinal photocoagulation in patients with DR is assessed based on the degree of the retinal neovascularization suppression, regression of macular edema, visual function improvement or stabilization. According to the listed above criteria, the laser therapy efficacy varies between 60–99% [7, 8]. Despite its high efficiency, laser therapy has a number of limitations: severe diabetic macular edema [9], prominent fibrotic changes in the vitreoretinal interface, restrictions on the repeated sessions of laser photocoagulation.

The emergence of drugs designed to inhibit VEGF in ophthalmic practice made it possible to change the treatment strategy in patients with retinal neovascularization. This treatment type is focused directly on the pathophysiological target in DR. However, despite high efficiency of using the angiogenesis inhibitors, a number of case studies revealed some non-inflammatory adverse events (cataract, elevated intraocular pressure, retinal artery occlusion, vitreous hemorrhage, rhegmatogenous retinal detachment) and inflammatory complications (sterile intravitreal inflammation, brolocizumab-associated retinal vasculitis, post-injection endophthalmitis) [10]. Short duration of therapeutic effect (to an average of three months), the need for repeated injections, and all the listed above risks are considered the disadvantages of this treatment method.

The literature indicates that new foci of neovascularization and proliferation often emerge in various terms after the panretinal laser photocoagulation. Given the limitations on the repeated sessions of laser photocoagulation and the risks of ophthalmic complications after the intravitreal injection of the angiogenesis inhibitors, extraordinary situations, when there are negative results of treatment with the use of the described above technologies in one eye and disease progression in the single eye with preserved vision, become a serious problem when performing treatment. The study was aimed to assess the efficiency and safety of laser photocoagulation of the optic disc peripapillary neovascularization in patient with proliferative diabetic retinopathy.

Clinical case

Patient M. aged 30 contacted the Research Center of Ophthalmology, Pirogov Russian National Research Medical University, in April 2017 for routine funduscopy. It was known from the case history that the patient had type 1 diabetes mellitus since he was nine; no cardiovascular disorder was revealed. In 2007, the patient was diagnosed with bilateral proliferative diabetic retinopathy and therefore subjected to panretinal laser photocoagulation. Intravitreal angiogenesis inhibitor administration was performed in 2008 due to proliferative retinal changes in the right eye, and was complicated by the central retinal artery occlusion with sudden loss of vision.

After admission to the Research Center of Ophthalmology, Pirogov Russian National Research Medical University, the patient underwent a comprehensive ophthalmic examination, which included standard diagnostic tests (visometry for uncorrected visual acuity (UCVA) and best corrected visual acuity (BCVA), indirect ophthalmoscopy with the MaxField indirect lens (Ocular Inc.; USA)) and specific assessment methods (multispectral imaging with various filters (Blue-,

Green-, Infrared Reflectance, MultiColor) performed with the Spectralis HRA+OCT, OCT2 module at 85,000 Hz (Spectralis HRA+OCT, Heidelberg Engineering, Inc.; Germany). The maximum follow-up period was 4 years.

Laser photocoagulation was performed with the VISULAS Trion ophthalmic laser system, 532 nm (Carl Zeiss; Germany).

During the initial patient assessment the following was revealed: visual acuity of the right eye (OD) — hand motion close to the face (eccentric); UCVA of the left eye (OS) 0.03, BCVA 0.7, in corrigible. Ophthalmoscopy OS revealed pale-pink optic disc with well-defined margins; the lace-like pattern of the newly formed vessels, running from the optic disc to the periphery and spreading in a fan-like manner, was observed predominantly in certain quadrants of the peripapillary region (upper nasal, lower nasal, lower temporal). Retinal vasculature: the artery to vein (A/V) ratio was 2/3, the vessel course remained unchanged, perivascular pigmented coagula were observed along the superior and inferior vascular arcades. Cellophane macular reflex, and weakly pigmented coagula (except for the avascular zone) were revealed. Pigmented coagula, reaching almost the optic disc to a distance of 1800 µm were found in the mid-periphery and far-periphery (Fig. 1A, B).

The following diagnosis was established based on the patient's medical history and the comprehensive ophthalmic examination: proliferative diabetic retinopathy OS, the condition after panretinal laser photocoagulation. Epiretinal fibrosis. Peripapillary neovascularization of the optic disc.

Taking into account the history of complication in the right eye, which developed after the intravitreal injection of the angiogenesis inhibitor and resulted in vision loss (the complication made it impossible to use the anti-VEGF drugs), a decision was made to perform custom laser treatment, which included staged laser photocoagulation: coagulation of the remaining intact peripapillary retinal area between the boundary of the old laser coagula and the zone within 500 µm from the optic disc edge at the beginning, assessing the effect of retinal photocoagulation and the visual function indicators a week later, with subsequent decision on the need for the next stage of focal laser photocoagulation of the newly formed blood vessels.

At the first stage, almost circumferential (except for the zone of papillomacular bundle) focal retinal laser photocoagulation was performed in the peripapillary region between old coagula and the zone within 500 µm from the optic disc edge. The chequerwise laser spots were applied using the following energy parameters: wavelength of 532 nm, power of 60–80 mW (until obtaining the first degree laser burn with the minimum possible parameters), exposure time of 0.08–0.1 s, and spot size of 100 µm. Visual acuity remained stable a week after the first-stage retinal laser photocoagulation. Ophthalmoscopy OS revealed the following: pigmented laser coagula were observed in the peripapillary region (up to 500 µm from the optic disc edge), the lace-like pattern of the newly formed vessels remained active (Fig. 2A, B).

After assessing the left eye (in a week) and detecting the visual function stability, the second-stage focal laser photocoagulation of the newly formed blood vessels (primarily the medium-sized vessels) was performed using the following energy parameters: power of 50–80 mW, exposure time of 0.06–0.1 s, spot size of 100 µm. The second stage was prolonged selectively and involved minimizing bleeding risks and assessing the effectiveness in four sessions performed with an interval of 3–4 weeks.

Examination performed 4 months after the second-stage focal laser photocoagulation of the newly formed blood vessels (four sessions) showed that visual acuity OS was stable: UCVA

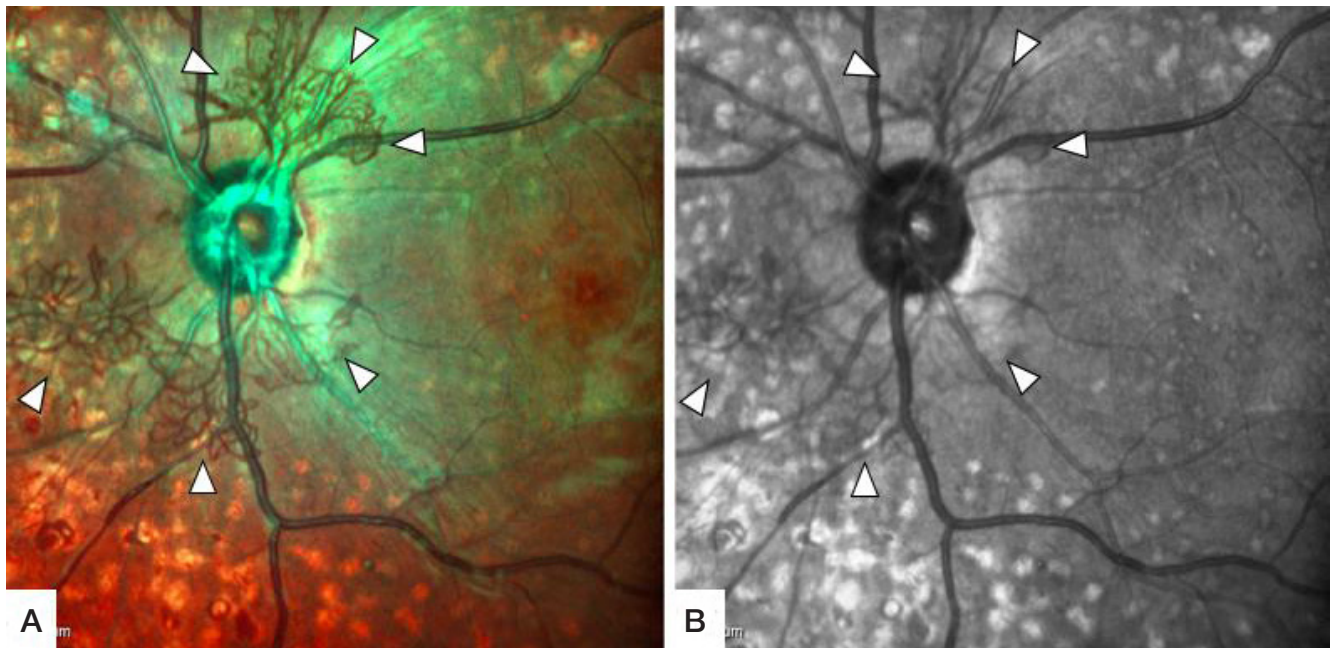


Fig. 1. Prior to laser therapy. **A.** Multispectral image; **B.** Infrared scanning laser ophthalmoscopy: network of the newly formed blood vessels is visible primarily in the upper nasal, lower nasal, and lower temporal sectors of the peripapillary region (white arrows)

was 0.03, and BCVA was 0.7. Ophthalmoscopy OS revealed the emptied newly formed vessels in the peripapillary region (Fig. 3A, B).

The follow-up examination performed four years later showed the unchanged visual acuity. Ophthalmoscopy OS revealed a complete regression of the optic disc network of the newly formed vessels in the peripapillary region (Fig. 4A, B).

Clinical case discussion

Diabetic retinopathy remains the leading cause of visual impairment and blindness in the world. More than one third of 285 million people all over the world, who suffer from diabetes mellitus, have DR, and one third of them (approximately

31.7 million) have a vision-threatening proliferative diabetic retinopathy [11]. Currently, the main treatment methods for proliferative diabetic retinopathy are as follows: retinal laser photocoagulation, intravitreal administration of angiogenesis inhibitors, treatment with corticosteroids, and vitreoretinal surgery. All the listed above treatment methods can be used in clinical practice as monotherapy or combination therapy.

The clinical case reported demonstrates the resource capabilities of the proposed peripapillary zone laser photocoagulation technique in the context of inability to use angiogenesis inhibitors due to the complication of the use of those, which have resulted in vision loss in the other eye.

The number of coagula, spot size and energy of the laser beam irradiating the retina should be selected individually

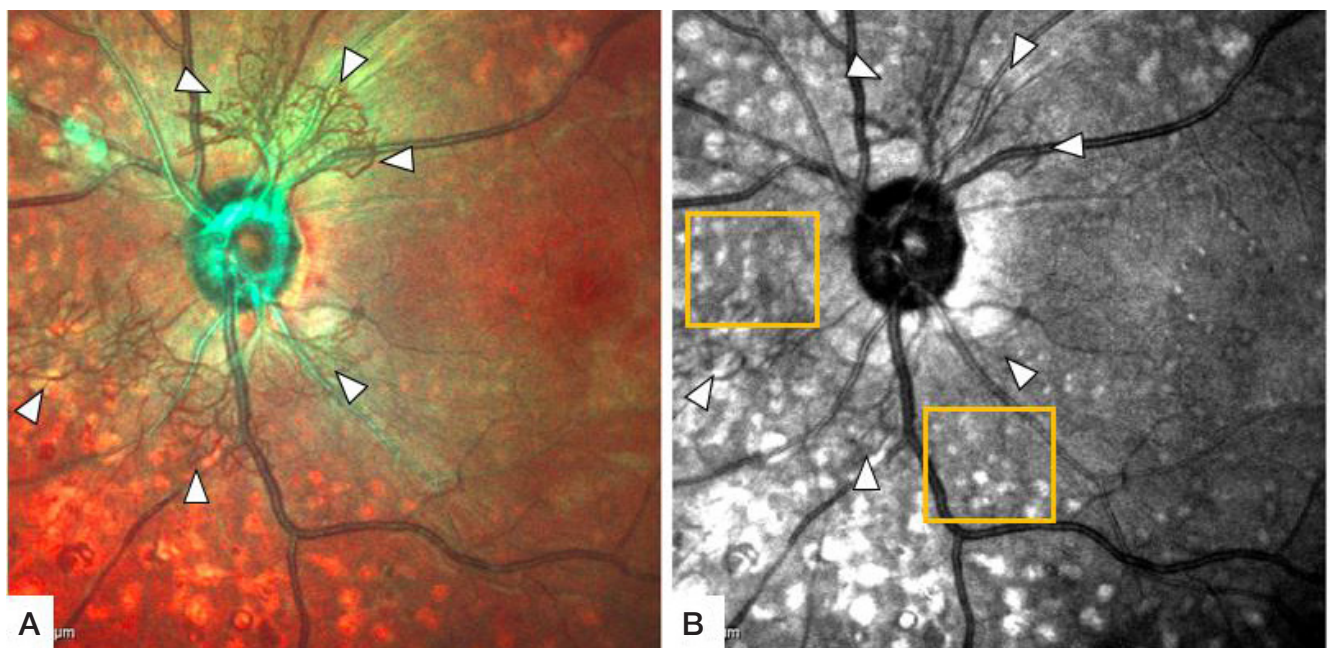


Fig. 2. A week after the first stage of laser photocoagulation. **A.** Multispectral image: network of the newly formed blood vessels in the peripapillary region is still active (white arrows). **B.** Infrared scanning laser ophthalmoscopy: network of the newly formed blood vessels in the peripapillary region is still active (white arrows), fresh coagula are observed in the peripapillary region (yellow square)

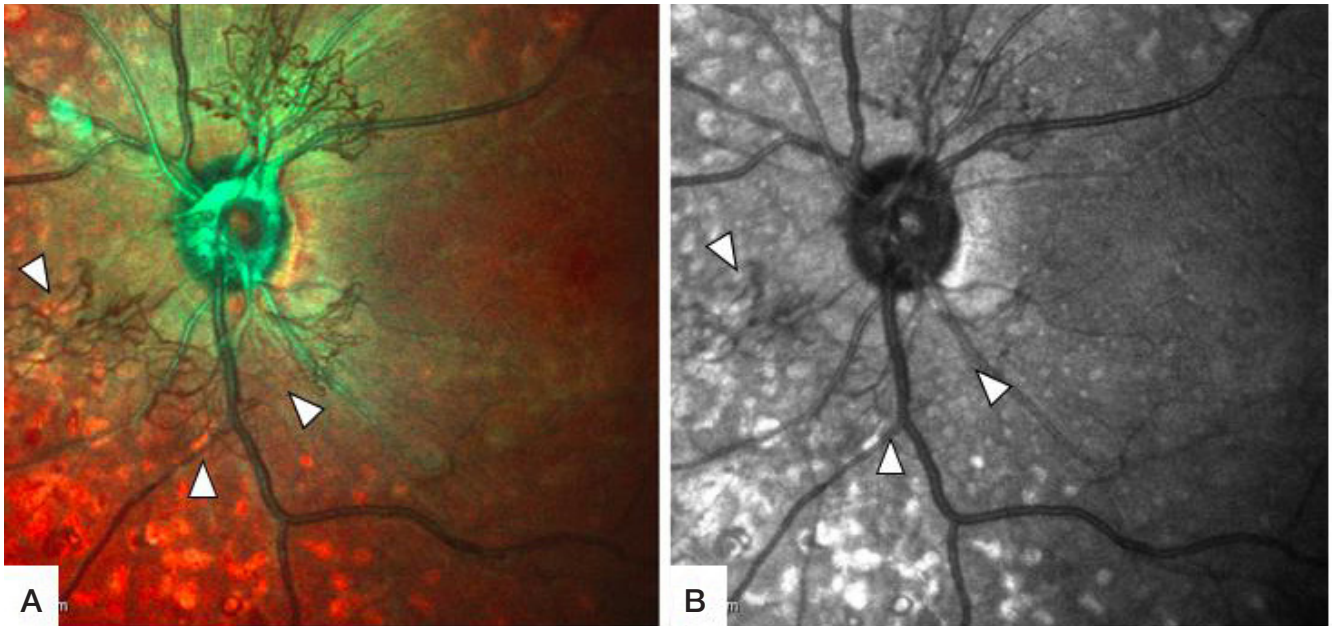


Fig. 3. Four months after the second-stage laser photocoagulation of the newly formed blood vessels. **A.** Multispectral image. **B.** Infrared scanning laser ophthalmoscopy: emptied newly formed vessels are visible in the peripapillary region (white arrows)

for a particular patient and oriented towards the lowest possible energy level. Laser exposure of the retinal areas, located most close to the optic disc, reduces “hypoxia” in these zones and, therefore, the new blood vessel formation intensity in the most reactive zone of proliferation, the optic disc. Thus, such preconditioning (performed at the first stage of treatment) of the peripapillary retinal area, with which the lace-like pattern of the new vessels is formed, results in reduced blood flow in these vessels, allowing for the more efficient second-stage treatment, the focal photocoagulation of the newly formed blood vessels. To minimize bleeding risks, one should start with blood vessels not exceeding the medium size, step-by-step in multiple sessions. Such approach allows the older coagula to contribute to blood vessel emptying, reduced blood flow and, therefore, the decreased risk of complications during subsequent photocoagulation.

The proposed laser treatment technique involves the use of the minimum possible energy parameters, allowing for the good morphofunctional outcome that consists in the complete optic disc peripapillary neovascularization regression and baseline visual function preservation.

CONCLUSION

Thus, the findings suggest that the use of the proposed focal laser photocoagulation technique for treatment of the optic disc peripapillary neovascularization ensure the regression of the newly formed blood vessels and preserve the baseline visual functions. The use of focal laser photocoagulation in the proposed peripapillary region expands the possibilities of treating the optic disc neovascularization. The practical effect demonstrates the results of using laser microsurgery in the adjacent areas of the optic disc with visual function preservation.

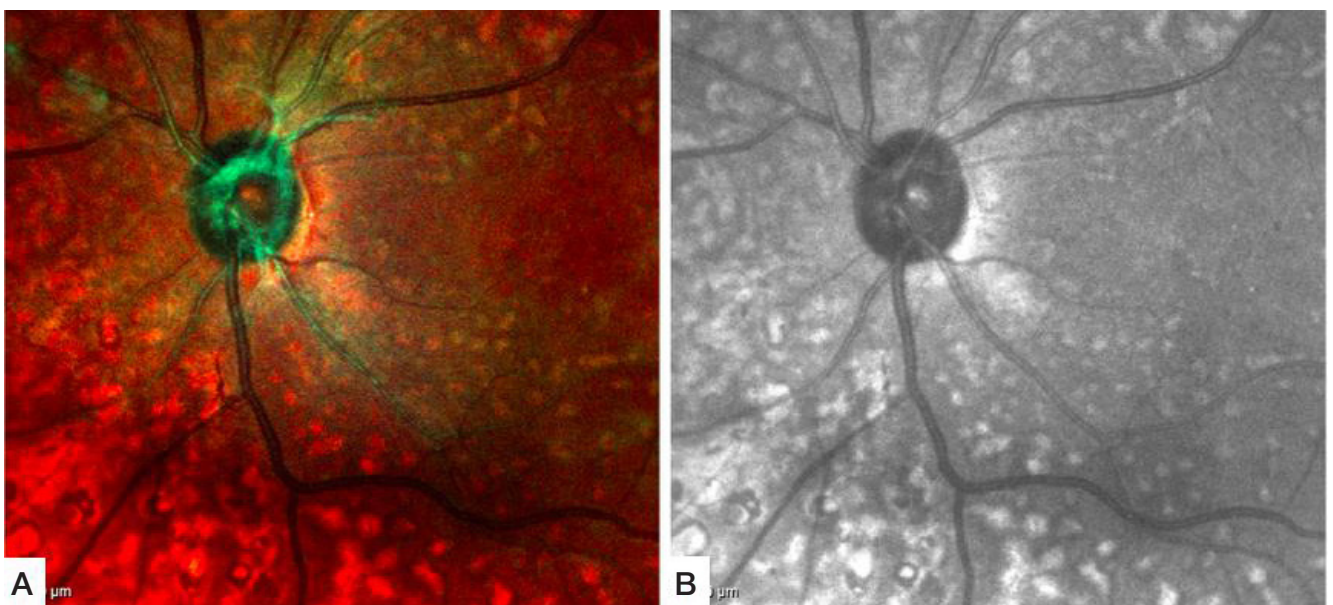


Fig. 4. Four years after the second-stage laser photocoagulation of the newly formed blood vessels. **A.** Multispectral image. **B.** Infrared scanning laser ophthalmoscopy: complete regression of the optic disc network of the newly formed vessels is observed in the peripapillary region

References

1. Stewart MW. Treatment of diabetic retinopathy: Recent advances and unresolved challenges. *World J Diabetes*. 2016; 7 (16): 333–341.
2. Klein R, Knudtson MD, Lee KE, Gangnon R, Klein BE. The Wisconsin Epidemiologic Study of Diabetic Retinopathy XXIII: the twenty-five-year incidence of macular edema in persons with type 1 diabetes. *Ophthalmology*. 2009; 116 (3): 497–503.
3. Sergushev SG, Homjakova EN. Anti-VEGF preparaty v terapii pacientov s diabeticheskim makuljarnym otekom. *Klinicheskaja oftal'mologija*. 2019; 25 (4): 238–44. Russian.
4. Federal'nyj registr saharnogo diabeta RF, realizuemyj FGBU «NMIС jendokrinologii» Minzdrava Rossii. Dostupno po ssylke: https://www.endocrincentr.ru/sites/default/files/all/EVENTS2019/NEWS%20SUM/13.03.19%20Prof.komissia/VIK_Exp_13.03.19.pdf.
5. Smirnova OM. Diabeticheskaja retinopatija. Rezul'taty mezhdunarodnyh mnogocentrovyh issledovanij. *Saharnyj diabet*. 2010; 13 (1): 80–87. Russian.
6. Bosma EK, van Noorden CJF, Klaassen I, Schlingemann RO. *Diabetic Nephropathy*. Springer, 2019. DOI: 10.1007/978-3-319-93521-8_19.
7. Burjakov DA, Kachalina GF, Pedanova EK, Kryl LA. Ocenka bezopasnosti povtornyh seansov subporogovogo mikroimpul'snogo lazernogo vozdeystvija pri lechenii diabeticheskogo makuljarnogo oteka. *Sovremennye tehnologii v oftal'mologii*. 2015; 3: 19–21. Russian.
8. Zajka VA, Shhuko AG, Arhipov EV, Bukina VV. Ocenka dolgosrochnoj jeffektivnosti panretinal'noj lazernoj koaguljacji pri saharnom diabete 2-go tipa. *Sovremennye tehnologii v oftal'mologii*. 2020; (1): 34–36. Russian.
9. Gacu MV, Bajborodov YaV. Kliniko-topograficheskaja klassifikacija diabeticheskikh makulopatij. *Saharnyj diabet*. 2008; 11 (3): 20–22. Russian.
10. Jacob T. Cox, Dean Elliott, and Lucia Sobrin. Inflammatory Complications of Intravitreal Anti-VEGF Injections. *J Clin Med*. 2021; 10 (5): 981.
11. Yau JW, et al. Meta-Analysis for Eye Disease (META-EYE) Study Group. Global prevalence and major risk factors of diabetic retinopathy. *Diabetes Care*. 2012; (35): 556–64.

Литература

1. Stewart MW. Treatment of diabetic retinopathy: Recent advances and unresolved challenges. *World J Diabetes*. 2016; 7 (16): 333–341.
2. Klein R, Knudtson MD, Lee KE, Gangnon R, Klein BE. The Wisconsin Epidemiologic Study of Diabetic Retinopathy XXIII: the twenty-five-year incidence of macular edema in persons with type 1 diabetes. *Ophthalmology*. 2009; 116 (3): 497–503.
3. Сергушев С. Г., Хомякова Е. Н. Анти-VEGF препараты в терапии пациентов с диабетическим макулярным отеком. *Клиническая офтальмология*. 2019; 25 (4): 238–44.
4. Федеральный регистр сахарного диабета РФ, реализуемый ФГБУ «НМИЦ эндокринологии» Минздрава России. Доступно по ссылке: https://www.endocrincentr.ru/sites/default/files/all/EVENTS2019/NEWS%20SUM/13.03.19%20Prof.komissia/VIK_Exp_13.03.19.pdf.
5. Смирнова О. М. Диабетическая ретинопатия. Результаты международных многоцентровых исследований. *Сахарный диабет*. 2010; 13 (1): 80–87.
6. Bosma EK, van Noorden CJF, Klaassen I, Schlingemann RO. *Diabetic Nephropathy*. Springer, 2019. DOI: 10.1007/978-3-319-93521-8_19.
7. Буряков Д. А., Качалина Г. Ф., Педанова Е. К., Крыль Л. А. Оценка безопасности повторных сеансов субпорогового микроимпульсного лазерного воздействия при лечении диабетического макулярного отека. *Современные технологии в офтальмологии*. 2015; 3: 19–21.
8. Зайка В. А., Щуко А. Г., Архипов Е. В., Букина В. В. Оценка долгосрочной эффективности панретинальной лазерной коагуляции при сахарном диабете 2-го типа. *Современные технологии в офтальмологии*. 2020; (1): 34–36.
9. Гацу М. В., Байбородов Я. В. Клинико-топографическая классификация диабетических макулопатий. *Сахарный диабет*. 2008; 11 (3): 20–22.
10. Jacob T. Cox, Dean Elliott, and Lucia Sobrin. Inflammatory Complications of Intravitreal Anti-VEGF Injections. *J Clin Med*. 2021; 10 (5): 981.
11. Yau JW, et al. Meta-Analysis for Eye Disease (META-EYE) Study Group. Global prevalence and major risk factors of diabetic retinopathy. *Diabetes Care*. 2012; (35): 556–64.